UNIVERSITY OF BERGAMO

Faculty of Engineering

Department of Industrial Engineering

PhD in Energy and Environmental Technology

XXII cycle – year 2010

SMALL-SCALE BIOMASS POWER GENERATION

Supervisor: Prof. Antonio Perdichizzi

Co-examiner: Prof. Giuseppe Franchini

Thesis by:

Samuel Carrara

Fatti non foste a viver come bruti,
ma per seguir virtute e canoscenza.
(Ye were not made to live like unto brutes,
But for pursuit of virtue and of knowledge.)

Dante Alighieri, The Divine Comedy,
Inferno, Canto XXVI, lines 119-120

Abstract

In recent years considerable attention has been paid to power generation from biomass, especially in small scale plants. Several plant configurations have been proposed and investigated, but so far, definitely preferable technological solutions have not been found yet. Moreover, a comparison of their performances is often difficult, due to the fact that working assumptions are not always consistent.

The aim of the present work is to provide a full overview on small scale technologies regarding biomass exploitation (particularly woody one) for power generation, in order to define the most interesting solutions from a thermodynamic and economic point of view. Existing configurations or those which are expected to be potentially available on the market in the near future have been considered. Three plant sizes have been focused: 100 kW_{el}, 1 MW_{el} and 5 MW_{el}. Internal combustion engines (ICE), (micro) gas turbines (mGT/GT), both internally and externally fired, and organic Rankine cycles (ORC) have been taken into account as power plants, while direct combustion and gasification have been considered for biomass.

Simulations show that the externally fired gas turbine is the most promising technology at small scale (100 kW_{el}), if a high temperature heat exchanger is available. A gasifier coupled with an internal combustion engine is instead preferable at larger scales (1 MW_{el} and 5 MW_{el}).

An also proposed sensitivity analysis concerning moisture effects shows that biomass drying with flue gas is generally disadvantageous, even if sometimes (e.g. in gasifiers) necessary, because of the dryer cost.

Acknowledgements

After twenty-one years, my career as a student comes to an end with this thesis. In this moment I am thinking back to the people who accompanied me and to the episodes which occurred during these years: if I had to list all of them, I should probably write another book! However, someone once said that one book per time is enough, when it is not too much, then I will just greet and thank the people who were important during the PhD period and who helped me reach this further goal, starting from the university teaching staff who bore me again after my bachelor and master degrees.

My dutiful thanks go to my Supervisor, Prof. Antonio Perdichizzi, for giving me once more the chance to collaborate with his research group and to develop this thesis under his guidance.

I am very grateful to my Co-examiner, Prof. Giuseppe Franchini, for having me always granted a huge support: working with him has always been stimulating and pleasant.

My thanks also go to Prof. Gianpietro Cossali, Prof. Giovanna Barigozzi and all the other professors who have always proven to be very helpful.

I warmly hug all PhD and post-doc students whom I met in these years and who shared with me the serenity of the positive moments and discouragement of the difficult ones: I will miss the PhD office and the lunches at Gattopardo's or Centrale's!

Naturally, I cannot but thank my parents, my brother, my grand-mother and all my other relatives, who helped me be what I am now.

My loving thanks go Laura and her family: the gratitude that I fell towards them cannot be described in few words; my thanks also to Mrs. Schroeder for the appreciated support.

Obviously I want to thank all friends of mine and all the other people who have been close to me and that cannot be cited here.

Finally, my special thanks to the ones who, without being seen, help me every single day from up above.

Table of contents

Nomenclature

Symbols

A	Area	m^2
C	Heat capacity	W/K
c	Biomass cost	€/t
H	Hydrogen content in biomass	-
h	Moisture	-
h	Yearly heat sale hours	h
K	Green certificate multiplicative factor	-
m	Mass	kg, t
$\dot{m}$	Mass flow rate	kg/s, t/h
P_{ch}	Chemical power	kW
P_{el}	Electric power	kW
p	Pressure	Pa, atm
p	Thermal energy sale price	$c€/kWh_{th}$
Q	Thermal power	kW
q	Latent heat of evaporation/condensation	MJ/kg
R	Universal gas constant	J/(kmol·K)
R*	Specific gas constant	J/(kg·K)
s	Entropy	J/(kg·K)
T	Temperature	°C, K
U	Overall heat transfer coefficient	$W/(m^2 \cdot K)$
X	Molar fraction	-
Y	Mass fraction	-

Greek symbols

α	Air to fuel ratio (mass)	-
α_{st}	Stoichiometric air to fuel ratio (mass)	-
β	Gas turbine pressure ratio	-
ε	Heat exchanger effectiveness	-
η_{el}	Electrical efficiency	-
η_{g}	Gasifier cold gas efficiency	-
η_{th}	Thermal efficiency	-
η_{I}	First law efficiency	-
λ	Air to fuel ratio to stoichiometric air to fuel ratio (mass)	-
ν	Air to fuel ratio (volumetric)	-
ν_{st}	Stoichiometric air to fuel ratio (volumetric)	-
ρ	Density	kg/m^3

Acronyms

ASU	Air separation unit	
(B)IGCC	(Biomass) integrated gasification combined cycle	
CCS	Carbon capture and storage	
CHP	Combined heat and power	
CI	Compression ignition	
COT	Combustor outlet temperature	°C, K
C/N	Carbon-nitrogen content ratio	
db	Dry basis	
DG	Distributed generation	
EBIT	Earning before interest and taxes	k€
EFGT	Externally fired gas turbine	
ETBE	Ethyl-Tertiary-Butyl-Ether	
FC	Fuel cell	
FC	Fixed carbon	

GC	Green certificate	c€/kWh$_{el}$
GHG	Greenhouse gas	
GT	Gas turbine	
ICE	Internal combustion engine	
IFGT	Internally fired gas turbine	
IGV	Inlet guide vanes	
IRR	Internal rate of return	-
HDI	Human development index	
HHV	Higher heating value	kJ/kg, MJ/kg kJ/Nm^3, MJ/Nm^3
HRSG	Heat recovery steam generator	
HWR	Hot water recovery	
IFGT	Internally fired gas turbines	
IRAP	Imposta regionale sulle attività produttive (regional tax on productive activities)	-
IRES	Imposta sul reddito delle società (tax on the corporate income)	-
LHV	Lower heating value	kJ/kg, MJ/kg kJ/Nm^3, MJ/Nm^3
MCFC	Molten carbonate fuel cell	
MDM	Octamethyl-trisiloxane	
mGT	Micro gas turbine	
MSW	Municipal solid waste	
MW	Molecular weight	kg/kmol
NPV	Net present value	k€
PAFC	Phosphoric acid fuel cell	
PBT	Payback time	years
PEM	Polymer electrolyte membrane	
PV	Photovoltaic	
SCR	Selective catalytic reduction	
SFR	Short rotation forestry	
SI	Spark ignition	

SOFC	Solid oxide fuel cell	
STIG	Steam injected gas turbine	
TIT	Turbine inlet temperature	°C, K
TO	Tariffa omnicomprensiva (all-inclusive tariff)	c€/kWh$_{el}$
TOT	Turbine outlet temperature	°C, K
VM	Volatile matter	
wb	wet basis	
w/w	Weight terms	

Subscripts

a	Air
c	Cold
ch	Chemical
dry	Dry conditions
el	Electric(al)
f	Fuel
g	Gas
h	Hot
i	Inlet
min	Minimum
o	Outlet
th	Thermal
V	Volume
wet	Wet conditions

List of Figures

List of Tables

Chapter 6

Introduction

It is now generally accepted that human activities have substantial effects on global warming and that the reduction of greenhouse gas emissions is a vital goal for the coming decades: for instance, the Kyoto protocol and the EU 20-20-20 plan are international agreements based on these assumptions. The use of renewable energy sources for power generation can make a major contribution in this direction. Amongst them, biomass seems to be particularly interesting, because it combines the main advantage of renewable energies (CO_2-neutrality) with the ability to be accumulated and exploited through a combustion process, coupling its conversion with more traditional technologies, thus also allowing combined heat and power (CHP) production. Besides, a considerable potential of this resource is available almost all over the world, and signally in Europe and Italy. In particular woody biomass is the most abundant typology and is suitable for power generation also thanks to its versatility.

Biomass power generation is mostly realised in large plants, but its exploitation can be even more interesting on small sizes, due to the difficulty in supplying large quantities of raw material to feed plants, the higher possibility of performing a cogenerative waste heat recovery and the very low environmental impact of the installations. Besides, small plants often enjoy higher economic incentives than larger ones, as occurs in Italy.

Small-scale biomass power plants have been widely investigated in recent years: literature is proposing several technical solutions. Nevertheless, undoubtedly preferable plant configurations have not been identified yet, which is also due to the recent development in the sector. Moreover, a comparison of their performances is often difficult because investigations are being carried out referring to different operating conditions.

Basing on these considerations, the aim of the present thesis is to perform a full assessment of small-scale biomass fired power generation technologies, focusing on woody resource, in order to allow a complete comparison and identify the most promising solutions from a thermodynamic and an economic point of view. Existing

plant configurations or those which are expected to be potentially available on the market in the near future have been considered.

Three plant sizes have been focused: 100 kW_{el}, 1 MW_{el} and 5 MW_{el}. Indeed, the former two scales are more relevant, since the latter can actually be considered a medium-size for biomass power plants (it has been taken into consideration in order to obtain comparison values).

Wood combustion and gasification are the biomass conversion processes taken into account, while pyrolysis has been neglected since it is not considered a forthcoming technology. On the other hand, internal combustion engines (ICE), (micro) gas turbines (mGT/GT), both internally and externally fired, and organic Rankine cycles (ORC) have been considered as power plants.

Starting from these base technologies, a large number of plant configurations has been assembled and investigated. In particular, thermodynamic performance simulations have been carried out using the commercial Thermoflex™ software. Setting the different configurations, power generation maximisation (e.g. providing regeneration when possible) has been focused, but low-temperature waste heat recovery is being realised in order to fully exploit biomass lower heating value (LHV), producing hot water. The most performing solutions then have been subject to an economic analysis, carried out basing on the Italian legislation, which provides considerable economic incentives for power generation from renewable energy sources.

The first chapter of the thesis is dedicated to the biomass resource. Firstly its importance in the energy scenario and its potential development are being discussed, referring in particular to the Italian context. Chemical, physical and energy characteristics of wood are then presented, followed by the description of the conversion technologies (i.e. combustion, gasification and pyrolysis, as mentioned).

The second chapter provides an overview on small-scale power plants, and in particular on the three adopted typologies, i.e. internal combustion engines, gas turbines and organic Rankine cycles. The last part of the chapter is dedicated to a brief description of the other technologies which, for different reasons, have not been considered in this thesis (Stirling engines, steam engines and fuel cells).

The operative part of the work begins in the third chapter, discussing all the technical hypotheses on which the thermodynamic simulations are based. Firstly the

computational Thermoflex™ tool is presented, especially dealing with the gasification model reliability and the issues related to the proper modelling of biomass syngas burning in power plants. Thereafter all design parameters adopted in the simulations are listed and discussed.

Thermodynamic analysis is the topic of the fourth chapter: firstly all investigated solutions are presented, also showing Thermoflex™ drawn plant schemes, then electrical and first law efficiency results are reported and discussed. Improved gasification solutions are additionally studied.

The thermodynamically most performing solutions have then been considered in the economic analysis, which is described in the fifth chapter. Also in this case, working hypotheses concerning the economic assumptions are indicated at first and then results are presented. A sensitivity analysis carried out varying some significant parameters is also proposed.

The sixth and last chapter of the thesis is finally dedicated to a complementary analysis, aiming at the investigation of moisture effects. In particular, it is studied how moisture affects plant performance and which is the effect of wood drying, both at thermodynamic and economic level.

Chapter 1
Biomass and technologies for its exploitation

1.1 Introduction

In this chapter an overview on the biomass resource is provided, focusing in particular on woody one, the type which is being considered in this work. After presenting its chemical, physical and energy properties, conversion technologies (pyrolysis, combustion and gasification) that allow its use in power plants are described.
However, first of all it is necessary to introduce the present world energy scenario and briefly discuss why biomass can play an important role in power generation. In addition, an outline of the Italian situation is also presented, showing the potentiality of biomass use for energy purposes in this country.

1.2 The energy issue and biomass role

Past studies have unequivocally demonstrated the existence of a strong correlation between social and economic development of a country and per-capita energy consumption, with particular reference to electricity: this concept is clearly shown in Figure 1.1, where the well-being of a country is quantified by the HDI (Human Development Index) indicator. Consequently, it is not surprising that developing countries (such as China, India and Brazil) are registering increasing energy consumption associated to their economic growth and that, on the other hand, due to the economic crisis a decrease is predicted for the OECD area in 2009.
Apart from this, total world energy consumption without any structural interventions is expected to grow constantly in the next decades (Figure 1.2).

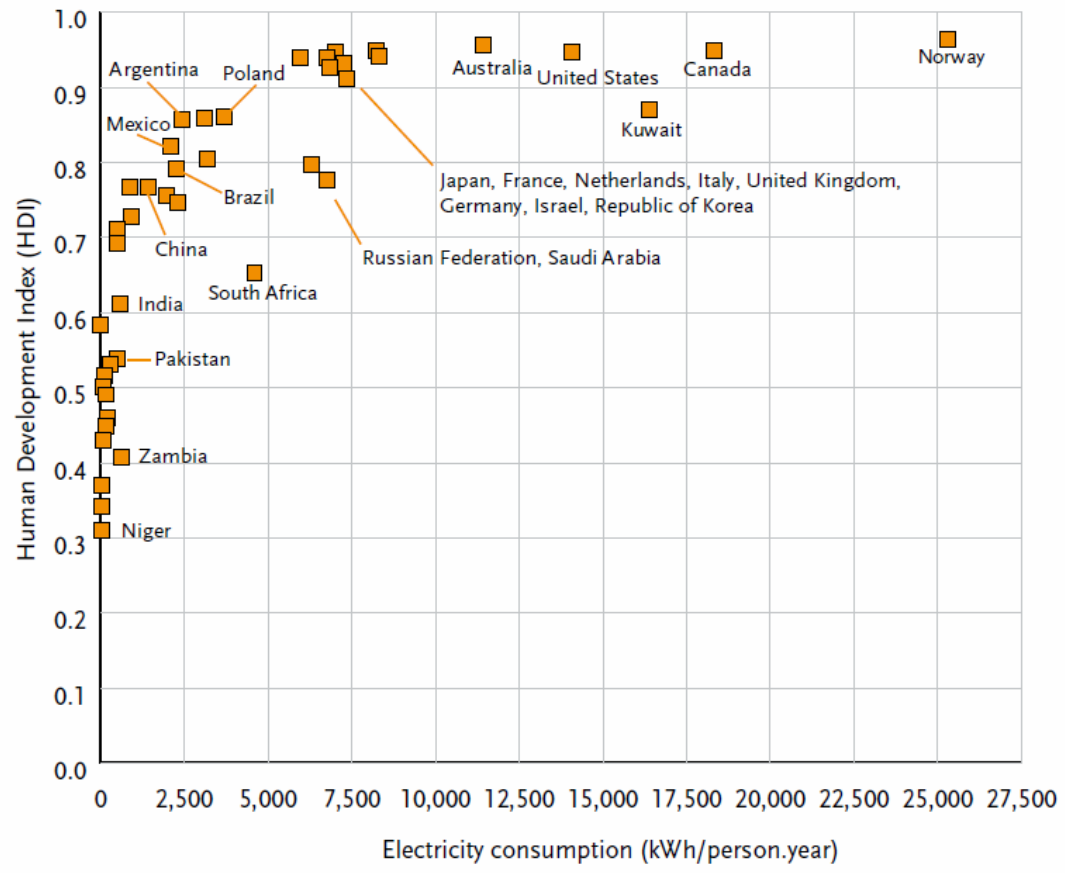

Figure 1.1 – Correlation between HDI and electricity consumption [1.1].

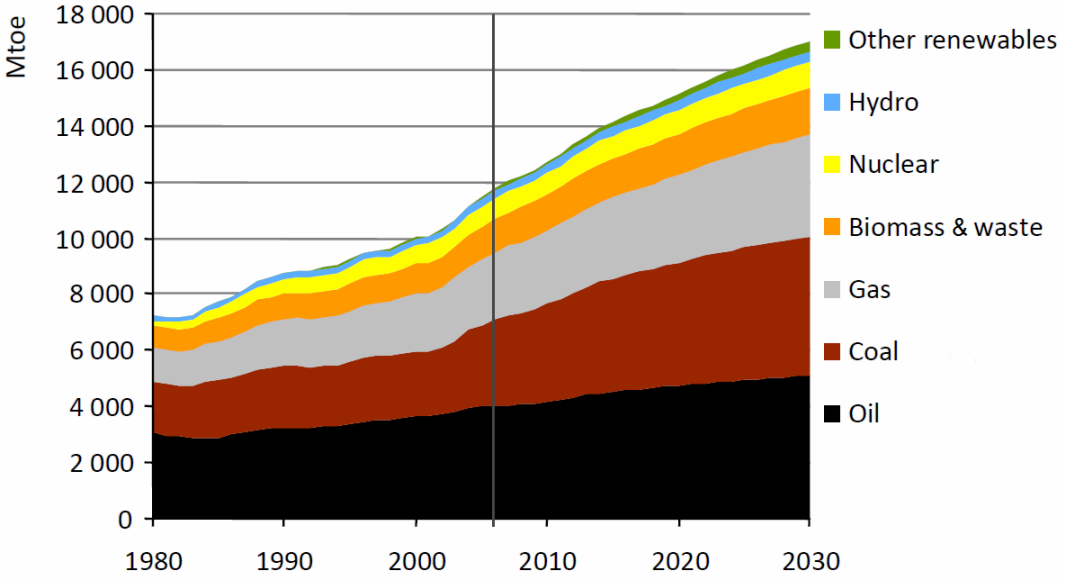

Figure 1.2 – World primary energy demand by fuel [1.2].

As one can see in Figure 1.2 and as summarised in the two pie charts in Figures 1.3 and 1.4, energy needs are mainly met by the combustion of fossil fuels: their incidence is nowadays 81% in terms of total primary energy and 67% for electricity production.

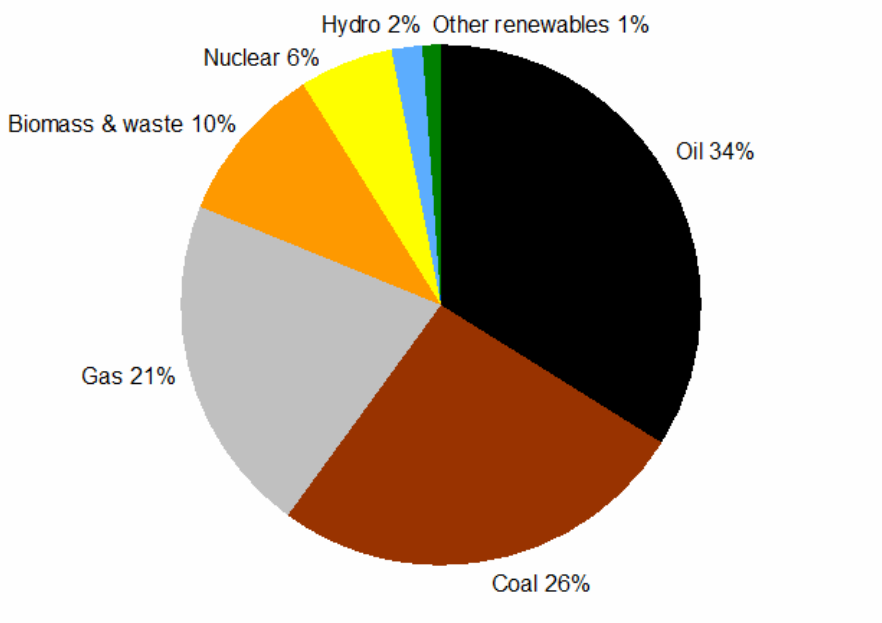

Figure 1.3 – World primary energy consumption by fuel (adapted from [1.3]).

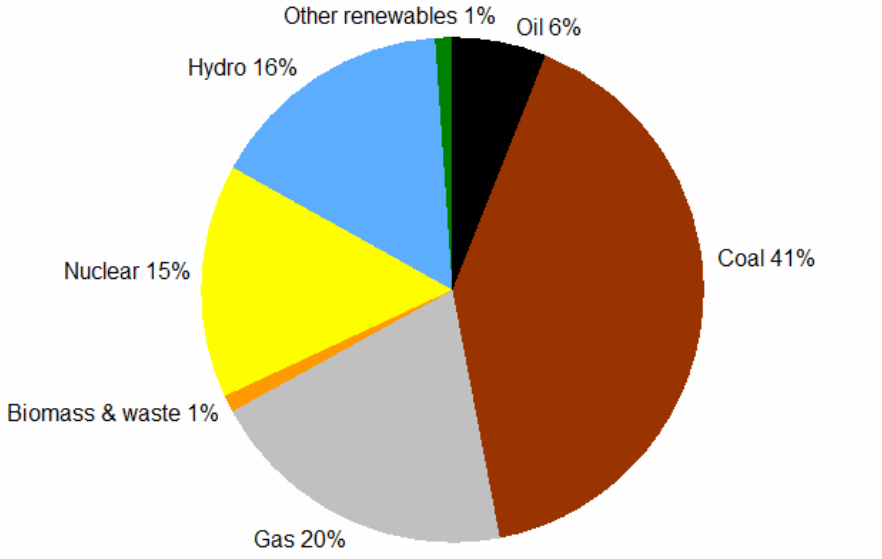

Figure 1.4 – World electricity production by energy source (adapted from [1.3]).

This fact involves the emissions of large quantities of greenhouse gases (GHG), above all carbon dioxide: its concentration in atmosphere has already reached levels never seen in past ages (about 385 ppm, see Figure 1.5) and a heavy increase is expected in the near future (Figure 1.6), mostly due to the developing countries, according to what mentioned above.

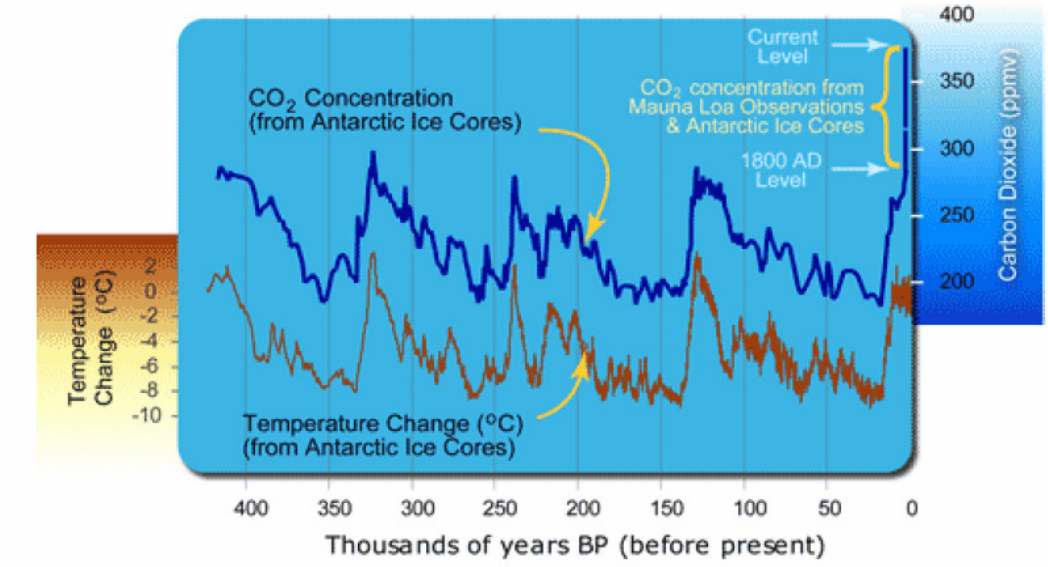

Figure 1.5 – Historic carbon dioxide concentration in atmosphere (note the heavy increase after the Industrial revolution, 1800 ca.) [1.4].

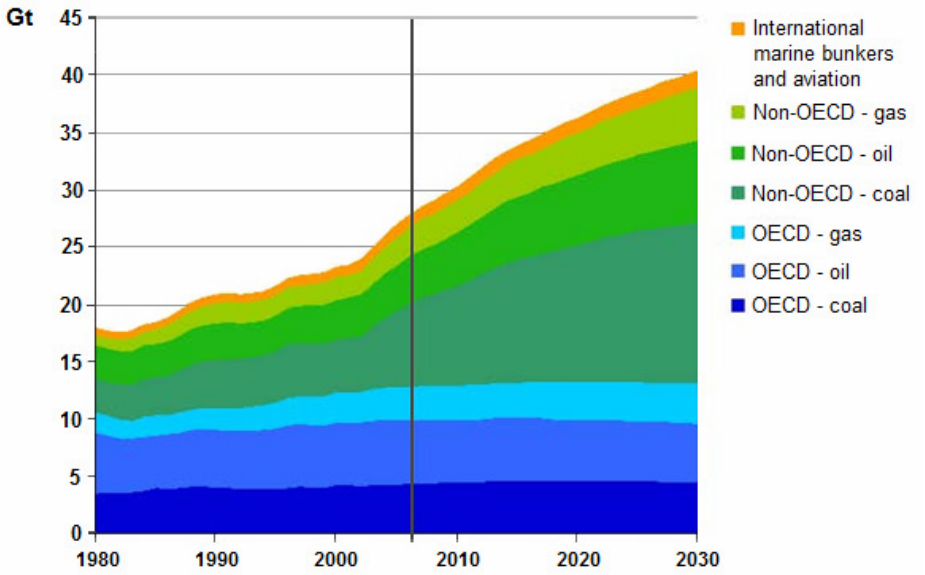

Figure 1.6 – Projected increase of carbon dioxide annual emissions [1.2].

Basing also on the likely relationship between historic temperature change and carbon dioxide concentration (see again Figure 1.5), it is commonly accepted that these emissions will probably lead to an increase of average temperature of Earth's near-surface air and oceans (the so called Global warming), with dramatic consequences on environment and, consequently, on world population [1.5].

It is therefore essential to adopt effective strategies to limit the emission of CO_2 and the other greenhouse gases. The Kyoto Protocol [1.6] represented the first actual international agreement in this sense, even if its practical results have been quite unsatisfying, mainly because it did not provide any limitations for emissions in the developing countries. Pending the conclusions of the United Nations Climate Conference that will be held in Copenhagen in December 2009, European Union in 2008 fixed the so called 20-20-20 plan: the aim is to reach by 2020 a 20% reduction in greenhouse gas emissions compared with 1990 levels, a 20% cut in energy consumption through improved energy efficiency and a 20% increase in the use of renewable energies (in particular, biofuels incidence in transports will have to be 10%) [1.7].

International Energy Agency (IEA) has recently proposed alternative plans, called 550 and 450 Policy Scenarios, for the evolution of GHG emissions (Figure 1.7), that aim at a long term stabilisation of the CO_2 concentration in atmosphere at 550 ppm or 450 ppm, thus limiting the temperature increase respectively to 3°C or 2°C compared to the pre-industrial age, that should avoid or limit environmental consequences [1.2].

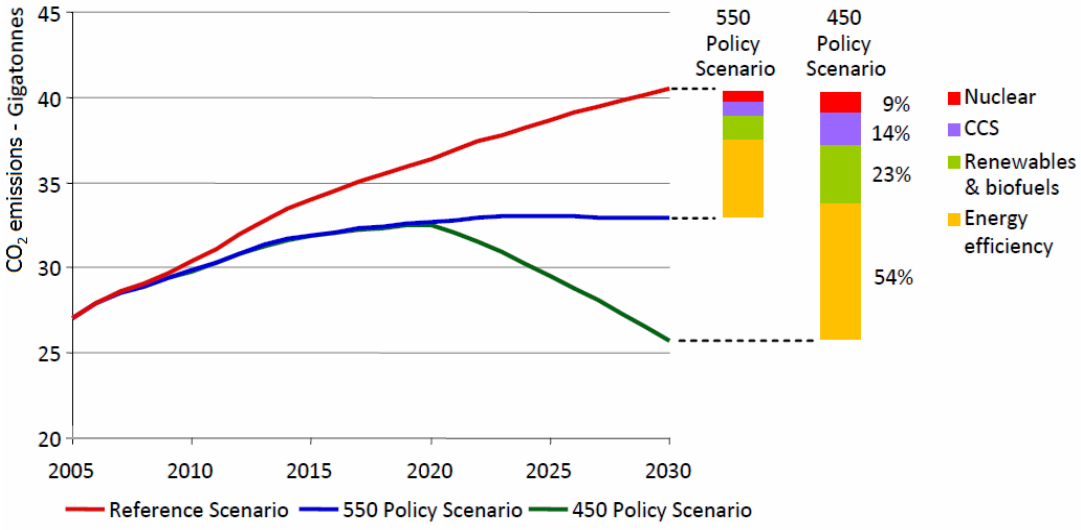

Figure 1.7 – IEA 550 and 450 Policy Scenarios [1.2].

As can be observed, this result would be achieved basing on four great pillars:

- a higher global efficiency, referring both to power plants and, above all, on the rationalisation of energy end-use: this point represents the most important contribution;
- a wider use of renewable energies and biofuels;
- the adoption on large scale of the CCS (Carbon Capture and Storage) techniques, that allow to separate carbon dioxide and confine it in underground geological formations or oceans;
- the construction of new nuclear power plants.

Renewable sources are therefore meant to be widely used in the near future for energy production, also considering, apart from greenhouse gas emissions issues, the problems related to unstable prices of fossil fuels and to their provisioning, that can be sometimes difficult.

Thanks to its peculiar characteristics that will be discussed hereinafter, biomass can play a very important role amongst them. Presently it already represents a considerable energy source and in particular, as shown in Figures 1.3 and 1.4, its share is the largest among the renewable sources (excluding hydro for power generation): it supplies 10% of the whole primary energy demand and 1% of the electricity production. It should be noted that statistics generally associate biomass and waste, but the former provides the most important contribution, above all for the first datum, which is due to the fact that biomass is often the unique energy source in undeveloped countries, being used for food cooking, heating by direct combustion, etc.

In detail in 2005[1] the incidence of biomass on gross domestic energy demand was 3.5% in OECD area, 4.6% in EU (with peaks of 16% in Finland, 15% in Sweden and 12% in Austria) and 19% in undeveloped countries, with frequent values of 30-40% and even 90% in the poorest ones: OECD countries consume 50% of the world primary energy, but only 17% of total biomass.

Obviously in OECD area biomass is exploited with modern technologies for power, heat (in case district heating) and CHP production: 80% of electricity production from

[1] Previous figures are based on 2006 global data, while detailed data, disaggregated for the different areas, are available for the year 2005: possible differences are however considered negligible for this discussion.

solid biomass and almost the totality of that from biogas occur in these countries. In particular biomass incidence on the domestic electrical production is 2% in EU, while is negligible in underdeveloped countries.

In absolute terms, biomass energy consumption in the European Union was 84 Mtoe (of which about 80% from solid biomass), compared with a total demand of 1815 Mtoe, while the maximum yearly amount of energy that could be derived from biomass in the area is estimated at about 400 Mtoe [1.8]. EU Commission in 2005 set the goal of a 149 Mtoe consumption by 2010 ÷ 2012 [1.9], nevertheless this ambitious target will hardly be reached: EurObserv'ER predicts that in 2010 the amount will be about 104 Mtoe, thus 46 Mtoe less than anticipated in the plan[2] [1.10].

1.2.1 Italian situation and perspectives

1.2.1.1 Primary energy

There are several assessments concerning total biomass consumption in Italy, often considerably different one from the other. These differences are mainly due to the difficulty in evaluating properly the actual consumption in the many small heating devices that were installed in the last years. Referring to the year 2005, in the Position Paper on the use of renewable energies, the Italian Government estimates it at 3.53 Mtoe [1.11], while IEA states 4.2 Mtoe, as reported in [1.8]. Nevertheless, the most reliable value is probably the one given by ITABIA (Italian Biomass Association), just because its assessment is also based on a deep survey on small-scale heating plants: the value is fixed in 5.65 Mtoe [1.12], which means a rate of about 3% on the whole domestic energy demand, which was 198 Mtoe in that year [1.13]. It must be specified that in every case all municipal solid waste (MSW) is included: basing on an assessment on waste-fired power plants performed by ENEA (Ente per le Nuove tecnologie, l'Energia e l'Ambiente) [1.14], its incidence can be evaluated in about 1.2 Mtoe.

[2] These last two values take into account only the biodegradable fraction of municipal solid waste; however the remaining part just amounts to 5 ÷ 6 Mtoe, so its incidence on the total value is quite low.

Concerning future scenarios, the goals fixed for Italy by the EU 20-20-20 plan require that in 2020 total primary energy deriving from biomass will have to be 16 ÷ 18 Mtoe. Data and perspectives contained in the Italian Government Position Paper are expressed according to those reference values and, basing on this document, in the cited publication ITABIA estimates biomass potential consumption for that date in 19.5 Mtoe (even if 3.6 Mtoe will be represented by imported biofuel necessary to satisfy transport fuel demand, so domestic contribution is expected to be limited to 15.9 Mtoe), that will substitute 16.5 Mtoe of fossil primary energy: the gap is essentially due to the different conversion efficiencies of power plants for the two types of feeding. Besides, MSW share is expected not to exceed 2 Mtoe. As in 2020 primary energy consumption should be about 215 ÷ 239 Mtoe [1.13], biomass would represent about 8 ÷ 9% of the total. Moreover, 20-20-20 goals would impose to limit the whole demand at 165 ÷ 175 Mtoe [1.15]: in that case the share would be obviously higher, about 11 ÷ 12%, but it is quite unlikely that this aim will be reached.

Values reported above must be compared to the total biomass availability in the country: ITABIA estimates it in 24 ÷ 30 Mtoe (excluding MSW), subdivided as shown in the Table 1.1, that is therefore theoretically sufficient to cover the predicted demand.

Energy source	**Availability [Mtoe/year]**
Residues from:	
- agriculture and agroindustry	5
- forestry and wood industry	4.3
- public parks	0.3
- livestock holdings	10 ÷ 12
Firewood	2 ÷ 4
Dedicated crops	3 ÷ 5
Total	**24 ÷ 30**

Table 1.1 – Potential biomass energy availability by source in Italy [1.12].

A wide literature concerning biomass availability in the different Italian regions or provinces has been produced in the last years. For the purposes of this work it is not necessary to enter into details, however it may be interesting to report some of those papers: [1.16], [1.17] and [1.18].

1.2.1.2 Electric energy

More up-to-date and specifically referred to "natural" biomass (thus excluding municipal solid waste) data are available concerning electricity generation, even because it is simpler to carry out statistical analyses in this field.

According to the GSE (former Gestore dei Servizi Elettrici, now Gestore dei Servizi Energetici), in 2008 the installed capacity in Italy was 936 MW_{el} [1.19], whereas the whole net capacity of the country was technically 98.6 GW_{el}, the available capacity was 63.5 GW_{el} and the peak demand was 55.3 GW_{el} [1.20]. The annual energy production from biomass was 4410 GWh_{el}, i.e. 1.4% of the total (319 TWh_{el}). In particular, power and energy generation were shared among the different biomass types as follows (as one can see, solid biomass represents the most important contribution):

- solid biomass: 449 MW_{el} – 2746 GWh_{el}
- biogas: 366 MW_{el} – 1599 GWh_{el}
- liquid biofuel: 121 MW_{el} – 65 GWh_{el}

For completeness, it must be said that waste-fired power plants had a capacity of 619 MW_{el} and generated 3112 GWh_{el}.

Also in this case there are several assessments concerning potentiality and future perspectives of power generation from biomass. Forecasts made by the Italian Government in 1999 [1.21] indicated the aim of reaching an installed capacity of 2300 MW_{el} with biomass feeding, in addition to 800 MW_{el} fed by MSW, by the years 2008 ÷ 2012, but these goals are far from being achieved, above all the first one. In the cited 2005 Position Paper, the Italian Government has then formulated less ambitious programmes: the installed capacity of biomass power plants by 2020 is predicted to be 1615 MW_{el}, from which about 10500 GWh_{el} energy would derive. In detail, 1123 MW_{el}, giving 7300 GWh_{el}, should be referred to solid biomass, while 492 MW_{el}, giving 3200 GWh_{el}, should derive from biogas (bioliquids were not taken into account). In addition again 800 MW_{el} of MSW plants are calculated, with a production of 4000 GWh_{el}. Finally, in another research work [1.22], the theoretical capacity of power plants considering only solid biomass is fixed in 2618 MW_{el}.

Moreover, here it is important to note that such an evaluation is also dependent on the fact that the raw material can be shared differently among the different applications

(power or heat demand, transports, etc.) and results are strongly influenced by this choice. However, in conclusion, the installed capacity that could likely be reached in the near future can be roughly fixed at about 2000 MW_{el}, at least half of which from solid biomass: this value, even if in the next decade total available capacity is expected to grow up to about 90 GW_{el} [1.23], makes biomass an important option for power generation in Italy for the near future.

1.3 Biomass and its chains

1.3.1 The resource

The term biomass defines a broad category of compounds characterised by an organic matrix and produced by living organisms (vegetable or animal). In general biomass directly or indirectly originates from the process of photosynthesis and thus constitutes an important renewable energy source derived from the Sun. However, fossil fuels (coal, oil and natural gas), though they were formed in past eras starting from organic vegetable and animal matter, and their derivatives (such as plastics) are not considered biomass. The following materials are instead included in the definition:

- woody and herbaceous species deriving from agricultural crops and forestry;
- agricultural and forestry residues (straw, brushwood, barks, etc.);
- agro-industrial residues (rice husk, olive residues, bagasse, etc.);
- livestock residues (animal manure, etc.);
- organic fraction of municipal solid waste, also called humid fraction[3].

As one can see, most of these species has vegetable origin and also concerning livestock residues, it must be noted that vegetables are the basic element of animal feeding.
Some examples of biomass are shown in Figure 1.8.

[3] As discussed above, this point is often the base of the different criteria adopted in conducting statistical surveys: sometimes it is not possible to distinguish between organic and inorganic fraction of MSW, and so it is taken into account on the whole; in other cases also the humid fraction is considered separately and so a distinction between natural biomass and waste is made.

Figure 1.8 – Some examples of biomass.

Depending on its origin, biomass can also be classified in:

- residual biomass;
- biomass derived from dedicated energy crops.

Residues and waste matter of agricultural, agro-industrial and forestry origin obviously fall within the first case, together with the humid fraction of MSW. Energy recovery from residual biomass is doubly advantageous because on one hand it reduces dependence from fossil fuels and on the other hand it alleviates environmental problems related to their disposal and to methane emissions that occur in their degradation process (it must be remembered that methane is twentyfold more powerful than carbon dioxide as a greenhouse gas).

Dedicated energy crops can additionally be divided into:

- oleaginous crops (rape, soy, sunflower, etc.), from which vegetable oils and biodiesel are produced;
- alcoholigen crops (sugarcane, sorghum, beet, etc.), used to produce bioethanol;
- lignocellulosic crops (that include woody perennial species like poplar, black locust, etc. and perennial or annual herbaceous species like miscanthus etc.), dedicated to solid fuel production.

Several reasons at environmental, economic and social level can be found to explain why biomass is so widely used for energy production and why its importance can become greater and greater in the near future. In particular, beside CO_2-neutrality that is common to all renewable energies, its main advantages are listed below:

1. it is an abundant resource and widespread almost all over the world;
2. it can be accumulated, and then used when necessary, thus solving or at least limiting the supplying uncertainty that is typical of the other renewable energies;

3. it can be converted in solid, liquid or gaseous fuels and then utilised through a combustion process – coupled with well known technologies, tailored to the purpose (steam cycles, reciprocating engines, turbines, etc.) – that allows not only power but also heat production (while the other renewable energies are mostly used only for power generation);
4. it allows the exploitation of unemployed areas with dedicated crops or the conversion of agricultural lands, generating positive occupational implications.

It is important to note that an energy source is considered renewable if it is naturally replenished at a rate that is greater or at least equal to the consumption one. Hence for an environmentally sustainable utilisation of biomass, it is necessary to couple the collection of natural material with a following process of reinstatement (reforestation, etc.) and not to just collect (as indeed occurs in many parts of Earth).

On the other hand, biomass is penalised by some disadvantages (that, however, are not likely to affect the whole attractiveness of the resource):

1. it has low energy density, both in terms of lower heating value (LHV), that for dry solid biomass is about 15 ÷ 20 MJ/kg (versus 42 MJ/kg of oil and 50 MJ/kg of methane) and, more in general, in terms of land productivity, since wide areas are required to produce significant quantities of raw material (typical values are 15 ÷ 25 t/ha per year);
2. due to the previous point, logistics (concerning transport, storage and handling) is complex and expensive;
3. production is generally not constant during the year and it is strongly dependent on weather and environmental conditions;
4. production is not cost-free, because crops need irrigation and fertilisers (a similar concept is valid for livestock holdings).

In particular, the first point is a key factor for biomass power plants and must be discussed. In fact it can be calculated that 1 MW_{el}-size plants consume about 5000 t of dry raw material per year: this implies that, considering the above mentioned values of land productivity, a cultivated area of 200 ÷ 350 ha is required, but due to the presence of other crops or urban territories, the area actually interested is much wider (at least ten fold). Moreover, this is valid for dedicated crops: the evaluation is still more onerous if residues are used. Therefore it is easy to understand that it is difficult to supply large

quantities of raw material, which is then made more complex by the strong incidence of logistics. Consequences are obvious: first of all plant sizes are limited (maximum $50 \div 60$ MW_{el}) and secondly, in general, supplying and logistics optimisation occurs on small scales[4]. These considerations make biomass exploitation particularly interesting in this last case, which moreover involves higher possibility of performing a cogenerative waste heat recovery and very low environmental impact of the installations.

1.3.2 Photosynthesis

Biomass chemical energy directly derives from solar energy via the photosynthesis process, so that biomass actually constitutes a sophisticated storage form of the energy sent by the Sun to Earth. Synthetically, by means of the chlorophyll, that is the green pigment of leaves, solar radiation activates a chemical conversion mechanism that involves carbon dioxide present in the air and water absorbed from the ground through the roots (or even absorbed from the air itself), generating organic compounds, afterwards forming the plant structure, and oxygen, being freed in air. As the organic compound originally being synthesised is glucose ($C_6H_{12}O_6$), photosynthesis can be schematised with the following elementary reaction:

$$6\ CO_2 + 6\ H_2O + \text{energy} \rightarrow C_6H_{12}O_6 + 6\ O_2 \qquad (1.1)$$

Glucose is then converted into complex molecules (such as cellulose, lignin, proteins, etc.), each one with a specific function in the plant. The reaction is made possible by the catalysing action of some substances absorbed by the roots, such as nitrogen, potassium, chlorine, etc., that can be naturally present in the ground or, in case, artificially added with appropriate fertilisers and that are then partly found in the raw material after the collection. Roughly, one can think that the growth of a cubic metre of vegetable matter is related to the absorption of a ton of carbon dioxide, of which 250 kg are stored as wood carbon while 750 kg are released as oxygen in the atmosphere [1.24].

[4] Moreover, basing on what said, the concept itself of small, medium and large scale must be redefined for biomass plants in respect to fossil fuel ones: in general "small scale" is used if capacity is lower than 1 MW_{el}, "medium scale" if it is in the range $1 \div 5$ MW_{el}, "large scale" if it is higher than 5 MW_{el}.

At the end of their life cycle, vegetables return the energy and the substances previously stored. This can happen by natural decomposition (also called cold combustion), a slow and unusable process, or by an actual combustion, where the energy is rapidly released by the oxidation process and then employed for useful purposes. In both cases the chemical reaction is however the same and is the exact opposite of (1.1):

$$C_6H_{12}O_6 + 6\ O_2 \rightarrow 6\ CO_2 + 6\ H_2O + \text{energy} \qquad (1.2)$$

In this process the oxygen produced during photosynthesis is consumed, while carbon dioxide and water, that were previously the reactants, are now released. Therefore the whole process is a sort of closed cycle, with globally no emissions of carbon dioxide, thus proving CO_2-neutrality of biomass. Naturally, this cannot be considered completely true because one has to take into account the primary energy consumption (and the consequent emissions) related to collection, transport and conversion phases. Indeed, this point is common to all renewable energies (e.g. production and installation of photovoltaic panels, wind turbines, etc.).

Photosynthetic process is quite inefficient, in terms of chemical energy fixed in biomass (and then available as lower heating value) compared to the incident solar radiation. Firstly, only visible fraction of sunlight (the one having wavelength included in the range 0.4 ÷ 0.7 μm), that represents about half of the total, is effective for photosynthesis. Part is then reflected by the leaf or passes through it or is transmitted to it in the form of heat, thus determining that just 40% of solar radiation is actually available for the process. In particular, red and blue fractions of the light are mostly absorbed, while the green one is mainly reflected, thus giving the leaves their characteristic colour. Then obviously the process is not ideal, but presents a thermodynamic efficiency that is typically around 30%. Finally, part of the energy thus produced (about 40%) is used for the internal metabolism of the plant, so that maximum theoretical efficiency is limited to 7% (moreover, this is valid only for the most efficient plants, otherwise it can be equal to the half, or even less). Due to imperfect conditions in terms of light, temperature, water and feeding availability, real efficiencies are then much lower and typically settle at 0.15 ÷ 0.50%. Table 1.2 summarises the progressive contributions of these loss factors and the achievable efficiencies.

Process/factor	Progressive percentage energy losses
Solar radiation out of effective spectrum	50%
Reflection, transmission, crossover	10%
Photosynthesis process losses	28%
Plant metabolism need	5%
Total energy losses	**93%**
Maximum theoretical efficiency	**7%**
Average real efficiency	**0.15 ÷ 0.50%**

Table 1.2 – Photosynthesis energy losses and efficiencies (adapted from [1.25]).

Despite this poor performance and even considering that biomass is obviously not present on the entire global surface, since Earth every year receives a huge amount of energy by the Sun (about 92,000 Gtoe, net of reflection, that would correspond to eight thousand times world primary energy needs – see figure 1.2), in this period about 200 billion tons of CO_2 are fixed in biomass through photosynthesis: the equivalent energy is about 72 Gtoe, that is still six times higher than the annual world primary energy consumption. Of course this is a theoretical potential that cannot be completely exploited, as easily inferable from the values shown in Section 1.2 [1.8].

1.3.3 Conversion principles and chains

There are several methods that allow the conversion of biomass into energy, but as general concept it is always at first transformed in an easily manageable form (solid, liquid or gaseous) and then used for different purposes.

Biomass composition strongly influences the choice of the conversion process. In particular two factors are decisive in this sense: water content (i.e. moisture) and carbon-nitrogen content ratio (C/N). If the former is lower than 30% and the latter is greater than 30, thermochemical processes, in which heat exchanges are strongly involved, are more suitable; on the other hand, if moisture is higher than 30% and C/N ratio is lower than 30, biochemical process (in which biological species, such as bacteria, take part) are preferred. If then biomass is rich of oils (that for the most used seeds can reach 35 ÷ 50% of the total composition), chemical-physical processes are

used: the aim is to extract raw vegetable oils, that afterwards are, in case, subject to chemical transformation to biodiesel by esterification. Processes of peeling, compaction, etc. that involve solid biomass to facilitate its transport, storage and utilisation fall in this category too.

Basing on these considerations, according to the biomass characteristics and the desired end use, different chains can be developed, as summarised in Figure 1.9.

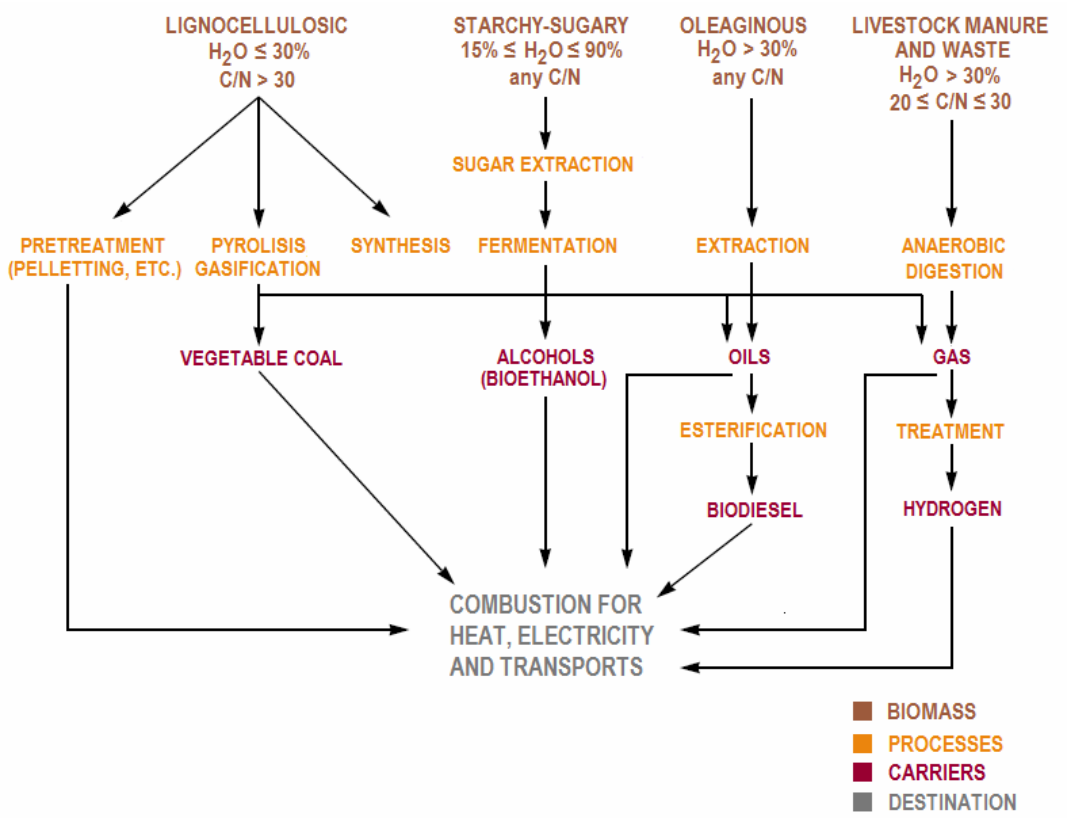

Figure 1.9 – Main biomass chains for energy conversion (adapted from [1.26]).

As already indirectly mentioned in Section 1.2, there are then three main end uses:

1. power generation;
2. heat generation;
3. fuel production for transports (essentially liquid).

In this work, focus has been put on the first point, i.e. power generation. Really all considered plants are CHP type, in the perspective of overall thermodynamic optimisation, so that low-temperature thermal production using waste heat was taken

into account. However systems specifically dedicated to heat generation, like for instance domestic boilers, have not been considered.

Besides, lignocellulosic biomass (and, signally, woody one) was chosen as reference fuel for the simulated plants. This because liquid biofuels (bioethanol and biodiesel) are mainly used for transports, and so starchy, sugary and oleaginous plants, from which they are produced by alcoholic fermentation and oil esterification, can be neglected in this work (even if, in general, these fuels can be used for power or heat generation too). Biogas produced by anaerobic digestion starting from livestock manure, as well as from humid fraction of municipal solid waste, is instead used for power (or CHP) generation, but this represents a quite specific and limited chain, while woody biomass is the most abundant and available type, and its chain is thus the most relevant.

As visible in Figure 1.9 and as discussed hereinafter, lignocellulosic biomass has an high carbon and a low nitrogen content, so that C/N ratio is typically much greater than 30, and a limited moisture level (in case, it can be easily reduced under 30% if starting value is higher): this implies that the most suitable conversion processes are the thermochemical ones. These will be fully described in Section 1.5, after discussing woody biomass properties. For completeness, instead the most important biochemical and physical-chemical processes are here briefly presented (see ref. [1.25]).

1.3.3.1 Alcoholic fermentation

Alcoholic fermentation is a micro-aerophyl process that operates a transformation of carbohydrates in ethylic alcohol (C_2H_5OH), that is thus called bioethanol, according to the following elementary reaction:

$$C_6H_{12}O_6 \rightarrow 2\ C_2H_5OH + 2\ CO_2 \qquad (1.3)$$

Hence this process is applied to sugary materials, like sugarcane, beet, some fruits, etc. and to starchy ones, like corn, barley, potato, etc. Alternatively bioethanol can be produced from lignocellulosic biomass, like straw or wood waste: in this case the material is hydrolysed by treatment with sulphuric acid in order to produce sugars, that are then subject to fermentation adopting genetically modified bacterial floras.

Bioethanol can be used in spark ignition (SI) internal combustion engines as gasoline additive up to 15% without requiring any modifications to the engine, or it can be combined with isobutene to produce ETBE (Ethyl-Tertiary-Butyl-Ether), which is currently done in Brazil, where this has become the only fuel, replacing gasoline.

1.3.3.2 Vegetable oil esterification

Biodiesel production is based on the reaction of transesterification (also called alcoholysis), where a vegetable oil, derived by pressing oleaginous plants seeds (sunflower, rape, soy, palm, etc.), reacts with an excess of methyl alcohol (methanol, CH_3OH) in the presence of a catalyst. The reaction can be summarised as follows:

$$\text{Oil} + 3\ CH_3OH \leftrightarrow \text{Methyl ester} + \text{Glycerine} \qquad (1.4)$$

Beside the methyl ester, that is the biodiesel, there is then also a production of glycerol, that must be gradually removed, because it is partly soluble in the reaction mixture. However the removed glycerine has a high economic value, considering its applications in cosmetics and in the pharmaceutical industry, and so it can be sold generating an additional return.
Reaction temperature depends on the catalyst nature: the most common solution is the use of alkaline catalysts (such as caustic soda or potassium hydroxide), that lets the reaction take place at ambient temperature, but it is also possible to adopt acid catalysts (like sulphuric or hydrochloric acid), that however require a temperature above 100°C.

1.3.3.3 Anaerobic digestion

Anaerobic digestion is a biological process where organic matter is broken down by some pathogenic bacteria in the absence of oxygen (hence the name). The product is the so called biogas, constituted by methane (50 ÷ 80%) and carbon dioxide. Given its composition, it is an excellent gas for combustion purposes, since it has a high lower heating value, that obviously depends on the CH_4/CO_2 ratio, typically varying in the

range 17 ÷ 29 MJ/Nm^3, and it has no dangerous contents (syngas obtained from gasification, instead, has not these good properties, as will be shown in Section 1.5.3).
As already said, this technique is typically applied to livestock manure or, more in general, to organic residues. As the starting fuel is waste material, that otherwise would be destined for disposal, economic and ecologic benefits of this process are indeed clear. Additionally, the resulting matter of the process is an excellent fertiliser because nitrogen, that could have been lost in the form of ammonia, is present in fixed form and hence is directly usable by plants.

1.3.3.4 Aerobic digestion

Aerobic digestion is a biochemical process, suitably applied in farms or livestock holdings, effected by micro-organisms whose proliferation, differently from anaerobic one, is allowed by the presence of oxygen. These bacteria metabolise organic matter, converting complex substances into simpler compounds, freeing carbon dioxide and water and thus heating the substrate (the lowering biomass layer that has not been digested yet). The generated thermal power can then be recovered by means of a fluid exchanger and used for heating purposes. As for anaerobic digestion, there are the additional advantages related to the reduction of residues, that would be brought to landfill, and to the production of compost; indeed, these are the real main aims of aerobic digestion, since the application is quite poor in terms of energy production (low-temperature heat against high quality biogas in the anaerobic process).

1.4 Woody biomass properties

In this section, chemical, physical and energy properties of woody biomass are presented. However, firstly it must be noticed that the resource can be supplied in different ways and typically:

- directly from coppice, in the perspective of a good forest management;
- adopting the so called Short Rotation Forestry (SFR), a modern cultivation technique that aims at the production of wood specifically for energy purposes,

optimising the efficiency both in spatial and temporal terms, i.e. maximising the density per cultivated hectare and reducing the biomass collection cycle to one or two years;

- using waste products of wood industry (sawmills, furniture factories, etc.).

The latter point, a part from being obviously convenient in global terms, is particularly suitable in the Italian context, where there are several wood industry districts (especially in the northern part of the country) and where it is then possible a coordinated exploitation of the resource (see for instance ref. [1.27]).

1.4.1 Chemical properties

As already said, woody biomass belongs to lignocellulosic species: this because its main constituents are cellulose, hemicellulose and lignin.

Cellulose is a complex polysaccharide, composed by glucose molecules (in number of 500 ÷ 1500) bounded together to form a long linear chain. The resulting chemical formula is $(C_6H_{10}O_5)_n$. It is the main component of the cell wall in all vegetable cells, giving strength to the plant, and it represents about 40 ÷ 50% of the wood.

Hemicellulose is a polysaccharide with a low molecular weight, constituting 10 ÷ 20% of wood, that is present in plant cell walls, in the spaces let free by cellulose. While the latter is crystalline, strong, and resistant to hydrolysis, hemicellulose has a random, amorphous structure with little strength and is easily hydrolysable.

Lignin is the component that differentiates wood from the other vegetable organisms and represents the remaining 20 ÷ 40%. It is constituted by a mixture of low molecular weight phenolic polymers. Its main functions are to provide rigidity to the cell walls and to allow the connection between the cells of the wood, creating a material highly resistant to impact, compression and bending.

In addition to these three main elements, in wood there are several others components: organic (like resin, rubber, fats, etc.), present in lumen and cell wall, and inorganic (like calcium, magnesium, sodium salts), that can be found in ashes after the combustion.

These considerations are valid in general for all wood types, but it is obvious that different species have different (though similar) specific composition. Generally this information is provided with two criteria: proximate and ultimate analyses. Proximate

analysis is a more immediate evaluation that distinguishes between volatile matter (VM, the part of biomass that is released as gas during a heating process) and fixed carbon (FC, the part that in the same process remains as solid char), only. On the other hand, ultimate analysis gives the elemental composition of biomass, thus indicating, independently from their form, the quantity of carbon, oxygen and hydrogen (the main components) and, normally, of nitrogen, sulphur and chlorine. Both of the analyses, however, consider moisture and ash separately. Compositions of some woody biomass types on dry basis (db), thus neglecting moisture, are presented in Table 1.3.

Name	FC	VM	Ash	C	H	O	N	S
Beech	24.15	75.20	0.65	51.64	6.26	41.45	0.00	0.00
Black Locust	18.26	80.94	0.80	50.96	5.71	41.95	0.57	0.01
Douglas Fir	17.70	81.50	0.80	52.30	6.30	40.50	0.10	0.00
Ponderosa Pine	17.17	82.54	0.29	49.27	5.99	44.36	0.06	0.03
Poplar	14.74	84.61	0.65	51.64	6.26	41.45	0.00	0.00
Red Alder	12.50	87.10	0.40	49.56	6.06	43.78	0.13	0.07
Redwood	16.10	83.50	0.40	53.30	5.90	40.30	0.10	0.00
Western Hemlock	14.20	83.80	2.00	50.90	5.80	41.10	0.10	0.10
Yellow Pine	15.45	83.24	1.31	51.59	7.00	40.10	0.00	0.00
White Fir	16.58	83.17	0.25	49.00	5.98	44.71	0.05	0.01
White Oak	17.20	81.28	1.52	49.61	5.38	43.13	0.35	0.01
Madrone	12.00	87.80	0.20	48.94	6.03	44.76	0.05	0.02
Mango Wood	11.38	85.64	2.98	46.24	6.08	44.42	0.28	0.00

Table 1.3 – Composition of some woody biomass types (% w/w, db) ([1.28] and [TF]).

As one can see, volatile matter is largely prevalent, as it represents about 75 ÷ 87% of the total, while fixed carbon seldom exceeds 20%, as well as ash is typically limited to 0.5 ÷ 1.5% (the value rises to about 5 ÷ 8% in the bark). Also ultimate composition is very constant: carbon percentage is always around 50%, oxygen is slightly above 40% while hydrogen is limited in the range 5 ÷ 7%. Finally, nitrogen and sulphur are present in very small quantities (chlorine datum would be analogous to sulphur one), which is a positive point as regards emissions. Therefore biomass is quite different from coal, that is instead characterised by low volatile matter (normally not higher than 40%) and high ash (even more than 10%) and sulphur (up to 5%) contents.

1.4.2 Physical properties

Moisture and density are wood physical features having a relevance on conversion processes. In particular, the former is a factor of paramount importance, because it also influences chemical and energy characteristics of biomass, and the density itself.
Moisture indicates the water content (both in free or bound form) in the wood, which can be evaluated both on dry (1.5) or wet basis, wb (1.6), the latter being largely more used (unless otherwise specified, this expression will be considered henceforth):

$$h_{dry} = \frac{m_{tot} - m_{dry}}{m_{dry}} \cdot 100 \quad (\%) \tag{1.5}$$

$$h_{wet} = \frac{m_{tot} - m_{dry}}{m_{tot}} \cdot 100 \quad (\%) \tag{1.6}$$

where m_{tot} represents the total mass, thus including moisture, m_{dry} is the mass of the dry substance, while the difference between the two indicates the moisture mass, obviously.
Moisture in wood is variable: it can have different values after felling depending on species, age, part of the tree and season. Generally it is lower in broad-leaved plants rather than in conifers, in the bottom parts of the plant rather than in the top ones and in summer rather than in winter. However, typical values are about 40 ÷ 50%. If then biomass is subject to a natural drying in air (seasoning), moisture can decrease below 20% (complete removal, instead, is possible only by artificial way). The influence of moisture on energy performance is being discussed in the next section.
Density is an important parameter too, since it expresses the quantity of mass in the unit of volume: obviously it is more advantageous if, given a certain volume (and thus a certain burden in terms of logistics), the mass there included is higher. In fact this implies a greater LHV per unit of volume and thus a lower relative incidence of transport, storage and handling in the economy of the chain. For these reasons, many compaction treatments have been developed to increase feedstock density, signally dedicated to wood residues having small granulometry (wood shaving, sawdust, etc.): the most important ones are pelleting (pellets are small cylinders of 5 ÷ 10 mm diameter

and 20 ÷ 40 mm length) and briquetting (briquettes are blocks having parallelepiped or cylinder shape with dimensions in the range 50 ÷ 300 mm). Apart from high energy density, stability and uniformity of the shape, these densified products are also characterised by low moisture percentage (lower than 10%, thanks to artificial drying treatments). Obviously, compaction processes are not applied to big wood pieces. However, in order to make the composition more homogeneous, these materials are normally subject to chipping, that is a mechanical operation reducing different size wood stocks in small chips (thus the name). This is a very important operation, as biomass dimensional homogeneity is vital for combustion efficiency.

1.4.3 Energy properties

From an energy point of view, the most important feature of a fuel is its heating value, that quantifies the heat generated by complete combustion of a unit mass of the material. As well known, a distinction is made between lower and higher heating value (LHV and HHV), depending on whether the latent heat of condensation of the water vapour produced in the combustion process is recovered (HHV) or not (LHV). HHV is mostly used in America, while LHV is preferred in Europe: actually in most cases water is discharged in atmosphere with flue gases in vapour phase, so LHV is more proper (and is always used in this work). For completeness, the relationship between these two parameters is presented:

$$LHV_{dry} = HHV_{dry} - 9 \cdot H \cdot q \qquad (1.7)$$

where H is the hydrogen content in the dry biomass (5 ÷ 7%, as mentioned before) and q is water condensation heat, that is equal to 2.4 MJ/kg; the subscript dry obviously indicates that the values are referred to dry basis, while the factor 9 relates to the fact that the produced water quantity is nine times higher than the hydrogen content. It must be noted that, precisely because discussion has been done on dry basis, here water vapour is only related to the presence of hydrogen in the structure of the fuel, that gives water in the combustion process, and is not associated to the moisture content: thus the formula. The difference between HHV and LHV is typically equal to 1 ÷ 1.5 MJ/kg.

Lower heating value strongly depends, as obvious, on chemical composition of biomass: in particular high carbon and hydrogen contents will result in higher LHV, while high oxygen, ash and nitrogen contents will determine an opposite effect. Nevertheless, as woody biomass composition is rather constant in the different species (see Table 1.3), lower heating value varies in a very limited range, that is about 18 ÷ 20 MJ/kg (hence HHV_{dry} results 19 ÷ 21.5 MJ/kg).

Then the real parameter that strongly influences the lower heating value is moisture, that works in two ways: firstly its simple physical presence determines a diminishing fuel ratio on the total mass and secondly, as mentioned before, there are energy losses due to the latent evaporation heat that is absorbed by water during the combustion process and is not being recovered later. The actual LHV is then calculated starting from LHV_{dry} as follows:

$$LHV = (1 - h) \cdot LHV_{dry} - h \cdot q = LHV_{dry} - h \cdot (LHV_{dry} + q) \qquad (1.8)$$

where h is moisture (on wet basis, naturally). The relation shows that real LHV, thus the energy actually recoverable from a combustion process, linearly decreases with increasing moisture and falls to zero with h ≅ 88 ÷ 90% (Figure 1.10).

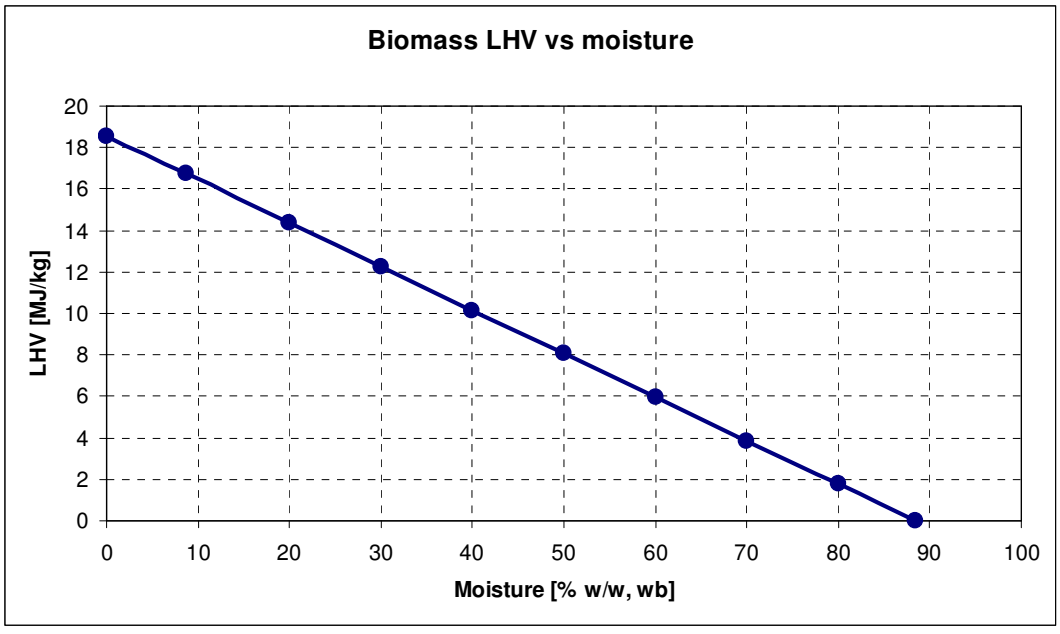

Figure 1.10 – Biomass LHV variation with moisture (own elaboration based on [TF]).

Table 1.4 shows lower heating value of some woody biomass species at different moisture levels (in case indicated in brackets). In particular conifers have a higher LHV than broad-leaved plants, because their resins have a greater lignin content. LHV of other fuels is also provided for comparison purposes: in particular, wheat-straw, representing lignocellulosic non woody biomass (however, both of them generally have very similar characteristics), and some fossil fuels.

Energy source	LHV [kJ/kg]
Broad-leaved plants (20%)	14,200
Broad-leaved plants (dry)	19,000
Conifers (20%)	14,900
Conifers (dry)	20,000
Wheat-straw (10%)	15,500
Coal (10%)	27,200
Oil	41,860
Diesel	41,860
Butane	45,600
Methane	50,200 (35,000 kJ/Nm^3)

Table 1.4 – LHV of some fuels (adapted from [1.29]).

1.5 Woody biomass conversion technologies

As already discussed, woody biomass is mainly exploited via thermochemical processes, where it is essentially burnt, either directly (combustion) or after a prior chemical conversion (pyrolysis or gasification). Only direct combustion and gasification have been taken into account in this work, while pyrolysis, the less mature technology, has been neglected (nevertheless, it will be briefly described).

Actually, these three phenomena can take place within the same process (pyrolysis and gasification are always intermediate phases of combustion, as well as pyrolysis and combustion occur in gasification), thus it is rather difficult to describe them separately. However, one can roughly say that these processes have different main purposes: to burn a solid fuel for combustion; to produce a liquid fuel for pyrolysis; to get a gaseous fuel for gasification (obviously both of the latter are afterwards burnt).

1.5.1 Combustion

Combustion is a complex exothermic oxidation reaction, where carbon and hydrogen contained in the fuel react with oxygen, producing carbon dioxide and water and releasing energy in the form of heat, as already shown in (1.2) equation.
The whole process occurs essentially in three stages (Figure 1.11), that can overlap in the combustion site, especially for large biomass particles:

1. drying;
2. thermal degradation (pyrolysis/gasification);
3. actual combustion (oxidation).

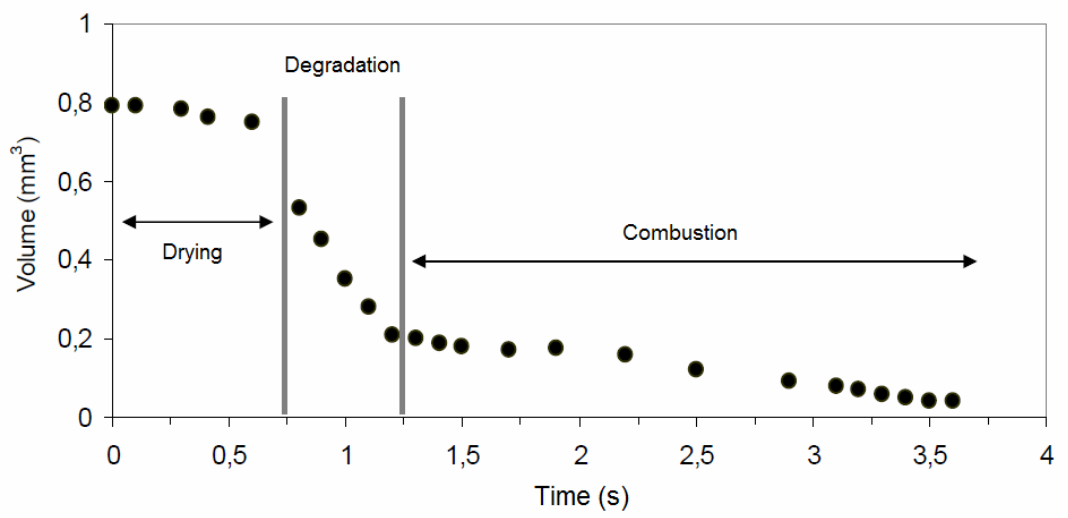

Figure 1.11 – Stages of the combustion of a small wood particle (adapted from [1.30]).

During the first phase, wood is being heated and moisture is being converted into vapour. The latter phenomenon already occurs before 100°C. Since vaporisation uses energy released from the combustion reaction itself, it determines a diminishing temperature in the combustion chamber, which slows down the combustion process. Indeed, if in Section 1.4.3 it has been shown that LHV wipes out with moisture levels around 90%, combustion cannot take place anymore when this exceeds 65 ÷ 70% already, because wet wood requires so much energy to evaporate water and then to heat vapour, that temperature is reduced below the minimum level to sustain the process (practically 60% is the maximum value found in real applications).

The second stage starts at 200°C, when wood begins to be subject to thermal degradation that leads to the evaporation of its volatile components (devolatilisation). As already shown in Table 1.3, this matter represents more than 75% of the total weight of biomass, so combustion will mostly occur in gaseous phase. As one can observe in Figure 1.12, the first component of the wood that undergoes the degradation is hemicellulose (300°C), followed by cellulose (325 ÷ 375°C). In this first phase, devolatilisation rate increases as temperature rises; thereafter, at around 400°C, most of the volatile matter has been freed and the process rate decreases rapidly. However, a low volatilisation is still observed in the temperature range 400 ÷ 500°C because of the lignin decomposition, that actually occurs throughout the whole temperature range, but is here more relevant in terms of weight loss.

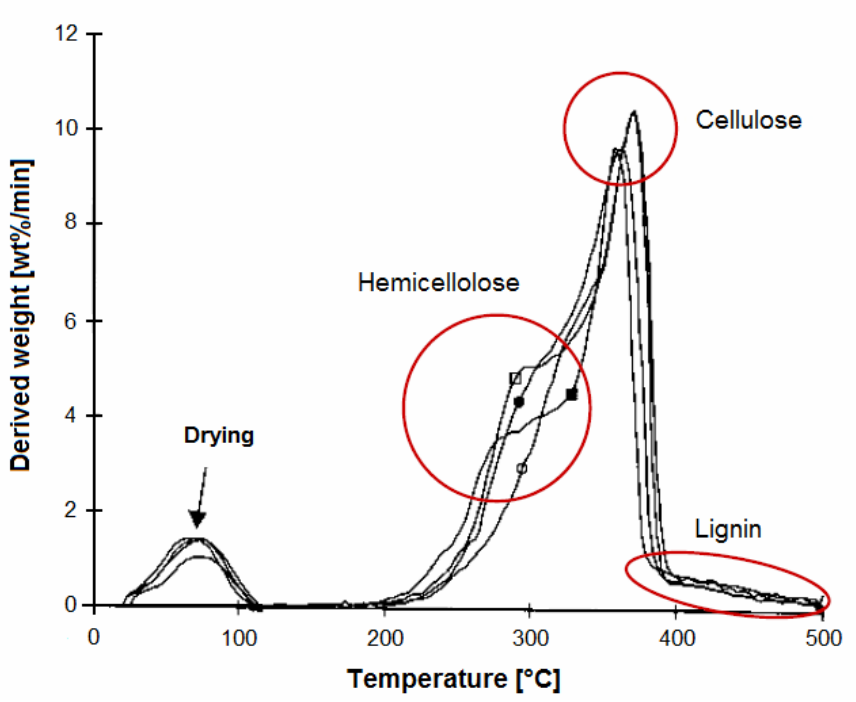

Figure 1.12 – Devolatilisation rate as a function of temperature (adapted from [1.30]).

Finally, combustion, i.e. complete oxidation of the resulting solid, liquid and gaseous matter, can take place. In particular, gas combustion begins at about 500 ÷ 600°C and protracts to 1000°C; in the range 800 ÷ 900°C solid char (composed by a carbonaceous residue and inorganic ash) and tars are burnt.

1.5.1.1 Combustion devices

From a conceptual point of view, combustion systems fed by biomass are not different from those fed by conventional fuels, being constituted by a burner or combustion chamber, where biomass is burnt, followed by a recovery section, where the generated heat is transferred to a fluid (water, thermal oil, air, etc.). On the other hand burning biomass naturally involves specific issues that must be considered in furnace design.

There are three main combustion technologies (in addition to a great number of innovative solutions under investigation), summarised in Figure 1.13:

- fixed bed (essentially grate furnaces);
- fluidised bed (bubbling or circulating);
- pulverised biomass combustion.

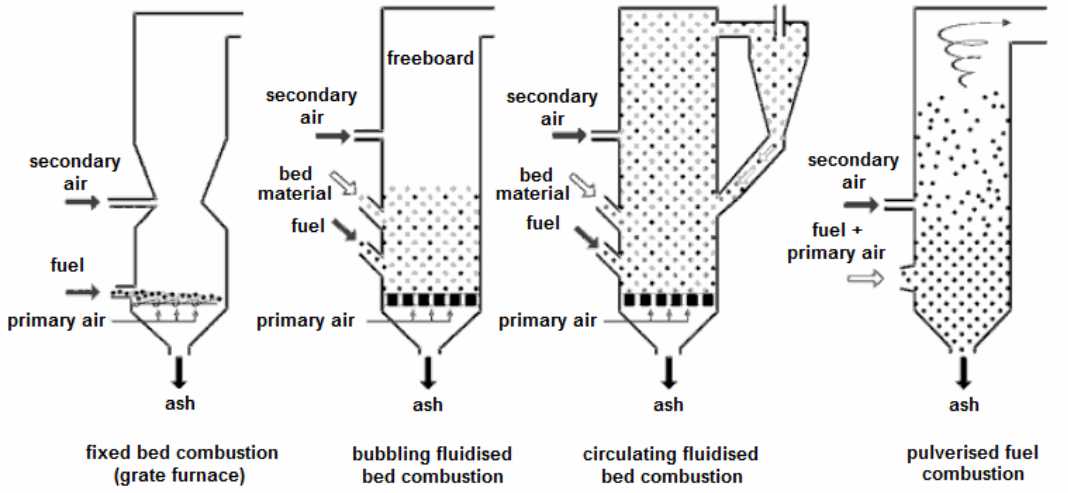

Figure 1.13 – Biomass combustion technologies [1.30].

In **fixed bed furnaces** (the most common case) primary air passes through a fixed biomass bed, lying on a grate (air or water-cooled), where drying, gasification and solid char combustion take place, while gases are burnt, after secondary air injection, in an upper zone. Classification is normally based on the movement of the grate, that can be fixed, moving, travelling, rotating or vibrating. These systems are quite flexible, in fact they allow the use of different type of woody biomass, having variable dimensions and high moisture and ash content. It is necessary to distribute biomass homogeneously on

the grate, in order to well adjust primary air injection: if this is done, they can work efficiently also at part load (down to 25% of the design point), right thanks to primary air injection control. Fixed grate is mostly used when the desired thermal power is lower than 500 kW_{th}, while moving grate, with its different versions, is more suitable above this value (up to some thermal megawatts).

For larger scales, i.e. tens of megawatts, **fluidised bed furnaces** are instead more efficient. In these plants grate is no more necessary because the bed (formed by biomass and a refractory, typically sand, the latter having the aim of homogenising heat distribution) is kept in suspension by primary air that is insufflated from the bottom. This involves a better mixing of fuel and air, and thus a better combustion quality and a lower production of unburnt. Moreover, this determines the possibility to provide a lower excess air (the air quantity percentage exceeding the stoichiometric need), that can be limited to 10 ÷ 20% for circulating beds (for fixed bed at least 30 ÷ 40% is required, but values up to 100% can also occur). Fluidised bed furnaces are flexible in terms of different fuel types input, but are quite rigid concerning biomass size and part load operation. They can operate at ambient pressure or be pressurised (up to 25 bar). Temperature is limited to 800°C (in fixed bed plant it can be 100 ÷ 200°C higher) to avoid bed sintering: this can be achieved with heat exchangers, gas recirculation or water injection. Moreover, this fact has positive effects on NO_x production. In bubbling type devices, the bed is kept in suspension but not in a turbulent condition (primary air velocity is the minimum required to keep the bed fluidised, i.e. 1 ÷ 3 m/s), while in circulating type ones, thanks to higher air velocity (5 ÷ 10 m/s) and lower bed particle size, sand and biomass are dragged out with hot gases, separated in cyclones and the re-injected in the bed: the higher turbulence in the bed involves a better heat exchange and a more uniform temperature, and thus a higher efficiency, but costs are higher as well.

In **pulverised biomass furnaces** (sawdust, wood shavings, etc.), where peak temperature are much higher (up to 1500°C), the solid fuel is pneumatically injected into the device through the primary combustion air. Obviously biomass particles must be very small (smaller than 10 mm, and preferably than 2 mm), thus gasification and char combustion occur very quickly, while gases are afterwards burnt by the secondary air. A low moisture content (lower than 20%) is also required. Typically the air/fuel mix is injected tangentially in the cylindrical furnace in order to obtain a vortex flow that

facilitates the process (although this determines the erosion of the furnace walls). However, biomass dust is mostly used as additional fuel (5 ÷ 10%) in coal-fed plants, in order to exploit the resource in more efficient and already existing plants, that besides thus become partially renewable (this is the so called co-combustion).

1.5.1.2 Emissions

When a combustion process takes place, pollutant emissions are released together with thermal energy. Several factors influence their production (heat transfer mechanism, air excess, moisture level, thermal inertia, etc.) but, of course, biomass composition is the most relevant point. The effects of the various elements present in the biomass are briefly discussed in this section, while a deeper analysis of polluting substances of syngas from gasification will follow afterwards, together with the description of the abatement technologies (which indeed are analogous in both cases).

As shown in Section 1.4.1, apart from carbon, oxygen and hydrogen, the main components of biomass are nitrogen, chlorine, sulphur and ash: pollutants are mostly formed starting from them[5].

Nitrogen compounds generated during combustion are mainly NO_x, harmful for human health because they determine ozone destruction and several diseases (affecting blood, lungs). When temperatures are limited to 800 ÷ 1100°C, like for biomass combustion, NO_x are mainly formed starting from the nitrogen contained in the fuel (fuel NO_x), that therefore must preferably be present in small quantities[6].

Chlorine vaporises almost completely during combustion, forming on one hand Cl_2 and HCl, discharged in gaseous form at the stake, with possible formation of dioxins and furans (carcinogens compounds) and on the other hand alkali chlorides which condensate, with diminishing temperature, on the surface of volatile ash particles (fly-ash) and of the exchangers, having corrosive effects. Dioxins and furans formation takes

[5] In addition, all the compounds produced as a result of a potential incomplete combustion, such as CO, soot, etc., should obviously be taken into account.

[6] Instead, when flame temperature is higher, like for pulverised biomass or fossil fuels (in the latter case it can even reach 2000°C), the dissociation of air nitrogen takes place: it then reacts with oxygen supplying the largely most substantial contribution of NO_x (in this case called thermal NO_x).

place by means of a heterogeneous reaction on the surface of fly-ash particles in the presence of carbon and oxygen at temperatures included between 250 and 500°C: hence little quantities of fly-ash particles in the flue gases, as a result of a complete combustion, are decisive to limit their production, together with low air excess and low concentration of chlorine in the biomass input.

Sulphur is converted into SO_x and alkali sulphates during the combustion process. Similarly to what happens to chlorine with HCl, sulphur compounds mainly pass in vapour phase during the combustion and then, as gases get colder, condensate on the surface of fly-ash particles and pipes, generating corrosion phenomena.

Ash represents the non-aqueous solid residue of the combustion of a fuel, mainly composed by highly oxidised substances, having high melting and boiling points, such as ionic compounds of metals (especially carbonates and oxides). In general the most important issues in biomass combustors or boilers are:

- the formation of fused or partly-fused agglomerates and slag deposits at high temperatures within furnaces;
- the formation, on the other hand, of bonded ash deposits at lower temperatures on solid surfaces;
- the accelerated metal wastage of the furnace components, due to corrosion, erosion and abrasion phenomena related to ash deposits or particle impacts;
- the formation and emission of sub-micron aerosol and fumes.

Indeed, ash of woody biomass has a high melting point (> 1000°C), so these issues are less onerous compared with herbaceous one (whose ash can have a melting point lower than 700°C). However, in addition to the previous points, handling and subsequent utilisation or disposal of ash residues must be taken into account. In this sense, it is important to note that wood ash can be used as a fertiliser (after proper treatments).

Basing on particle size, ash is classified in the following three types:

- bottom-ash, the heaviest one, that remains on the grate or in the sand bed after the combustion (it represents about 60 ÷ 90% of the total ash);
- cyclone-ash, a lighter class, that is swept away by the gases but can easily be separated by inertial systems, like cyclones (10 ÷ 35%);
- fly-ash, the smallest fraction, that require more complex separation devices to be removed (2 ÷ 10%) [1.30].

1.5.2 Pyrolysis

Pyrolysis is a thermochemical process, mainly applied to lignocellulosic materials, consisting in a degradation of organic polymers and mineral substances of biomass obtained by means of heat supplied in absence of oxygen, at temperatures varying between 400°C and 800°C. The main product is normally considered the liquid phase (bio-oil), essentially composed of tars, oils and water, but solid char and a gaseous phase (a mixture of CO, CO_2, CH_4, etc.) are also produced. These products are then used in substitution of conventional fuel in many applications.

Indeed, operative conditions (above all in terms of temperature and reaction time) are fixed in order to regulate the mutual proportion of the products. As a general rule, increasing temperature and reducing residence time determine a gradual increase in the production of lighter phases. In fact in the so called slow pyrolysis (400 ÷ 500°C and very long reaction time, of the order of minutes) the production of charcoal is maximised (for this reason the process can be also called carbonisation), achieving 35% in weight, corresponding to 50% of energy content, with analogous proportion of the other two phases; in fast pyrolysis one can have a maximisation (even > 80% in weight) either of the liquid production, with temperatures ranging in 500 ÷ 650°C and reaction times equal to one or some seconds, or of the gaseous one, with temperatures higher than 700°C and faster reactions (less than one second: in this case the phenomenon is often called flash pyrolysis); finally, conventional pyrolysis leads, at temperature lower than 600°C and medium residence time (tens of seconds), to an intermediate composition, with a certain preponderance of the bio-oil (roughly 50% versus 25% of the other two phases).

1.5.3 Gasification

Gasification is a thermochemical process consisting in the conversion of solid or heavy liquid fuels (coal, biomass, tars) into gaseous ones, by means of a incomplete oxidation at high temperature (800 ÷ 1000°C) with a controlled substoichiometric amount of oxygen (pure or contained in air or steam): the equivalence ratio, i.e. the ratio of oxidant supplied to that required for complete combustion, is typically 0.25 ÷ 0.40.

High volatility, carbon reactivity, low content of sulphur and ash are all chemical properties that make biomass particularly suitable for gasification. In fact the process, compared to other materials (signally coal), can be conducted at lower temperature, taking less time and with fewer problems regarding emissions and corrosion of the reactor walls. On the other hand, biomass moisture and low energy density are two significant disadvantages.

Not much differently from combustion (indeed, as mentioned before, the processes often overlap), the gasification process is composed of four stages: drying, devolatilisation, solid char and volatile products partial oxidation and final reactions (mainly reduction type) among the gases previously given off. A scheme of the main reactions taking place in a gasifier is shown in Table 1.5.

Reactions	**Enthalpy of reaction [kJ/mol]**
Heterogeneous reactions	
Combustion	
$C + ½ O_2 \rightarrow CO$ (partial oxidation)	-110.6
$C + O_2 \rightarrow CO_2$ (total oxidation)	-393.7
Pyrolysis	
$4 C_nH_m \rightarrow m CH_4 + (4n – m) C$	exothermic
Gasification	
$C + CO_2 \rightarrow 2 CO$ (Boudouard)	158.7
$C + H_2O \rightarrow CO + H_2$ (carbon reforming)	131.4
$C + 2 H_2 \rightarrow CH_4$ (hydrogasification)	-74.9
Homogeneous reactions	
Gas-phase reactions	
$CO + H_2O \rightarrow CO_2 + H_2$ (water gas shift)	-40.9
$CO + 3 H_2 \rightarrow CH_4 + H_2O$ (methanation)	-206.3

Table 1.5 – Main reactions in a biomass gasification process (adapted from [1.29]).

As already mentioned, the main product of the process is a gaseous fuel, called syngas (sometimes product gas or producer gas[7]), although solid charcoal and liquid tars are also produced. Syngas is mainly composed of incomplete combustion products (above all CO, in addition light hydrocarbons, such as CH_4) and of H_2 and CO_2. However,

[7] In this case the gas is named syngas after the clean-up treatment only.

actual composition depends on several parameters: gasifier type, biomass type, working temperature, pressure and so on. Among these, one of the most important is the adopted oxidant agent. In fact, as one can see in Table 1.6, there is a big difference whether air, oxygen or steam are used.

	Air	**Oxygen**	**Steam**
CO	15-25	30-37	32-41
CO_2	5-15	25-29	17-19
H_2	10-20	30-34	24-26
CH_4	1-3	4-6	11-12
C_2H_4	0-1	1	2-3
N_2	43-55	2-5	2-3
LHV [MJ/Nm³]	**4-6**	**9-11**	**12-15**

Table 1.6 – Typical syngas molar percentage composition as a function of the oxidant agent (own elaboration based on several data).

In particular, one can observe that in the first case a conspicuous quantity of nitrogen (derived from air) is found in the syngas (its content is about half of the total), having a diluting action, so that LHV results much lower than in the other two cases. It must be also noted that reported compositions are on dry basis, since water, that is present in different percentages at gasifier output, is normally separated.

It is quite easy to understand that all small-scale plants, like those considered in this work, use air as oxidant agent, as they require simple and inexpensive devices and, for instance, it would not be justified to install an air separation unit (ASU), necessary to extract oxygen from air in case of gasification with this agent, as well as all the systems required for steam production.

Gasifiers require thermal feeding for their operation: normally the process is fed by the combustion of part of the solid biomass (direct feeding), but heat can also be provided from outside by means of exchangers (indirect feeding), again burning part of the solid biomass or of the syngas as well.

Since gasification is an energy conversion process, it is affected by some losses, essentially heat dissipations or those related to the LHV and/or the sensible heat of the discharge matter (charcoal, ash), which however are generally limited to some percentage points. Nevertheless, since the syngas leaves the gasifier at high temperature,

it owns a relevant part of the energy output in the form of sensible heat (roughly 20%), but since before or during the necessary cleaning process it is cooled, this energy contribution is normally lost (it can be partly recovered using heat exchangers). Consequently, the parameter that quantifies the gasifier performance, understandably called cold gas efficiency, considers the syngas LHV the only useful output against the solid fuel power input, being defined as follows:

$$\eta_g = \frac{(\dot{m} \cdot LHV)_{SYNGAS}}{(\dot{m} \cdot LHV)_{BIOMASS}} \tag{1.9}$$

where the meaning of the terms is immediate, remembering that fuel power is given by the product of mass flow rate and lower heating value. Basing on what mentioned above, typical values of this parameter are 70 ÷ 80%.

Nevertheless, despite the process losses, the conversion of solid fuel in a gaseous one involves a great number of advantages: it can be easily transported and stored, the emission related to its burning are lower and, above all, combustion efficiencies are higher and the fuel can be used in high-efficiency gas-fed power plants. In this regard, it must be remembered that syngas can have several applications (e.g. it can be burnt in boilers for heat generation or used in chemical processes for liquid biofuels synthesis, like the Fischer-Torpsch one,) but the main aim of this work is to focus right on power generation, hence this will be the only purpose taken into consideration. Exactly as solid biomass, syngas can be burnt in existing natural gas plants (co-combustion) or can be fired in dedicated plants: the typical solution on large scales is BIGCC (Biomass Integrated Gasification Combined Cycle), while on smaller ones, as it will be discussed, CHP with internal combustion engines, micro/small gas turbines, etc. is more proper.

Finally, as mentioned above, it is important to remember that the gasification unit is constituted not only by the gasifier, but also by two other main components, i.e. the syngas cooling and cleaning systems, in addition to all the other complementary devices (dedicated to biomass storage and pretreatment, ash disposal, etc.). In fact syngas at gasifier output is rich in impurities which have to be removed and since this process normally cannot be globally carried out at high temperature, it is necessary to cool the syngas first.

1.5.3.1 Gasifiers

Gasification is not as completely proven technology, but several solutions are available at commercial level. From an operating point of view, similarly to combustors, gasifiers can be characterised by a fixed, fluidised or entrained bed (the latter corresponding as a matter of fact to pulverised biomass combustors). In the first case, basing on the direction of the relative flow between air and biomass, they can be further distinguished in updraft (counter current), downdraft (co-current) and crossdraft type, while in the second one, basing on the characteristics of the bed, a distinction can be made again in bubbling, circulating and also dual type.
Table 1.7 summarises typical values of the main parameters of these reactors.

		Reaction temperature [°C]	Output gas temperature [°C]	Tar [mg/Nm³]	Particulate [mg/Nm³]
Fixed bed	**Updraft**	1000	250	High ($10^4 \div 10^5$)	Low (100 ÷ 1000)
	Downdraft	1000	800	Low (50 ÷ 1000)	Modest (100 ÷ 8000)
	Crossdraft	900	900	High	Modest
Fluidised bed	**Bubbling**	850	800	Medium ($10^3 \div 10^4$)	High ($10^4 \div 10^5$)
	Circulating	850	850	Medium	Very high ($5 \cdot 10^4 \div 10^5$)
	Dual	800	700	High	High
Entrained bed		1000	1000	Low	Very high

		Biomass size [cm]	Maximum moisture [% w/w]	Input flow capacity [t/h]	Power capacity [MW_{el}]
Fixed bed	**Updraft**	0.5 ÷ 10	50	10	1 ÷ 10
	Downdraft	0.1 ÷ 10	20	0.5	0.1 ÷ 1
	Crossdraft	1 ÷ 10	20	1	0.1 ÷ 2
Fluidised bed	**Bubbling**	< 2	30	10	1 ÷ 20
	Circulating	< 1	30	20	2 ÷ 100
	Dual	< 2	30	10	2 ÷ 50
Entrained bed		< 0.2	20	20	5 ÷ 100

Table 1.7 – Typical operating parameters of gasifiers (adapted from [1.31] and [1.32]).

One can observe that fixed bed reactors are used on small scales, because of the necessity of maintaining a stable and compact bed that limits these plants dimensionally, while fluidised and entrained bed gasifiers are more suitable on larger scales, analogously to combustors (besides they would be unjustified for small sizes). As one can see, plant size is reported in electrical terms: obviously to obtain the related thermal capacity the value must be multiplied by 2.5 ÷ 5 (corresponding to average electrical efficiencies of 20 ÷ 40%).

The different types of gasifiers will now be described, mainly focusing on fixed bed reactors, as obvious: all the figures showing the plant scheme are taken from [1.31].

In **updraft** or **counter-current gasifiers** (Figure 1.14) biomass and air/syngas move in opposite directions: the former is charged from the top, via a hopper (equipped with seals to avoid the leakage of syngas), and moves downwards, being hit by the hot gas flow that goes up from the bottom.

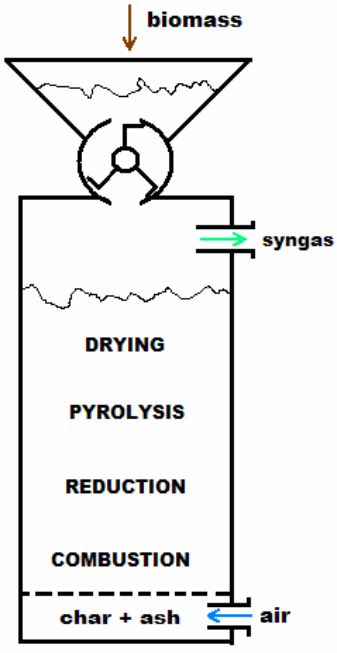

Figure 1.14 – Scheme of an updraft gasifier.

Biomass first encounters the drying zone, where the solid fuel frees itself from moisture thanks to the hot upward flow; pyrolysis reactions take place in the lower layer: here, always using the heat owned by the hot gases, biomass is decomposed in charcoal, tar

and pyrolysis gas, releasing its volatile matter; then there is the reduction zone and finally combustion reactions, fed by the air (or, in case, oxygen) there injected, take place on the bottom grate, where charcoal is burnt producing mainly H_2O and CO_2 at high temperatures. The combustion products go up through the interstices of the charcoal bed and transform part of the stored thermal energy in chemical energy (related to the LHV of H_2, CO, etc.) through the globally endothermic reduction reactions, thus forming the syngas.

Since the pyrolysis zone is the last one passed by the gas flow (except for the drying zone, that however is not relevant in chemical terms), the syngas exits the gasifiers rich in condensable volatile products, i.e. tars, as shown in Table 1.7. This is a favourable point from an energy point of view, because tars raise syngas LHV, but it involves some practical problems, as their condensation can produce occlusions on pipes or nozzles: for this reason such syngas is not directly usable in ICEs or GTs because the fouling in combustion chambers or valves would not be acceptable.

As already mentioned, in its upward motion, the syngas releases part of its sensible heat to the biomass, yielding a full drying and a considerable pre-heating of the solid fuel, and thus leaving the reactor at low temperature. This firstly allows to feed the plant with very wet biomass (up to 50%) and then to achieve high cold gas efficiencies, because part of the energy required by the process is supplied by the syngas itself.

These last considerations concerning tar contents, moisture acceptability and syngas output temperature do not apply for **downdraft** or **co-current gasifiers**, as one can understand from the schemes shown in Figure 1.15, where two of the most adopted patterns are reported: throated (or Imbert) and open-core (or stratified). In general, in such plants biomass and the oxidiser pass through the reactor in the same direction, towards the bottom[8], even if the actual scheme is quite different in the two cases.

In throated gasifiers, the oxidiser is injected through a set of nozzles positioned by a reduction in the reactor section, that is normally at about one third of the gasifier height, where the combustion process takes place, fed by the volatiles produced in the pyrolysis process (hence the low content of tars in the syngas). The latter occurs in the upper

[8] In some configurations, understandably called “inverted”, the syngas proceeds upwards while the biomass has been previously charged on the grate filling the whole volume. However, this solution is used only for simple domestic applications, where the syngas is burnt immediately after being produced.

layer, involving the material that has not reacted yet and that is supported by the throat, and is fed by the heat released in the combustion itself. The charcoal generated during the pyrolysis forms a incandescent bed under the throat, supported by a perforated grate: the gaseous combustion products pass through this bed, being involved in the reduction reactions and transforming in syngas, that then crosses the grate and exits the reactor. The char instead is gradually consumed until it is reduced in dust and then falls, together with ash, in a cinerary below the grate: the material collected here represents 2 ÷ 10% of the input biomass (ash content can vary in the range 10 ÷ 50%). In case, charcoal can be separated from ash and then used for energy purposes (e.g. in the process itself), being characterised by a good LHV (roughly 20 MJ/kg).

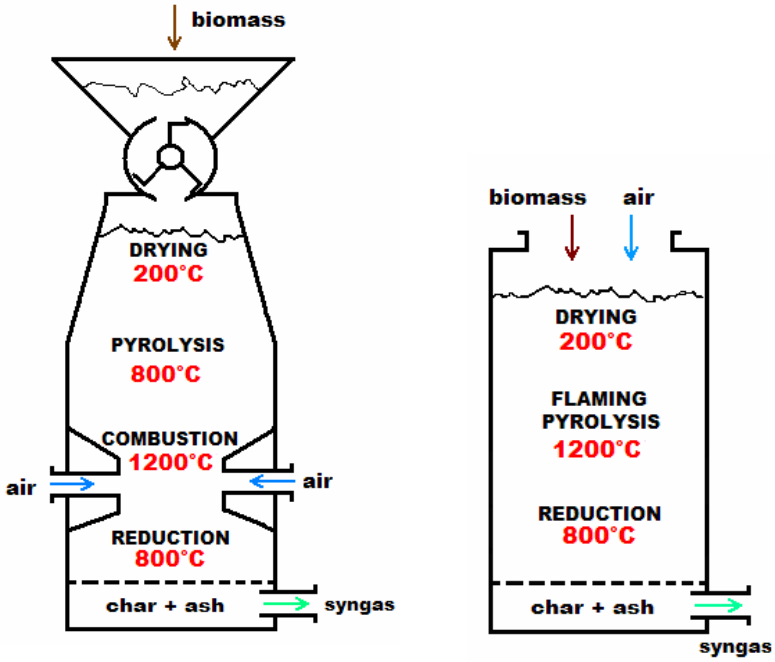

Figure 1.15 – Schemes of downdraft gasifiers: throated (left) and open-core (right).

Since the syngas exits soon after the reduction phase, its sensible heat is not recovered in the reactor. Therefore its output temperature is much higher than in the updraft case, while cold gas efficiency is lower (a following recovery of syngas sensible heat is then required for a thermodynamic optimisation of the process). Besides, the drying phase is not fed by the hot syngas, but simply by the heat transferred from the lower layers: hence drying capacity is not as high as in the previous case and input biomass has to be

less wet (maximum accepted moisture content is generally about 20%). Nevertheless, on the other hand, low tar content makes possible to couple these gasifiers with ICEs or GTs (directly or after some treatments, that however are much less onerous than those which would be required in the updraft case), and this is a crucial point that makes these plants more suitable for power generation plants feeding.

The size of the biomass pieces must be sufficiently large (at least 10 mm), because the bed is self-supported on the throat, and regular, in fact pieces having oblong or irregular shape may cause phenomena of bridging, i.e. the formation of an obstruction in the descent of the material resulting in temperature fluctuations, and channelling, i.e. the fall of non-pyrolysed biomass in the reduction zone, causing high production of tars and non reacted material (for these reasons, gasifiers are generally equipped with vibrating or mixing systems). Another disadvantage of this configuration is the limitation in the scaling-up of plants, that is due to the injection method of the oxidiser, that can not reach the centre of the biomass bed if the throat diameter is too wide.

The open-core configuration has been developed to plug these gaps, essentially eliminating the throat. As visible in the figure, both biomass (that now can have a smaller size) and air/oxygen enter in the gasifier from the top and proceed together downwards. Therefore the oxidiser mixes uniformly with the solid material from the very beginning, thus solving the problems related to the difficult penetration of the jet from the nozzles (and thus to the plant scaling, at least partially). After the drying phase, right thanks to this early mixing, there is a zone in which pyrolysis and combustion occur together as a matter of fact (the phenomenon is called “flaming pyrolysis”), since the volatile products freed by the pyrolysis are immediately burnt by the oxidiser. However, a part from this point, the whole process is analogous to the throated case.

Crossdraft gasifiers (Figure 1.16) are a middle way solution between the two previously described: biomass is still charged from the top, while the oxidiser is injected at high velocity through a nozzle from one side and syngas leaves the reactor by the other one. The reaction volume is very small, surrounded by layers of ash, charcoal and biomass: this is advantageous in terms of thermal dissipation and allows the use of inexpensive materials for the gasifier walls, that are subject to lower thermal stress. Their main quality is however the low inertia, yielding good response to load changes and quick starting, due to the small biomass quantity involved in the reactions: for this

reason, these gasifiers are normally adopted in small size applications where several starts and stops occur during the day (e.g. automotive), even if generally their use is quite limited nowadays.

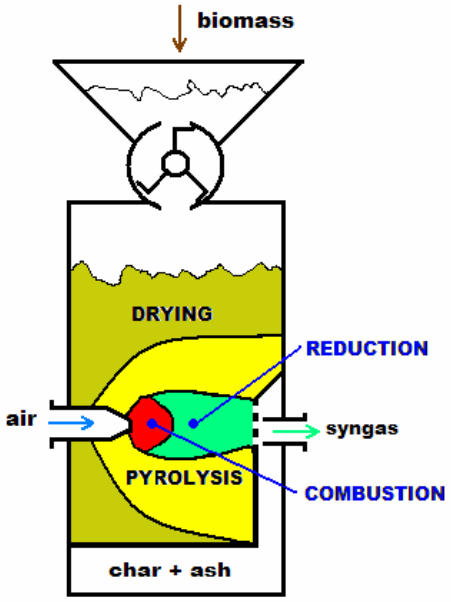

Figure 1.16 – Scheme of a crossdraft gasifier.

Fluidised and entrained bed gasifiers represent the state of art of gasifiers.

The first ones, as can be noted in the schemes shown in the next page, are substantially identical to the analogous combustion devices. Indeed these gasifiers are combustors that work in substoichiometric conditions and whose aim is then not to completely burn the solid biomass to generate hot flue gases, but to convert the biomass in syngas: apart from that, plant structure and operating principles are actually the same. The only difference lies in the necessity to add in the bed some proper catalysts (e.g. alumina or dolomite), together with the solid biomass and the inert, in order to reduce the formation of tars.

Therefore, for **bubbling bed gasifiers** (Figure 1.17) the injected air velocity is the minimum required to keep the bed in suspension in a fluid state and the bed itself is clearly distinguished from the topping section of the reactor where only syngas is present, apart from a small quantity of dragged particles, mainly composed of ash and removed in a cyclone.

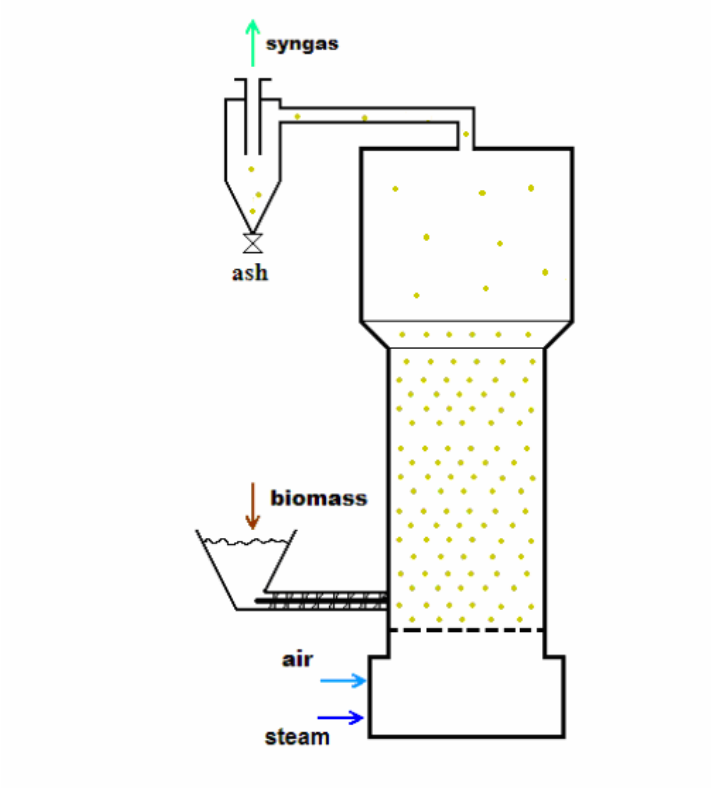

Figure 1.17 – Scheme of a bubbling fluidised bed gasifier.

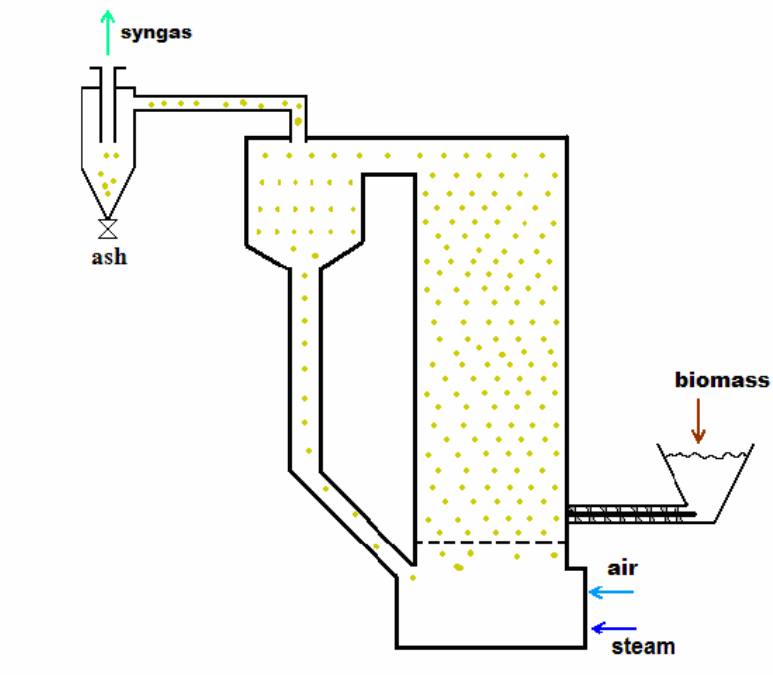

Figure 1.18 – Scheme of a circulating fluidised bed gasifier.

For **circulating bed gasifiers** (Figure 1.18), instead, higher velocity results in a complete mixing between the solid and the gaseous phases and it is not possible to identify a free surface in the bed: particles (of biomass and inert) that are dragged out from the bed are separated from the syngas in a cyclone, cooled in an exchanger and then reinserted in the bed. Then another cyclone separates ash from syngas, as in bubbling bed reactors. Circulating bed reactors are more compact compared with the latter, thanks to higher flow velocities, and has fewer problems concerning heat transfer, since this takes largely place out off the combustion zone, and therefore has a better performance; nevertheless it is more complex in terms of design, setting and running and is hence more expensive.

Due to the homogeneous distribution of the temperature inside the bed, in fluidised bed gasifiers, differently from fixed bed ones, there are not separate reaction zones: drying, pyrolysis, combustion and reduction occur gradually in every particle. Indeed, only for these plants gasification temperature is properly defined: in fact fixed bed gasifiers (and, partly, also entrained bed ones, as will be discussed below) present different zones inside the reactor, dedicated to the various stages of the process, each one having a different temperature and therefore a gasification temperature is not univocally identifiable (generally, as shown in Table 1.7, in these cases the combustion temperature is used as reference). However, the main advantage of these devices is indeed the easy control of temperature, via air/fuel ratio, that is kept uniform: this leads to high efficiencies. Finally, the possibility of operating in pressurised conditions makes these plants suitable to be coupled with gas turbines.

Dual fluidised bed gasifiers are devices made up of two different reactors: in the first one pyrolysis reactions take place, while in the second one volatiles are burnt. The combustion produces the necessary energy to feed pyrolysis in the first reactor, heating the bed. Syngas thus produced has a medium LHV, but high contents of tars and particulate. The plant is however complex and expensive, therefore this solution is not frequently adopted.

Concluding, **entrained bed** (or flow) **gasifiers** are reactors typically used on large sizes (> 10 MW_{el}), being quite complex and expensive. As already mentioned, biomass must be fed in dust form, therefore it must be ground in pieces not larger than 2 mm before entering the reactor, making these plants similar to pulverised fuel combustors.

As shown in Figure 1.19, biomass dust and the oxidiser (normally oxygen) are introduced, together with the portion of charcoal recirculated from the cyclone, in the bottom part of the reactor, where the combustion takes place. Its products go up passing through a diffuser, that reduces their velocity, and enter the second stage, that is the reduction zone, where additional biomass is fed. Since the solid fuel is present in dust form, contact surfaces are very high and hence reaction times are very short. The process happens at very high temperature (and normally at high pressure, in this case also allowing a coupling with GTs) so that firstly the syngas results completely free from tars (that are in vapour form) and secondly ash melts, being then collected on the bottom of the reactor in the form of slag. On the other hand, high temperature causes low thermal efficiencies and syngas must be cooled after leaving the gasifier. Moreover, these devices are often cooled by means of boiling water jackets and the produced vapour can be used in the process or in other applications [1.31].

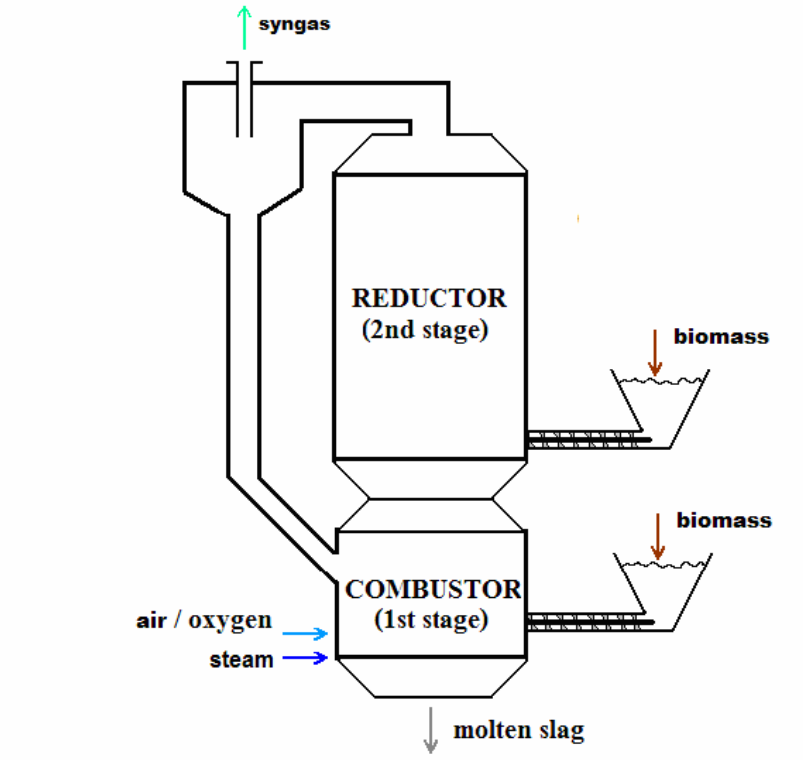

Figure 1.19 – Scheme of a circulating entrained bed gasifier.

1.5.3.2 Syngas treatment

Syngas exiting the gasifier can be directly used only if it feeds a burner for direct combustion and the user is at short distance from the output duct of the reactor. In all the other cases it has to be previously cleaned up, because otherwise the impurities contained in syngas would heavily damage pipes and the user device itself. The syngas cleaning system downstream of the reactor is an integral part of the whole gasification plant and is not less important than the reactor itself; indeed, the main problems that affect gasification technology and limit their definitive commercial rise mainly lie in this section, as will be discussed further on.
Table 1.8 gives a full overview on the main contaminants that can be found in syngas, the problems related to them (concerning plant operation but also human health, considering pollutant emissions) and the technologies mostly used for their treatment.

Contaminant	Examples	Problems	Clean-up method
Particulates	Ash, char, fluidised bed material	Erosion	Filtration, scrubbing
Alkali metals	Sodium, potassium compounds	Hot corrosion	Cooling, adsorption, condensation, filtration
Fuel-bound nitrogen	Mainly ammonia and HCN	NO_x formation	Scrubbing, SCR
Tars	Refractive aromatics	Clog filters, difficult to burn, deposit internally	Tar cracking, tar removal
Sulphur, chlorine	HCl, H_2S	Corrosion, emission	Lime or dolomite scrubbing, absorption

Table 1.8 – Syngas contaminants, their problems and clean-up methods [1.33].

The choice of the plant configuration, concerning both the reactor and the cleaning system, and signally the necessity to focus on some types of contaminants rather than on others, depends on the final use of syngas (heat generation, co-combustion, furnaces,

ICEs, GTs, Stirling engines, etc.), each one having specific requirements. It is quite obvious that, as a general rule, the cleaning need is stronger in internal combustion plants rather than in external combustion ones[9]. However, it must be noted that the literature is not rich of reliable data on the gas quality requirements and moreover they are often quite contrasting.

Focusing on internal combustion engines and gas turbines, the most important types of power plant that can be fed by syngas, generally the former are more tolerant of contaminants than the latter. Alkali and sulphur compounds, which corrode the blades, have the most deleterious effects on gas turbines. Also chlorine compounds, that interact with several metals, have corrosive effects, and this is worsened by the change from reducing (gasifier) to oxidising (plants combustion chamber) environments. Particulate matter damages the moving parts, eroding them (again, more heavily on GTs than on ICEs). Turbines are not very sensitive to tars, as the high gas temperatures keep them in vapour form, nevertheless these condensate on the piping system (causing fouling of heat exchangers, for instance) and it is a potential problem if syngas has to be compressed, as it will deposit in the compressor. For this reasons, requirements for tars in global terms are quite strict, more than for internal combustion engines [1.34]. Table 1.9 provides some limit values of the contaminants content for these two power plants.

	Tar [mg/m³]		**Particles [mg/m³]**	
	Maximum	Desired	Maximum	Desired
Gas engines	< 100	< 50	< 50	< 5

	Tar [mg/m³]	**Particles [ppm]**	**Na [ppm]**	**K [ppm]**	**S [ppm]**	**HCl [ppm]**	**Other metals [ppm]**
Gas turbines	5	< 1	< 1	< 1	1	< 0.5	< 1

Table 1.9 – Required values of the gas quality for the use in ICEs and GTs [1.35].

[9] Indeed, syngas is normally produced precisely to be used in internal combustion devices, since external combustion ones can be fed by burning solid biomass, avoiding the complexity of gasification process; however, specific considerations can lead to use syngas also in these plants in certain cases.

However, as discussed above, it is important to remember that these data have to be considered only as a rough guide (for instance, in [1.36], the limit of particulate content for gas turbine is fixed in 30 mg/Nm^3).

Finally, a description of the main removal devices is provided.

There are two main categories of systems for **particulate** removal: dry and wet. In the first case particles are separated adopting physical or mechanical methods, without adding anything to syngas, while in the second case, called scrubbing, a liquid is properly used.

Concerning dry systems, the mostly used devices (often adopted in combination in the same plant) are: cyclones, electrostatic precipitators, fabric filters and candle filters.

Cyclones, that have already been mentioned in fluidised bed combustor and gasifiers, are vertical-axis cylinders, with a conical lower part, which are tangentially entered by raw syngas: the solid particles are carried towards the walls by the centrifugal force and then fall in the bottom hopper, while clean syngas comes out from the top of the cylinder. They can efficiently (> 90%) remove particles having diameter higher than 5 μm (PM5) and moderately (> 50%) particles whose diameter is higher than 1 μm (PM1), but are ineffective at lower sizes. On the other hand, they are cheap and can also be used at high temperature.

In electrostatic precipitators (ESP) syngas passes between two high voltage electrodes: the wiry emitting one (negative) charges the particles (while syngas is not involved), that are then attracted by the receiver (positive), having plate form, on which they settle. Afterwards they are removed mechanically (in this case they can be used at high temperature, i.e. at about 500°C) or using a thin water film (which limits the operating temperatures below 100°C). Removal efficiency is about 95% for PM1.

Fabric filters (FF) are essentially bags, made up of various types of fabric, through which raw syngas is forced to pass: the particles are blocked by the filter structure and are then removed by shaking or insufflating air in the direction opposite to the flow. Operating temperature depends on the fabric type, but normally is not higher than 350°C. Their efficiency is very good: it can be higher than 99.5% for PM1.

Candle filters consist of a series of rigid and porous cylinders, supported by a common tube sheet, that capture syngas dust passing through them and then discharge it in a lower sink, while cleaned syngas is collected in the upper space of the vessel and then

blown out. Obviously a periodic clean-up is to be planned, to avoid the formation of deposits and the consequent head losses. They can be composed of metallic (e.g. Inconel) or ceramic material: in the first case they work at medium-high temperature (600°C), so that syngas must be partially cooled, while in the second case operating temperature (850°C) is analogous to the syngas one at the gasifier output, so that it is no more necessary to perform the cooling. This represents an enormous advantage, that would allow syngas to keep its sensible heat, nevertheless this technology cannot be considered proven yet. However these devices are particularly suitable for very fine and light charcoal particles and have excellent removal efficiencies (about 99.8%), even if they denote some problems of clogging due to soot accumulation deriving from tar cracking.

On the other hand, as mentioned above, in wet scrubbers dust removal is effected using liquid droplets that capture the particles present in raw syngas. The adopted liquid is normally water (even if other types of fluid are used or under investigation): since it obviously has not to evaporate, syngas must be cooled below 100°C. Water droplets are then removed from syngas stream (by coalescence, sedimentation or, in case, using cyclones). There are several specific techniques through which the process is effected: the most simple solution is the spray tower, a vertical device in which raw syngas and water droplets are simply made flow in counter-current (similarly to evaporative cooling towers in steam power plants, even if the phenomenon is obviously different), but the most used is the Venturi scrubber. In this system, raw syngas is made flow through a Venturi tube, whose throat is connected to the water source: the pressure drop occurring here attracts the liquid that, thank to low pressure and high flow velocity, is easily sprayed, increasing the contact surface with syngas and thus capturing a higher quantity of particles. Removal efficiency is therefore very good, being 99.9% for PM2 and 95 ÷ 99% for PM1.

As seen, syngas is normally cooled below 600°C: at these temperatures **alkali compounds** (sodium, potassium salts, etc.) precipitate in or on particles and therefore the previously described technologies (filters, precipitators, scrubbers) can be suitably used to remove them. On the other hand, to clean the gas and preserve high temperatures, only ceramic candle filters can be used. Besides, high temperature removal via solid adsorbers (e.g. silica or alumina) is a solution under investigation.

As for combustors, due to relative low temperatures, NO_x formation mainly derives from the **nitrogen** contained in the biomass. In particular during the gasification it is mainly converted into ammonia, NH_3 (and, to a lesser degree, into hydrogen cyanide, HCN), that is then converted into NO_x during the combustion of the syngas. In order to keep down the emissions, several methods can be applied. First of all, it is always useful to supply biomass having low nitrogen content and, on the other hand, adopt low-NO_x combustion techniques. Concerning removal systems, they can be focused either on the syngas NH_3 or on flue gases NO_x downstream of the power plant. Ammonia can be removed with wet scrubbing (obviously at low temperature) or with high temperature (800 ÷ 900°C) catalytic decomposition, by means of metal (e.g. iron, nickel based) or non-metal (dolomite, zeolite) catalysts; on the other hand, a catalytic method, called Selective Catalytic Reduction (SCR), is also used for flue gas NO_x, brought to react with an ammonia-based reducing substance at about 250 ÷ 350°C, yielding water and free nitrogen.

Tars must always be removed if syngas is cooled or compressed before being used and in particular, as previously discussed, if it is used in internal combustions engines or gas turbines. Their concentration strongly depends on the reactor type, but also on operating temperature (it decreases with increasing temperature) and fuel type (in general biomass produces more tars than coal). Their efficient removal still remains the main technical barrier for the successful commercialisation of biomass gasification and this represents the main reason why downdraft gasifiers are largely the most used solution on small scales. However, two main systems are adopted: physical or chemical. In physical systems, tar droplets are made condense and are then removed by means of devices similar to those used for particulate, mainly wet scrubbers (but, for instance, also wet electrostatic precipitators have been studied). Tars can then partly be separated and used for energy purposes, but this process is complex and require a complicated management of wastewater. On the other hand, chemical systems are based on tar cracking, i.e. tars are decomposed in simpler molecules. This can be done in catalytic, adopting solutions analogous to those described for NH_3, or thermal way, by means of partial oxidation (adding air or oxygen) or direct thermal contact with hot surfaces (in both cases the process obviously occurs at high temperature, 800 ÷ 1000°C). Again, they are complex and not yet proven technologies.

Sulphur compounds are generally not a major problem, given the low content of this element in biomass (contrary to coal). Nevertheless, in case of adoption of biomass syngas for gas turbine feeding, the restrictive requirements for such plants (1 ppm) call for sulphur removal, since its concentration in raw syngas is about 100 ppm. A substantial reduction is actually achieved if dolomite has been previously used for tar cracking, however a chemical absorption unit, consisting in a hot bed of zinc monoxide that brings the concentration below 0.01 ppm, is generally installed. **Chlorine compounds** instead are normally removed either via adsorption, with active materials materials installed both in the gasifier or in a secondary reactor, or wet scrubbing.

In conclusion, it has been shown that, among the proven technologies, only cyclones allow a high-temperature operation, while all the other ones essentially require syngas gas cooling, causing an energy loss, partially reduced if a heat recovery process is provided [1.37].

Chapter 2
Small-scale power plants

2.1 Introduction

After having discussed the characteristics of woody biomass and technologies for its energy conversion, this chapter provides a description of the main small-scale power generation plants.

In this work three specific sizes have been taken into account: 100 kW_{el}, 1 MW_{el} and 5 MW_{el}, focussing on the first two ones. In fact, basing on what already mentioned in the previous chapter, the latter cannot properly be considered small size, nevertheless it has been taken into account in order to get a sort of upper limit reference values, also considering that all the power technologies adopted for 100 kW_{el} and 1 MW_{el} cases can be generally used for the 5 MW_{el} case too.

Commercially available technologies and those that are expected to be potential in the near future have been taken into consideration, based on internal combustion engines (ICE), gas turbines, in case in the micro configuration (mGT/GT), both internally and externally fired, and Organic Rankine Cycle (ORC) plants. However, the less developed and used solutions are also briefly presented in the last part of the chapter.

For the time being, it is important to note that the internal combustion plants are described in their classic configuration, i.e. considering natural gas feeding: issues related to the use of syngas in such plants are just mentioned here, while they will be fully discussed in the next chapter.

Concluding, it may be useful to specify that the solution mostly used on large scales is the traditional steam cycle plant one, which, however, is affected by low electrical efficiency (averagely 25 ÷ 30%), since their low power capacity (in absolute terms) results in the necessity to contain investment costs, requiring modest thermodynamic cycle parameter values and extreme plant simplicity. Higher efficiencies (35 ÷ 40%) are achievable with BIGCC, where a gas turbine, fed by gasification syngas, is coupled

with a bottoming steam cycle, although this is a more complex and less diffused technology [2.1]. However, as discussed, the most convenient solution is probably co-combustion in large-scale coal plants, avoiding construction of new dedicated facilities and allowing exploitation of biomass in relatively high-efficiency plants.

2.2 Small-scale power generation and CHP

Small-scale power generation falls within the broader concept of Distributed Generation (DG), consisting in on-site power production, i.e. next to the final user (that may be a single house as well as mid-sized factories), with handover to low or medium-voltage grid of electric surplus. This allows to easily follow the variations of the power load and to avoid losses, consisting in several percentage points in terms of equivalent electrical efficiency, related to the transmission and distribution processes, necessary in case of centralised production in large-scale plants. On the other hand, in the classic case of natural gas feeding, DG results heavily penalised compared to large-scale plants in all cost determinants:

- investment, being higher in specific terms (€/kW_{el}) and split over a lower number of yearly working hours;
- fuel, being affected by higher unit costs and lower electrical efficiencies (which can reach 60% in large combined cycles, while they do not exceed 30% on 100 kW_{el}-size and 40% on 1 MW_{el}-size in internal combustion engines, which are the most performing solution);
- O&M (Operation and Maintenance), whose incidence is relatively higher.

Basing on these considerations, methane-fed[1] DG has a sense, both in energy and economic terms, only if waste heat is recovered, i.e. if a combined heat and power production is being carried out.

The basic concept of cogeneration or CHP is well known: in every thermodynamic power cycle, that yields mechanical or electric power adopting high-temperature heat (normally deriving from a combustion process) as an energy source, it is necessary to

[1] In this work natural gas and methane are normally used as synonyms.

release part of the heat at a lower temperature, normally to the environment. This heat, directly discharged in form of flue gases and/or indirectly with a exchanger, is normally a considerable share of the energy input and is a loss penalising the energy performance of the plant. On the other hand, if it is partly or completely recovered for useful purposes, a CHP process is realised, with clear positive effects, since the process is more efficient in respect to separate production of the two goods in two different dedicated plants. In fact, as suitably schematised in Figure 2.1, electricity is normally produced in plants having about 40% electric efficiency, where waste heat is normally discharged at low temperature (for instance, in steam plants condensation heat is released at 30 ÷ 40°C) or however a proper recover is not effected; on the other hand, heat is normally produced via furnaces or boilers having high thermal efficiency[2] (even 90%), but it is subject to a heavy thermodynamic degradation, being produced at a temperature higher than 1000°C and then absorbed by a fluid whose temperature is normally lower than 150 ÷ 200°C (in all civil applications, i.e. domestic heating, and in most industrial ones). This fact enables to utilisation of waste heat from power cycles (obviously also for steam plants, with proper cycle modifications, i.e. increasing condensation temperature), thus allowing the saving of fuel that would be necessary in the corresponding furnace: with the same net energy output, the overall fuel saving can be even higher than 30%.

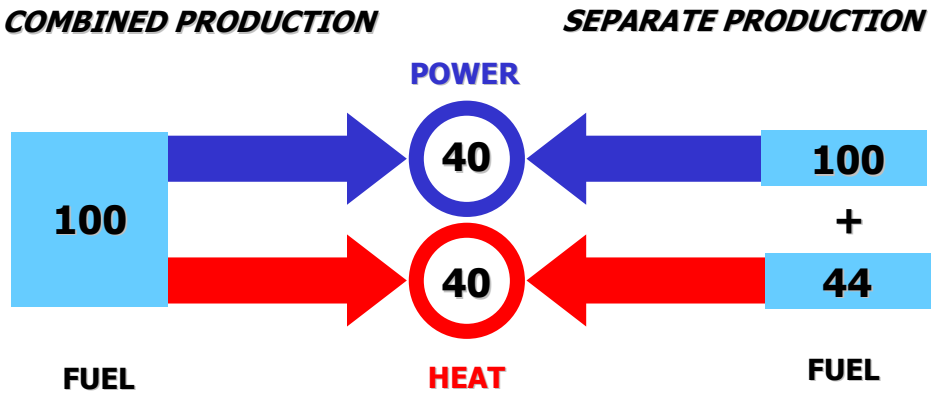

Figure 2.1 – Energy flows diagram in combined and separate production.

[2] Electrical and thermal efficiencies are defined as the ratio between, respectively, generated power or heat and fuel power input (given by the product of fuel mass flow rate and its LHV).

As a consequence, CHP justifies the adoption of small-scale plants and makes them competitive with larger ones, because their lower electrical efficiency is compensated by heat production. Obviously CHP is also applied on large scales[3], but their performance in terms of first and second law efficiencies[4], differently from the mere electrical efficiency, is not much higher than that of small plants [2.2].

The above explanations generally also apply for biomass, since it is exploited through a combustion process (directly or after being converted into syngas), nevertheless the heat recovery necessity becomes less pressing, mainly because of two factors.

First of all, differently from methane-fed plants, concerning biomass the performance of large-scale plants is substantially comparable to that of small-scale ones. In fact, as will be shown in the next chapters, 25% electrical efficiency of large steam cycles is easily achieved by 1 MW_{el}-size plants, as well as 35 ÷ 40% of BIGCC plants is reached by some 5 MW_{el}-size devices. Indeed, it is important to always remember that "large scale" for natural gas plants means roughly 300 ÷ 500 MW_{el}, while, as already discussed, for biomass plants it means even 10 ÷ 20 MW_{el}, therefore the distance in absolute terms between small and large size is low and favours the limitations in performance differences.

Secondly, small-scale power generation from renewable sources enjoys conspicuous economic incentives, that are not provided for heat production, whose incidence is therefore lower, as will be shown in Chapter 5.

It is also for this reasons that in this work focus has been put primarily on the maximisation of power generation, even if the effect of thermal production starting from waste heat has been taken into account, since it obviously contributes to an overall plant optimisation. Summarising, one can affirm that CHP production is a necessity on small-scale methane-fed plants, while it is generally not mandatory in case of biomass feeding, even if it can obviously be relevant.

[3] Actually its diffusion started right from these plants.

[4] First law efficiency is given by the ratio between the net output (power + heat) and the fuel power and is thus equal to the sum of electrical and thermal efficiencies; second law efficiency is calculated in a similar way, but since heat is a less valuable energy form than electricity, its contribution is multiplied by a reducing factor, normally the Carnot efficiency related to the heat supplying temperature.

2.3 Internal combustion engines

Internal combustion engines (Figure 2.2) are machines historically developed for the automotive industry, that in the last decades have been used for industrial cogeneration and, recently, also in civil and tertiary sectors. They are available in a wide range of sizes, that is 1 kW_{el} ÷ 10 MW_{el}[5], thus perfectly covering the three cases being considered in this work. Indeed, the smallest engines, dedicated to applications in residential buildings or little business activities, have not yet reached an industrial level of development (although some models are available on the market): the considerations reported below generally apply for engines having a capacity higher than about 30 kW_{el}.

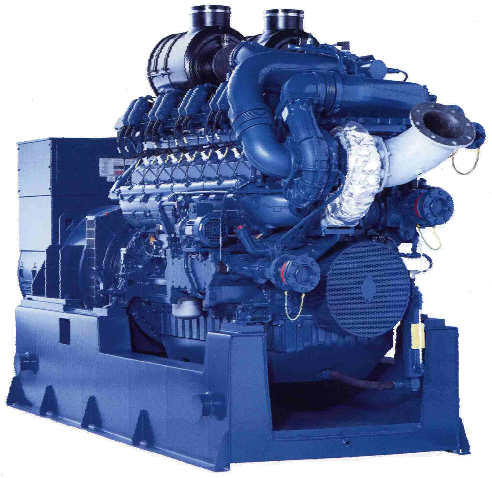

Figure 2.2 – An internal combustion engine for cogenerative use [2.3].

These engines are normally reciprocating, with various processes occurring inside the cylinders according to piston movement. It is commonly known that there are two main engine types:

- spark ignited (SI), based on Otto cycle;
- compression ignited (CI), based on Diesel cycle.

In SI engines the fuel is injected in the air flow during the intake phase, the mixture is adiabatically compressed, then ignited by a spark produced by a plug and finally it

[5] Large-scale marine-derivative Diesel engines, whose capacity can be even 50 ÷ 60 MW_{el}, are neglected, because they are not used for power generation.

expands, again adiabatically, producing useful work. Hot gases are then discharged and the cycle is being repeated. Figure 2.3 shows a schematisation of the process. The high temperature reached in the compression phase could result in mixture self-ignition (knocking), which must be avoided: for this reason, the compression ratio is generally limited to 10 ÷ 14.

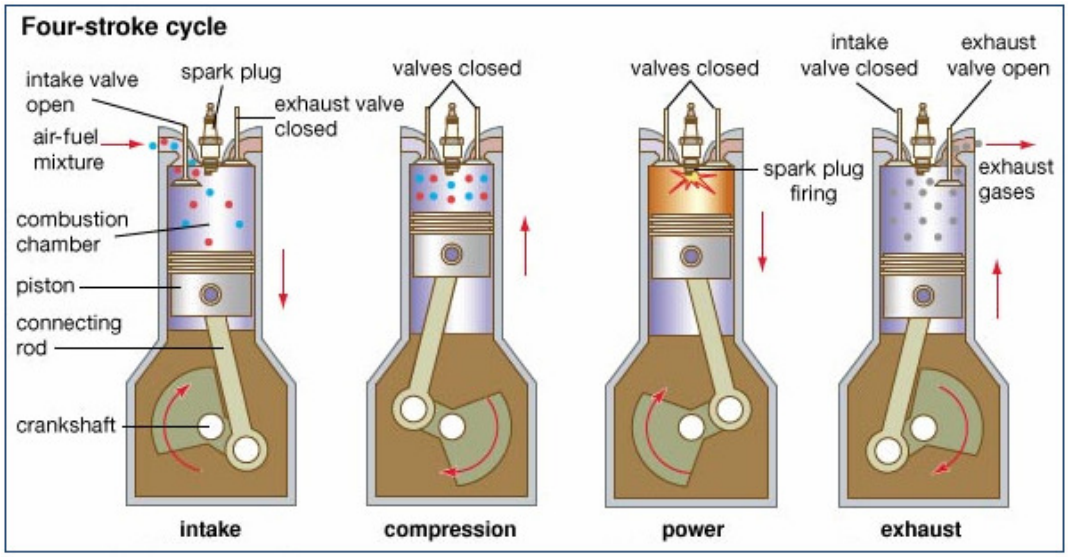

Figure 2.3 – Four-stroke cycle in a SI internal combustion engine [2.4].

As one can see, the four-stroke configuration is proposed in the figure. The name is due to the fact that the whole work cycle is realised by means of four movements (strokes) of the piston, two upwards and two downwards, each one roughly corresponding to a thermodynamic process. Two-stroke engines, where the cycle occurs in just two movements, may be realised too, but their environmental performance is poor, so that they are not generally adopted for CHP applications.

The operating concept in CI engines (intake - compression – combustion – expansion-discharge) is analogous, but here only air is compressed, then the fuel is injected at high pressure into the cylinder and the mixture self-ignites because of the air high temperature (the phenomenon to be avoided in SI engines): the combustion process is more gradual and one can assume that it occurs at constant pressure, while the combustion takes place instantaneously (at least ideally) in SI engines and can thus be considered isochoric. Besides, compression ratio can be higher (up to 20).

In general, ICEs can use a wide variety of fuels, but in CHP applications natural gas is normally adopted, due to its features of environmental compatibility, constant availability and relatively low costs.

Since methane is also characterised by a good anti-knock behaviour, it is suitable for use in SI engines, that is the mostly used solution. The mixture in these machines can be stoichiometric or, more often, lean (lean burn), i.e. the air to fuel ratio is higher than the stoichiometric one: this is done in order to limit NO_x production. SI methane engines can be built up according to a dedicated project or else, as often occurs, they derive from CI engines, adapted to the new type of operation (plugs are added, power capacity is reduced to 60 ÷ 80% to avoid knocking, etc.).

Natural gas can also be used in CI engines but, due to its anti-knock behaviour, a percentage of diesel oil must be added (1 ÷ 10%) to achieve self-ignition of the charge. The natural gas can be supplied either at low pressure in the intake together with air or at high pressure directly into the combustion chamber with diesel oil: according to the described issues, in the former case, power output must be reduced to 80 ÷ 95%, while, in the latter case, power capacity is substantially unvaried, but a gas compressor is required if methane supplying pressure is not high enough, with consequent power consumption, typically about 5% of the generated power. Besides, compressor cost and potential problems related to its operation have to be taken into account: therefore, unless natural gas is directly available at high pressure (which normally does not happen), making compressor installation unnecessary, low-pressure injection of gas in the intake duct is normally preferred.

Apart from some models having capacity lower than 200 kW_{el}, reciprocating engines are always supercharged through a turbocharger: the turbine is fed with the engine flue gases and drives the compressor, that enhances air pressure, increasing its density and thus power output (in addition efficiency increases also, while emissions decrease). An intercooler with the aim of cooling the air at the compressor output to further increase density and, at the same time, reduce the engine compression work is normally also provided. It is important to note that in vehicles the heat released at the intercooler is rejected in the air, while in CHP engines it can be recovered for useful purposes by water flow (even if its temperature is generally low, about 40 ÷ 50°C). The integration of the turbocharger with the engine is schematised in Figure 2.4.

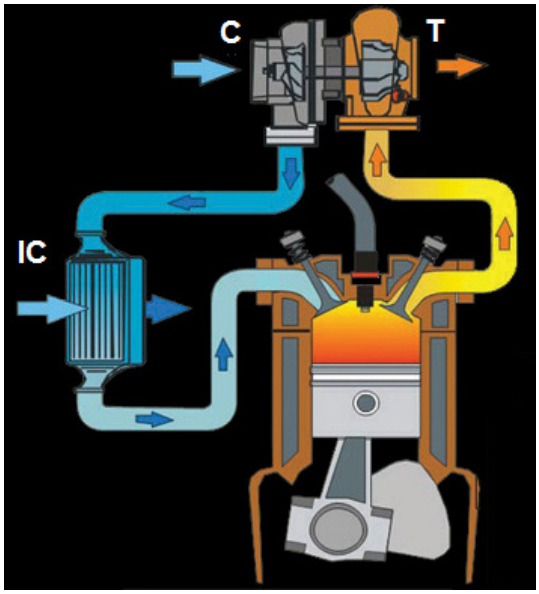

Figure 2.4 – Scheme of an ICE equipped with turbocharger (C: compressor, T: turbine, IC: intercooler) (adapted from [2.5]).

The main advantages of internal combustion engines are:

- high reliability, since it is a proven and diffused technology;
- low specific cost (800 ÷ 1200 €/kW_{el});
- high electrical efficiency;
- high service life (60,000 ÷ 80,000 hours);
- high flexibility, i.e. ability in following the load with good efficiencies under various operating conditions.

In particular, in Figure 2.5 the electrical efficiency of a great number of cogenerative SI internal combustion engines is shown (however, CI engines performances are analogous). As one can see, this parameter is averagely 30% for 100 kW_{el}-capacity, 35 ÷ 40% for 1 MW_{el}, while 45% is reached at 5 MW_{el}.

On the other hand, these plants are affected by some defects:

- high O&M costs (1 ÷ 1.5 c€/kWh_{el});
- considerable noise and vibrations;
- it is necessary to adopt emission control systems, i.e. catalysts, since reciprocating operation involves production of high quantity of pollutants (NO_x and CO, for instance, are thus typically limited to 500 mg/Nm^3) [2.2].

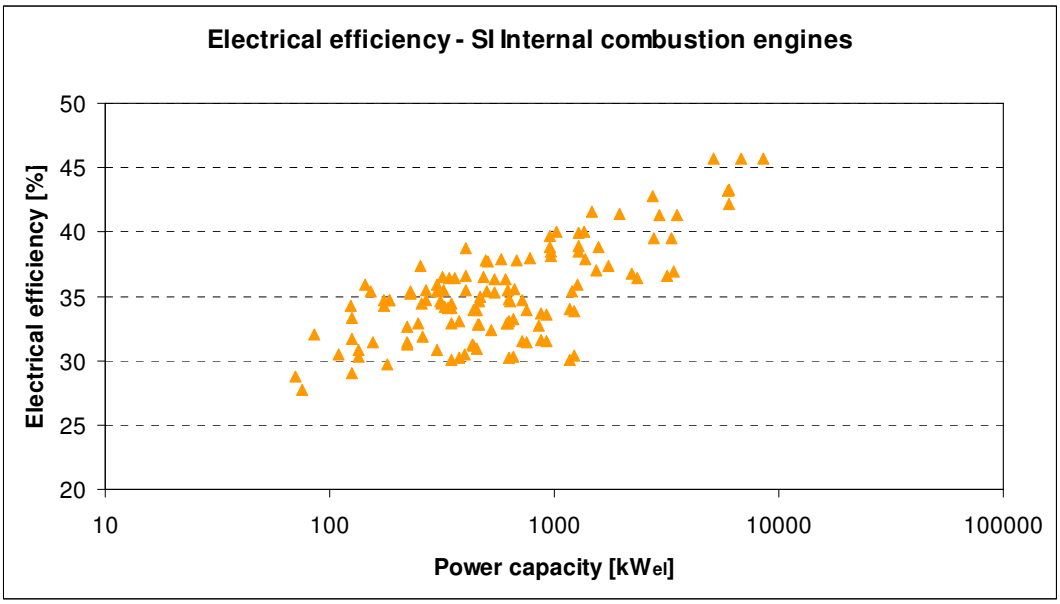

Figure 2.5 – Electrical efficiency of SI internal combustion engines as a function of size (own elaboration based on [TF]).

Apart from the disadvantages reported above, high efficiency and reliability make internal combustion engines the most adopted solution for CHP applications on small scales. As shown in Figure 2.6, power generation is performed coupling the driveshaft with an alternator, while heat can be recovered both from hot flue gases, that leave the engine at 350 ÷ 550°C, and from the cooling water (cylinders jackets, lube oil) normally available at 90°C (in case intercooler heat can then be taken into consideration).

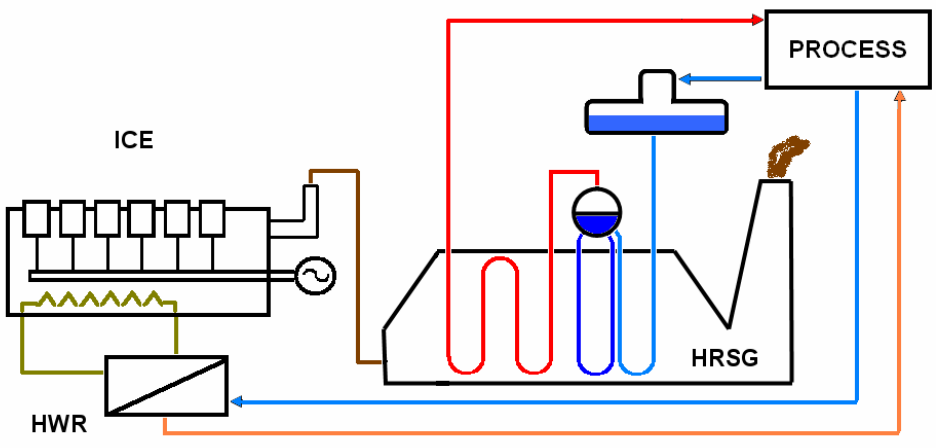

Figure 2.6 – Scheme of heat recovery in a CHP internal combustion engine.

In particular, flue gases can be used in a HRSG (Heat Recovery Steam Generator) to produce low-temperature and pressure steam (normally up to 200°C and some bars) or hot water (e.g. for heating purposes); obviously concerning the cooling circuit (in the figure indicated by HWR, Hot Water Recovery), the latter is the only available solution. Finally, some typical energy flows in a 1 MW_{el} engine, having 41% as electrical efficiency, are presented in Figure 2.7. Considering that flue gas heat cannot be completely recovered (normally gases are cooled down to 120 ÷ 150°C, so the useful share would be about 25%) and neglecting intercooler contribution, first law efficiency would be about 80 ÷ 85%. On lower scales, up to 85 ÷ 90% are instead being reached, obviously with lower electrical efficiencies. However, values are very attractive in both cases.

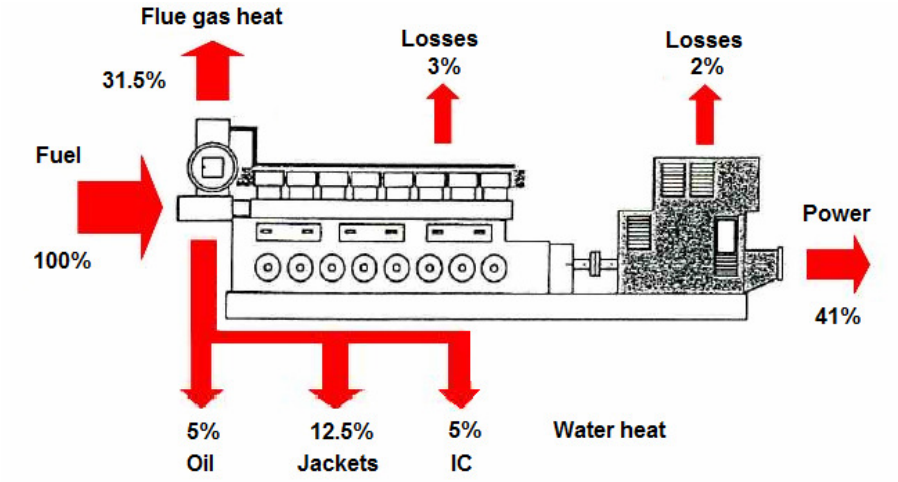

Figure 2.7 – Energy flows in a typical 1 MW_{el}-size CHP engine (adapted from [2.6]).

2.4 Gas turbines

Gas turbines (Figure 2.8), like internal combustion engines, are machines originally developed for propulsion purposes, even if in this case focus was pointed on aeronautical applications. First plants were realised at the end of the thirties, but it was only after the Second World War that gas turbines started strong development, initially as aircrafts engines (first military and then civil) and afterwards, especially in the last decades, for stationary employments, where they are typically adopted to drive work-

absorbing machines (mechanical drive), such as methane compressors in pipelines, or for power generation (the major interest in this work), either alone or in combined cycle with a bottoming steam plant, exploiting the heat owned by the hot flue gases. Applications for propulsion of other transport means (especially ships) have also to be mentioned for completeness.

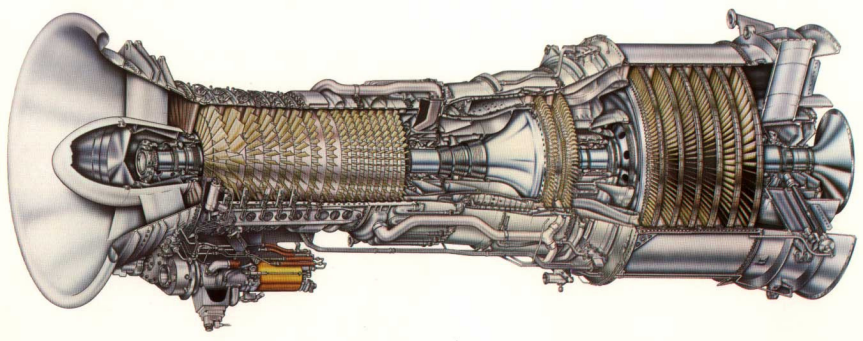

Figure 2.8 – An example of gas turbine [2.7]

As known, gas turbines are based on the Joule-Brayton cycle, composed of an adiabatic compression, an isobaric heating, an adiabatic expansion and an isobaric cooling. Except for rare cases, they adopt an open cycle in which air is compressed and then sent in a combustion chamber where fuel (natural gas or kerosene for propulsion) is added and combustion takes place, subsequenltly, the hot gases expand through the turbine and finally they are discharged in the open air: a simple scheme is represented in Figure 2.9 (the meaning of the symbols is immediate).

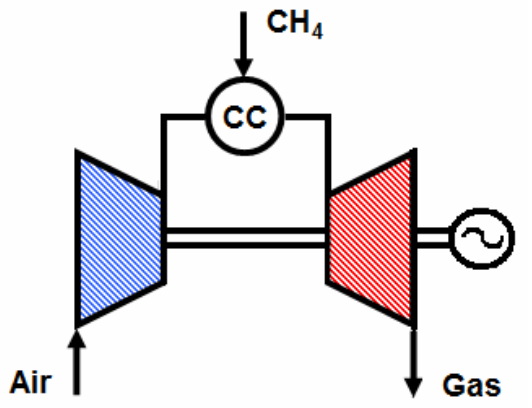

Figure 2.9 – Simplified scheme of a gas turbine for power generation.

Gas turbines are very complex machines, whose design involves a great number of relevant issues concerning aero and fluid dynamics, heat transfer, metallurgy, etc.: only some of them are mentioned in these pages, above all the ones that allow comparison with the other power plants taken into consideration.

In their base configuration, these plants cover a very wide range of power capacity, that is about 500 kW_{el} ÷ 350 MW_{el}, even if actual competitiveness is normally reached starting from 5 ÷ 10 MW_{el} only. The reason lies precisely in the high technological content of these turbomachines, required to achieve good efficiencies and inapplicable or unjustified on small plants. For instance, it is well known that an improvement of the performance mainly involves turbine inlet temperature (TIT) increase, which implies the adoption of sophisticated materials and metallurgical techniques[6] coupled with advanced methods for turbine's first stages cooling: in small-scale turbines the cooling system is very simple or often is even missing, limiting TIT to 900 ÷ 1000°C, against 1100 ÷ 1400°C reached by the larger types, with consequent performance fall. Indeed, the increase of TIT must be accompanied by a contextual calibrated increase of maximum pressure, which implies the installation of additional stages to the machines, with consequent additional costs, that would be unjustified in small plants. Besides, the overall plant performance is particularly sensitive to compressor and turbine efficiencies, that are penalised by inevitable size effects on small scales. This happens also because small turbines are a simple scale-down of the larger models, whose basic architecture is conserved: in particular the machines are always axial (obviously multi-stage), except from some cases limited to the smallest sizes (500 kW_{el} ÷ 1 MW_{el}), where low mass flow rates suggest the adoption of radial configurations. Finally, it is important to remember that only large-scale turbines (i.e. having capacity higher than about 40 ÷ 50 MW_{el}) can be directly coupled with an alternator, while small ones require a higher rotational speed and thus a transmission system, gradually more and more onerous with diminishing size (as speed increases).

The electrical efficiencies as a function of size of the turbines available on the market are shown in Figure 2.10, exactly as done for internal combustion engines.

[6] The use of ceramic materials, that would be decisive in this sense, is still subject to R&D, mainly due to their poor mechanical performance.

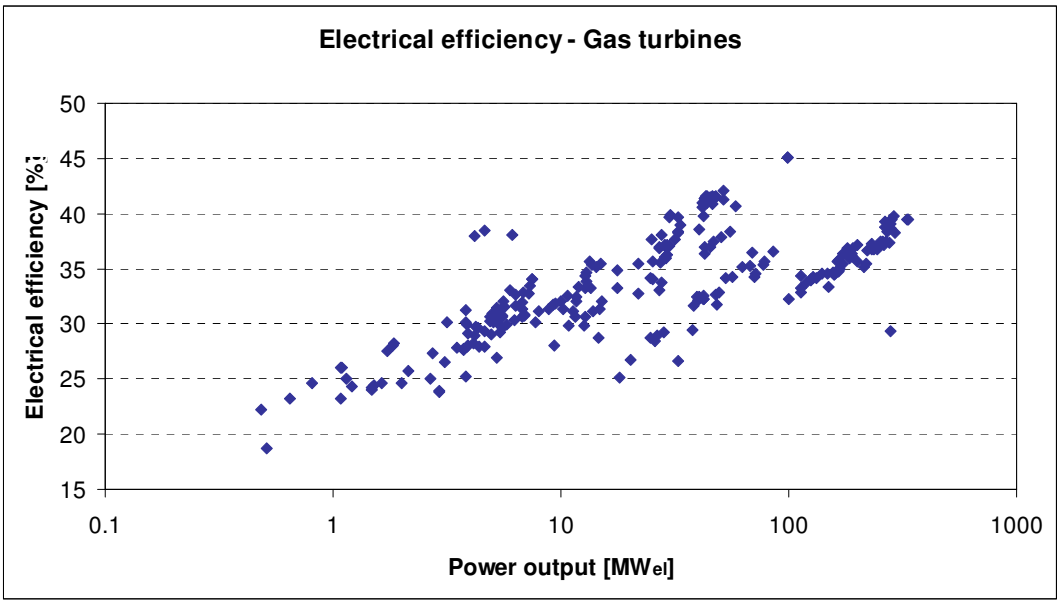

Figure 2.10 – Electrical efficiency of gas turbines as a function of size (own elaboration based on [TF]).

As one can see, efficiency of the smallest models varies from 20 ÷ 25% (these are very poor values) up to 40 ÷ 45% as regards the most performing ones. In particular, one can observe two main development lines: the higher one is limited to about 50 MW_{el} (apart from one specific model), where the best efficiencies are reached, while the lower one extends to the highest sizes, getting near to 40%. These two ideal lines are associated to two different families of gas turbines dedicated to power generation: aero-derivative and heavy-duty. As suggested by the name, the former is constituted by turbines deriving from engines specifically designed and developed for aeronautical propulsion, with as little as possible modifications, characterised by extreme operating parameters, with the goal of efficiency optimisation. On the other hand, heavy-duty turbines are directly developed for stationary applications and are therefore characterised by a more essential design, even because they are typically used in combined cycles and the main aim is no more the performance optimisation of just the gas turbine but of the whole plant, which requires less advanced parameters [2.8].

If the efficiencies of small gas turbines are quite low, it is clear that unacceptable performance would characterise models having an even smaller size (< 500 kW_{el}) if machine architecture and operating features were not reconsidered. For this reason,

several configurations, differing from the original scheme described above, have been proposed and investigated (a good synthesis is reported in [2.9]), but the largely prevalent solution, developed in last years, is given by the regenerative open cycle: indeed, the expression micro gas turbine, that should be referred to all the various plant typologies on these scales, normally indicates implicitly this specific solution. However, also externally fired gas turbines represent an interesting option and are being taken into account in this work, even if their commercialisation is still at an early stage.

2.4.1 Micro gas turbines

Differences between "classic" gas turbines and micro gas turbines (mGT, Figure 2.11) concern almost all the main components of the plant (except for the combustor).

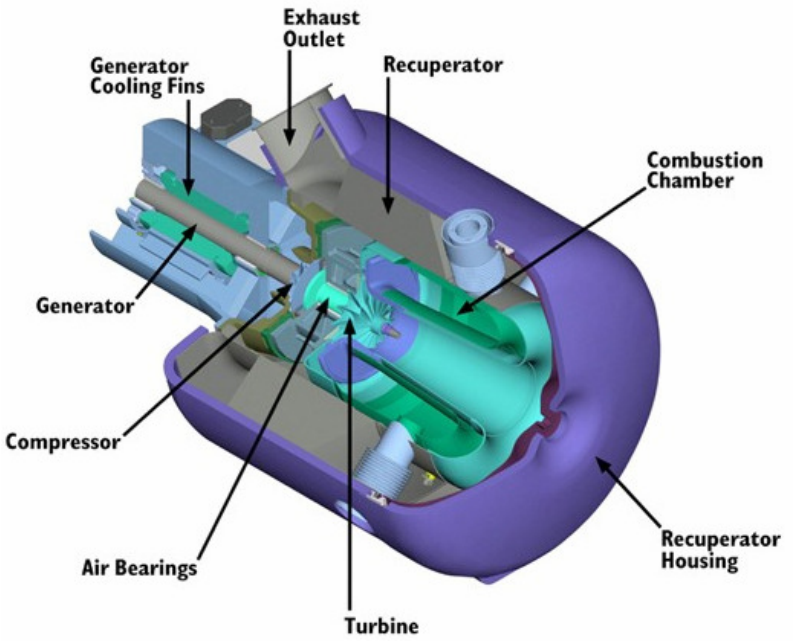

Figure 2.11 – An example of micro gas turbine (scheme) [2.10].

The main unit is composed of a centrifugal compressor and a centripetal turbine, both single-stage and mounted on a shaft operating at a very high rotational speed (50,000 ÷ 120,000 rpm), necessary to reach good performance with low mass flow rates (and thus small machines): the device is analogous to an ICE turbocharger. A recuperator is always installed: before entering the combustion chamber, air exiting the

compressor passes through it, absorbing heat from hot gases at the turbine outlet. After combustion, hot gases expand through the turbine and cross the recuperator, as already mentioned. Finally they are discharged or, more often, since they normally have a good heat content (temperature is about 250 ÷ 300°C), pass through a cogenerative exchanger, which allows the production of useful heat, in the form of hot water or low-pressure steam. In most models, in order to avoid the adoption of a mechanical reduction gear, a permanent magnet generator is mounted on the shaft and produces high frequency electricity, then rectified and finally inverted to 50 Hz (or 60 Hz) AC, which allows a good part-load adjustment. A picture of a mGT rotor and a scheme of a CHP mGT are shown, respectively, in Figures 2.12 and 2.13.

Figure 2.12 – A rotor of a micro gas turbine (generator, compressor and turbine).

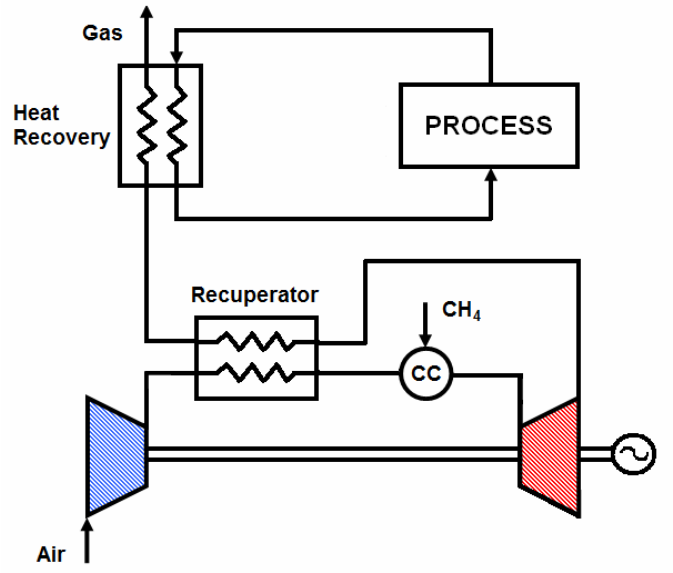

Figure 2.13 – Scheme of a cogenerative micro gas turbine.

The adoption of the recuperator is vital to achieve good efficiencies even with the limited pressure ratio (normally 4 ÷ 4.5[7]) allowed by single-stage radial machines. In fact, in case of simple cycle, with such a low pressure ratio, temperature would be very high at turbine outlet and very low at combustor inlet, which would imply unacceptable efficiencies. On the other hand, a pressure ratio increase would require the adoption of multi-stage machines, with consequent increase in investment costs. The installation of a recuperator solves these problems, because it exploits the energy contained in the flue gases to heat the air entering the combustor. Indeed, as shown in Figure 2.14, a further pressure ratio increase would be disadvantageous, because of losses due to inefficiency of the machines, that grow proportionally to the work and thus to the pressure ratio [2.2].

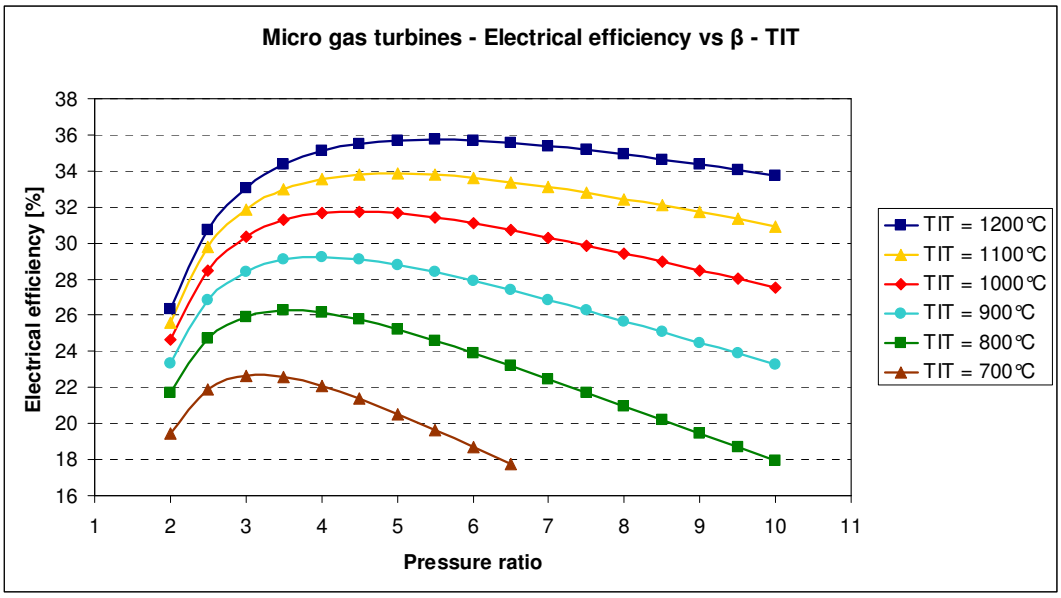

Figure 2.14 – Electrical efficiencies of mGT regenerative cycles as a function of pressure ratio (β) and turbine inlet temperature (TIT)[8].

Turbine inlet temperature is normally 900 ÷ 950°C, since turbine cooling is not performed: the corresponding optimum pressure ratio is, not by chance, 4 ÷ 4.5, as

[7] In small simple-cycle turbines pressure ratio is generally 8 ÷ 15.

[8] Results have been obtained via simulations in Thermoflex™ adopting average design values (being a complementary analysis, details are not discussed). The software will be described in the next chapter.

mentioned above. Under these conditions, one can achieve an electrical efficiency of about 30%, which is a value that simple-cycle gas turbines reach at about 5 MW_{el}-scale (see Figure 2.10). Higher efficiencies would obviously be possible with higher turbine inlet temperatures: in this sense, R&D is currently more directed towards investigation of ceramic materials (see for instance [2.11]) rather than integration of cooling systems.
Considering the importance of the recuperator, it may be interesting to analyse the incidence of its effectiveness on the electrical efficiency. However, first of all, it is important to note that there are two commonly used definitions of this parameter. In Thermoflex™ (and thus in this work) the following is adopted:

$$\varepsilon = \frac{Q_{ACTUAL}}{Q_{MAXIMUM}} \tag{2.1}$$

where Q_{ACTUAL} is the actual rate of heat transfer, while $Q_{MAXIMUM}$ is the maximum heat transfer rate that would be transferred by a counter-flow heat exchanger of infinite size with zero losses, associated with zero pinch temperature difference.
The other definition is given by the ratio of temperature change in the stream with lower heat capacity to the difference between the incoming temperatures of the two streams. For example, referring to the T-Q (temperature-heat transfer) diagram of a generic counter-flow heat exchanger shown in Figure 2.15, it is defined as follows:

$$\varepsilon = \frac{T_{h,i} - T_{h,o}}{T_{h,i} - T_{c,i}} \tag{2.2}$$

Equation (2.2) is actually a simpler special case of the previous definition and can be suitably used if working fluids are incondensable gases or if operating conditions are far from phase transitions, nevertheless they may lead to some problems if used to describe a heat exchanger where a phase transition takes place. In fact in these cases the pinch point may be located not at the exchanger ends, but in an intermediate zone, thus making this formula inappropriate. In order to avoid such problems and to use an always valid definition, Equation (2.1) is therefore being preferred here.

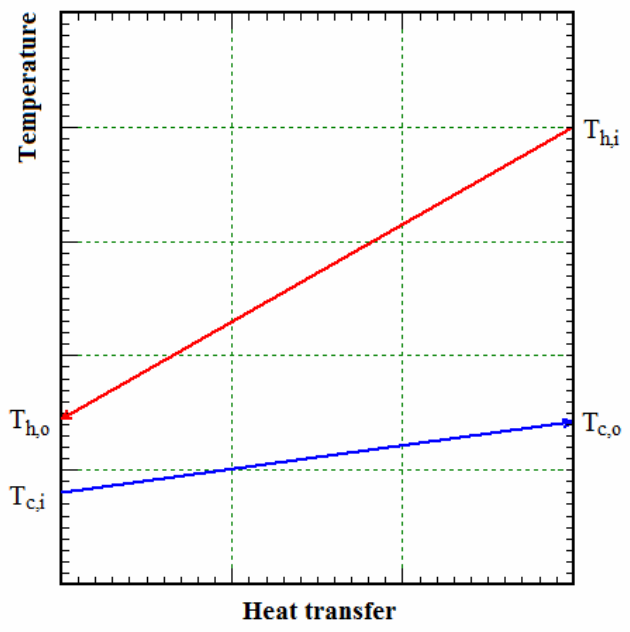

Figure 2.15 – T-Q diagram of a generic heat exchanger.

Getting to the heart of the matter, in Figure 2.16 one can observe the progress of electrical efficiency (fixing TIT at 950°C) as a function of pressure ratio and heat exchanger effectiveness, the latter varying in the range 80 ÷ 90% (previous results were obtained with ε = 85%).

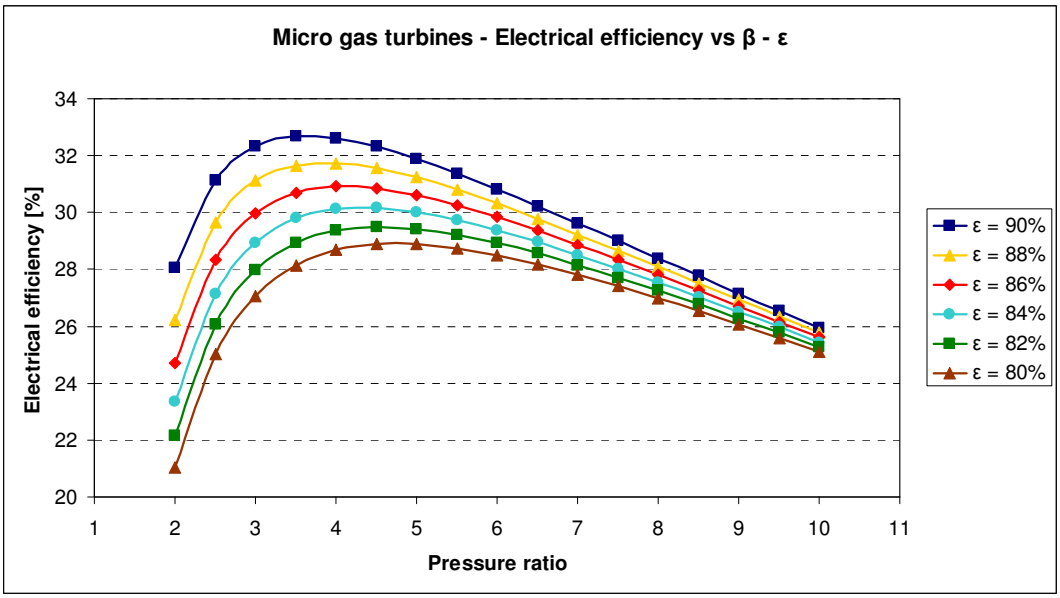

Figure 2.16 – Effects of the heat exchanger effectiveness on mGT electrical efficiency.

One can observe that, as predictable, electrical efficiency increases with increasing heat exchanger effectiveness, even if all curves finally converge in one single point, corresponding to the maximum pressure ratio that makes regeneration possible. The maximum point of the curves gradually moves towards low values of pressure ratio, from 4.5 to 3.5 (with $\varepsilon = 100\%$, the optimum β would be about 2, while it is equal to 1 in case of ideal cycles, as well known). Besides, the progressive electrical efficiency increase becomes more and more considerable, thus justifying the effort to achieve higher and higher effectiveness. However, regarding this, it has to be taken into consideration that increasing effectiveness implies heat exchanger size increase (and consequently costs increase, too), becoming dramatic above 90%, as shown in Figure 2.17, where size is expressed with the dimensionless parameter NTU (Number of Transport Units), defined as follows:

$$NTU = \frac{U \cdot A}{C_{min}} \tag{2.3}$$

In the formula, U is the overall heat transfer coefficient, A is the exchange area, while C_{min} is the lower heat capacity between the two streams. As a consequence, practical trade-off values are normally fixed in the range $85 \div 90\%$ (this is valid not only for recuperators, but also for heat exchangers in general terms) [2.8].

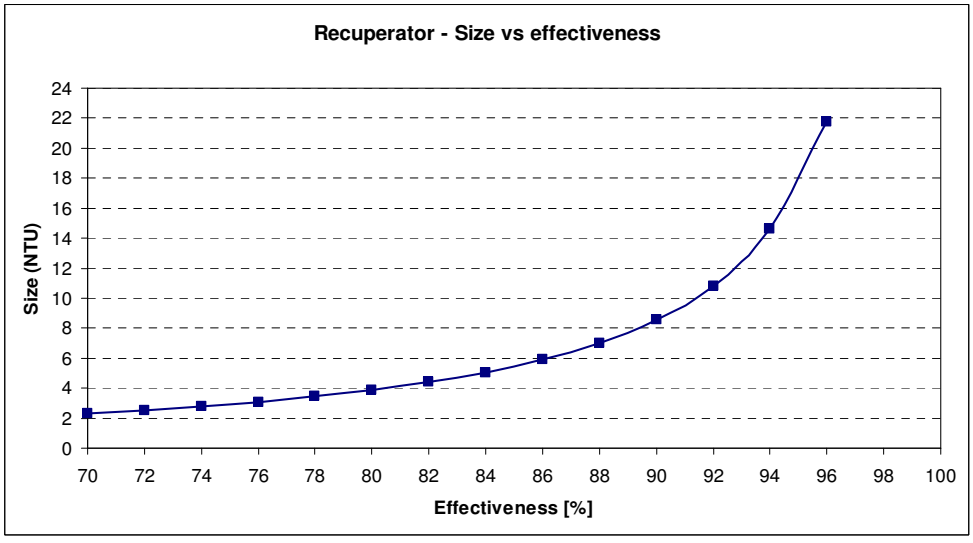

Figure 2.17 – Relation between effectiveness and size for counter-flow recuperators.

Returning to microturbines, at the moment there are eight models available on the market, having a power capacity ranging between 30 ÷ 250 kW_{el}, with corresponding efficiencies of 25 ÷ 33%, as shown in Figure 2.18.

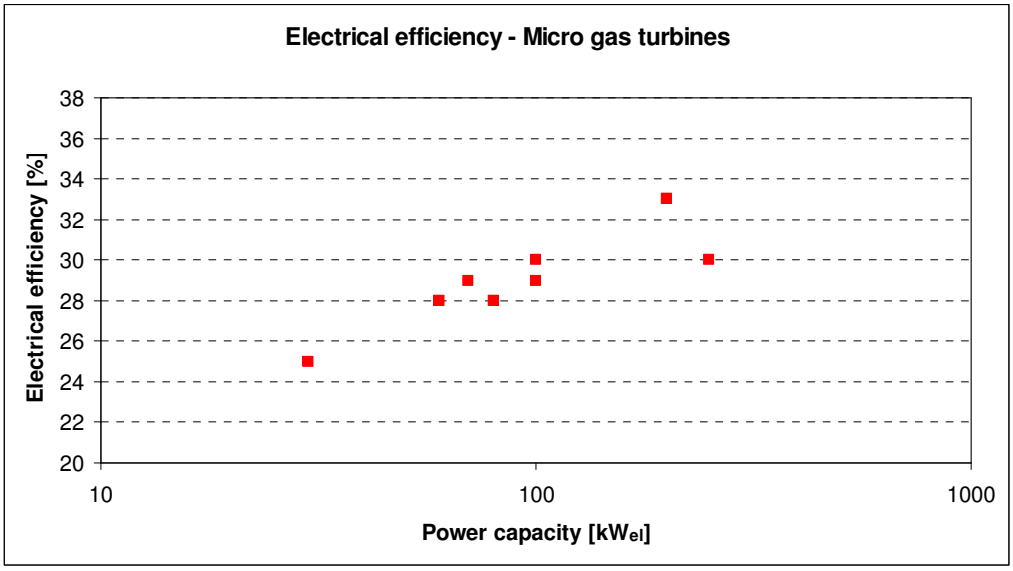

Figure 2.18 – Electrical efficiency of micro gas turbines as a function of size.

Comparing this figure with Figure 2.5, it appears that microturbines performance is comparable with the one of internal combustion engines, although being slightly lower (see next section for deeper considerations). Besides investment costs are a little higher (1100 ÷ 1400 €/kW_{el}) and reliability cannot be considered analogous to the engines one, although generally, it has been demonstrated.

On the other hand, the great advantage granted by micro gas turbines consists in the very low level of pollutant emissions, resulting about one order of magnitude lower than those of reciprocating engines (e.g. CO and NO_x emissions are lower than 100 ppm @ 15% O_2) Besides it has to be taken into consideration that all waste heat usable for cogenerative purposes is contained in the medium-high temperature flue gases, while in internal combustion engines it is shared (averagely in equal measure) between high-temperature gases and low-temperature water: in practical cases this could be a constraint regarding adoption of one solution rather than the other.

Anyway, apart from this point, the solution represented by internal combustion engines is more frequently adopted, except from specific cases of particularly strict

environmental requirements. Indeed, great R&D efforts are being made and it is easily predictable that in the next years, microturbines will become fully competitive with reciprocating engines.

2.4.2 Comparison among ICE, GT and mGT

In the previous sections, performance of the presented technologies, in terms of electrical efficiencies, has been discussed. In order to carry out some preliminary hypotheses concerning the results of this work, it may be interesting to compare those values, and in particular the ones relating to the considered scales (100 kW_{el}, 1 MW_{el} and 5 MW_{el}), compressing Figures 2.5, 2.10 and 2.18 in one single graph, as shown in Figure 2.19.

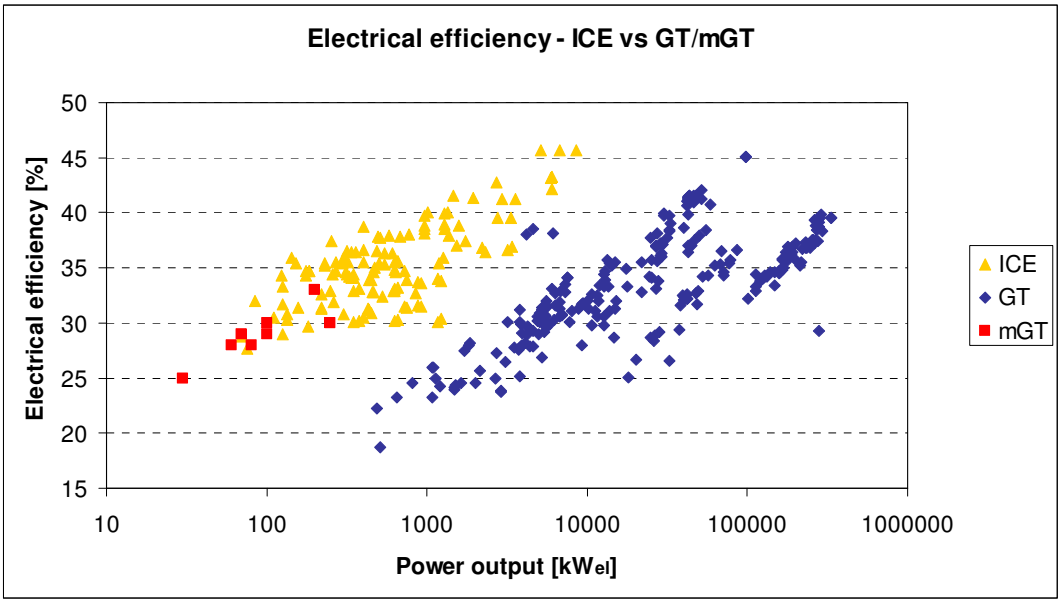

Figure 2.19 – Electrical efficiency of ICEs, GTs and mGTs as a function of size.

As mentioned in the previous section, at 100 kW_{el} reciprocating engines and micro gas turbines have a similar electrical efficiency, being about 30%. On the other hand, gas turbines on the two larger sizes are available in the classic simple-cycle configuration, which, as discussed, is strongly penalised by size effects, while internal combustion engines are here present with their most performing models. GTs efficiency is in fact

about 25% at 1 MW_{el}, being much lower than 35 ÷ 40% of internal combustion engines: a difference of 10 ÷ 15%. The same applies for 5 MW_{el}, where efficiencies of both the technologies increase by about 5%: GTs reach 30% and analogously ICEs grow up to 45%. Only adopting regenerative[9] or STIG[10] solutions, gas turbine can achieve about 38%, which, however, is still significantly lower than ICEs result.

Basing on these data, one can hypothesise that, also in case of biomass feeding, reciprocating engines and turbines will be competitive at 100 kW_{el}, while the former will result absolutely favoured on the two larger scales: actually, this is roughly what happens, as will be discussed hereinafter.

Finally, it must be pointed out that the ORC technology also considered in this work has not been taken into account in this particular analysis because it is an externally-fired solution. In fact its performance is similar independently from the feeding fuel and would result too much penalised by a comparison with internally-fired internal combustion engines and turbines, enjoying the advantages of natural gas feeding, but requiring significant modifications to allow the use of biomass. A similar concept is applicable for externally fired gas turbines, for which, moreover, performance data of commercial plants are not available.

2.4.3 Externally fired gas turbines

As the name suggests, externally fired gas turbines (EFGT) are plants in which combustion does not involve the working fluid that flows through the turbine, but occurs in a combustor placed downstream of this component. Thus fluid heating, that is simply air, is performed by means of a heat exchanger, as shown in the scheme of Figure 2.20 (heat recovery for CHP is also taken into account). As one can see, it is very similar to the micro gas turbine, with a “simple” (but obviously significant) position reversal between the turbine and the combustion chamber.

[9] On these scale, low pressure ratios imply that turbine outlet temperature is higher than compressor outlet one, thus allowing a regenerative process. Nevertheless it is rarely being applied because increasing efficiencies normally do not justify higher bulks and costs.

[10] STIG (STeam Injected Gas turbine) is a technology based on the injection of steam, produced using hot flue gases, in the turbine combustion chamber, which allows to enhance efficiency and power output.

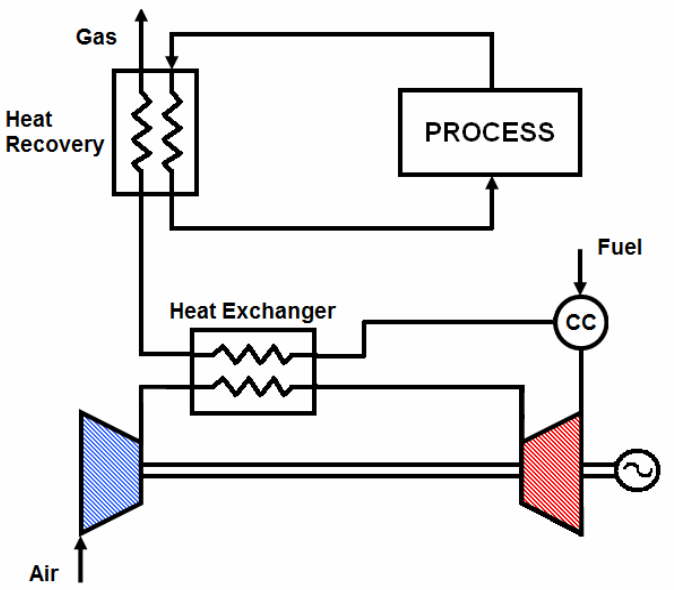

Figure 2.20 – Scheme of a cogenerative externally fired gas turbine.

This configuration has been profoundly investigated and developed with the aim of eliminating one of the gas turbine's major limitations, i.e. the necessity to feed the plant with clean fuels in order to avoid erosion, deposition and corrosion phenomena on the expander: feeding with solid and/or dirty fuels (coal, biomass, tars) is now accepted, without requiring any previous conversions (pyrolysis or gasification), since exclusively air flows through the turbine (obviously the cited problems may concern the heat exchanger, but here they are in general less onerous than on the turbine). It is important to note that these plants were originally studied referring to coal feeding in large scale turbines [2.12]: these scales are presently investigated, too [2.13], but considering also the excellent performance of the corresponding methane-fired internal combustion turbines, this technology seems to be more interesting on small scales with biomass feeding [2.14].

Another advantage consists in the fact that combustion (almost) occurs at ambient pressure, and not under pressurised conditions as in internally-fired turbines, which is a good point especially for solid fuels. Besides, the combustion chamber is normally placed downstream of the turbine, in order to recover the air sensible heat in the combustion process, even if it could theoretically be fed directly with cold ambient air.

The main limitation of this technology lies in the achievable low turbine inlet temperature. In fact this value is related to the heat exchanger's thermal characteristics (now not being a simple recuperator anymore) and the currently used classic metallic devices normally withstands a 800°C working temperature on the hot gas side, implying a turbine inlet temperature equal to about 700 ÷ 750°C. Higher temperatures, mandatory to reach good efficiencies, are achievable adopting superalloys or, above all, ceramic materials. Apart from high costs, there is a debate in literature concerning the actual applicability of this solution, mainly with respect to reliability and durability (see for instance [2.15] and [2.16]). Anyway, this is undoubtedly not a commercially proven technology.

Similarly to what done in Figure 2.14 for micro gas turbines (that could be called Internally Fired Gas Turbines, IFGT, by analogy with EFGTs), the performance of externally fired gas turbines as a function of pressure ratio and maximum cycle temperature is shown in Figure 2.21 (results have been obtained in simulations performed adopting the same design parameters of the previous case).

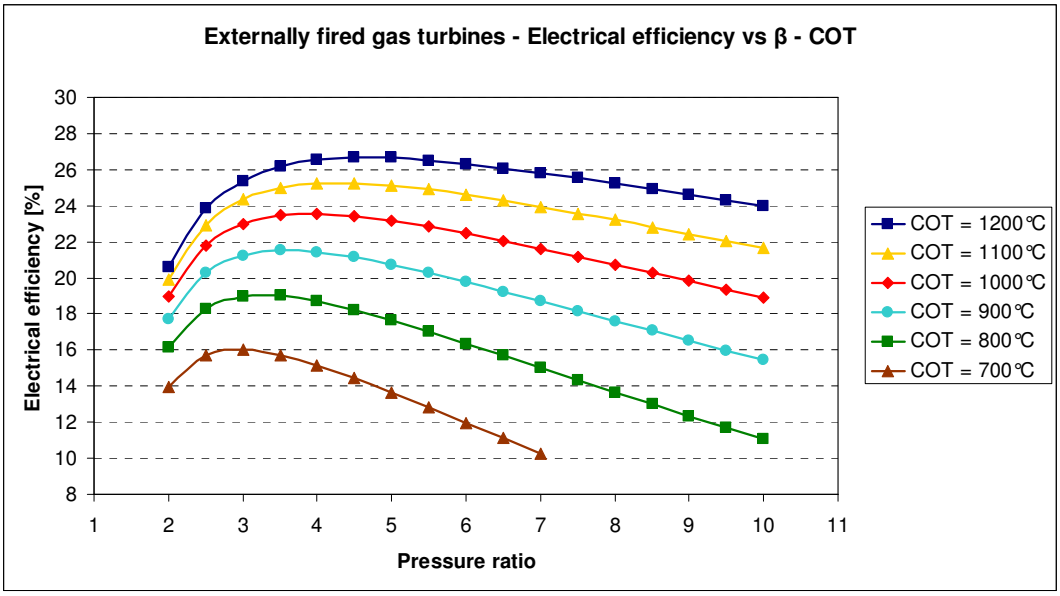

Figure 2.21 – Electrical efficiencies of EFGTs as a function of pressure ratio (β) and combustor outlet temperature (COT).

First of all, one can see that the maximum cycle temperature is no more the turbine inlet temperature, TIT, but COT, standing for Combustor Outlet Temperature. In fact in IFGTs they coincide (at least on first approximation) and one usually refers to TIT; on the contrary, in EFGTs these values are different due to the plant architecture and therefore COT must be used. However, the curves progress is similar to the previous case: as indeed predictable, efficiency reaches a maximum here, too and then decreases with increasing pressure ratio, even if maximum values are detected in a smaller range of pressure ratios (3 ÷ 4.5 against 3 ÷ 5.5); on the other hand, values are significantly lower: in particular differences in the maximum efficiencies are about 7 ÷ 9% in absolute terms, that is 30 ÷ 40% in relative terms. As obvious, this is mainly due to the different role of the heat exchanger and in fact TIT, that is the real main operative parameter, is now considerably lower than the corresponding COT: indeed with ε = 100%, COT and TIT would be equal and the efficiencies themselves would also be almost equal. Of course there would be several other factors (even conflicting, e.g. the stream flowing through the turbine in EFGTs has lower mass flow rate and specific heat capacity in respect to the IFGT case, but fuel compressor consumptions are also lower, etc.), but they are of minor importance.

Finally, the incidence of the heat exchanger effectiveness on EFGTs electrical efficiency is shown in Figure 2.22 (in this case COT is fixed at 950°C).

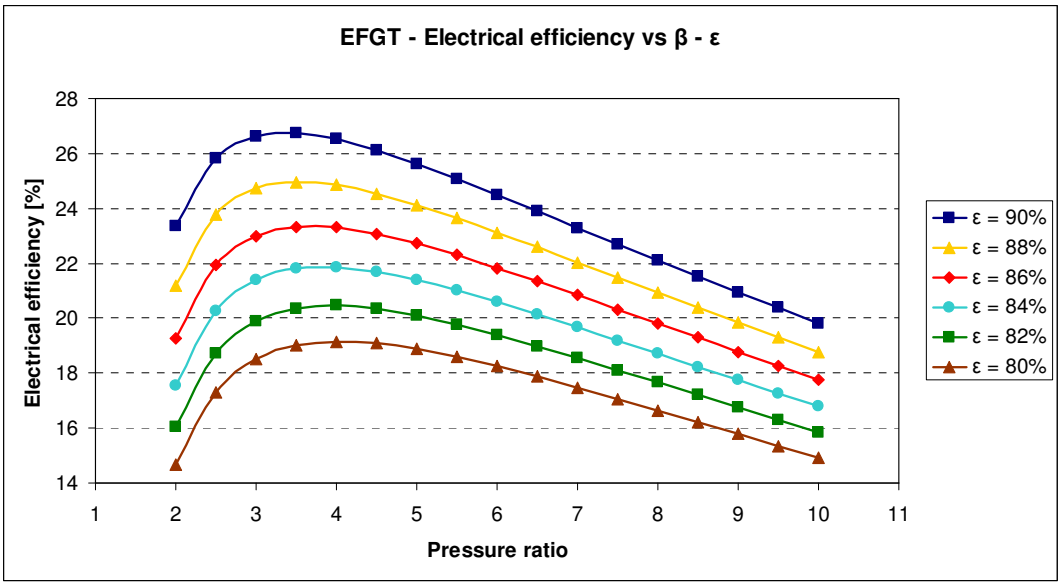

Figure 2.22 – Effects of the heat exchanger effectiveness on EFGT electrical efficiency.

The progress of the curves is analogous to the mGT case and, again, optimum pressure ratios are found in a more limited range (3.5 or 4). Nevertheless, the curves converge at a much higher pressure ratio (if convergence occurs before zero efficiency) and, above all, they are more distant one from the other, demonstrating that the heat exchanger performance is now even more important that in IFGT turbines.
Similarly to what discussed in the previous section, these comparisons may also be very useful in view of prediction of the results that will be obtained in the simulations with biomass feeding.

2.5 Organic Rankine cycles

Organic Rankine Cycles (ORC) represent a technology originally applied in the field of geothermal energy conversion, which, in recent years, has been affected by considerable diffusion in small-size cogeneration, especially using biomass as energy source. Commercial solutions are normally available in the power capacity range of 200 kW_{el} ÷ 2.5 MW_{el}, therefore only 1 MW_{el} size, among the three considered in this work, would be available. Nevertheless the other two scales can also be taken into account. On one hand, in fact, it is sensible to suppose that the 100 kW_{el} solution will be developed in the near future, since technological modifications necessary to this operation starting from the 200 kW_{el} models are not expected to be dramatic. On the other hand the upper size limit is not due to technological constraints, but essentially to the availability of the heat source: customised solutions up to 10 MW_{el} can be produced on demand [2.17]. Moreover, ORCs denote essentially no size effects on energy performance, the smallest plants as well as the larger ones being characterised by the same electrical efficiency: it may therefore be hypothesised that 5 MW_{el} capacity is reached adopting more than one smaller plant in series.
As the name suggests, the technology is based on a closed Rankine cycle, where the working medium is no more water but an organic fluid, more suitable than the former when the feeding heat source is at medium-low temperature (say 70 ÷ 400°C), which implies working pressures and temperatures that lead to high specific volumes and volumetric flow rate if water were used. For this reason, ORC plants are applied in

exploitation of the mentioned geothermal energy, but also in the solar thermal energy field (especially coupled with parabolic concentrators) or in waste heat recovery (e.g. from exhaust gases exiting internal combustion engines, gas turbines, industrial furnaces, etc.). In this sense, the use of biomass, that is obviously burnt in a furnace, is not an optimum solution from an exergy point of view, because the hot valuable gases produced in the combustion are used to feed a power cycle that is thermodynamically quite poor; nevertheless there are other features, discussed below, that make this option interesting: this configuration will be considered hereinafter.

Figure 2.23 shows a complete scheme of an organic Rankine cycle plant fed via biomass combustion.

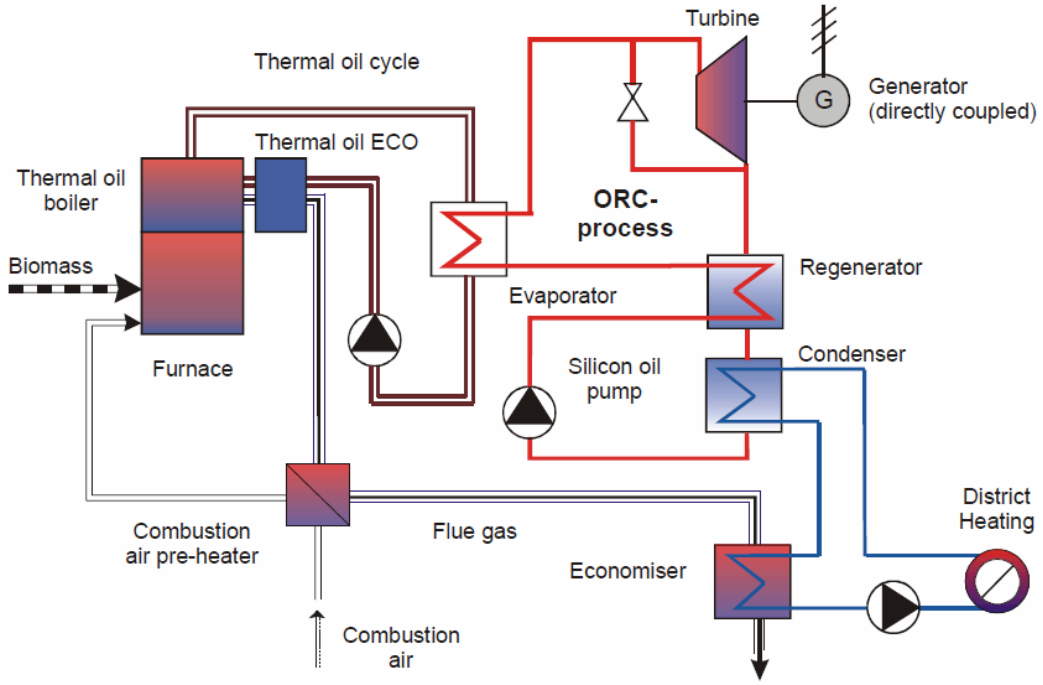

Figure 2.23 – Scheme of a biomass-fired ORC plant [2.18].

The combustion takes place in a furnace where heat is not directly transferred to the working fluid, but is absorbed by an intermediate thermal oil, typically at a temperature of 300°C. Higher values are not allowed because oil must remain at liquid phase: this limits the maximum cycle temperature even when a hotter heat source could be available. The oil is being sent to the ORC unit evaporator, where it releases heat to the working fluid, like in classic Rankine cycles. The latter evaporates, then flows through

the turbine, yielding mechanical power that is converted to electric by means of the alternator. The fluid still being in vapour phase at the turbine output (this point will be discussed below), enters a regenerator and is finally being sent to the condenser, where it releases its latent heat to the thermal user. The liquid is then being pumped and, after crossing the regenerator, it returns to the evaporator. On the other hand, hot gases exiting the furnace are normally used first to pre-heat the combustion air and then to provide a further thermal power to the process (obviously in case of high heat demand, the pre-heater can be by-passed, although at the expense of electrical efficiency). In case of waste heat recovery, the furnace is substituted by a simple heat exchanger, where the hot stream heats the thermal oil (which can be heated just up to 200 ÷ 250°C if available temperatures are low).

Figure 2.24 gives an overall view of an ORC unit (thus excluding the biomass furnace, if present): it can be noted that condenser and regenerator are clearly the largest components.

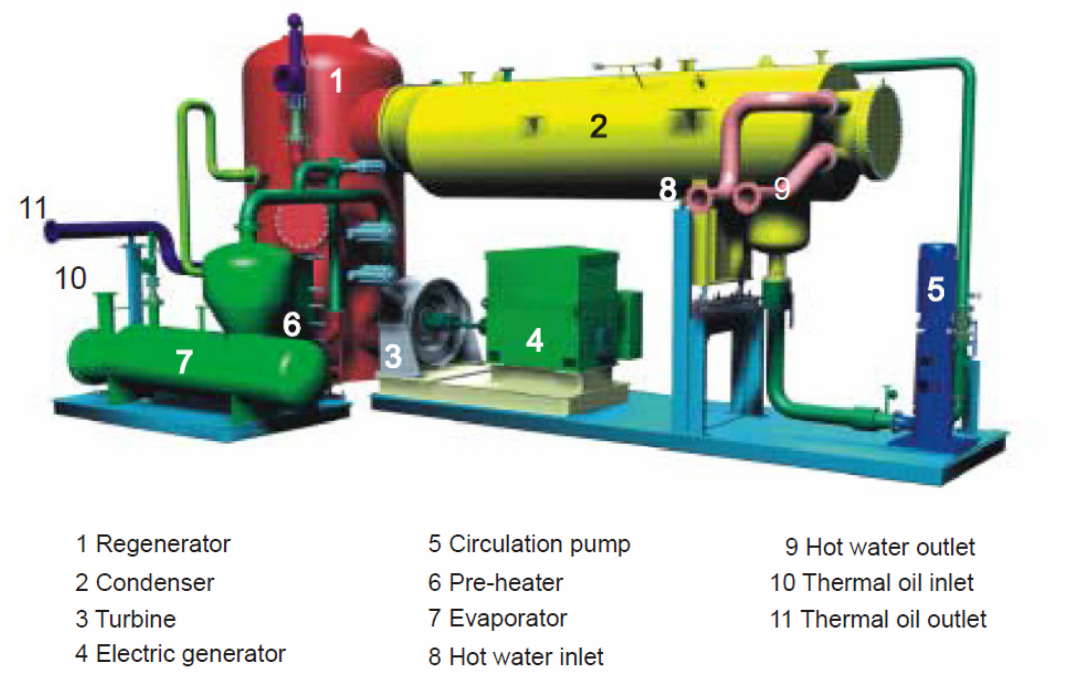

Figure 2.24 – Picture of an ORC plant [2.18].

A typical energy balance of a biomass fired ORC plant is instead shown in Figure 2.25: as one can see, electrical efficiency is about 15%, but the recovery of the condensation heat allows to reach a very high thermal efficiency, about 75%. As a result, first law efficiency can achieve even 90%[11].

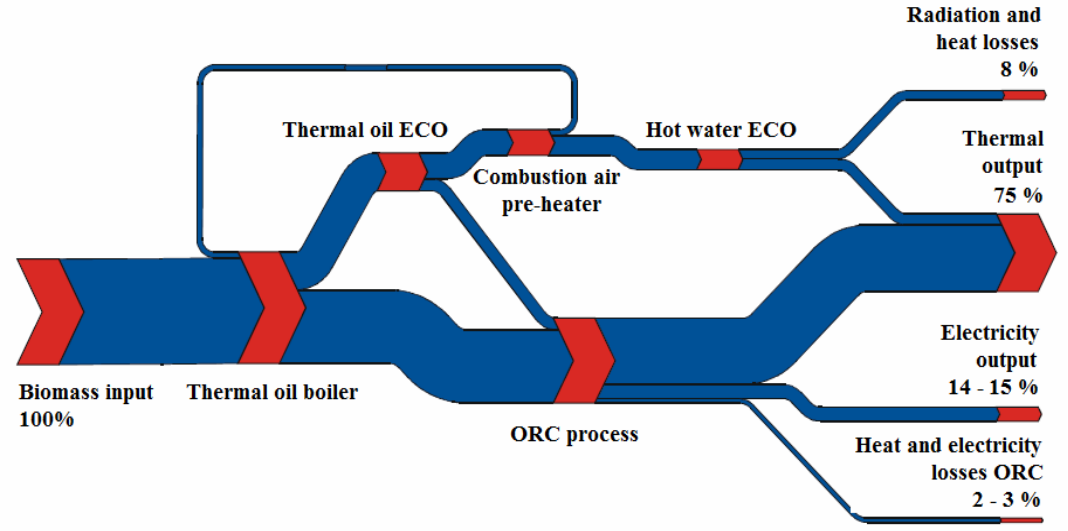

Figure 2.25 – Typical energy balance of a biomass-fired ORC plant [2.18].

As one can see, electrical efficiency is significantly lower than the one reached by internal combustion engines and gas turbines, even considering penalisation due to the fact that it is an external combustion plant. Indeed, this parameter is variable adjusting the condensation temperature. In fact, the case described above refers to the typical configuration in which the organic fluid condensates at 90°C, thus allowing the production of hot water for heating purposes, but it can be lowered down to 40 ÷ 50°C: in this case electrical efficiency raises to about 20%, but it is clear that useful heat recovery is no more possible (neglecting contribution of flue gases). This is why the CHP configuration is normally preferred.

Concerning the thermodynamic cycle, given the low-temperature heat source, a superheated approach like in traditional Rankine cycles is not appropriate. Actually, a little superheating is always performed in order to prevent formation of liquid droplets at the intake of the turbine, that would damage the component, but it generally does not

[11] These values are quite standardised among the various commercial solutions (that indeed are not numerous yet).

exceed 10°C and thus the fluid exiting the evaporator is almost in saturated conditions [2.19]. It is therefore advisable not to use wet fluids, but to adopt dry or isentropic ones. This distinction is being made based on the slope of the upper limit curve in the T-s (temperature-entropy) diagram, as shown in Figure 2.26.

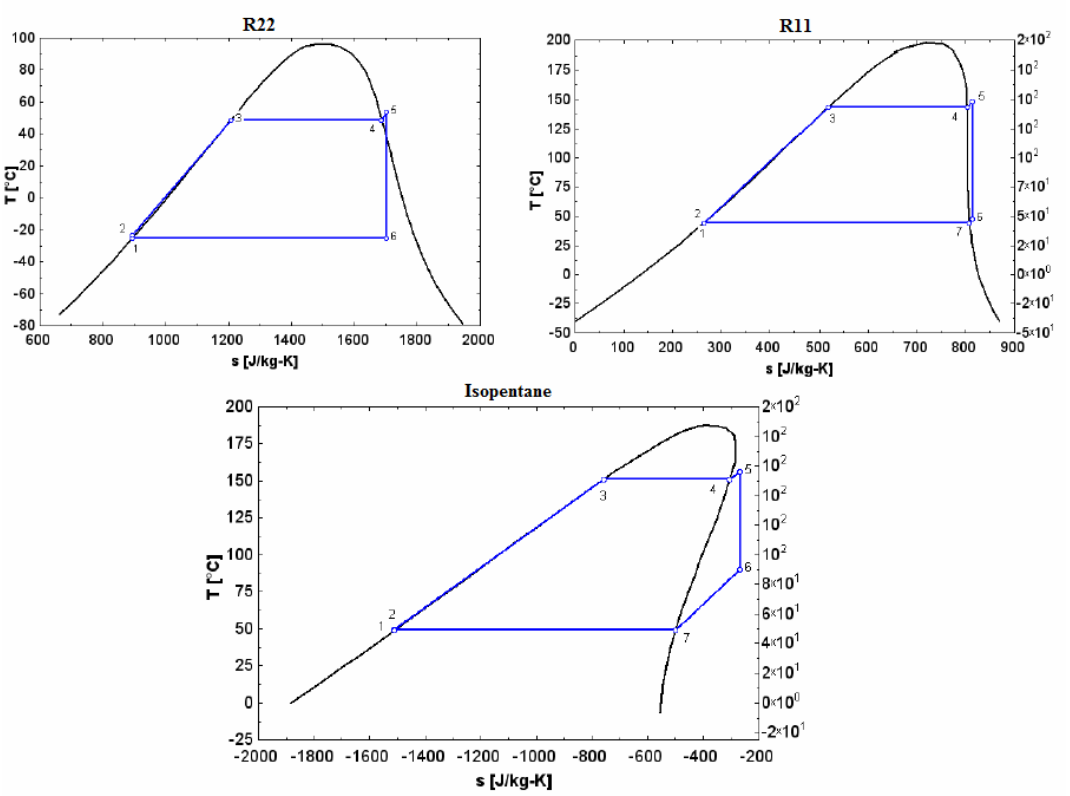

Figure 2.26 – Wet (left), isentropic (right) and dry (bottom) vapour saturation curves with the corresponding Rankine cycle [2.20].

In case of wet fluids, almost all the expansion occurs inside the two-phase region and, again, this must be avoided because of the damage which the condensate would produce on the expander. The preferable solution would be to adopt isentropic fluids, as the saturation curve fits very well the isentropic expansion line in the cycle, but the dry solution is suitable too, even because, since the fluid at the end of the expansion is still in superheated conditions, it lends itself to the adoption of regenerator that is simple a vapour-liquid heat exchanger, that yields an enhancement of the efficiency. In addition to this point, being relevant for the simulations of plant operation, the working fluid must have several other features to be suitable for use in an ORC plant: low

flammability, low freezing point, high stability at changing temperature, high vaporisation heat, low toxicity, low cost, good availability, high density, etc. [2.20]. Dry fluids are normally used also because it is not easy to find isentropic fluids with all these characteristics. Normally silicon oils are being used: in particular octamethyl-trisiloxane (normally shortened to MDM) [1.27].

As mentioned before, thermal oil working temperature limitations determine a considerable exergy loss, at least in case of biomass combustion. On the other hand this implies that the boiler works under atmospheric conditions and, since in many European countries skilled operators are required to run pressurised boilers, this means manpower cost savings: actually the operation is running totally unmanned (only few hours per week are required for maintenance and inspections [2.18]). Further advantages of the ORC technology are listed below:

- high turbine isentropic efficiency (up to 85%);
- low mechanical stress in the turbine, due to the low rotational speed (allowed by the high molecular weight of the organic fluid);
- direct turbine coupling with the alternator, without need of a gear box, due to the same reason;
- no turbine blade erosion, as a consequence of completely dry expansion;
- long unit life, thanks to the working fluid characteristics, not eroding and corroding pipes, valves and blades, as water does;
- excellent possibility of part-load (down to 10% of the nominal power), with good performance;
- high reliability and availability;
- water treatment system not required;
- simplicity of start-stop and load modulation procedures;
- low noise operation [2.21].

Among these, the most significant features are undoubtedly reliability and easy running, which, despite high investment costs (about 1000 ÷ 2500 €/kW_{el} for the ORC unit, 1500 ÷ 3000 €/kW_{el} for the thermal oil boiler, obviously decreasing with increasing size) and not excellent efficiencies (at least in pure electrical terms), sometimes make this technology preferable to other solutions, e.g. gasification, granting higher performance but being also more complex.

2.6 Other technologies

Apart from those described in the previous sections, there are other technologies that could be potentially used for power generation starting from biomass. They have not been considered in this work for various reasons: immaturity of the technology, poor performance, high costs, etc., or because they do not represent a possible solution on the considered scales. However, some of them deserve a brief description: in particular, Stirling engines, steam engines and fuel cells have been taken into account.

2.6.1 Stirling engines

Stirling engines (Figure 2.27) like ICEs, are reciprocating machines, but differently from the latter they are not interested by internal combustion, being fed with heat coming from an external source: a combustor, where any fuel (obviously including biomass) can be burnt, possibly also waste heat, etc. Working cycle is thus closed and therefore working fluid (a gas) can be anyone: helium, nitrogen, air, etc.

Figure 2.27 – Pictures of a 9 kW_{el} CHP Stirling engine package [2.2].

Stirling engines are based on the thermodynamic cycle bearing the same name. As schematised in Figure 2.28, it is composed of an isothermal compression (1-2), performed by heat release to a cold medium, that can be the water stream designed for a cogenerative use, an isochoric process (2-3), where fluid absorbs heat passing through a hot porous regenerator, an isothermal expansion (3-4), realised supplying heat from the hot source, and a final isochoric process (4-1), where hot working fluid releases heat to the aforementioned regenerator.

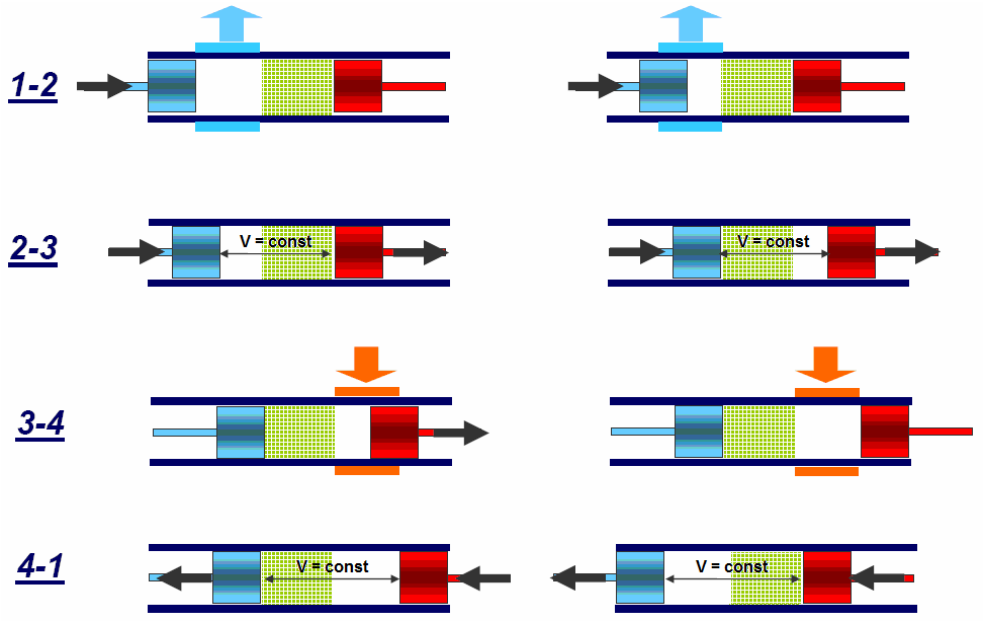

Figure 2.28 – Representation of a Stirling engine's working phases [2.22].

Stirling engines have not been taken into account in this work because they are essentially available on very small scales (< 100 kW_{el}). Electrical efficiency is strongly dependant on size, as it can range from 12 ÷ 15% of 1 kW_{el} machines to 30 ÷ 35% of 50 ÷ 100 kW_{el} ones (the latter being competitive values with other technologies). However, in the future they are supposed to be mainly used on very small scales for domestic distributed generation (in particular, CHP), last not least thanks to their high first law efficiency, which can reach up to 95%.

External feeding, as mentioned, allows the use of any fuel, because the flue gases are not involved in the working process. Besides it permits more regular operation, with low noise, vibrations, emissions (comparable with microturbines) and necessity of maintenance. Useful life is good as well (40,000 ÷ 60,000 hours). On the other hand, installation costs are quite high, at least on small scales: they can range from 2500 ÷ 3000 €/kW_{el} for few kilowatts capacity to about 1200 €/kW_{el} for tens of kilowatts (again, comparable with ICEs); besides, due to the high thermal inertia of the system, start-up time is significant.

Stirling engine cannot be considered a completely proven technology yet, even if there are several manufactures on the global market. However, energy supplying is always meant to be effected with methane, while biomass applications are still at an early stage.

2.6.2 Steam engines

Reciprocating steam engines (Figure 2.29) represent the steam exploiting solution for power purposes on small scales (capacity range is about 25 kW_{el} ÷ 1.5 MW_{el}), where steam turbines cannot be adopted. Working cycle is obviously analogous: steam is produced in a boiler, fed with any fuel (e.g. biomass, too), being then sent to the machine, where the expansion takes place supplying mechanical energy (subsequently converted in electric one by a generator); finally it is condensed (releasing its latent heat to a thermal process in case of CHP) and water is repumped into the boiler.

Figure 2.29 – A 1.5 MW_{el} reciprocating steam engine [1.24]

Inlet pressure is normally 6 ÷ 60 bar. Pressure ratio is averagely 3, up to a maximum value of 6: in case, multi-stage engines may be applied, in order to fully exploit the pressure drop and yield higher power. Moreover, doing so, electrical efficiency can raise from single-stage engine 6 ÷ 10% to 12 ÷ 20%: acceptable values (if heat recovery is being performed, obviously). Besides they are solid and proven units. However, installation of all devices required for a steam cycle (high pressure boiler, water treatment system, etc.), making the total cost rise to 2500 ÷ 4000 €/kW_{el} (depending on size), is generally not justified and this is why this solution is not widespread.

2.6.3 Fuel cells

All power technologies described up to now have the common characteristic of being based on exploitation of fuel through a combustion process (or, in some cases, of another heat source). In this reaction, the fuel chemical energy is released in the form of

heat owned by the hot product gases; heat is then used to feed a thermodynamic cycle (e.g. gas or steam cycle), where it is partly converted into mechanical work (by means of steam or gas turbines, ICEs, etc.), which in turn is transformed in electrical energy through a generator. Obviously in this chain some losses occur, but even if the process were ideal, thermodynamic limitations (i.e. Carnot efficiency) associated to the heat/work conversion would remain, determining an inevitable reduction (normally at least 20 ÷ 30%) with respect to the maximum theoretical work.

In Fuel Cells (FC, Figure 2.30), instead, the chemical energy content of the fuel is exploited in a completely different way, since it is directly converted into electrical energy by means of electrochemical reactions, thus avoiding the aforementioned chain with all its limitations: in particular no theoretical efficiency limits due to the second law of thermodynamics are present, since no heat/work conversion occurs. Obviously, due to the non-ideality of the cycle, there are losses present also in these plants, but thanks to what mentioned above, electrical efficiencies remain high, at about 40 ÷ 60%. As one can see, these are very high values, competitive with those of large scales power plants and, besides, they are coupled with exceptional environmental performance, since emissions are very low, as easily understandable. Moreover, these efficiencies can also be achieved by small-scale plants, as the technology is completely modular: plants are formed by a series of cells (hence the name), whose power can range from hundreds of watts to some kilowatts, up to a capacity of even some megawatts.

Figure 2.30 – Pictures of a 5 kW_{el} fuel cell package [2.2].

As schematised in Figure 2.31, in a typical FC the gaseous fuel (normally hydrogen, or however another gas rich in this element) is continuously being fed to the anode (the negative electrode, where oxidation of fuel and production of electrons take place),

while the oxidiser (e.g. air) is being supplied to the cathode (the positive electrode, where oxygen reduction with electrons coming from the external circuit connected to the anode occurs); the chemical reaction takes place by means of an ions exchange through the electrolyte and produces power by closing the circuit between the electrodes.

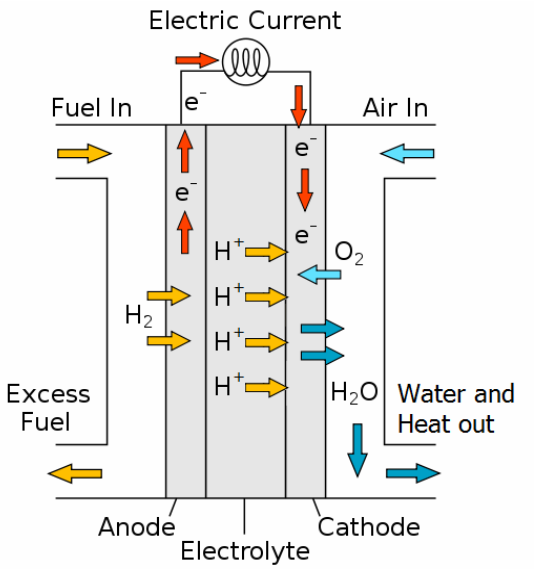

Figure 2.31 – Operational scheme of a fuel cell (adapted from[2.23]).

Fuel cells are normally classified according to the electrolyte type in the following families:

- Polymer Electrolyte Membrane (PEM) Fuel Cells;
- Phosphoric Acid Fuel Cells (PAFC);
- Molten Carbonate Fuel Cells (MCFC);
- Solid Oxide Fuel Cells (SOFC)

Among these, only PAFCs have reached a commercial stage, although investment costs are still considerably high (3000 €/kW_{el}). However, this value is expected to decrease significantly in the next years.

Possible CHP applications are due to the fact that some of these models work at medium (PAFC) or high (MCFC and SOFC) temperature, that is being kept by supplying heat (burning a share of the fuel), partly recoverable downstream of the process. Moreover, high-temperature fuel cells can be integrated with gas turbines,

realising the so called hybrid cycles, whose electrical efficiency could reach up to 70%: however, the development of this technology is still at a prototype stage.

As said, the typical fuel is hydrogen. Normally it is not directly available, so natural gas is being used, even if this implies the necessity of its conversion in hydrogen (by steam reforming, partial oxidation, etc.) in a dedicated part of the plant. Another possibility is to feed syngas (that, by definition, normally has a fair hydrogen content), produced by means of heavy fuel gasification, such as biomass. As reported in [1.34], several research investigations have been conducted on coupling of biomass gasification and fuel cells: however, this technology is far from being considered ready for use. In particular, syngas cleaning is a critical aspect, because requirements for fuel cells in this sense are much stricter than for internal combustion engines and gas turbines.

Chapter 3
Working hypotheses and preliminary analysis

3.1 Introduction

In the first two chapters biomass resource and small-scale power plants, representing the two main fields of this work, have been described: finally now the more operating phase of the thesis can begin. In particular, this chapter deals with issues and hypotheses introducing to simulations of thermodynamic performance achieved by the considered plants, whose results will be presented in Chapter 4.

As already mentioned, Thermoflex™ has been chosen to perform the aforementioned simulations: the first section will be dedicated to a brief description of this tool. This software, joined at its 18th version[1], has been used for several years by the Industrial Department of the University of Bergamo and can undoubtedly be considered proven. Nevertheless this version was the first one having a section specifically dedicated to gasification[2], thus requiring an analysis aimed at verifying the model's reliability. Besides, feeding power plants with gasification syngas involves the issues mentioned in Chapter 1, which have to be considered in the simulation parameters' definition and that will therefore be extensively discussed.

Finally all working hypotheses, concerning performance data of the reference plants (internal combustion engines, gas turbines, organic Rankine cycle plants as well as devices treating biomass) and all the other operating parameters will be presented in the last sections of this chapter. Analysed solutions will instead be described in the following one.

---

[1] Actually, version 19 has been released in 2009, but the cited version 18 has been used in this thesis work.

[2] Indeed, in the previous versions, a simple gasification model was available, but it was clearly inadequate for a thorough analysis.

3.2 Thermoflex™

Thermoflex™ is one of the various thermal engineering software products dedicated for power and cogeneration industries provided by Thermoflow Inc. Among these, one can mention GT PRO™ and GT MASTER™ (the former intended to gas turbines and combined cycles design, the latter to their performance simulation), STEAM PRO™ and STEAM MASTER™ (similar to the previous ones, but obviously concerning conventional Rankine cycles) and RE-MASTER™ (for designing and simulating repowering of conventional steam plants with gas turbines). As one can see, these are all tools specifically dedicated to single types of power plants.

Thermoflex™, instead, is a more general fully-flexible software, which can in case be integrated with the aforementioned ones, developed afterwards for modelling a great variety of thermal systems, i.e. not only gas turbines or steam cycles. It is a modular program with a graphical interface that allows the user to assemble a plant model from icons representing over one hundred different components (customised elements can also be created). An example of a simplified steam plant created in Thermoflex™ is shown for illustrative purposes in Figure 3.1.

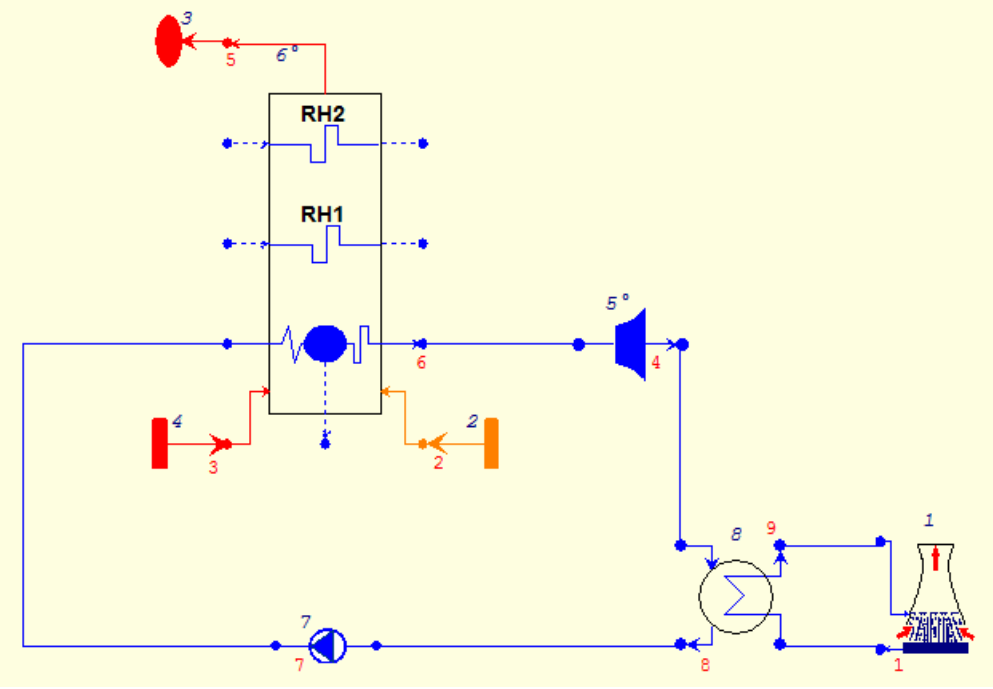

Figure 3.1 – A steam power plant modelled in Thermoflex™.

The meaning of the various components (boiler, turbine, condenser with a cooling tower and pump) is immediate. Obviously the steam generator has feeding air and fuel streams input and flue gases output.

As one can see, the different components present a specific colour depending on the treated fluid, and in particular[3]:

- red: gas (even combustion products);
- blue: water (in any phase);
- orange: fuel;
- purple: refrigerant (or however high molecular weight fluid);
- pink: thermal oil.

An option menu is associated to every component: here the user can define all design parameters (efficiencies, head or heat losses, desired pressure and temperature, etc.). Then the simulation can be run and results are finally shown, if it converged. Figure 3.2 schematises the logical process followed during the simulations: after drawing and editing phases, the software performs automatic checks in order to identify potential inconsistencies.

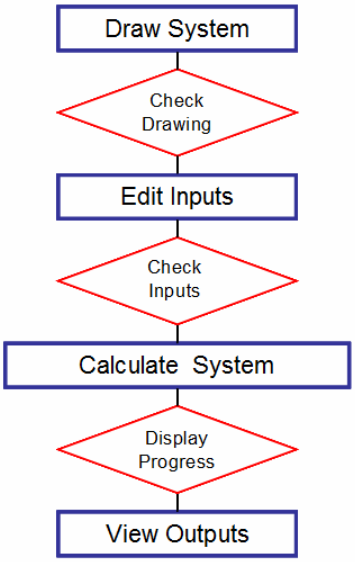

Figure 3.2 – Logical sequence of a Thermoflex™ plant simulation [3.1].

[3] Only the fluids considered in this work are listed here. These indications will be useful hereinafter, when all the simulated plant configurations will be presented.

Virtually every kind of information concerning the simulated plant is then provided:

- overall plant data (power output, electrical efficiency, heat rate, etc.);
- characteristic features of the various components (size and temperature-heat transfer diagram of a heat exchanger, steam expansion line in the enthalpy-entropy diagram for a turbine, produced or absorbed power, etc.);
- values of the thermodynamic parameters (temperature, pressure, enthalpy, steam quality in addition to mass flow rate), which may override the user's input data if necessary, in every point of the plant.

It must be specified that results implicitly refer to full-load steady conditions, while the transient phase is not analysed. On the other hand, once effected the design calculation, off-design simulations can be performed: indeed, Thermoflex™ is particularly powerful regarding this kind of analysis, although, not being required, it has not been considered in this work.

Another major Thermoflex™ feature consists in the broadness of its library, both concerning working mediums (gases, fuels, refrigerants, etc.) and, above all, pre-built commercial power plants, i.e. gas turbines and internal combustion engines. In particular, models of ICEs are very important for the purposes of this work, because they cannot be assembled starting from simpler components, but can only be used as single default machines. Gas turbines, instead, may be built up assembling compressor, combustor and turbine, in case looking elsewhere for design parameters [3.1].

3.3 Gasifier

If proper input data are supplied, Thermoflex™ can suitably simulate plants of any size. Nevertheless, it is quite inevitable that it gives greater emphasis to large combined cycles and steam plants. This point also becomes clear considering the models of gasifiers available in its library: in fact, apart from the user-defined general purpose gasifier, three specific models can be additionally chosen, but all of them refer to oxygen-blown commercial devices dedicated to coal gasification in large IGCCs. Therefore the former, that can obviously be fed with any fuel, has been taken into account in this work: it is shown in Figure 3.3.

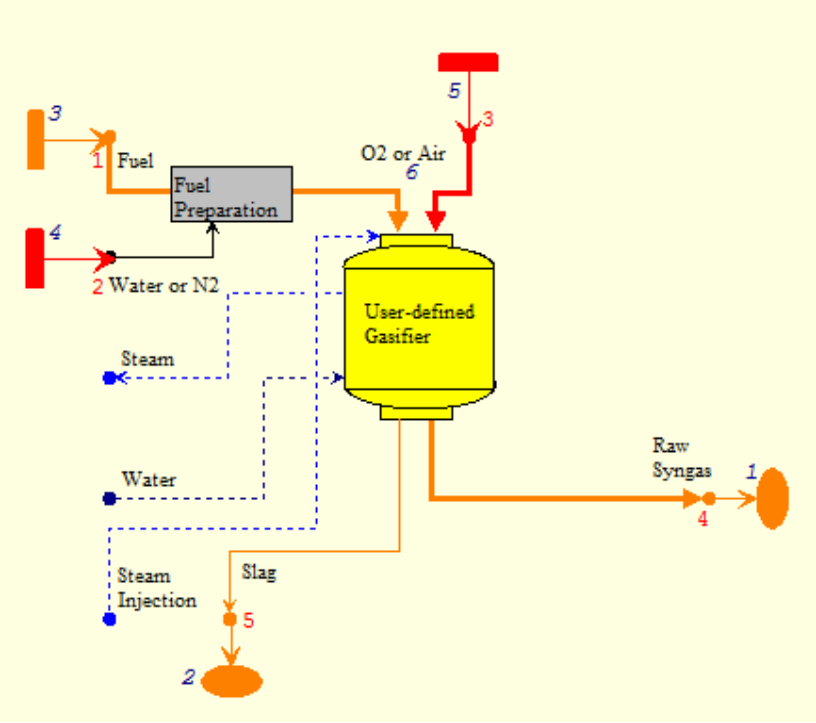

Figure 3.3 – User-defined gasifier model in Thermoflex™.

A fuel preparation unit is visible in the figure: it represents a legacy of large coal plants, where fuel is normally fed after being mixed with a water or nitrogen stream, which is necessary since those gasifiers are normally pressurised. Instead, this component is usually not present on small scales, mainly because gasifiers are normally at ambient pressure and fuel can be fed mechanically. However, Thermoflex™ forces to provide a water/nitrogen source in any case, as suggested by the solid line (while a dotted line indicates an optional input/output): simply, its mass flow rate has always been fixed equal to zero in all simulations[4]. Apart from that, then there are two input flows, the solid biomass and the oxidiser (theoretically oxygen or air), and two output flows, the raw syngas and the slag, composed of residual charcoal and ash (that actually is a fuel, hence the icon colour).

[4] For simplicity, this has also been done for pressurised gasifiers, since in case normal air would be probably used for injection, and thus the equivalent amount could be assumed to enter the gasifier by the main input duct.

The main input to define the gasifier are:

- type of oxidiser (air or oxygen: being small-scale plants, air is always being used; as one can see, water/steam can in case be fed another way);
- type of input specification by the user: air flow ratio or gasifier temperature, obviously with the respective datum (the latter was chosen in this work, letting then system fix the proper mass flow rate);
- gasifier pressure.

Other minor parameters then complete the model: auxiliaries power consumption, slag exit temperature, etc., while biomass type has previously been defined.
Syngas composition (in volumetric terms) and lower heating value as well as, given the mass flow rates, cold gas efficiency of the gasifier are the provided results.

3.3.1 Reliability of the model

As specified in the Introduction, the first operation is aimed at verifying reliability of the gasifier model supplied by Thermoflex™. Indeed, complete modelling of biomass gasification is not a purpose of this work, but is just one of the addressed issues, therefore it is sufficient here to verify that results provided by the software are in line with those found of literature or commercial plants, without discussing them too much in detail.
In particular this verification has been carried out considering two different references.
The first one is a computational code, designed for simulation of biomass gasification, available on the website of Savona Combustion Laboratory, Dipartimento di Macchine, Sistemi Energetici e Trasporti (DIMSET/SCL), University of Genoa [3.2]. It is a simple executable program, analogous to the Thermoflex™ model in terms of required inputs and provided outputs. It is quite obvious that the two models have been fed with the same wood type (weight composition: C – 50%, O – 44%, H – 6%, i.e. $CH_{1.44}O_{0.66}$ in molar terms; moisture: 10%) in the comparison analysis, varying gasification temperature in the range 500 ÷ 1200°C at ambient pressure and using air as oxidiser: results denote very good correspondence, as shown in Figures 3.4 ÷ 3.6 (the evolution of CO and H_2 content and of air/fuel ratio is presented for summary purposes, only).

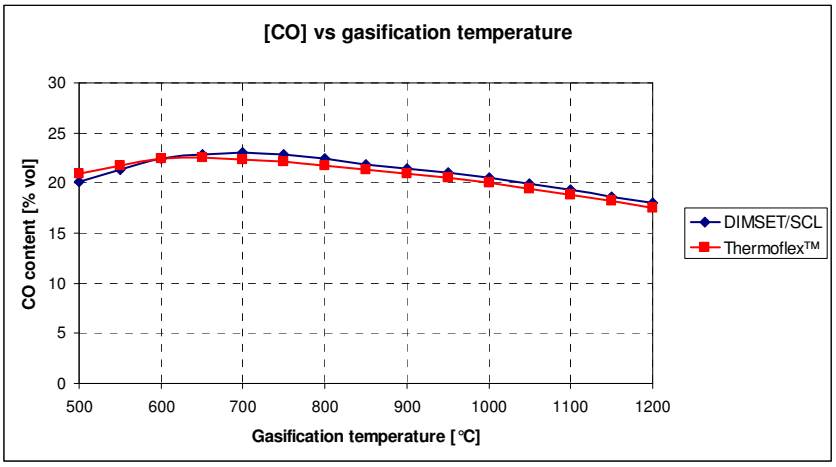

Figure 3.4 – Syngas CO content as a function of gasification temperature.

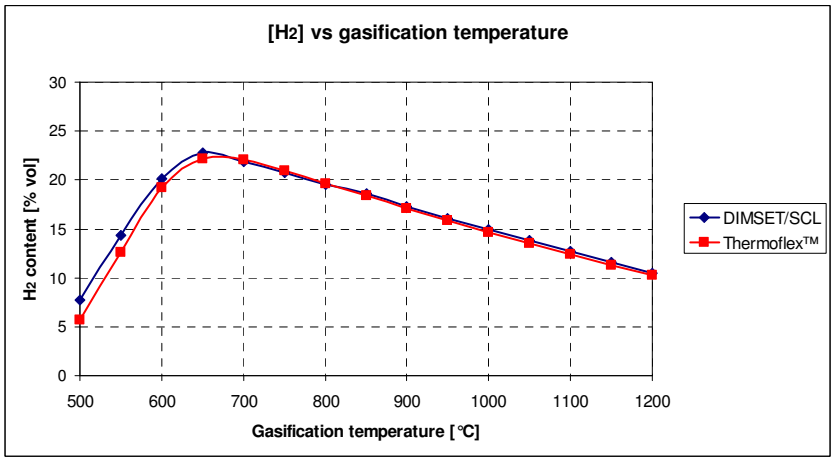

Figure 3.5 – Syngas H_2 content as a function of gasification temperature.

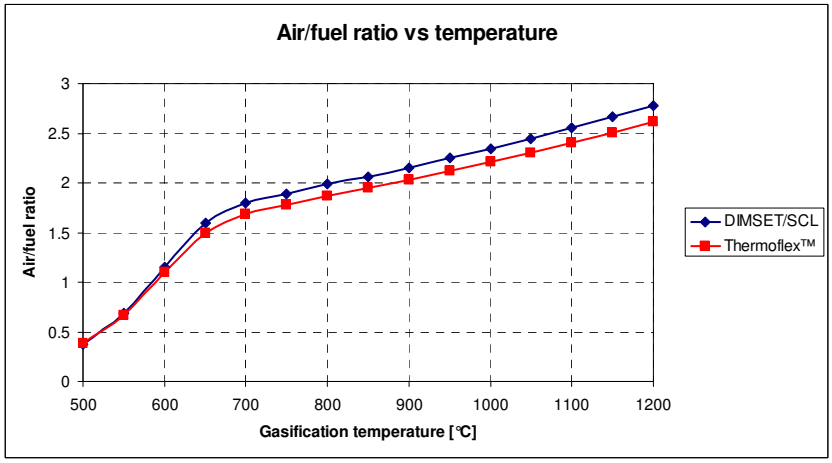

Figure 3.6 – Air to fuel ratio as a function of gasification temperature.

The second reference is paper [3.3], where the variation of syngas molar composition from biomass air gasification at different working temperatures and moisture levels is being studied using an in-house code. The adopted wood type is represented by $CH_{1.4}O_{0.59}N_{0.0017}$, that is C – 52.4%, O – 41.3%, H – 6.1% and N – 0.2% in mass fraction terms. Figure 3.7 shows the results of this analysis in the temperature range 1023 ÷ 1373 K (750 ÷ 1100°C) at two moisture levels, i.e. 0% and 30% (pressure is again equal to the ambient one).

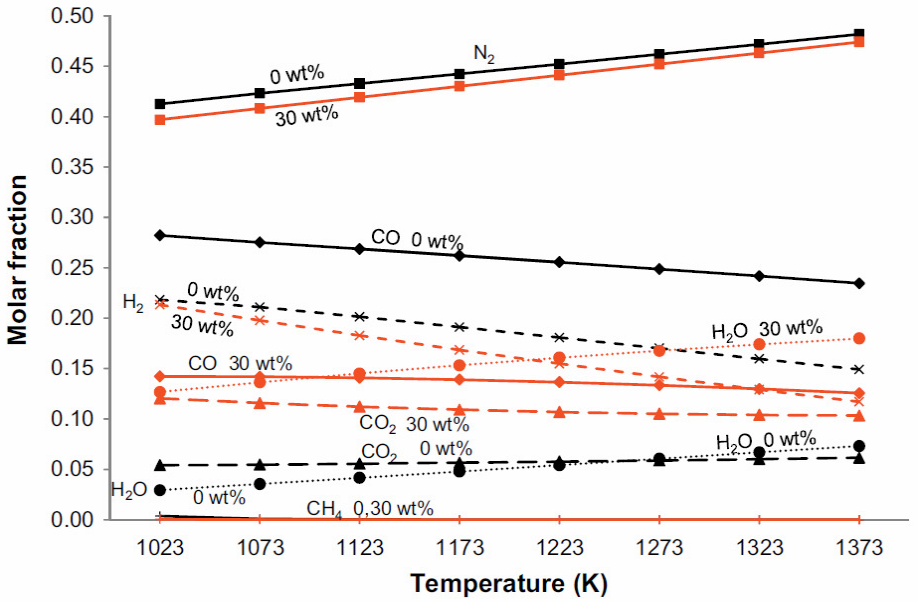

Figure 3.7 – Syngas molar composition as a function of gasification temperature and moisture [3.3].

Results obtained via Thermoflex™ simulations performed under the same conditions are instead shown in Figures 3.8 and 3.9. As one can see, the progresses of the curves at both moisture levels are absolutely analogous[5]: also in light of the previous results, one can therefore conclude that the gasification model provided in Thermoflex™ is reliable and can be suitably used for the simulations in this work.

[5] Syngas in Thermoflex™ also contains argon, deriving from air, and traces of COS and H_2S, which can cause little mismatches with reference values.

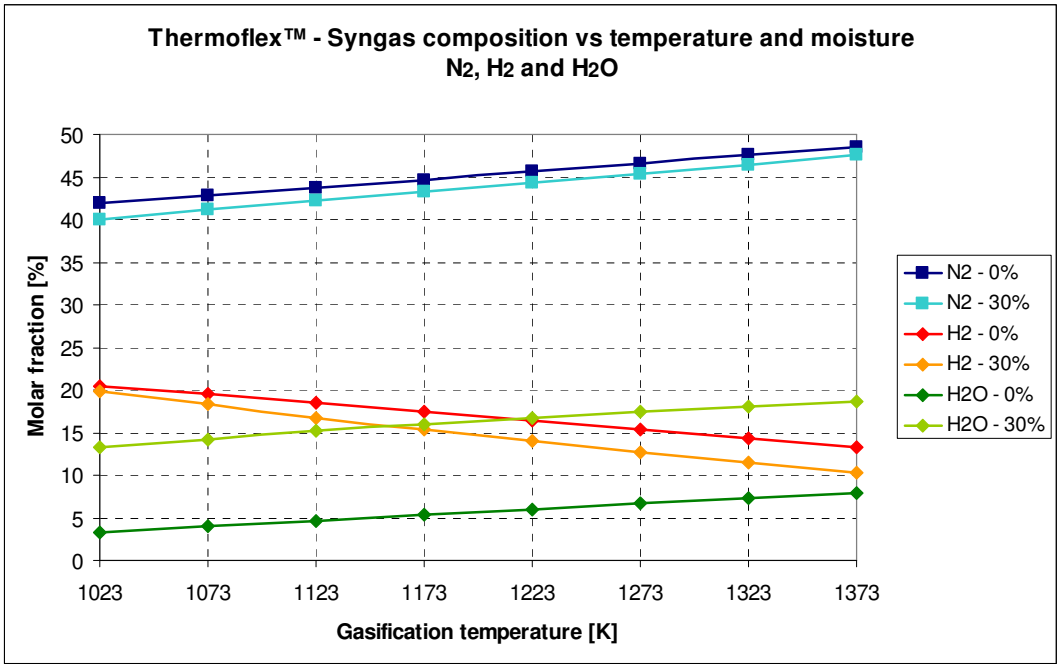

Figure 3.8 – Syngas molar composition as a function of gasification temperature and moisture: N_2, H_2 and H_2O (Thermoflex™ simulation).

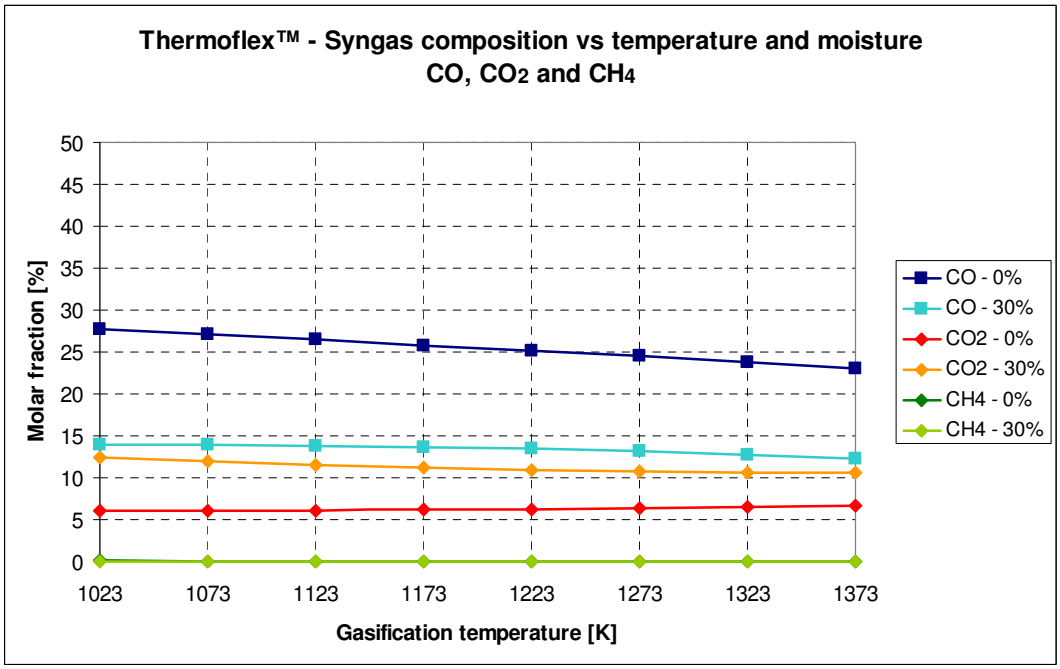

Figure 3.9 – Syngas molar composition as a function of gasification temperature and moisture: CO, CO_2 and CH_4 (Thermoflex™ simulation).

3.3.2 Reference plant

Gasifiers produced by Ankur Scientific and distributed in Italy by Caema are considered as reference in this work. They are fixed-bed downdraft air-blown gasifiers, working at ambient pressure, with the following nominal/average data [3.4]:

- combustion temperature: 1000 ÷ 1100°C
- reduction temperature: 600 ÷ 800°C
- syngas exit temperature: 500°C
- syngas composition (molar fraction, dry basis):
  - CO: 16 ÷ 18%
  - H_2: 16 ÷ 18%
  - CH_4: 2 ÷ 3%
- syngas LHV: 1200 kcal/kg (5000 kJ/kg)
- cold gas efficiency: 80%

Another important issue already stated in Chapter 1 has to be discussed at this point. A gasification temperature is in effect properly defined in fluidised bed gasifiers, but there are different reaction zones in fixed bed devices, each one with its own temperature: therefore it is not correct to refer to a single gasification temperature. Nevertheless the gasifier model available in Thermoflex™ requires indication of a unique value for this parameter[6]: it is thus necessary to indicate a sort of average equivalent temperature to properly model a fixed bed gasifier. In the present case, it is quite easy to foresee that an intermediate temperature, i.e. 800°C, will be suitable for the purpose. However, a quick analysis has been conducted also in this sense: Figures 3.10 and 3.11 show the progress of lower heating value (on dry basis) and cold gas efficiency as a function of temperature, feeding the gasifier with different types of wood, whose composition is indicated in Table 3.1 (moisture ranges from 0% to 20%, the highest value normally accepted by downdraft gasifiers).

[6] The two cases discussed in the previous section implicitly refer to this configuration.

Name	Ref.	FC	VM	h	Ash	C	H	O	N	S	Cl
Dry pine bark	[TF]	24.2	72.9	**0**	2.9	53.4	5.6	37.9	0.1	0.1	-
Wood pellets	[TF]	16.4	74.4	**8.7**	0.5	45.8	5.5	39.4	0.08	0.01	0.01
Wood chips	[3.5]	13.28[7]	66.4[8]	**20**	0.32	39.2	5.2	35.2	0.08	-	-

Table 3.1 – Proximate and ultimate analysis (% w/w, wb) of the considered wood types.

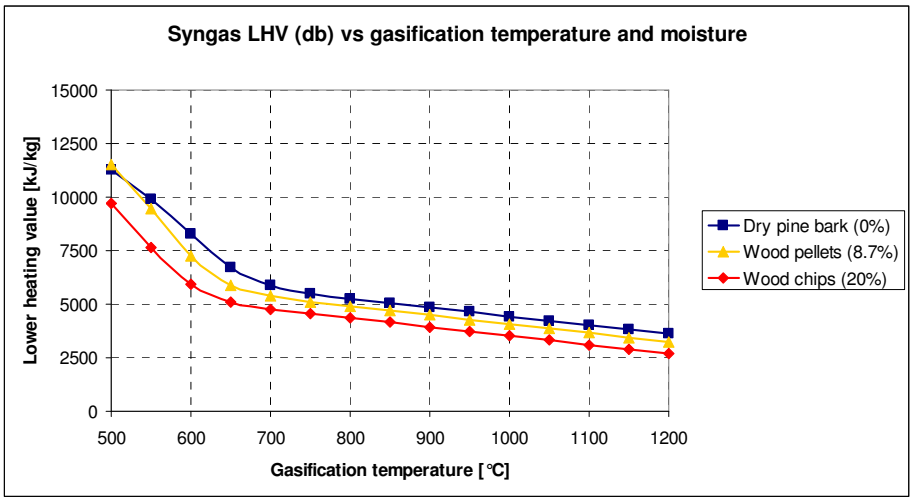

Figure 3.10 – Syngas LHV as a function of gasification temperature and moisture.

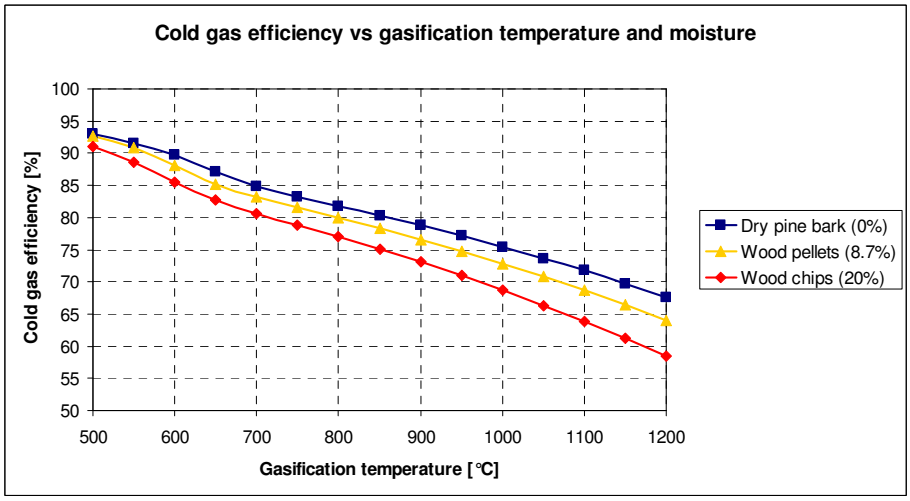

Figure 3.11 – Cold gas efficiency as a function of gasification temperature and moisture.

[7] These values were not reported in the paper and were thus hypothesised (VM: 83%, FC: 16.6 %, db).

Figures show how proper the choice of 800°C as equivalent gasification temperature is, since 5000 kJ/kg as LHV and 80% as cold gas efficiency are averagely achieved here (exit temperature of 500°C will then be reached via a cooler integrated in the gasifier). Indeed, as shown in Table 3.2, actual syngas composition slightly differs from the declared one (in particular CH_4 is practically not present), but lower heating value and cold gas efficiency are more important in terms of energy balance. Therefore results can be considered satisfying.

Name	Wet basis						Dry basis				
	CO	CO_2	CH_4	H_2	N_2	H_2O	CO	CO_2	CH_4	H_2	N_2
Dry pine bark	28.04	5.54	0.03	18.55	44.50	3.34	29.01	5.73	0.03	19.19	46.04
Wood pellets	22.27	8.83	0.03	20.00	41.65	7.22	24.00	9.52	0.03	21.56	44.89
Wood chips	16.38	10.94	0.01	19.90	40.66	12.11	18.64	12.45	0.01	22.64	46.26

Table 3.2 – Syngas molar composition (%) at 800°C as gasification temperature (argon contribution has been added to the nitrogen datum).

This configuration will be used in all simulations and, for simplicity reasons, also in 5 MW_{el} case, even if downdraft gasifiers are not applied here (indeed there is actually no distinction between the different types of devices in Thermoflex™). Besides pressurised gasifiers, based on the same configuration, will also be taken into account, although this solution is normally not applied on these scales.

3.4 Syngas issues

The use of biomass syngas in power plants is not a trivial matter. In particular there are three main aspects distinguishing this case from classic natural gas feeding and which have to be studied carefully:

- combustion process;
- syngas cleaning;
- syngas low LHV.

The first item involves all technological parameters that must be defined in the design of a burner and mainly depends on fuel composition: flame speed, temperature and stability, residence time, flammability limits, etc. In particular, due to its high flame speed and wide flammability limits (which forces to adopt diffusive combustion instead of a premixed one) and high flame temperature (which determines the necessity to evaluate its effects on mechanical strength of materials and however to provide methods, such as dilution with nitrogen, to limit its value and thus NO_x emissions), the presence of hydrogen is the most significant point in this sense for syngas. Wide literature is available regarding these issues (see for instance ref. [3.6], [3.7] and [3.8]). However, this is a specific topic and it is not being examined in detail here: in this work it is sufficient to hypothesise that the combustion device is properly designed and that the process occurs regularly. On the other hand, the two remaining items have to be discussed more extensively, which will be done in the next two dedicated sections.

3.4.1 Syngas cleaning

The potential problems caused by contaminants contained in syngas and the necessity of cleaning have already been shown in Chapter 1, together with the methods to accomplish this operation: this section presents the description of how the syngas cleaning phase is modelled in Thermoflex™. As real reference plant, Caema solution has been examined (in fact, it has already been stated that a gasification facility is formed not only by the gasifier itself, but also by all the other devices aiming at syngas treatment, therefore this was a natural choice). Figure 3.12 shows a complete Caema gasification plant coupled with an ICE, with the cleaning section consisting of:

- a dry multi-cyclone;
- an syngas-air heat exchanger;
- a wet scrubber;
- a compressor with water atomiser;
- a cyclone for water separation;
- a condenser;
- two biomass filters;
- a fabric filter.

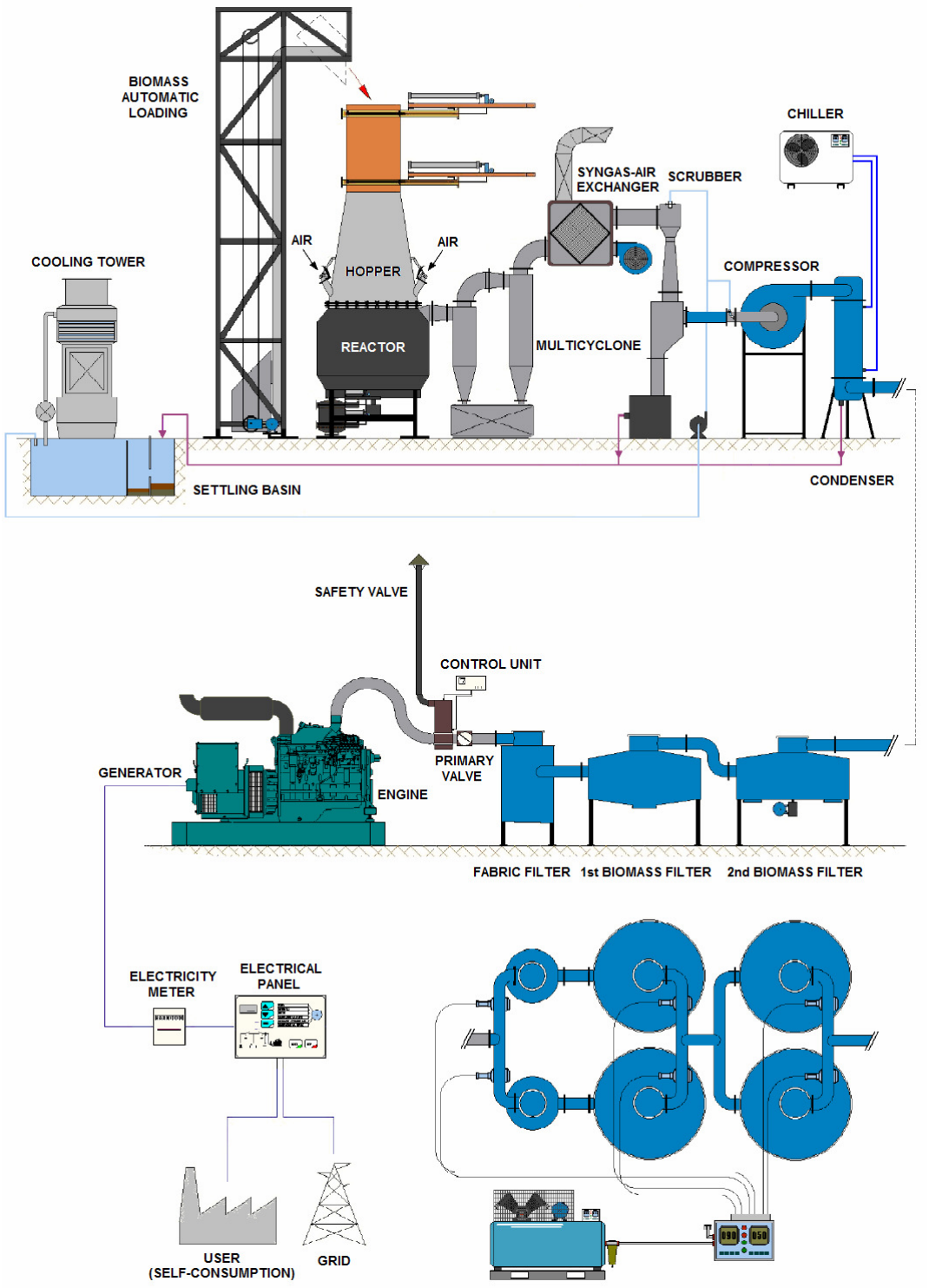

Figure 3.12 – Complete Caema gasification plant coupled with an ICE (adapted from [3.4]).

In the new section dedicated to gasification, Thermoflex™ provides models for all these components: theoretically, a cleaning section downstream the gasifier could therefore be assembled. Nevertheless, it was mentioned in the previous pages that syngas exiting the gasifier is actually already clean, being composed only by CO, CO_2, CH_4, H_2, H_2O, N_2 and Ar, apart from two sulphur compounds, i.e. H_2S (hydrogen sulphide) and COS (carbonyl sulphide), moreover not having any effect in the following power section. Thus all models of devices dedicated to syngas cleaning are actually useless and are only meant to complete the plant model under a visual aspect, as they just introduce head losses and, in case of scrubbing or wet compression, determine a moisture variation (which is always completely being removed at the end of the treatment chain). Considering that these components often lead to computational problems, it is easy to understand why the final choice was to condensate the cleaning section into two simple components, i.e. a heat exchanger, simulating the temperature decrease (down to 25°C) and head losses along the process, and a moisture separator. Power consumption of the various real components have instead been charged to the gasifier. The resulting Thermoflex™ model is shown in Figure 3.13 (note the presence of the aftercooler, fed by a hypothetic water flow, yielding the aforementioned temperature decrease from 800°C to 500°C at the gasifier output).

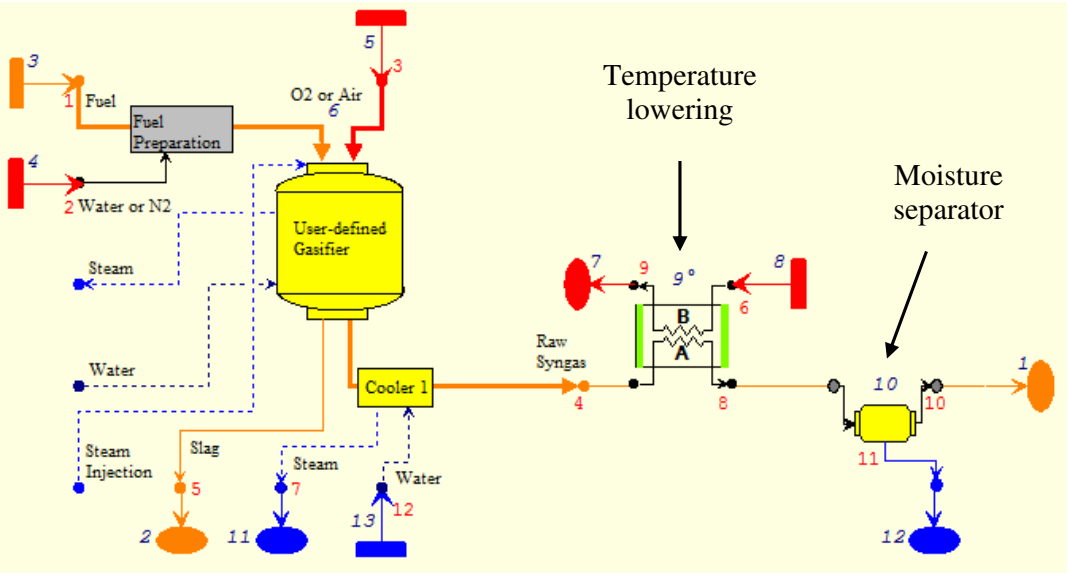

Figure 3.13 – Thermoflex™ simplified gasification and syngas cleaning model.

Actually a slightly different model was then adopted for the simulations performed in this work. In fact most of the sensible heat contained in the raw syngas is dissipated at the heat exchanger (exit temperature is normally about 60 ÷ 100°C; the remaining cooling is being achieved during the following cleaning operations). Therefore a heat recovery is always being performed already in the basic configuration: syngas sensible heat, otherwise lost in the exchanger, is absorbed by an air stream (blown by a fan to overcome head losses and whose mass flow rate is fixed so that heat exchanger effectiveness results 90%), afterwards used to dry biomass input (which is positive in thermodynamic terms, as will be discussed later on). Naturally, another heat exchanger simulating the final temperature decrease from 60 ÷ 100°C (the actual value was fixed in the minimum that avoids water syngas condensation in the heat exchanger plus a pinch difference of 20°C) to 25°C is provided in the model, together with the moisture separator. The model actually adopted in the simulations is shown in Figure 3.14.

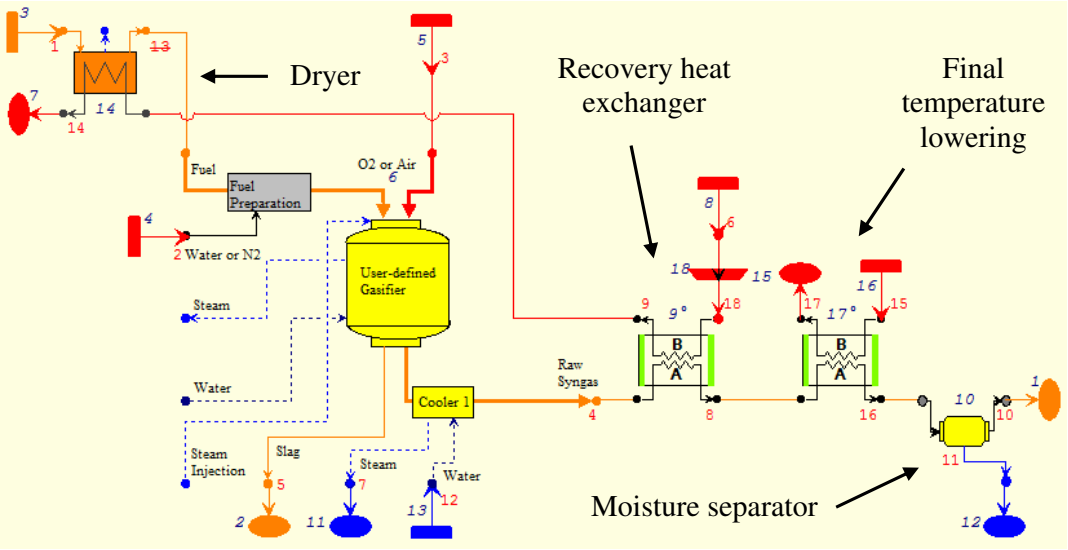

Figure 3.14 – Thermoflex™ complete gasification and syngas cleaning model.

3.4.2 Syngas low LHV

Biomass gasification with air as oxidiser produces syngas having a lower heating value of about 5 MJ per fuel unit, both in mass (as just shown) and in volume terms (see Table 1.6): density is in fact normally about 1 kg/Nm^3, as will be calculated later. Methane,

instead, has a LHV equal to about 50 MJ/kg and 35 MJ/Nm^3 (see Table 1.4), that means ten times in mass terms and seven in volumetric terms higher than syngas one, which implies a much higher fuel requirement to get the same power input or the same maximum temperature if syngas is used instead of methane for plant feeding. This involves some important implications on plants operation. As there are significant differences regarding these aspects between internal combustion engines and gas turbines, they will be analysed separately.

3.4.2.1 Internal combustion engines

Biomass syngas, like natural gas has a good anti-knock behaviour, therefore it can be suitably used in SI engines. It is also possible to use it in CI engines, but obviously only in dual-fuel configuration with pilot diesel injection [3.9]. This work will focus the first category. Moreover, again similarly to natural gas case, these engines can be specifically developed for syngas feeding or derive from CI machines: the former will be considered here.

Internal combustion engines in Thermoflex™ are pre-built components, supposed to be natural gas fuelled, as regards SI machines. They are reliable models, nevertheless they are little versatile, i.e. every model is characterised by default values of power output, electrical efficiency (thus fuel power input) and flue gas mass flow rate. Therefore if the engine is fed with a low-LHV fuel instead of methane, and thus a higher mass flow rate of this fluid is required, the software automatically lowers air input to compensate that increase and keep gas mass flow rate constant, always yielding the same power with the same efficiency. Only if the stoichiometric limit is reached, and then a further decrease of air mass flow rate would prevent the reaction to take place, stoichiometric conditions are kept and exhaust mass flow rate can raise accordingly (power output remains constant all the same). Apart from this last particular condition, it is therefore necessary to verify that the main assumption is correct, at least approximately, for the examined case: this can be done performing some calculations[8].

[8] In these calculations simplified air volume composition, i.e. 79% of N_2 and 21% of O_2, is being considered. Their ratio is exactly 3.76: for this reason the "air molecule" is indicated as $O_2 + 3.76\ N_2$.

The methane combustion reaction in air can be written as follows:

$$CH_4 + 2\,(O_2 + 3.76\,N_2) \rightarrow CO_2 + 2\,H_2O + 7.52\,N_2 \qquad (3.1)$$

This means that burning 1 m^3 of methane requires $2 \cdot (1 + 3.76) = 9.52$ m^3 of air. Bearing in mind that the chemical elements molecular weights (MW) in the reactants, expressed in kg/kmol, are: H – 1, C – 12, N – 14 and O – 16, stoichiometric mass air to fuel ratio, α_{st}, can be then easily calculated as follows:

$$\alpha_{st,CH4} = \frac{2\ MW_{air}}{MW_{CH4}} = \frac{2\ (2\cdot 16 + 3.76\cdot 2\cdot 14)\ kg_a/kmol}{12 + 4\cdot 1\ kg_f/kmol} = 17.16\ \frac{kg_a}{kg_f} \qquad (3.2)$$

On the other hand, in Section 2.3 it has already been explained that SI engines normally operate in lean conditions. In this regard, Figure 3.15 shows real air/fuel ratio values for commercial models[9].

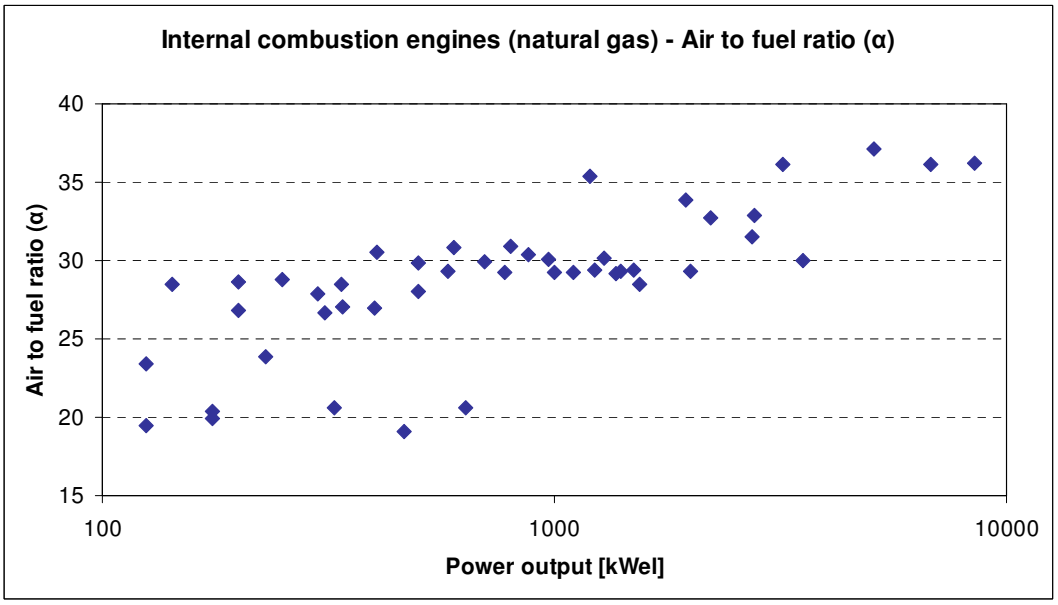

Figure 3.15 – Air to fuel ratio in methane-fed SI internal combustion engines.

[9] Data are taken from [TF] and several technical catalogues.

As one can see, α is an increasing function of size and is averagely about 25 ÷ 30 (that means that the parameter λ, defined as α/α_{st}, is about 1.45 ÷ 1.75; alternatively it can be said that the excess air is 45 ÷ 75%).
Considering that methane LHV is 50 MJ/kg, the resulting lower heating value of the air/methane mixture entering the engine (whose mass flow rate is then naturally equal to the flue gas one) will be:

$$LHV_{mixture,CH4} = \frac{LHV_{CH4}}{\alpha + 1} = \frac{50 \ \text{MJ/kg}_f}{(25 \div 30) + 1 \ \text{kg}_g/\text{kg}_f} \cong 1.6 \div 1.9 \ \frac{\text{MJ}}{\text{kg}_g} \qquad (3.3)$$

In order to perform an analogous calculation for biomass syngas, it is necessary to define its composition: the one reported in Table 3.3 is taken as reference (water-free syngas is considered). As one can see, it is provided both in molar (or volumetric) terms (X) as usual, and in mass terms (Y), the latter obtained weighting the former on MWs.

Compound	X [%,mol]	MW [kg/kmol]	Y [%,mass]
CO	20	28	23.1
CO_2	10	44	18.1
H_2	20	2	1.6
CH_4	1	16	0.7
N_2	49	28	56.5
Total	**100**	**24.28**	**100**

Table 3.3 – Reference syngas molar percentage composition.

Among the five reported compounds, CO_2 and N_2 are inert, thus only CO, H_2 and CH_4 take part in the combustion. Their oxidation reactions and stoichiometric air/fuel ratio are reported below (obviously methane is not indicated anymore):

$$2\ CO + (O_2 + 3.76\ N_2) \rightarrow 2\ CO_2 + 7.52\ N_2 \qquad (3.4)$$

$$2\ H_2 + (O_2 + 3.76\ N_2) \rightarrow 2\ H_2O + 7.52\ N_2 \qquad (3.5)$$

In both cases, (1 + 3.76) / 2 = 2.38 m^3 of air is then required to burn 1 m^3 of fuel.

Instead, calculations in mass terms would be:

$$\alpha_{st,CO} = \frac{MW_{air}}{2\ MW_{CO}} = \frac{2 \cdot 16 + 3.76 \cdot 2 \cdot 14\ \ kg_a/kmol}{2\ \ (12+16)\ \ kg_f/kmol} = \ \ 2.45\ \ \frac{kg_a}{kg_f} \tag{3.6}$$

$$\alpha_{st,H2} = \frac{MW_{air}}{2\ MW_{H2}} = \frac{2 \cdot 16 + 3.76 \cdot 2 \cdot 14\ \ kg_a/kmol}{2\ \ (2 \cdot 1)\ \ kg_f/kmol} = \ \ 34.32\ \ \frac{kg_a}{kg_f} \tag{3.7}$$

Finally it is possible to calculate the overall air amount necessary to burn a syngas unit, weighting the different α_{st} values on the mass fractions:

$$\alpha_{st,syngas} = \sum_i \alpha_{st,i} \cdot Y_i = \alpha_{st,CO} \cdot Y_{CO} + \alpha_{st,H2} \cdot Y_{H2} + \alpha_{st,CH4} \cdot Y_{CH4} =$$

$$= 2.45 \frac{kg_a}{kg_f} \cdot 0.231 + 34.32 \frac{kg_a}{kg_f} \cdot 0.016 + 17.16 \frac{kg_a}{kg_f} \cdot 0.007 = 1.24 \frac{kg_a}{kg_f} \tag{3.8}$$

Obviously this value depends on the actual syngas composition, however it is normally included in the range $1 \div 1.3\ kg_a/kg_f$.

As syngas is already diluted with a considerable amount of nitrogen (inherited from gasification air), the need to apply a lean burn configuration now becomes less pressing. Therefore these engines can generally work near to stoichiometric conditions [3.10]. On the other hand, larger amounts of air can also suitably be used: in order to cover a wide spread of possibilities, it can be assumed that λ ranges in $1 \div 1.5$ (i.e. an excess air of $0 \div 50\%$), that means a corresponding air to fuel ratio of about $1.2 \div 1.85\ kg_a/kg_f$.

In order to calculate syngas LHV for the examined case, the single values of the three fuel gases present in syngas have to be taken into account: they are shown in Table 3.4.

Compound	**LHV [MJ/kg]**
CO	10.1
H_2	120
CH_4	50

Table 3.4 – LHV of the three fuel gases present in the syngas [TF].

An weighted average operation, analogous to the one performed above, must be effected again (as mentioned, it is about 5 MJ/kg):

$$LHV_{syngas} = \sum_i LHV_i \cdot Y_i = LHV_{CO} \cdot Y_{CO} + LHV_{H2} \cdot Y_{H2} + LHV_{CH4} \cdot Y_{CH4} =$$

$$= 10.1 \frac{MJ}{kg_f} \cdot 0.231 + 120 \frac{MJ}{kg_f} \cdot 0.016 + 50 \frac{MJ}{kg_f} \cdot 0.007 = 4.6 \frac{MJ}{kg_f} \quad (3.9)$$

Finally, the resulting lower heating value of the air/syngas mixture entering the engine can be calculated as follows:

$$LHV_{mixture,syngas} = \frac{LHV_{syngas}}{\alpha + 1} = \frac{4.6 \ MJ/kg_f}{(1.2 \div 1.85) + 1 \ kg_g/kg_f} \cong 1.6 \div 2.1 \ \frac{MJ}{kg_g} \quad (3.10)$$

As one can see, the lower heating value of the air/fuel mixture is very similar in both cases, therefore with an analogous mixture mass flow rate (and thus gas mass flow rate), an analogous fuel power input is provided. Besides it must be remembered that ICEs specifically designed for low-LHV feeding are characterised by similar efficiencies with respect to their corresponding same size models fuelled with methane [3.11] (indeed, there are not many plants available on the market), therefore the hypothesis that engines keep the same electrical efficiency in case of syngas feeding, too, can be considered reasonable. Hence, if fuel power input and electrical efficiency are equal, electric power output will accordingly be equal.

After all, it has been demonstrated that Thermoflex™ assumptions are fully acceptable, at least for the purposes of this work: both in case of natural gas and syngas feeding, a certain size internal combustion engine (in terms of power output) is roughly characterised by the same gas mass flow rate and by the same electrical efficiency and therefore Thermoflex™ methane-fed ICEs models can suitably be used for the performance simulations also in case of syngas fuelling.

Another aspect must finally be discussed for completeness. This analysis has been conducted in mass terms, because energy balances (such as heat recovery downstream the engine, etc.), which are the real objective of the simulations, are regulated by mass

flow rates[10]. On the other hand, an analysis in volumetric terms just concerns the engine design (being the machine a volumetric one). However, as it may be interesting as well, some brief calculations are being presented.

Methane, as mentioned, has a LHV that in volumetric terms is equal to 35 MJ/Nm^3. It has been calculated (see Equation 3.1) that the stoichiometric amount of air for its combustion is 9.52 Nm^3. Considering the aforementioned excess air (45 ÷ 75%), this means that volumetric air to fuel ratio (hereinafter indicated with ν) is about 14 ÷ 16.5. Hence the volume LHV of the CH_4/air mixture is:

$$\mathrm{LHV_{V,mixture,CH4}} = \frac{\mathrm{LHV_{V,syngas}}}{\nu+1} = \frac{35\ \mathrm{MJ/Nm^3}}{(14\div16.5)+1\ \mathrm{Nm^3_g/Nm^3_f}} \cong\ 2\div2.35\ \frac{\mathrm{MJ}}{\mathrm{Nm^3_g}} \qquad (3.11)$$

Concerning syngas, firstly its density has to be calculated (the composition indicated in Table 3.3 is always to be taken as reference). Its specific gas constant R* can be obtained from the universal gas constant *R* and its MW:

$$\mathrm{R^*} = \frac{R}{\mathrm{MW}} = \frac{8314.5\ \mathrm{J/(kmol\cdot K)}}{24.28\ \mathrm{kg/kmol}} =\ 342.4\ \frac{\mathrm{J}}{\mathrm{kg\cdot K}} \qquad (3.12)$$

Referring to normal conditions, i.e.

$$\begin{cases} \mathrm{p = 1\ atm = 101{,}325\ Pa} \\ \mathrm{T = 0°C = 273\ K} \end{cases} \qquad (3.13)$$

density can finally be calculated as follows (as mentioned, it is about 1 kg/Nm^3):

$$\rho_{\mathrm{syngas}} = \frac{\mathrm{p}}{\mathrm{R^*\cdot T}} = \frac{101{,}325\ \mathrm{Pa}}{342.4\ \mathrm{J/(kg\cdot K)\cdot 273\ K}} =\ 1.08\ \frac{\mathrm{kg}}{\mathrm{Nm^3}} \qquad (3.14)$$

The lower heating value in volumetric terms can then easily be derived:

[10] In this sense it must be noted that specific heat capacity of flue gases is analogous in the two cases.

$$LHV_{V,syngas} = \frac{LHV_{m,syngas}}{\rho_{syngas}} = \frac{4.6\ \text{MJ/kg}}{1.08\ \text{kg/Nm}^3} = 4.26\ \frac{\text{MJ}}{\text{Nm}^3} \tag{3.15}$$

Remembering that ν_{st} is 2.38 both for CO and H_2 (see Equations 3.4 and 3.5), the stoichiometric amount of combustion air can be obstained, still performing a weighted average (in this case obviously referring to molar fractions):

$$\nu_{st,syngas} = \sum_i \nu_{st,i} \cdot X_i = \nu_{st,CO} \cdot X_{CO} + \nu_{st,H2} \cdot X_{H2} + \nu_{st,CH4} \cdot X_{CH4} =$$

$$= 2.38 \frac{\text{Nm}_a^3}{\text{Nm}_f^3} \cdot 0.20 + 2.38 \frac{\text{Nm}_a^3}{\text{Nm}_f^3} \cdot 0.20 + 9.52 \frac{\text{Nm}_a^3}{\text{Nm}_f^3} \cdot 0.01 = 1.05 \frac{\text{Nm}_a^3}{\text{Nm}_f^3} \tag{3.16}$$

Considering excess air ranging from 0 to 50%, the volumetric air to fuel ratio is about $1 \div 1.6$ and thus the volumetric LHV of the syngas/air mixture is:

$$LHV_{V,mixture,syngas} = \frac{LHV_{V,syngas}}{\nu + 1} = \frac{4.26\ \text{MJ/Nm}^3}{(1 \div 1.6) + 1\ \text{Nm}_g^3/\text{Nm}_f^3} \cong 1.65 \div 2.1\ \frac{\text{MJ}}{\text{Nm}_g^3} \tag{3.17}$$

In this case, there is a certain difference between the two values, which essentially relates to the different densities: the methane LHV is roughly $10 \div 20\%$ higher than the syngas one. This means that a given volumetric flow rate does not yield the same power input: an engine with a certain displacement fed with syngas will generate lower power than in case of methane fuelling, i.e. it is subject to derating. Indeed there are some methods to overcome this phenomenon, at least partially (increasing the engine compression ratio, performing a heavier turbo-charging, etc. [3.12]), but independently from that, this is a practical aspect that does not affect energy balances. For the purposes of this work, it was sufficient to verify that in both of the two different feeding cases the same power output corresponds to the same gas mass flow rate, as modelled by Thermoflex™. Then, it is not a problem if, due to the different density of the air/fuel mixtures, a syngas engine generating a certain amount of power has to be bigger (i.e. have a higher displacement) than a methane engine of the same power size.

3.4.2.2 Gas turbines

In case of methane feeding, fuel mass flow rate in gas turbines is normally equal to about 2% of the air one[11] (i.e. the air to fuel ratio α is about 50). Instead, if syngas is being used, and therefore a tenfold mass flow rate is being required, the incidence would increase to 20%, for the time being assuming that the compressor is working under the same conditions and thus treating the same air mass flow rate. The gas mass flow rate flowing through the turbine would increase accordingly. If this were possible, a mass flow rate increase would result in proportional increase as regards the expander power output and in a more considerable overall net power output increase (about 40%), as, in first analysis, the power absorbed by the compressor would be constant. Nevertheless, the gas mass flow rate increase in the turbine entails an input pressure increase: the compressor is therefore required to supply a higher pressure ratio. This implies that the operation point moves away from the design one, in particular towards the surge line: thus some actions are required to be taken on the plant. Ideally, the best solutions would be an increase in the turbine nozzle area or high-pressure stages addition to the compressor, but from a technical point of view these are burdensome interventions on an existing plant and, moreover, it is not granted that shaft and turbine can bear the higher power output. Therefore normally, air mass flow rate entering the compressor is being reduced, adjusting IGVs (Inlet Guide Vanes) and loosing part of the power increase [2.8]. Moreover, in case of pressurised gasifiers, air exiting the compressor may be partly separated and used to feed the gasifier itself, in order to compensate the fuel (and then gas) mass flow rate increase. On the other hand, it is obvious that these problems would not occur if the gas turbine were specifically designed for syngas feeding (many manufactures are working in this direction).

As will be shown in the next chapter, in this work a lot of plant solutions based on commercially available methane-fed gas turbines have been analysed. In particular they have been built up first ideally disassembling the reference plants and then re-assembling the various components (compressor, combustor, turbine, etc.) according to the new different configurations (EFGTs, hybrid solutions, etc.). In case of syngas

[11] The presence of the recuperator in micro gas turbines implies that this ratio is lower (about 1%) and the following values are accordingly lower, too. However the concept is absolutely analogous.

feeding, the turbine was ideally substituted by another one having the same features (essentially in terms of polytropic efficiency), but adapted to the new exhaust mass flow rate conditions (the air rate was instead kept constant). From a practical point of view, this would correspond to the aforementioned increase intervention in the turbine nozzle area or in the adoption of a specifically designed machine.

3.5 Reference power plants and design parameters

3.5.1 Common data

In all simulations, ambient conditions have been fixed to ISO ones (p = 1 atm = 101,325 Pa and T = 15°C = 288 K), with a relative humidity of 60%. Natural gas LHV is 48,671 kJ/kg, while its supplying pressure is equal to 0.02 bar

As already mentioned, waste heat recovery has always been performed, yielding low-temperature hot water for heating purposes (or any other compatible industrial application, of course). In this sense one specific plant has been taken as reference for each considered size: in particular the mGT at 100 kW_{el} and the ICEs at 1 MW_{el} and 5 MW_{el}. Process water mass flow rate has then been fixed so that it is interested by a heating from 50°C to 70°C in the hot gas recuperator(s), according to the design data described in the following sections. Afterwards in all the other plants of each size, this water mass flow rate is kept constant and, the return temperature being fixed at 50°C, the delivery one varies according to the heat availability, resulting included in the range 65 ÷ 100°C (with a little steam production sometimes). Mass flow rate values are respectively: 1.994 kg/s, 13 kg/s and 55 kg/s. Indeed, it is important to note that this hypothesis does not apply for ORC plants, where this quantity depends on the heat released at the condenser.

Technical data of power plants taken as reference are presented in the next sections. ICEs and GTs/mGTs are implicitly supposed to be fed with natural gas, while concerning ORCs, regardless of the feeding type, only the power section of the plant downstream of the thermal oil circuit is being considered. Design data of all devices regarding biomass are finally discussed in the last section of the chapter.

3.5.2 Internal combustion engines

Obviously, internal combustion engines as reference for the three considered sizes are all taken from [TF]: they are listed in Table 3.5. Table 3.6, instead, summarises the most relevant data of these plants.

Size	Model
100 kW_{el}	Cat 3306
1 MW_{el}	Deutz TBG 620 V12K
5 MW_{el}	Rolls Royce B35:40-V12 AG

Table 3.5 – Reference internal combustion engines.

Parameter	Unit	100 kW_{el}	1 MW_{el}	5 MW_{el}
Engine operating data				
Gas mass flow rate	kg/s	0.153	1.53	8.25
Exhaust gas temperature	℃	515	515	395
Cooling water circuit				
Cooling water inlet temperature	℃	80	82	80
Cooling water outlet temperature	℃	90	92	90
Cooling water mass flow rate	kg/s	3.387	11.16	45.49
Pump isentropic efficiency	%	85	85	85
Pump mechanical efficiency	%	97	97	97
Cooling water heat exchanger				
Effectiveness	%	42.1	23.9	25.1
Heat loss	%	1	1	1
Head loss (process water side)	%	0	0	0
Head loss (engine water side)	%	2	2	2
Exhaust gas heat exchanger				
Stack gas temperature	℃	120	120	120
Effectiveness	%	88.7	87.1	82.2
Heat loss	%	1	1	1
Head loss (water side)	%	0	0	0
Head loss (gas side)	%	0	0	0

(%)

Parameter	Unit	100 kW_{el}	1 MW_{el}	5 MW_{el}
Nominal performance				
Net electric power	kW_{el}	108.7	1008	5046
Electrical efficiency	%	30.1	39.6	45.3
First law efficiency	%	88.6	84.5	84.5

Table 3.6 – Reference internal combustion engines data.

It is important to note that engine operating and performance data, i.e. gas mass flow rate, exhaust gas temperature, electric power (neglecting the cooling water pump power consumption, depending on the chosen efficiencies), electrical and first law efficiency are all Thermoflex™ default parameters, while those concerning heat recovery can be chosen by the user. In particular, classic design parameters have been used (flue gases cooled down to 120°C and engine cooling water at 90/80°C, except for the intermediate model, for which technical data indicate 92/82°C [3.13]). Once the aforementioned two temperatures have been set, the heat amount that has to be discharged being known, cooling water mass flow rate is fixed by the system. The two heat exchangers effectiveness has been chosen in order to observe the given temperatures and mass flow rates.

Pressure drop on process water side has been fixed equal to zero in both exchangers, because the specific thermal process does not involve the power plant directly, therefore its losses do not have to be charged to the latter (indeed, the circulating pump consumptions would be negligible all the same). For computational reasons, the same has been done on the gas side of the exhaust heat exchanger.

Finally, efficiencies are in accordance with the values presented in Chapter 2: as mentioned, first law efficiency is a little higher in the smallest plant.

3.5.3 Gas turbines

Regarding gas turbines, reference has been made to [TF] for 1 MW_{el} and 5 MW_{el} plants, while a commercial plant, whose technical data have been found in literature and on the web, has been considered for 100 kW_{el} size (since [TF] does not include micro gas turbines, as mentioned). All turbine models are listed in Table 3.7.

Size	Model	Ref.
100 kW_{el}	Turbec T100	[3.14], [3.15]
1 MW_{el}	Solar Saturn 20-T1600	[TF]
5 MW_{el}	Solar Centaur 50 (SIM)	[TF]
	Solar Mercury 50 (REG)	[TF]
	Rolls Royce 501-KH5 (VAP)	[TF]

Table 3.7 – Reference gas turbines.

There are three reference plants for the 5 MW_{el} case. This is due to the fact that, in general, three gas turbine plant configurations have been considered, i.e. simple, regenerative and STIG cycles, and all of the three solutions are available on the market only on that size: acronyms reported in the table clearly show the corresponding solution (VAP stands for vapour). Note that the reported one is the only existing model both for regenerative and for STIG solutions. Besides Solar Mercury 50 essentially derives from Solar Centaur 50, which is the corresponding simple-cycle version (it has been chosen right for this reason). On the other hand, for each of the other two sizes there is only one plant typology available, namely the regenerative one for 100 kW_{el} and the simple one for 1 MW_{el}, hence the single reference model. However, in the latter case, a regenerative solution, feasible thanks to the working temperatures and pressures and realisable simply adding a recuperator, has also been considered. On the contrary, STIG solution is not deemed to be justified on these scales.

As easily understandable, not all technical data were known, concerning both Turbec T100 and the other models present in [TF]. In general global cycle parameters, such as pressure ratio, TIT and TOT (Turbine Outlet Temperature), air mass flow rate, power output and electrical efficiency are known, but more specific data, such as machines polytropic efficiencies, head and heat losses, etc., are unavailable. Therefore, the first operation within this work was assembling of plants with those characteristics, starting from the elemental components, making hypotheses about the unknown data and trying to comply with the design ones. These plants will be disassembled later on and the components will be used to built up the various simulated configurations.

Table 3.8 shows all technical data regarding the considered gas turbines. Obviously the recuperator at 1 MW_{el} is applied only in the regenerative solution (as shown in the table, its features are analogous to the 100 kW_{el} ones and this also applies for the 5 MW_{el}

regenerative case): performance data put into brackets at the bottom of the table refer to this particular case.

Parameter	**Unit**	**100 kW_{el}**	**1 MW_{el}**	**5 MW_{el} (SEM)**	**5 MW_{el} (REG)**	**5 MW_{el} (VAP)**
Compressor						
Air mass flow rate	kg/s	0.793	6.46	18.86	17.40	15.34
Pressure ratio	-	4.5	6.5	10.6	9.8	13.4
Polytropic efficiency	%	81.6	85	79	85	86
Mechanical efficiency	%	98	98.5	98.5	98.5	99
Inlet head loss	%	1	1	1	1	1
Recuperator						
Effectiveness	%	89.3	*89.3*	-	89.3	-
Heat loss	%	1	*1*	-	1	-
Head loss (cold side)	%	1.5	*1.5*	-	1.5	-
Head loss (hot side)	%	2.5	*2.5*	-	2.5	-
Combustor						
COT	℃	950	899	1054	1093	1054
Heat loss	%	1	0.5	0.5	0.5	0.5
Head loss	%	3	4	4	4	4
Δp/p fuel/water injection	%	40	40	40	40	40
Fuel compressor						
Polytropic efficiency	%	75	75	80	80	80
Mechanical efficiency	%	98	98	98	98	98
Inlet head loss	%	2	2	2	2	2
Outlet head loss	%	2	2	2	2	2
Turbine						
Polytropic efficiency	%	82.2	88	92	88	83.5
Mechanical efficiency	%	98	98.5	98.5	98.5	99
Outlet head loss	%	1	1	1	1	1
HRSG						
Effectiveness	%	-	-	-	-	96
Heat loss	%	-	-	-	-	1
Head loss (water side)	%	-	-	-	-	2
Head loss (gas side)	%	-	-	-	-	2.5
Pump isentropic efficiency	%	-	-	-	-	85
Pump mechanical efficiency	%	-	-	-	-	97

(%)

Parameter	Unit	100 kW_{el}	1 MW_{el}	5 MW_{el} (SEM)	5 MW_{el} (REG)	5 MW_{el} (VAP)
Recovery heat exchanger						
Effectiveness	%	91.8	91.8	91.8	91.8	91.8
Heat loss	%	1	1	1	1	1
Head loss (water side)	%	0	0	0	0	0
Head loss (gas side)	%	2.5	2.5	2.5	2.5	2.5
Shaft						
Rotational speed	rpm	70,000	22,516	14,950	14,180	14,600
Generator/motors						
Generator efficiency	%	92	93	95	94.5	95.5
Auxiliaries motor efficiency	%	92	92	92	92	92
Nominal performance						
Net electric power	kW_{el}	101.3	1068 *(1012)*	4109	4211	5547
Electrical efficiency	%	29.7	22.0 *(32.1)*	26.7	36.1	35.3
First law efficiency	%	78.7	84.6 *(81.3)*	85.1	83.8	61.1

Table 3.8 – Gas turbines design data.

Observing the nominal performance data, one can verify that they are in accordance with those reported in Chapter 2: the micro gas turbine has an electrical efficiency near to 30%; the 1 MW_{el} model is characterised by poor design data (e.g. low TIT) and thus by low electrical efficiency and only the presence of the recuperator makes this parameter exceed 30%; the 5 MW_{el} plant also has a lower efficiency with respect to regenerative plants of smaller size, while regenerative and STIG configurations reach 35 ÷ 36%. Naturally, simple cycle plants are on the contrary characterised by much better thermal efficiencies, so that first law efficiency is higher in this case, while it is a little lower in the regenerative case and much lower in the STIG solution (where most of the available heat is used to produce injection steam).

In this last case, the heat recovery steam generator has been modelled by means of a simple heat exchanger: effectiveness has been fixed at 96%, but this has not to be considered an excessive value, since it yields a pinch temperature difference of 50 ÷ 60°C. Steam production (in terms of mass flow rate and temperature) then varies accordingly.

For simplicity reasons, turbine cooling has never been considered (indeed, it should be applied only for 5 MW_{el} configurations): equivalent results have been obtained adjusting the other parameters.
As one can observe, the same cogenerative heat exchanger model has been used in all cases: pressure drop on water side has been fixed equal to zero, the same as for internal combustion engines.

3.5.4 Organic Rankine cycles

Organic Rankine cycle plants taken as reference in this work are those manufactured by Turboden [2.17], whose performance has already been mentioned in Chapter 2.
These plants use MDM as working fluid, but unfortunately it is not available in [TF]. Since it is not possible to add other fluids to those present in the library itself, the first operation was to find out among those being available a fluid having similar features regarding MDM to be used in the simulations. In particular benzene, which is actually studied as ORC fluid as well [3.16], has been chosen, as it presents an analogous T-s diagram form (it is a dry fluid too) and an almost equal critical temperature (289°C versus 291.2°C) with respect to MDM. On the other hand, the corresponding critical pressure is quite different (48.9 bar versus 14.4 bar) [2.19], thus operating pressures in the simulations were adjusted in order to match the desired temperatures.
Turboden supplies two plant configurations: the first one exploits a high-temperature heat source (e.g. gas from biomass combustion) and is designed for CHP applications, while the second one uses low-temperature heat (e.g. from a geothermal source, waste gases, etc.) and is designed for pure power generation. Naturally these two solutions can "cross" each other, so that only electrical production is possible in the first case, as well as cogeneration is theoretically applicable in the second one (although the latter is generally unjustified). Data concerning both solutions are presented in Table 3.9: as one can see, available data are quite few. In this regard, it is important to remeber that technical data and performance are similar for all sizes, thus the reported ones are valid for all the considered solutions. Again, it must be specified that the reported electrical efficiency is calculated referring to the thermal power of oil: biomass furnace will be considered later.

Parameter	Unit	High T - CHP	Low T - EL
Evaporator			
Thermal oil inlet temperature	°C	300	270
Thermal oil outlet temperature	°C	250	150
Condenser			
Cooling water inlet temperature	°C	60	25
Cooling water outlet temperature	°C	80	35
Nominal performance			
Electrical efficiency	%	18	19

Table 3.9 – Turboden plants design data.

In this work the first solution was considered in case of biomass combustion, while the second one in case of internal combustion engines and gas turbines bottoming the ORC plants, as will be shown.

Actually the high-temperature CHP solution provides two thermal oil circuits (one at 310/250°C and the other at 250/130°C) in the latest plants, however in this work the classic 300/250°C one is being considered, as also done in [1.27] and [2.19].

Turboden does not directly provide information concerning the thermodynamic cycle, nevertheless for the CHP solution these data have been found in literature (precisely in the just mentioned works). In particular the following temperature values are provided:

- vaporisation: 250°C
- superheating: 260°C
- condensation: 90°C

However, in this work the latter parameter has been fixed to 80°C, as inlet and outlet temperatures of the cooling water are not 60°C and 80°C, but 50°C and 70°C.

Basing on these data, and particularly keeping similar pinch temperature differences both in the evaporator (about 20°C) and in the condenser (10°C), the following temperature parameters were chosen for the low-temperature pure electric configuration:

- vaporisation: 170°C
- superheating: 180°C
- condensation: 45°C

Other technical data concerning the ORC unit are additionally provided in the aforementioned references (obviously they have been used for both cases):

- pump isentropic efficiency: 75%
- pump mechanical efficiency: 95%
- pump motor efficiency: 95%
- turbine mechanical efficiency: 95%
- generator efficiency: 97%

The other unknown parameters have instead been estimated as shown in Table 3.10. Again, they are valid for both solutions.

Parameter	Unit	Value
Thermal oil pump		
Isentropic efficiency	%	75
Mechanical efficiency	%	95
Motor efficiency	%	95
Evaporator		
Heat loss	%	1
Head loss (benzene side)	%	4
Head loss (oil side)	%	2
Turbine		
Isentropic efficiency	%	83
Regenerator		
Effectiveness	%	85
Heat loss	%	1
Head loss (water side)	%	2
Head loss (gas side)	%	2
Condenser		
Heat loss	%	0
Head loss (water side)	%	0
Recovery heat exchanger		
Effectiveness	%	91.8
Heat loss	%	1
Head loss (water side)	%	0
Head loss (gas side)	%	2.5

Table 3.10 – Other ORC plants design data.

Turboden indicates that turbine efficiency can achieve up to 85%, therefore 83% has been chosen. Evaporator effectiveness is not expressly indicated, as both inlet and outlet temperatures are fixed and thus the effectiveness itself is obtained accordingly: however, this parameter results equal to about 90% with the given values (that leads to the mentioned pinch difference temperature of 20°C). Recovery heat exchanger is applied in all cases in which exhaust hot gases, having any origin, are available. Duratherm 630 has been chosen as thermal oil: its working temperature range (-9.4 ÷ 329.4°C) makes it suitable for the application.

Concerning benzene mass flow rate, for the high temperature CHP case this parameter was chosen in order to generate about 100 kW_{el}, 1 MW_{el} and 5 MW_{el} in the three different cases, and in particular:

- 100 kW_{el}: 1 kg/s
- 1 MW_{el}: 10 kg/s
- 5 MW_{el}: 50 kg/s

On the other hand, given the thermodynamic parameters of the cycle, in low-temperature configurations, this mass flow rate depends on the available thermal power and consequently varies from case to case.

Concluding, it can be verified that with all these assumptions, simulations of such plants provide analogous results to those declared by the manufacturer and obtained in the cited literature works. Actual results will however be shown in the next chapter, in order to present them together with the performance of the other plants, thus allowing a clearer comparison.

3.5.5 Biomass devices

In this last section, design data of the biomass devices are finally presented. They are: gasifier (minor technical data are now shown, in addition to the main ones already discussed in Section 3.3.2), dryer, combustion devices (combustor for gas turbines and furnace for ORCs) and filters. Their features are summarised in Table 3.11.

It is important to point out that, differently from what happens with syngas in gasifiers, Thermoflex™ calculates the quantity of dust produced during the combustion of solid biomass and therefore filters have a concrete effect on flue gases cleaning. Nevertheless

the aspect concerning emissions is not interesting for this work and is therefore being neglected: filters are provided in the models just to account their head losses.

Parameter	Unit	Value
Gasifier		
Carbon conversion	%	98
Heat loss	%	1
Specific consumption	kWh/t	70
Slag exit temperature	℃	200
Air compressor isentropic efficiency	%	75 (80 at 5 MW_{el})
Air compressor mechanical efficiency	%	98
Air compressor motor efficiency	%	92
Dryer		
Fuel moisture evaporated	%	100
Dried fuel outlet temperature	℃	80
Head loss (gas side)	%	2.5
Specific consumption	kWh/t	5.5
Moisture evacuator isentropic efficiency	%	87
Moisture evacuator electromechanical efficiency	%	90
Syngas heat recovery		
Heat exchanger effectiveness	%	90
Heat exchanger heat loss	%	1
Heat exchanger head loss (air side)	%	2
Heat exchanger head loss (syngas side)	%	0
Air fan isentropic efficiency	%	75
Air fan mechanical efficiency	%	98
Air fan motor efficiency	%	92
Biomass combustor (GT)		
Heat loss	%	2
Head loss	%	5
Biomass furnace (ORC)		
Efficiency	%	83
Excess air	%	40
Heat loss	%	2
Head loss	%	2

(%)

Parameter	Unit	Value
Air pre-heater effectiveness	%	90
Air pre-heater heat loss	%	1
Air pre-heater head loss (cold side)	%	1.5
Air pre-heater head loss (hot side)	%	2.5
Air fan isentropic efficiency	%	75
Air fan mechanical efficiency	%	95
Air fan motor efficiency	%	95
Filters		
Head loss	%	1

Table 3.11 – Biomass devices design data.

As already anticipated, datum concerning gasifier specific consumption does not account the gasifier power need only, but also those relating to all the syngas cleaning devices that are neglected in this work. Small-scale gasifiers normally work at ambient pressure, but the pressurised solution has also been considered for gas turbine feeding (the mentioned air compressor is now required): in this case, the parameter depends on the required conditions in the combustor and thus varies from case to case.

The indicated percentage of evaporated fuel moisture for the biomass dryer is 100%: this means that in the basic cases a full drying is always performed, if available. However the variation effect of this parameter is investigated further on. As shown, drying operation in gasifiers is normally performed using the air stream previously adopted for syngas cooling, while in plants with solid biomass combustion hot flue gases are being used.

Performance of gas turbine biomass combustors is similar to the natural gas fuelled ones, although solid feeding involves some penalisation, as noticeable. Combustor outlet temperature, instead, varies in the different cases, as will be discussed in the next chapter.

Finally, [2.21] refers to a biomass furnace having 80 ÷ 83% efficiency, from which a 15% electrical efficiency is derived: 83% efficiency has been chosen here.

Chapter 4
Thermodynamic analysis

4.1 Introduction

After the presentation of all the working hypotheses that underlie the simulations of the investigated power plants performance, in this chapter results of the analysis are shown and discussed. The objective of this phase is to determine the most interesting solutions for biomass power generation from a thermodynamic point of view: in the next chapter, these will then be subject to an economic analysis, in order to determine the globally best solution for each power size.

Firstly the investigated solutions are being listed and described, afterwards results, in terms of electrical efficiency (η_{el}) and first law efficiency (η_I), are shown. The former parameter is the most important because the main interest of this work is power generation; nevertheless the latter is significant as well, since it provides information about the global energy efficiency of the plant. Finally, some possible gasification device variations are being discussed, in order to identify potential base configuration corrections allowing to reach better performance.

Wood pellets have been used as fuel in the analyses of this chapter. Their composition has already been shown in Table 3.1, while their lower heating value is 16,784 kJ/kg. Obviously this indication should not be taken literally, i.e. wood pellets are actually not supposed to be used for plants feeding (it would be technically and economically unreasonable): in this phase it was simply necessary to choose a reference fuel having good energy characteristics, and in particular a low moisture level, in order to obtain results not excessively influenced by this parameter[1]. The effect of using different fuel types, i.e. characterised by different moisture values, will be discussed in Chapter 6.

[1] On the other hand, to adopt a totally dry fuel would not have been a likely solution.

4.2 Investigated solutions

Seven plant configurations, with globally sixteen versions, based on internal combustion engines, gas turbines and organic Rankine cycles have been analysed in this work: they are listed and described below, with acronyms indicated for each of them. Respective plant schemes are shown in Figures 4.1 ÷ 4.16 at the end of the section.

4.2.1 ICE GAS – Internal combustion engine coupled with a gasifier

This solution (Figure 4.1) does not need any particular description: solid biomass is supplied to a gasifier (obviously working at ambient pressure) that produces syngas subsequently used to feed an internal combustion engine.

4.2.2 GT GAS – Gas turbine coupled with a gasifier

This configuration is corresponding to the previous one. Nevertheless there are now several possible plant versions, related to the turbine thermodynamic cycle (simple, regenerative or STIG) and to the gasifier working pressure (ambient pressure or pressurised). The combination of these different conditions leads to six possible solutions (the meaning of the various subscripts and acronyms is immediate and, moreover, they have partially been mentioned in Table 3.7):

- GT GAS SIM AMB: GT GAS with simple cycle and ambient pressure gasifier (Figure 4.2);
- GT GAS REG AMB – GT GAS with regenerative cycle and ambient pressure gasifier (Figure 4.3);
- GT GAS VAP AMB – GT GAS with STIG cycle and ambient pressure gasifier (Figure 4.4);
- GT GAS SIM PRES – GT GAS with simple cycle and pressurised gasifier (Figure 4.5);
- GT GAS REG PRES – GT GAS with regenerative cycle and pressurised gasifier (Figure 4.6);

- GT GAS VAP PRES – GT GAS with STIG cycle and pressurised gasifier (Figure 4.7).

The last three configurations are very similar to the former three ones, with only two details differing: syngas compressor is not required anymore (and is substituted by a control valve), as fuel is already pressurised, but on the other hand an air compressor is necessary to feed the gasifier.

4.2.3 GT EXT – Externally fired gas turbine with solid biomass feeding

Characteristics of externally fired gas turbines have already been described in Section 2.4.3, however, it is recalled that such plants are not available on the market, therefore these solutions must ideally be assembled referring to the technical data of the aforementioned classic internally fired gas turbines. For 100 kW_{el} and 1 MW_{el} scales there is no ambiguity, as the reference plant is just one, but for the 5 MW_{el} size three reference gas turbines have been considered (see Table 3.7), each one related to the three possible cycles: in this case the regenerative configuration has been chosen, as it is the most similar to EFGTs (the recuperator is analogous to their main heat exchanger; the technical data of the former have been used for the latter).

In this family two versions have been identified, as a function of the heat exchanger's allowable maximum temperature (from a plant scheme point of view, the two solutions are obviously identical, see Figure 4.8):

- GT EXT CER – GT EXT with ceramic (or however high temperature) heat exchanger;
- GT EXT MET – GT EXT with conventional metallic heat exchanger.

Particularly, in the first configuration combustor outlet temperature has been fixed so that turbine inlet temperature results equal to the design one in natural gas plants. With the chosen design data reported in the previous chapter, this implies a COT of 1033°C for the 100 kW_{el} solution (TIT = 950°C) and 971°C for the 1 MW_{el} one (TIT = 899°C). On the other hand, regarding the 5 MW_{el} solution TIT would be equal to 1093°C, which would imply a COT of 1178°C. Nevertheless this value appears excessive and therefore it has been limited to 1100°C, which leads to a TIT of 1023°C. Obviously these are still very high values but they seem reasonable for this analysis and also in a future

perspective (indeed, such and even higher values have been found in literature: see for instance [2.15], [4.1] and [4.2]).
On the contrary, regarding the metallic heat exchanger solution, maximum temperature has been fixed at 800°C, which limits turbine inlet temperature to 740 ÷ 750°C.

4.2.4 GT DIR – Gas turbine directly fed with solid biomass

This solution is given by classic internally fired gas turbines where only the natural gas combustor is substituted by a solid biomass fed one, keeping all design data unvaried. This type of plant represents the simplest solution for the use of biomass in gas turbines from a conceptual point of view and has already been investigated [4.3], nevertheless it is quite accepted in the literature that this solution cannot be applied from a practical point of view (see again [2.15], for instance), due to enormous problems related to the expansion of dirty flue gas in the turbine causing heavy damage to the component in short time. All the same it has been considered in this work, essentially for comparison purposes with the other solutions. Also in this case, the three gas turbine configurations have been taken into account, i.e.:

- GT DIR SIM – GT DIR with simple cycle (Figure 4.9);
- GT DIR REG – GT DIR with regenerative cycle (Figure 4.10);
- GT DIR VAP – GT DIR with STIG cycle (Figure 4.11).

4.2.5 ORC – Organic Rankine cycle fed by biomass combustion

Turboden plants in their high temperature configuration, i.e. with thermal oil at 300/250°C, both in CHP and pure electric version, are taken as reference.
Indeed, these plants can be characterised by several design versions and a little analysis aiming at defining the actual ORC plant configuration to be adopted in the simulations must be effected. Moreover, this gives the chance to actually verify the results with the ones declared by the manufacturer, which are reported in the previous chapter.
In particular the main point is to define the use of the hot gases exiting the furnace (their temperature is about 330°C). Three aspects must be assessed and precisely whether or not they effect these operations:

- biomass drying;
- air pre-heating;
- thermal recovery of hot gases.

A complete reference plant, modelled in Thermoflex™ is shown in Figure 4.12.

First of all, air-preheating has been compared with the case of simple heat recovery for thermal purposes (further water process heating after the condensation phase). Table 4.1 shows results in terms of electrical, thermal and first law efficiencies (in both cases full biomass drying is performed). Results correspond with the declared performance shown in the previous chapter: in fact, in both cases, electrical efficiency calculated referring to thermal oil power input is 18% (though values shown in the table are the overall net ones, thus including the combustion process efficiency).

Parameter	Unit	Pre-heating	Heat recovery
Electrical efficiency	%	17.06	15.13
Thermal efficiency	%	72.93	75.30
First law efficiency	%	89.99	90.43

Table 4.1 – Effect of air pre-heating compared to heat recovery in a cogenerative ORC.

Beneficial effects of pre-heating in terms of electrical efficiency are predictable, but it is important to note that the inevitable penalisation concerning thermal production is limited as well, so that first law efficiency results to be almost equal. Therefore air-preheating is always considered in ORC plants with biomass furnace.

On the other hand, the effect of providing biomass dryer and, again, recovery heat exchanger is studied in a crossed way, i.e. considering the four presence or absence combinations (obviously pre-heating is effected). Results are shown in Table 4.2.

Parameter	Unit	Drying + heat recovery	NO Drying + heat recovery	Drying + NO heat recovery	NO Drying + NO heat recovery
Electrical efficiency	%	16.92	17.16	17.06	17.30
Thermal efficiency	%	73.85	73.88	72.93	72.49
First law efficiency	%	90.77	91.04	89.99	89.79

Table 4.2 – Effect of biomass drying and/or heat recovery in a cogenerative ORC.

These results are quite interesting and show the two operations having almost no effect, as their benefits are balanced by auxiliaries consumption and/or head losses. However the best solution seems to be the second one, i.e. performing heat recovery but no fuel drying: electrical efficiency is slightly lower than the highest one (achieved without neither fuel drying nor heat recovery), but the corresponding first law efficiency is the best. Thus this solution has been adopted: it is schematised in Figure 4.13.
In case of pure electric production, the thermal process is substituted by a cooling tower and the recovery heat exchanger is accordingly removed (thermal production would be ridiculous). In this regard, it must be specified that the latter is not considered an independent solution, as the plant scheme is essentially the same and there is only a condensation temperature modification: therefore, two performance data will be provided for the ORC solution in the results section.

4.2.6 ICE/GT GAS ORC – Internal combustion engine or gas turbine coupled with a gasifier and bottoming ORC

In this solution ORC is fed with hot flue gases discharged by an internal combustion engine or a gas turbine fed by a gasifier, thus forming a sort of combined cycle. The integration of ICEs and GTs with ORCs has been widely investigated (see for instance [4.5] and [4.6]), but these studies always refer to the classic natural gas feeding and not to the integration with syngas-fuelled devices, like in this case. This solution is practically given by the combination of the presented first two plants (ICE GAS and GT GAS) with an ORC. Consequently, the related acronyms are:

- ICE GAS ORC
- GT GAS ORC

Right because this scheme derives from ICE/GT GAS, for the latter there would be additional six versions, related to those considered in that case. Besides, they should be multiplied by two, because the possible CHP or electric arrangement of ORC plant should be considered (for internal combustion engines only these two ones are present). Actually in STIG plants, exhaust gases leave the HRSG at 230 ÷ 250°C, a too low temperature to allow an integration with an ORC, thus only simple and regenerative cycles have been considered. However, like in the previous case, all these possible

configurations are not considered as independent versions, but a spread of possible results for these solutions will simply be provided. Moreover, a preliminary analysis will allow to cut off some of them. In Figures 4.14 and 4.15 two examples of possible configurations are shown (the other ones are however easy to figure out): ICE GAS ORC and GT GAS ORC REG PRES, both in the CHP version. In the first plant the process has been divided in two for heat recovery optimisation purposes. Finally, the gas/thermal oil heat exchanger has the following characteristics:

Parameter	Unit	Value
Effectiveness	%	85
Heat loss	%	1
Head loss (thermal oil side)	%	2
Head loss (gas side)	%	0 (ICE) 2.5 (GT)

Table 4.3 – Thermal oil-gas heat exchanger design data.

4.2.7 GT HYB – Hybrid gas turbine fed by solid biomass and natural gas

This is the only solution that is not exclusively fuelled by biomass. It has been proposed in [4.4] and is considered also in this work because, despite of not being completely renewable, it could represent an interesting solution given its relative plant simplicity. As one can see in Figure 4.16, it is essentially a methane-fed regenerative gas turbine with an afterburning fuelled with solid biomass (for this reason, as for EFGTs, the regenerative turbine plant has been taken as reference at 5 MW_{el}). This additional combustion re-heats flue gases, so they enter the recuperator at a higher temperature: air on the other side of the exchanger is subject to heavier heating and thus, fixed the turbine inlet temperature, a lower amount of natural gas is required. Obviously the electrical efficiency decreases, but there is the advantage of substituting part of the natural gas with biomass. In order to allow the use of a metallic heat exchanger, temperature of gases exiting the biomass combustor is fixed at 800°C.

4.2.8 Summary

Actually not all the described solutions have been considered for each scale: Table 4.4 provides a complete overview in this sense (the symbol ✓ indicates that the corresponding configuration has been analysed).

Group	Solution	100 kW_{el}	1 MW_{el}	5 MW_{el}
1	ICE GAS	✓	✓	✓
2	GT GAS SIM AMB	-	✓	✓
	GT GAS REG AMB	✓	✓	✓
	GT GAS VAP AMB	-	-	✓
	GT GAS SIM PRES	-	✓	✓
	GT GAS REG PRES	✓	✓	✓
	GT GAS VAP PRES	-	-	✓
3	GT EXT CER	✓	✓	✓
	GT EXT MET	✓	✓	✓
4	GT DIR SIM	-	✓	✓
	GT DIR REG	✓	✓	✓
	GT DIR VAP	-	-	✓
5	ORC	✓	✓	✓
6	ICE GAS ORC	-	-	✓
	GT GAS ORC	-	✓	✓
7	GT HYB	✓	✓	✓

Table 4.4 – Scheme of the investigated solutions on the different scales.

As mentioned in the previous chapter, concerning gas turbines the following solutions have been taken into account: at 100 kW_{el} only the regenerative one, at 1 MW_{el} simple and regenerative ones, while at 5 MW_{el} all three ones (simple, regenerative and STIG). Naturally, as EFGTs and hybrid turbine are based on the regenerative solutions, they have been considered for all three scales. Finally, combined ICE/GT and ORC plants are applied only on the largest scales, as it is necessary that the latter produces at least 100 kW_{el} (smaller plants cannot be built up, or are not commercially available anyway). Additionally, the internal combustion engines solution is not present at the 1 MW_{el} scale

because the thermal power contained in the exhaust gases is not sufficient in this sense (while it is for gas turbines[2]).

In conclusion, the following plant scheme pictures require some specifications. Firstly, the drying system in gasifiers appears a little more complex than that shown in Chapter 3: this is exclusively related to computational issues and does not concern simulation hypotheses. Besides, the various components that gradually appear in the different plant schemes are indicated with a tag (gasifier components have already been described in the previous chapter).

[2] It is recalled that thermal power discharge in gas turbines is entirely contained in hot gases, while it is divided into hot gases and cooling water in internal combustion engines.

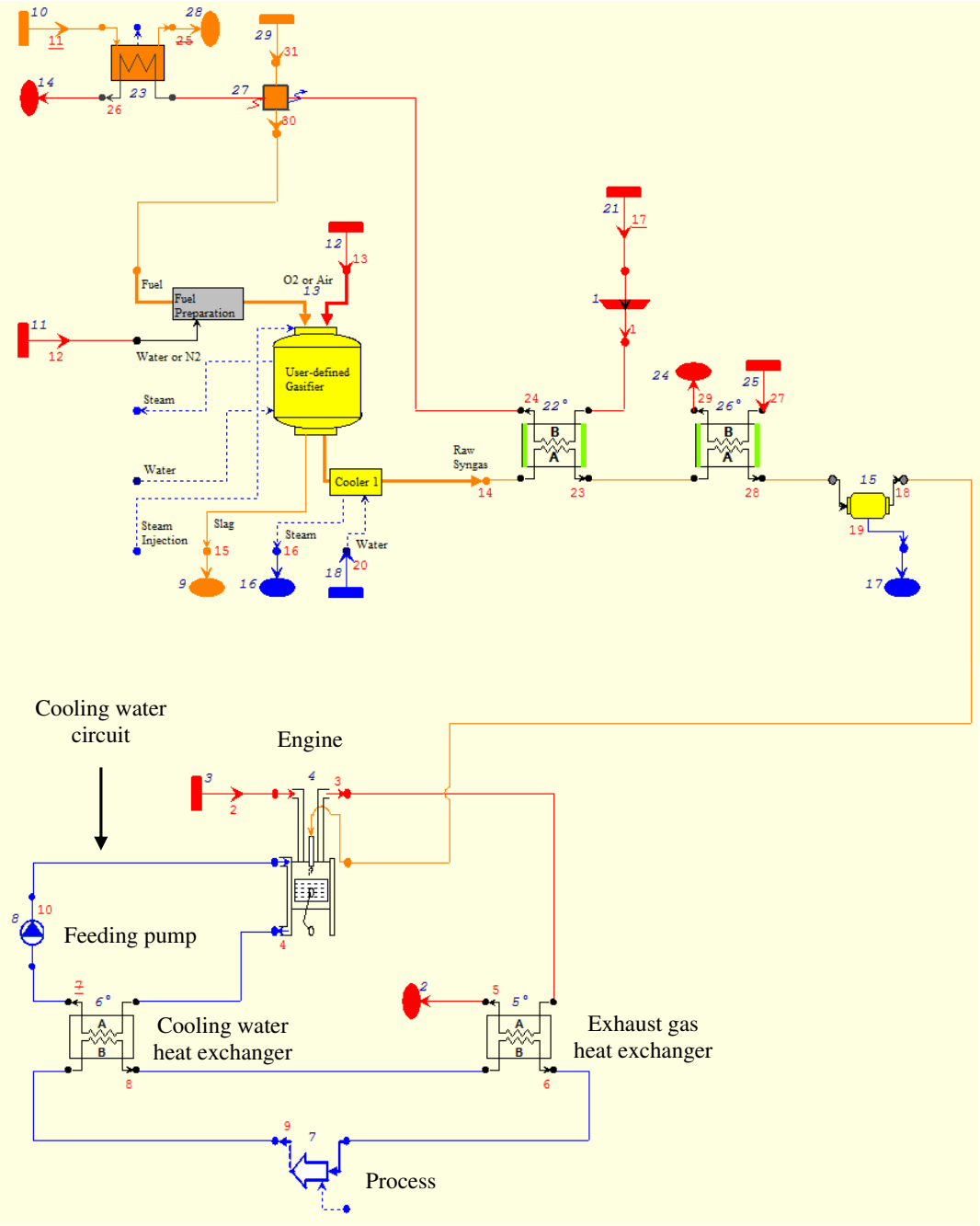

Figure 4.1 – ICE GAS: internal combustion engine coupled with a gasifier.

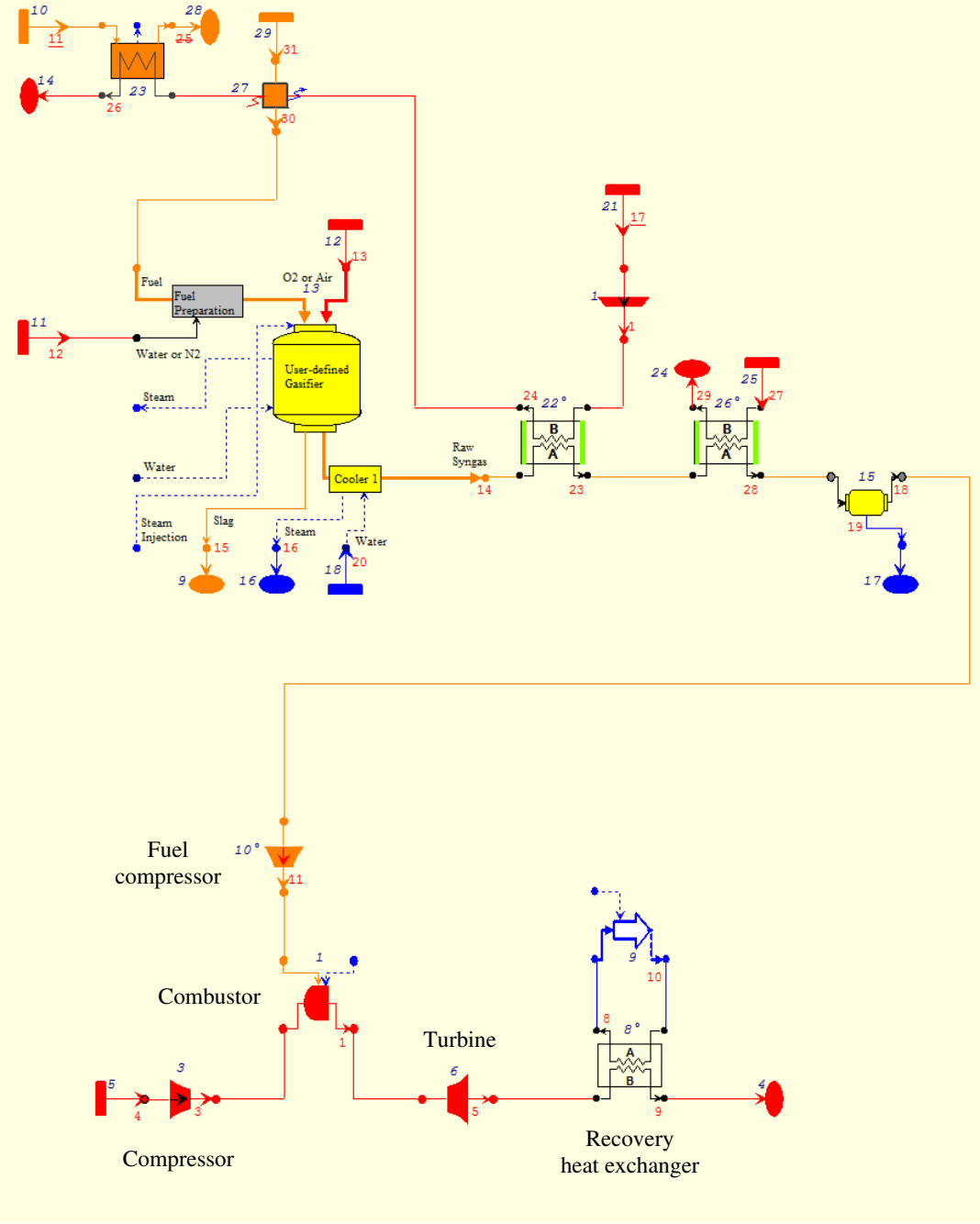

Figure 4.2 – GT GAS SIM AMB: simple-cycle gas turbine coupled with an ambient pressure gasifier.

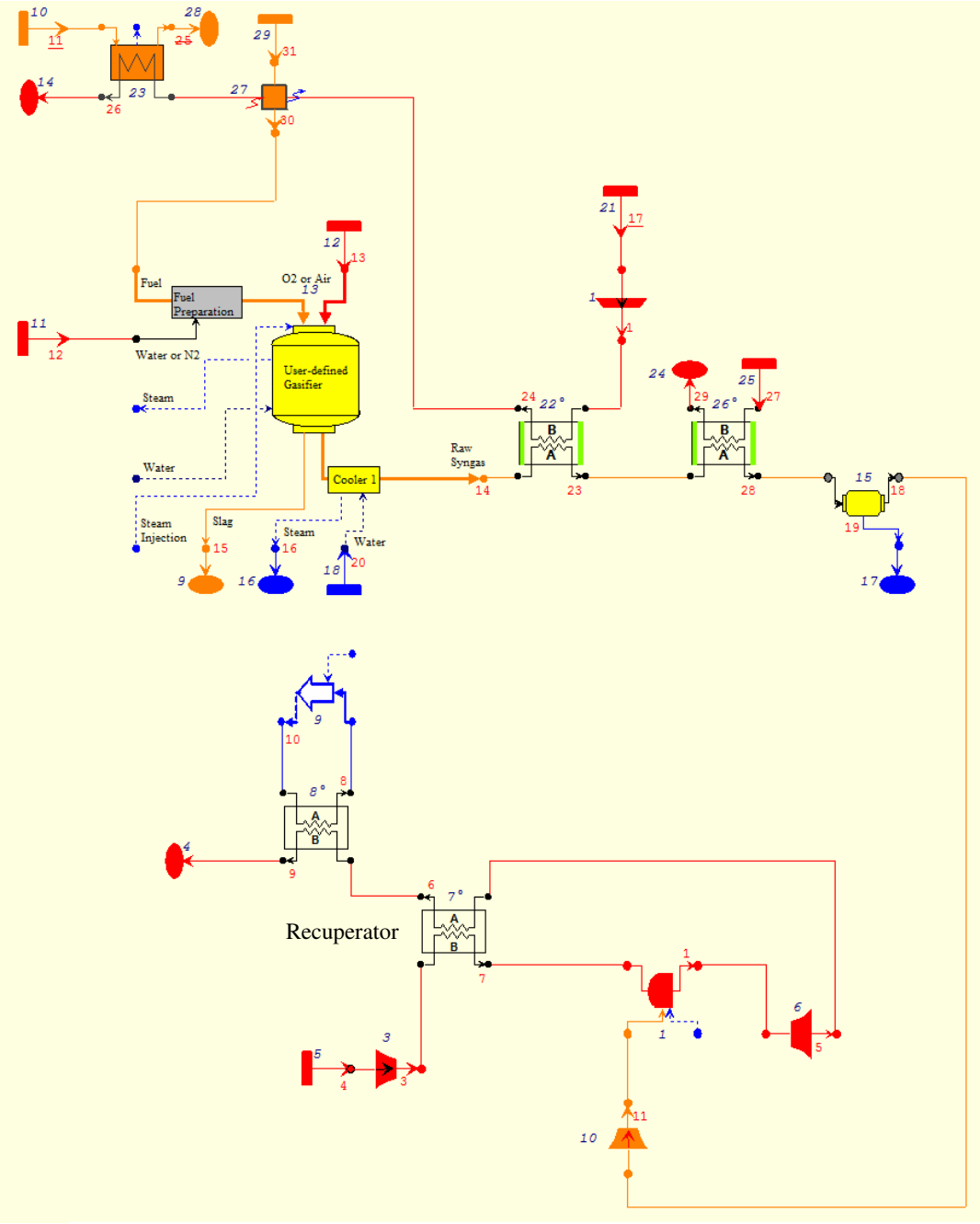

Figure 4.3 – GT GAS REG AMB: regenerative-cycle gas turbine coupled with an ambient pressure gasifier.

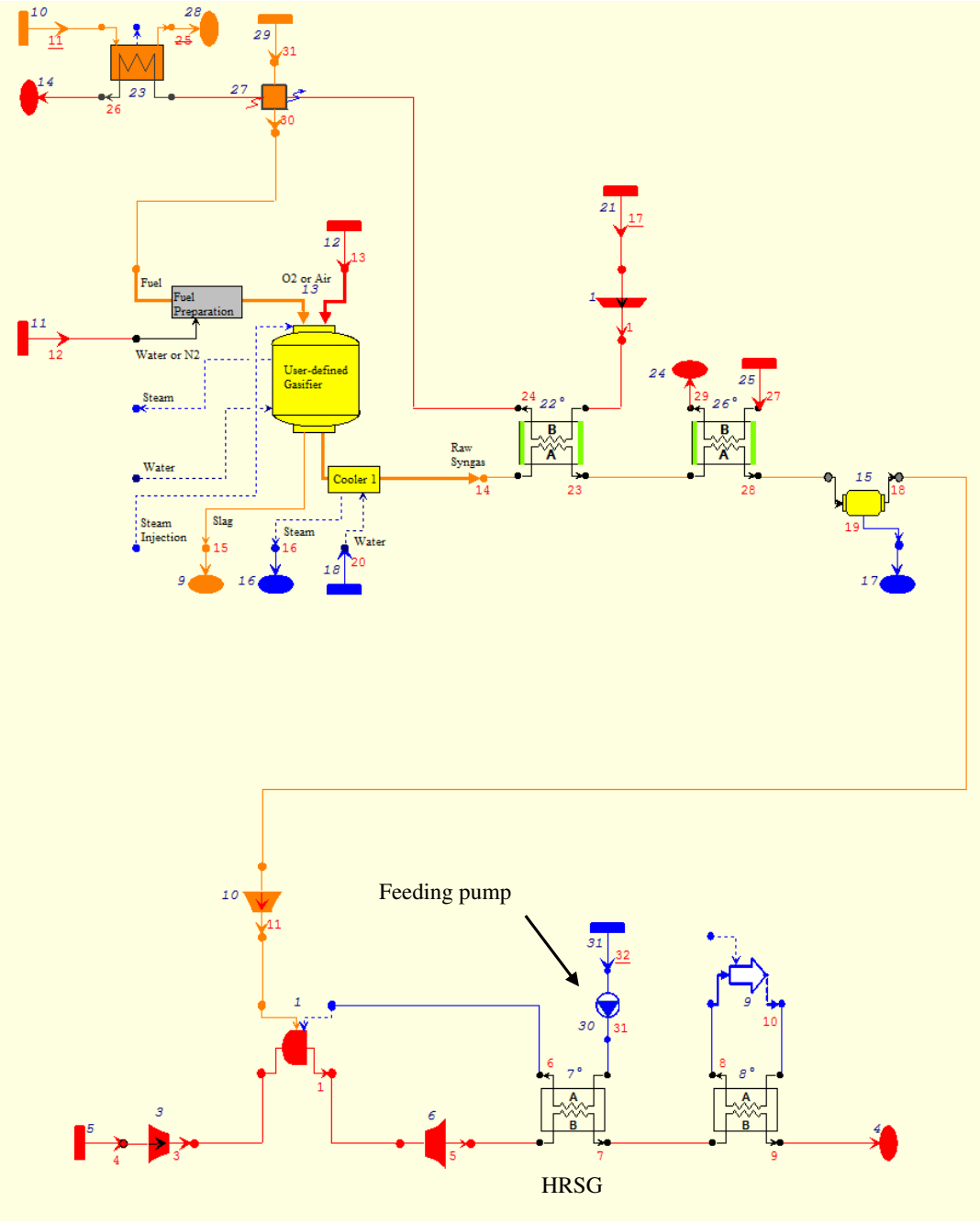

Figure 4.4 – GT GAS REG VAP: STIG-cycle gas turbine coupled with an ambient pressure gasifier.

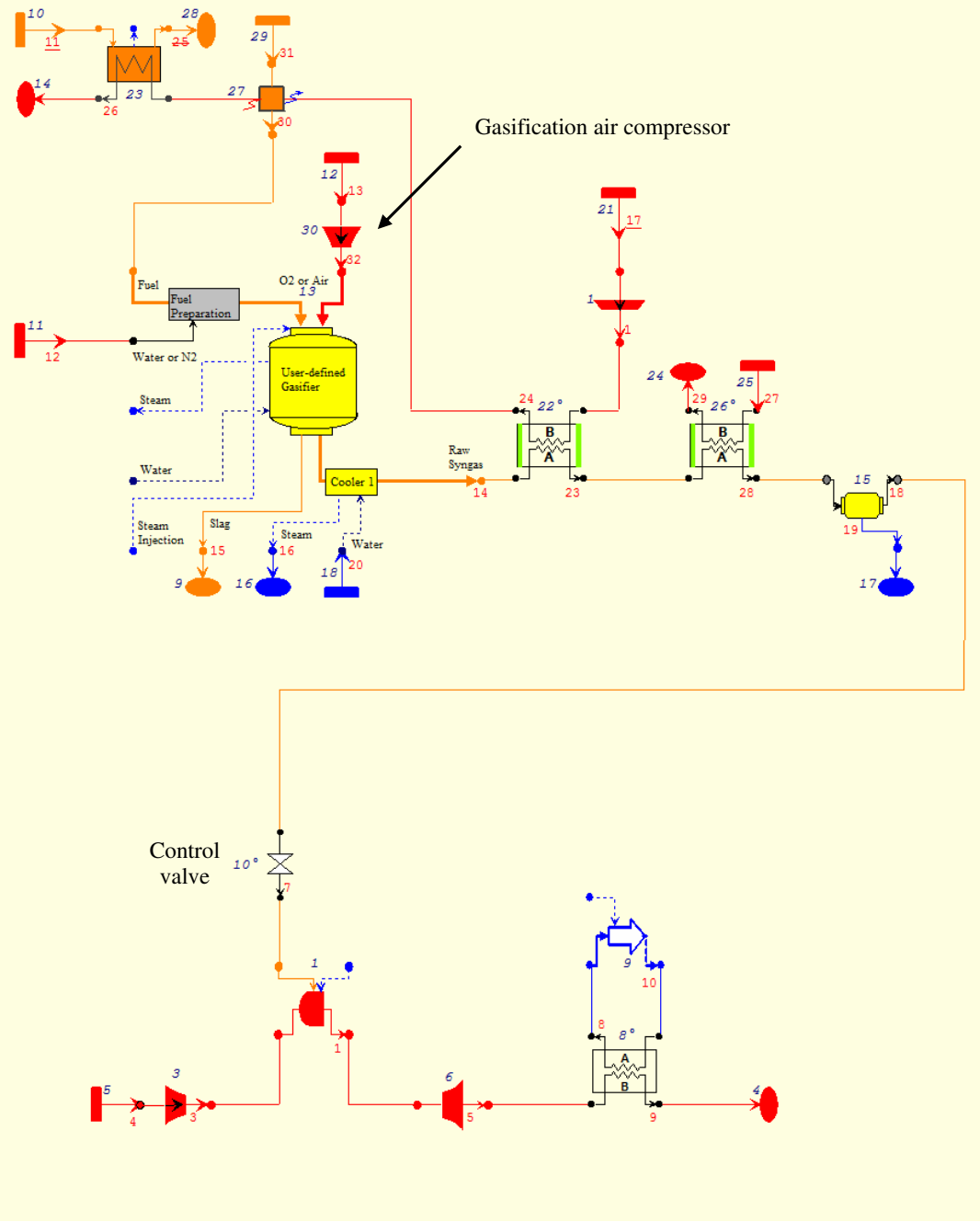

Figure 4.5 – GT GAS SIM PRES: simple-cycle gas turbine coupled with pressurised gasifier.

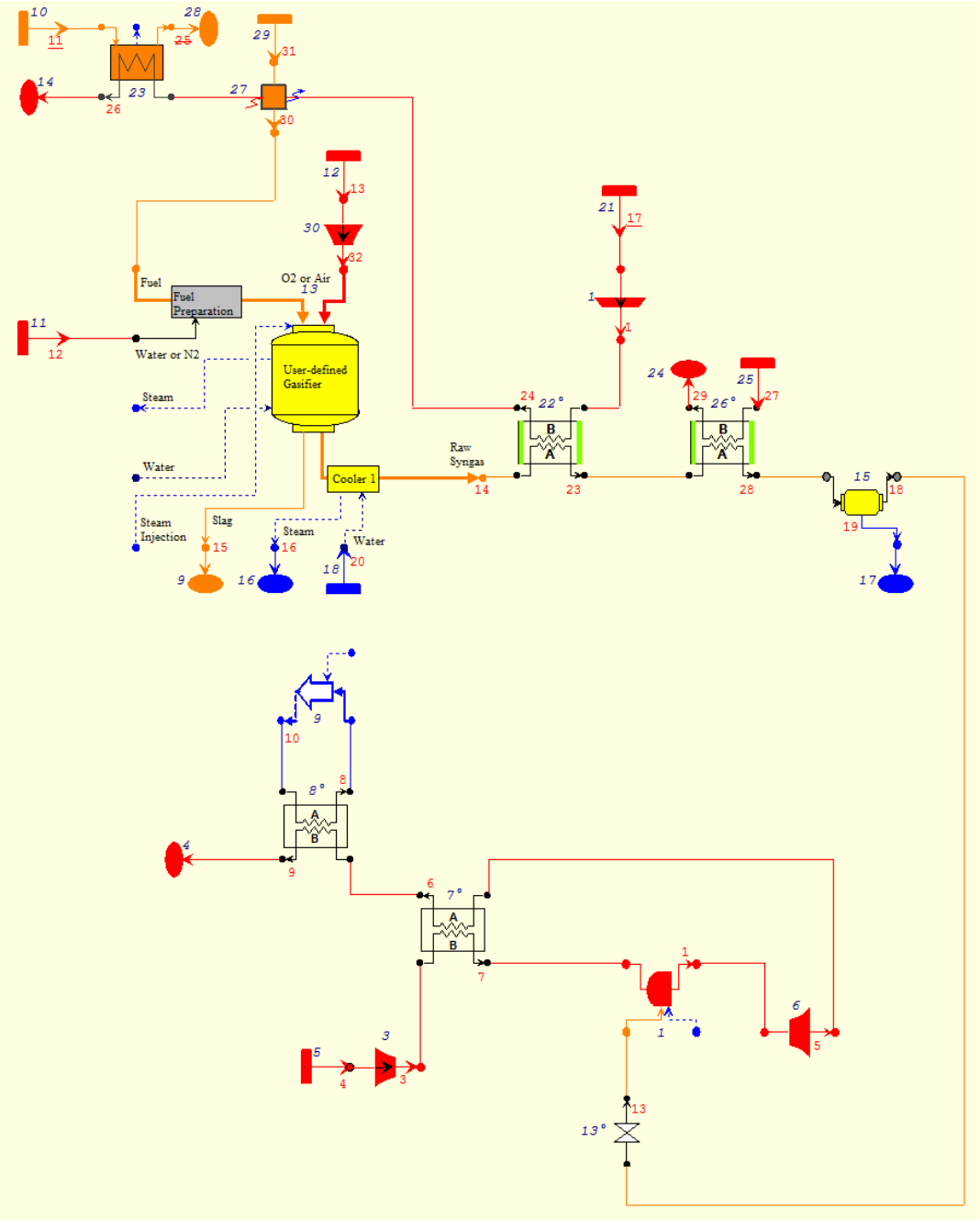

Figure 4.6 – GT GAS REG PRES: regenerative-cycle gas turbine coupled with pressurised gasifier.

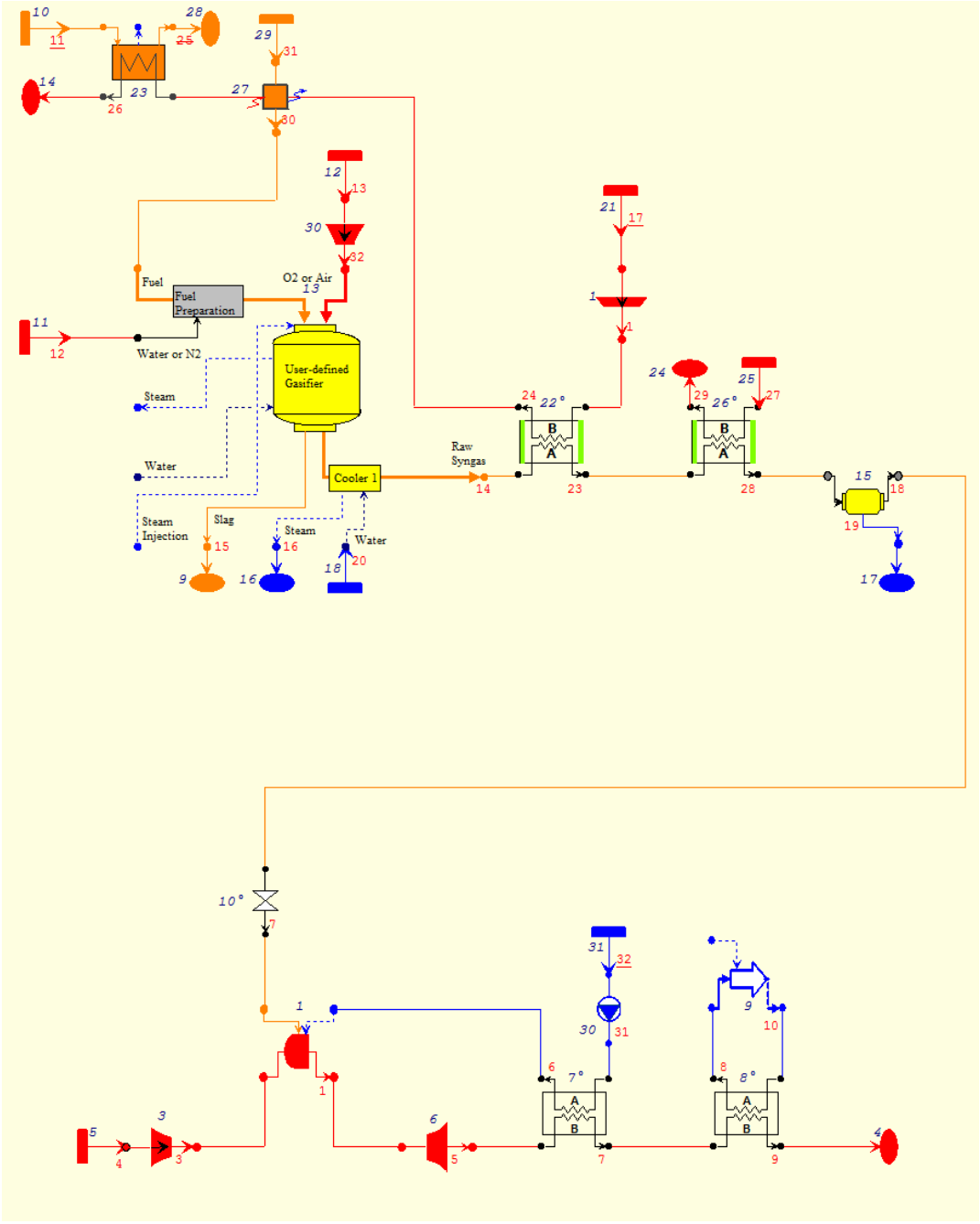

Figure 4.7 – GT GAS VAP PRES: STIG-cycle gas turbine coupled with pressurised gasifier.

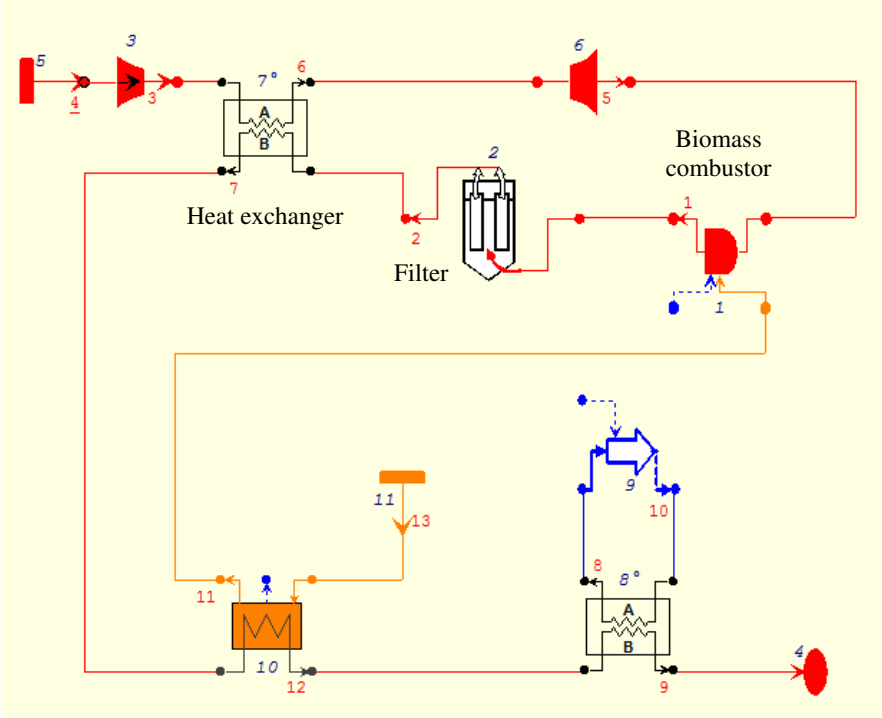

Figure 4.8 – GT EXT CER/MET: externally fired gas turbine fed with solid biomass (ceramic or metallic heat exchanger).

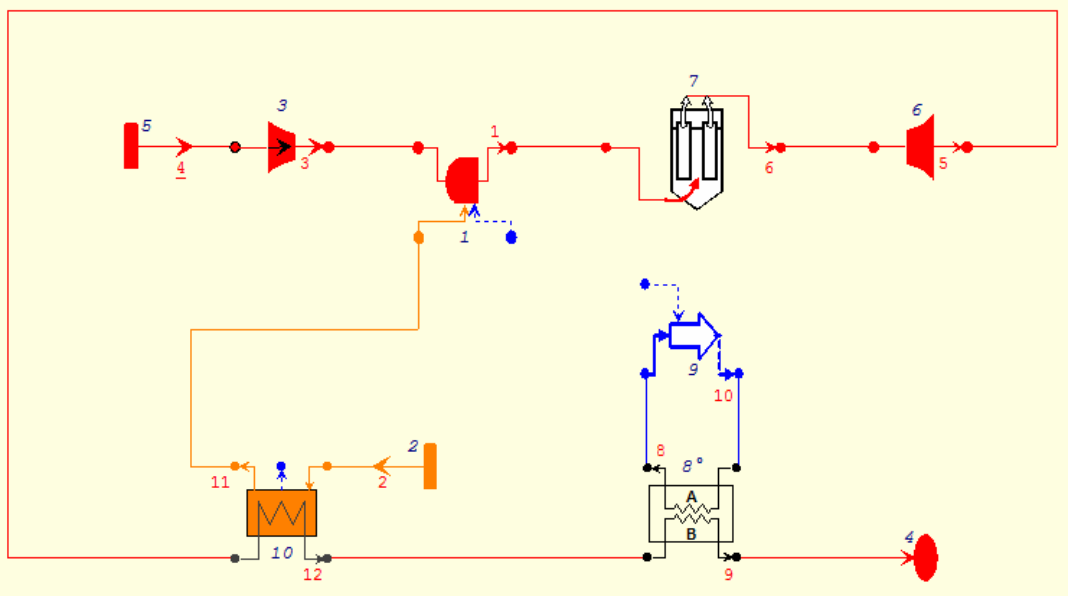

Figure 4.9 – GT DIR SIM: simple-cycle gas turbine directly fed with solid biomass.

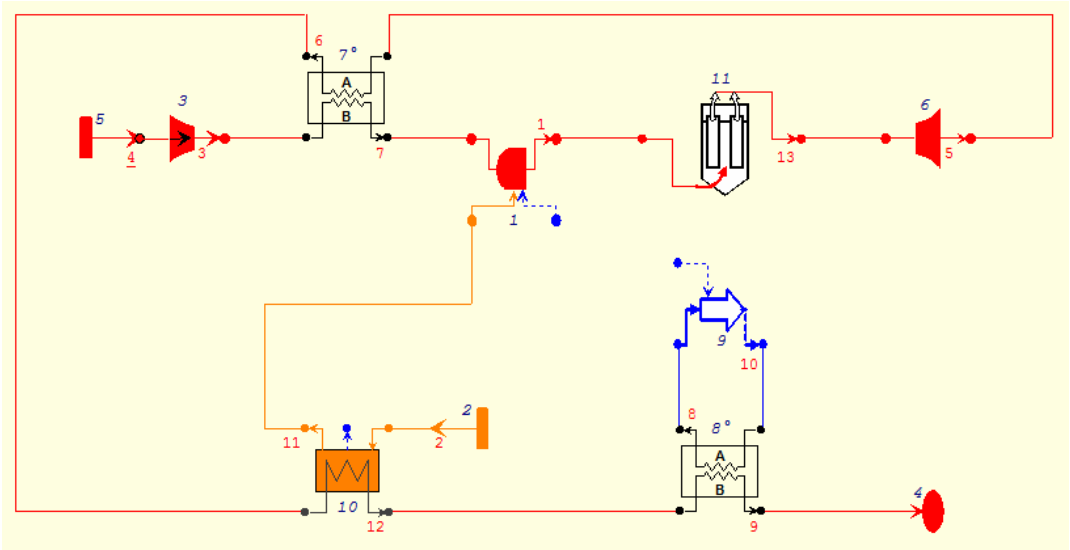

Figure 4.10 – GT DIR REG: regenerative-cycle gas turbine directly fed with solid biomass.

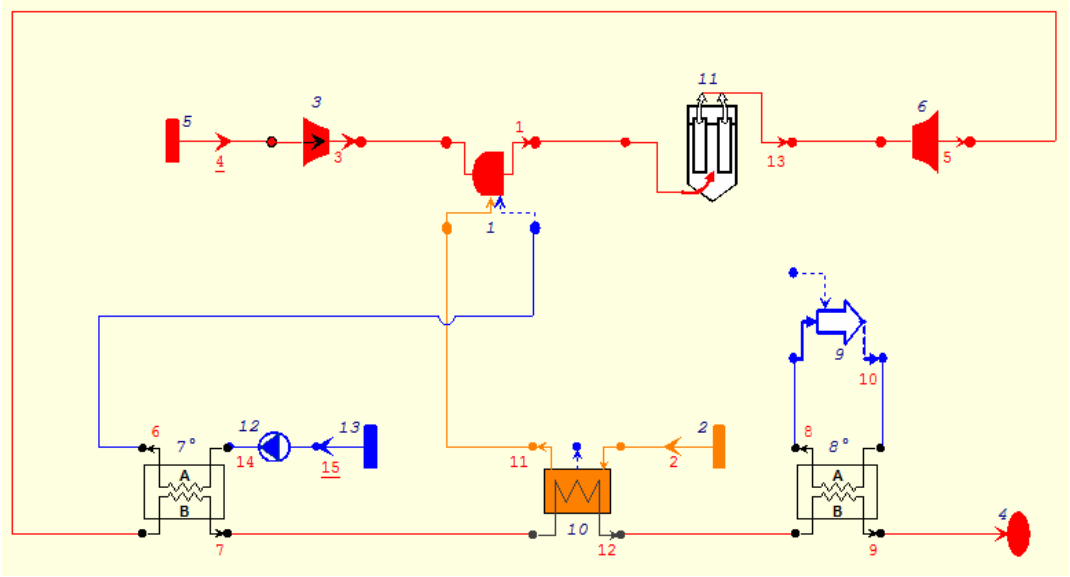

Figure 4.11 – GT DIR VAP: STIG-cycle gas turbine directly fed with solid biomass.

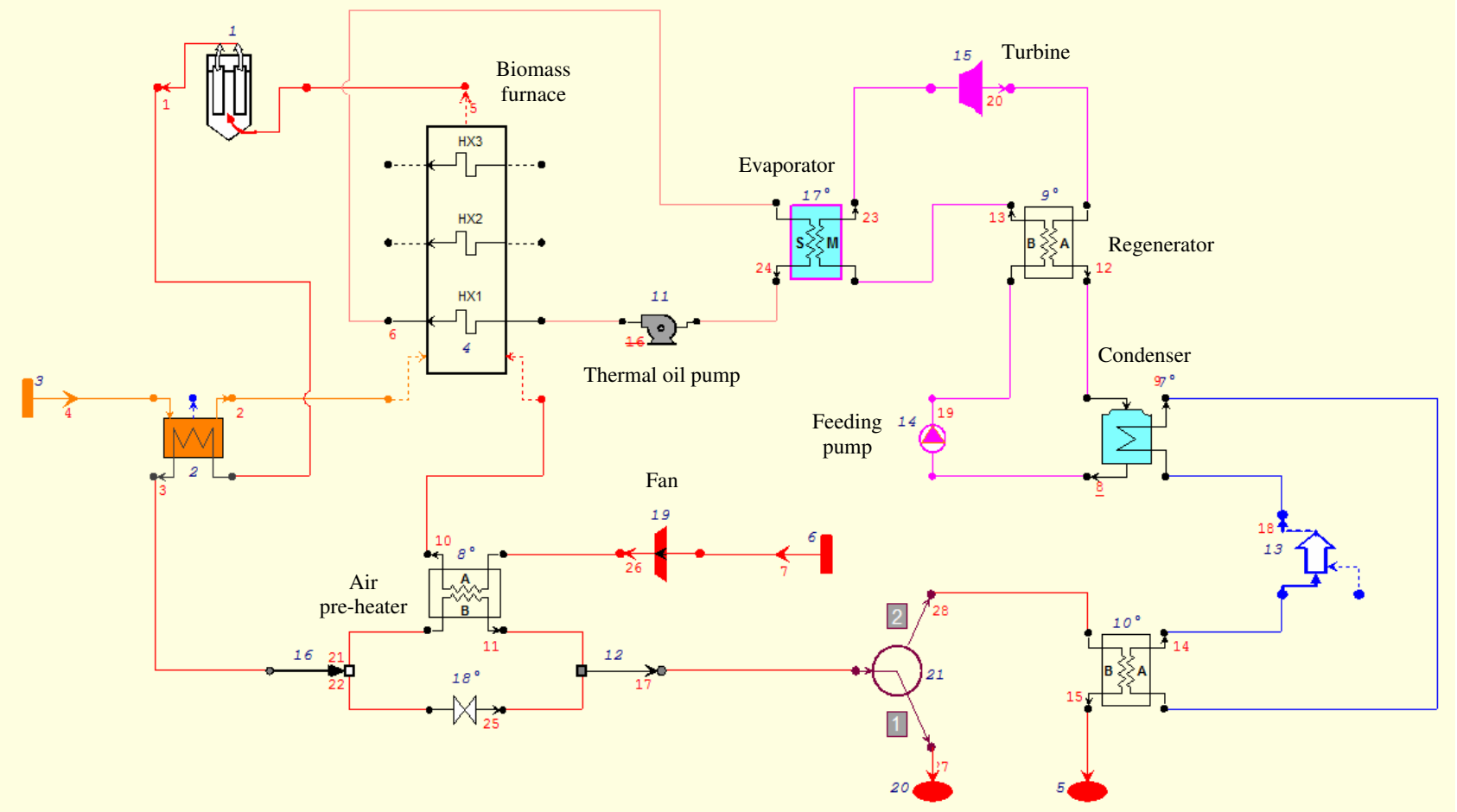

Figure 4.12 – ORC: organic Rankine cycle plant fed by biomass combustion (complete plant).

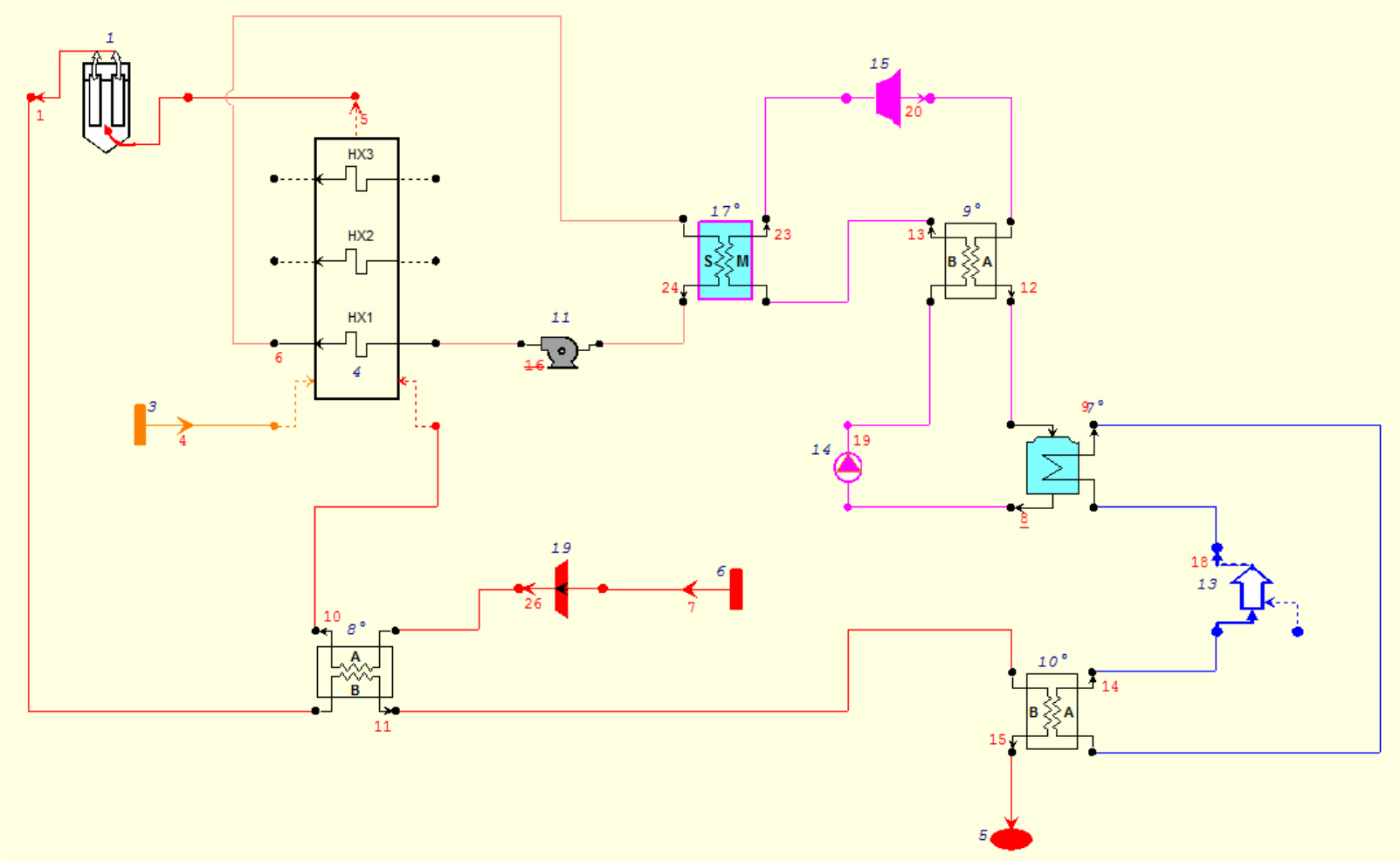

Figure 4.13 – ORC: organic Rankine cycle plant fed by biomass combustion (adopted plant: no drying).

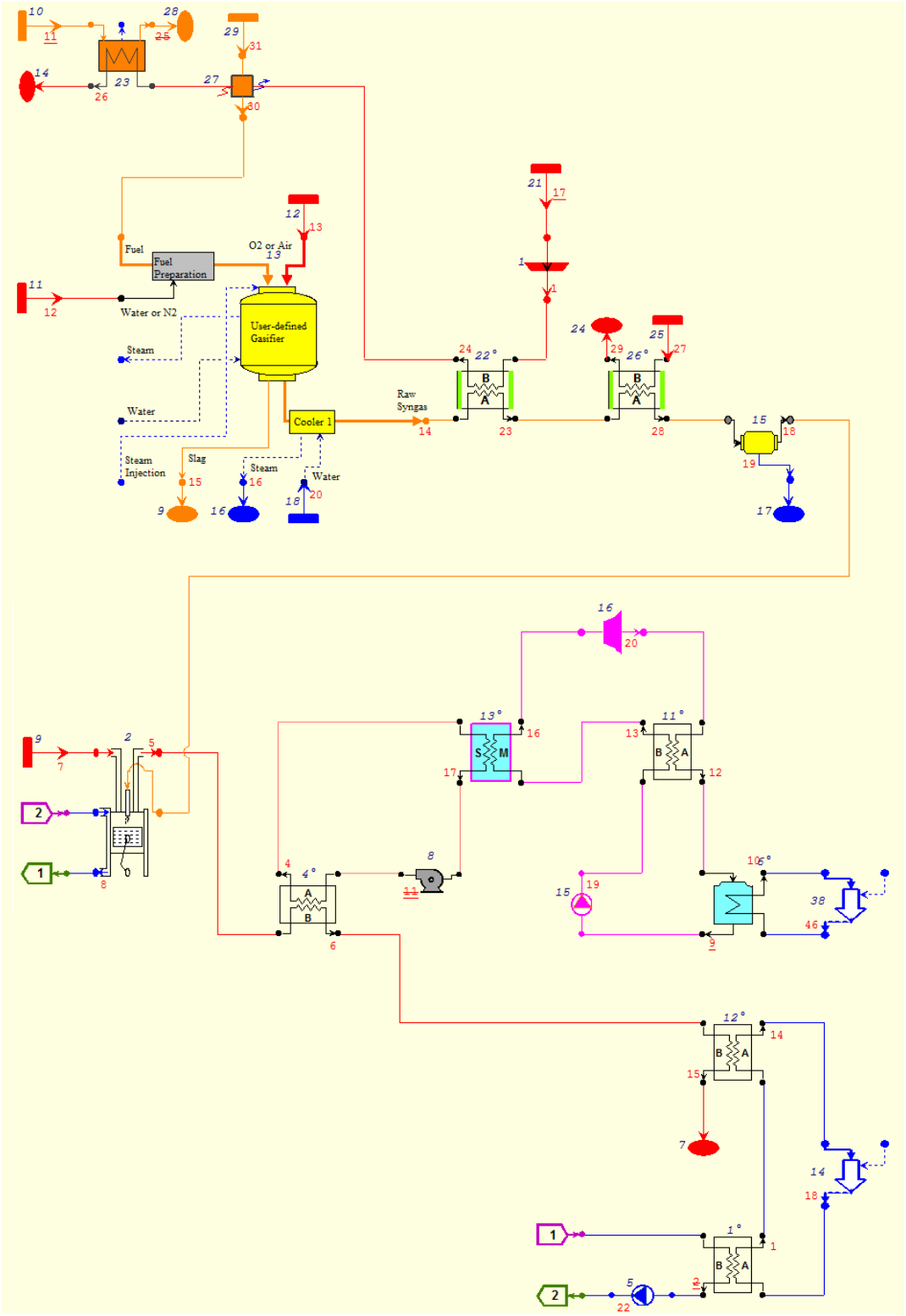

Figure 4.14 – ICE GAS ORC: internal combustion engine coupled with a gasifier and bottoming ORC.

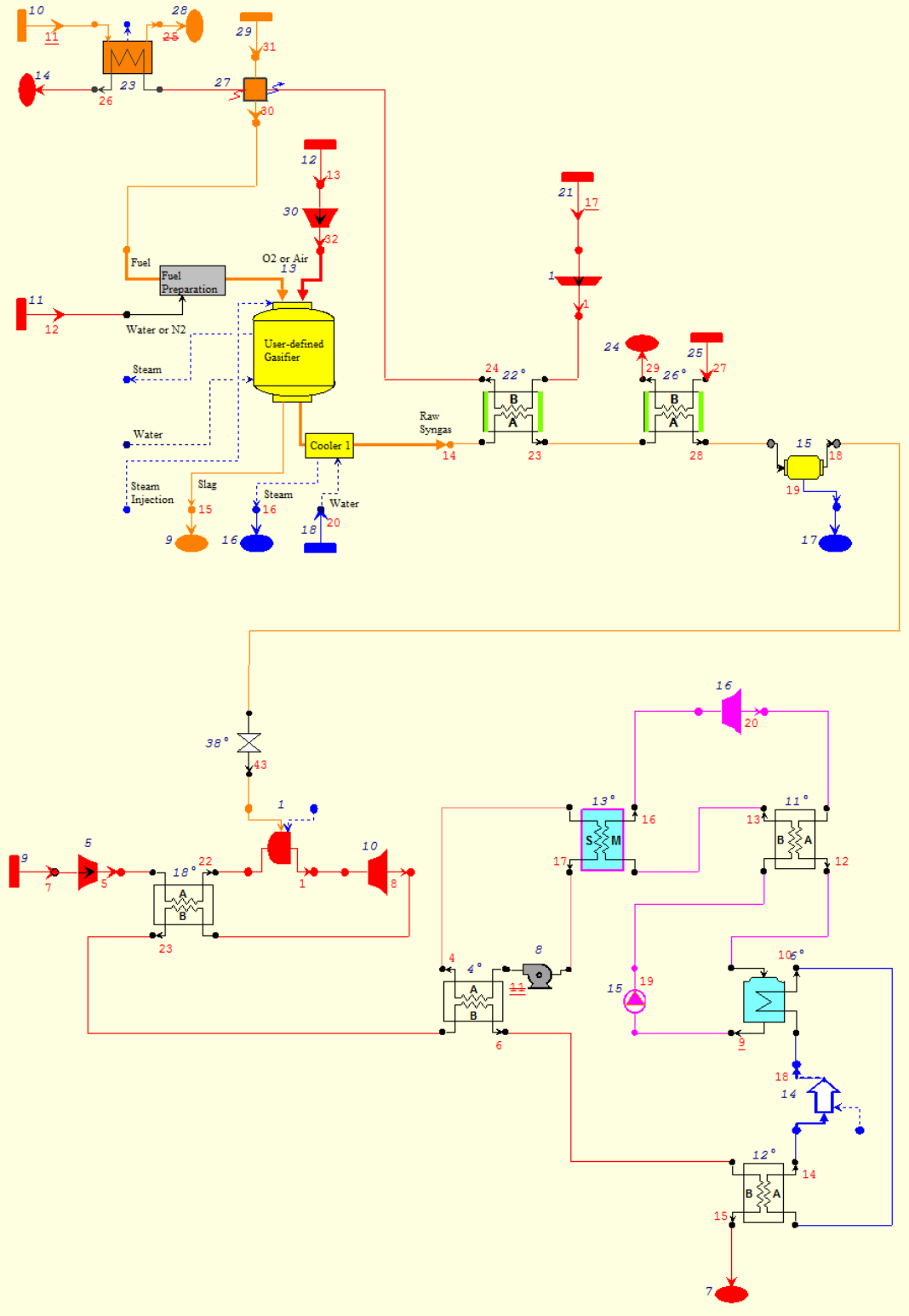

Figure 4.15 – GT GAS ORC REG PRES: regenerative-cycle gas turbine coupled with a pressurised gasifier and bottoming ORC.

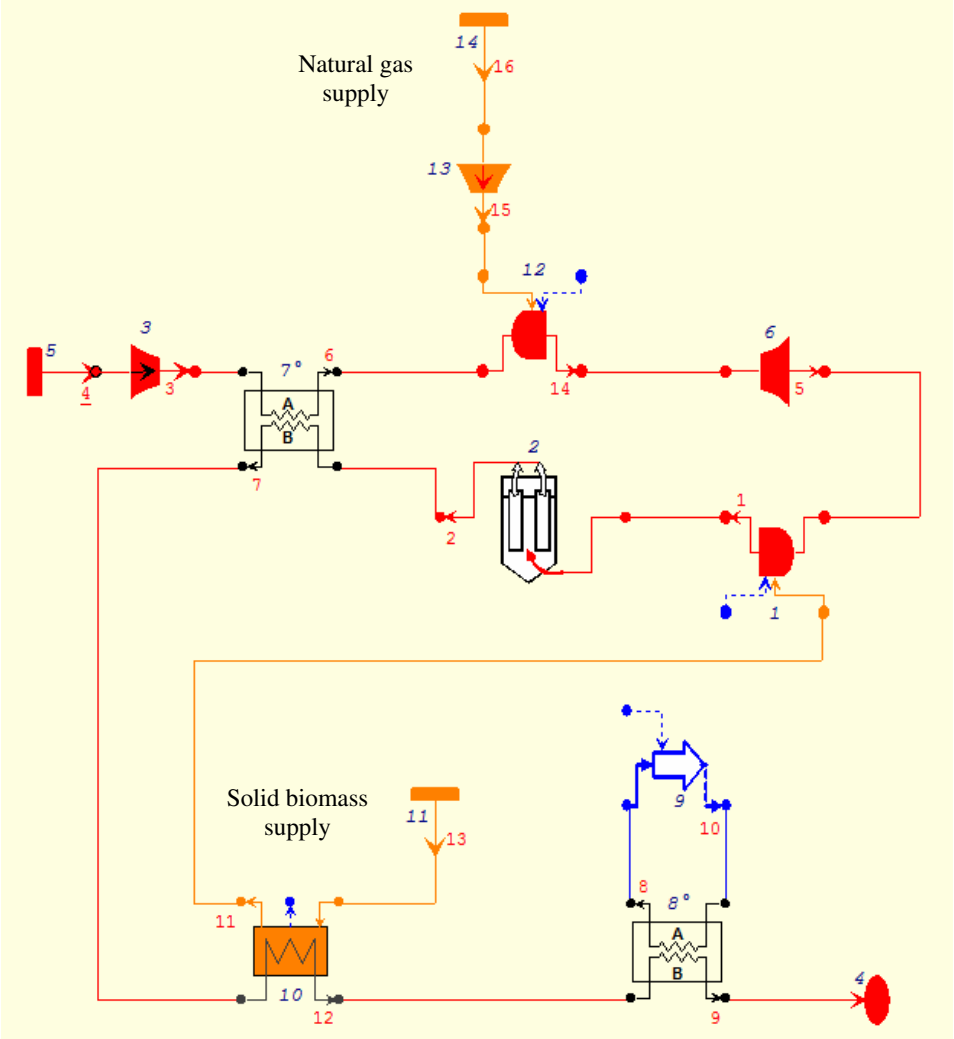

Figure 4.16 – GT HYB: gas turbine fed by natural gas and solid biomass.

4.3 Results

In this section results of the thermodynamic simulations are being presented, both in numerical terms and in chart form (histograms), where columns of the seven different groups are reported with different colours, in order to simplify the analysis. In particular, in case of gas turbine directly fed with solid biomass (group 4), a semi-transparent colouring has been chosen, in order to remember that it is a sort of ideal solution which actually cannot be applied and that its results have to be considered separately. As mentioned, results are supplied in terms of electrical (η_{el}) and first law (η_I) efficiencies, the former being the most significant.

4.3.1 100 kW_{el} size

According to Table 4.4, eight solutions have been considered at this scale. Their efficiencies are listed in Table 4.5 and graphically shown in Figures 4.17 and 4.18. The brighter portion at the top of the ORC column obviously indicates the difference between the cogenerative and the pure electric solutions.

Group	Colour	Solution	η_{el} [%]	η_I [%]
1	Green	ICE GAS	23.78	73.42
2	Red	GT GAS REG AMB	19.07	63.92
		GT GAS REG PRES	22.15	66.68
3	Gold	GT EXT CER	22.61	77.52
		GT EXT MET	14.43	74.75
4	Light brown	GT DIR REG	28.57	77.52
5	Blue	ORC	17.16 (CHP) 21.00 (EL)	91.04(CHP) 21.00 (EL)
7	Orange	GT HYB	23.62	76.82

Table 4.5 – 100 kW_{el}: electrical and first law efficiencies.

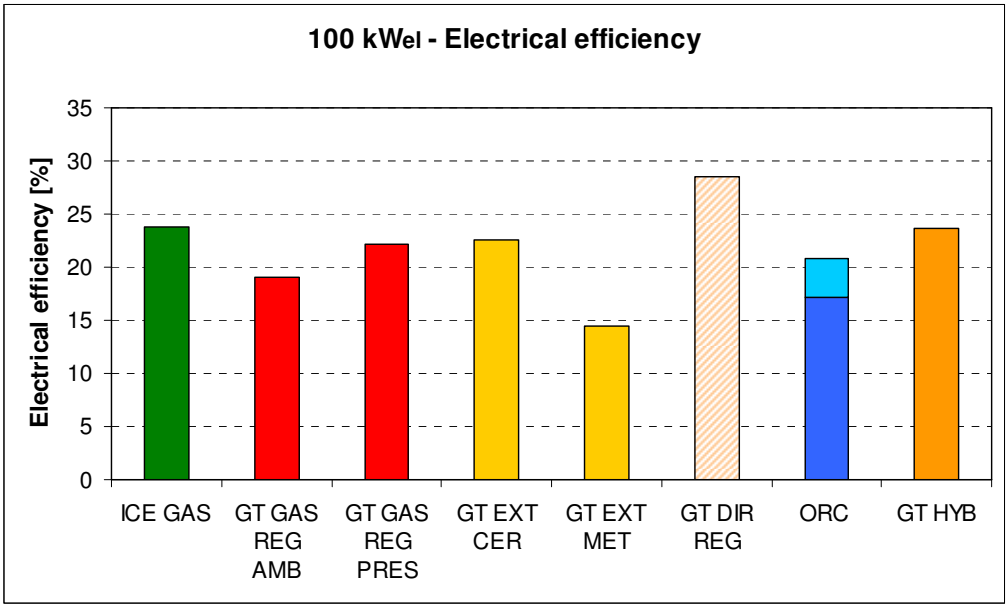

Figure 4.17 – 100 kW_{el}: electrical efficiency.

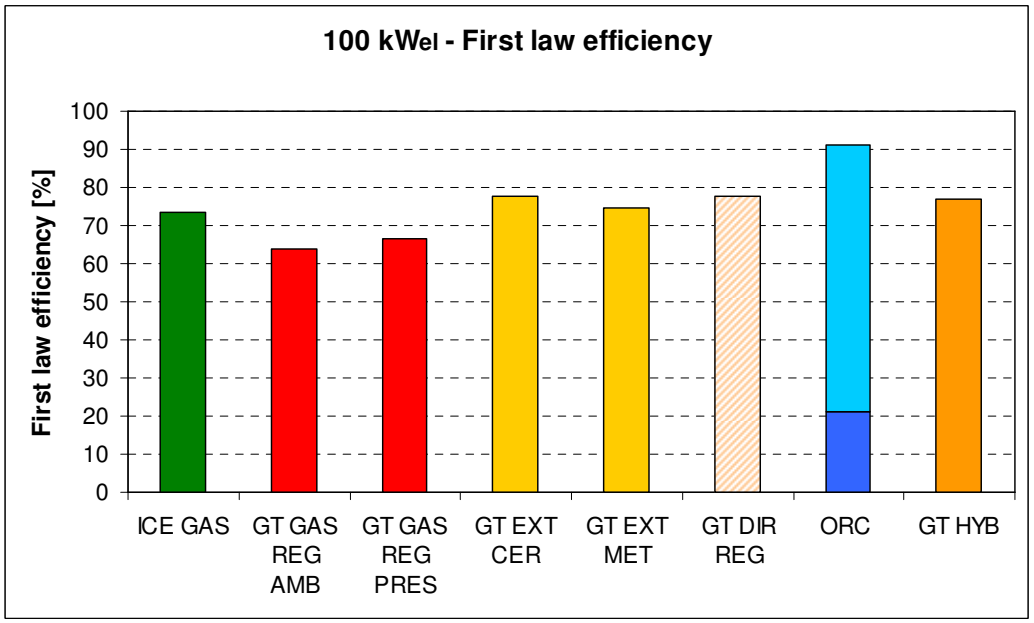

Figure 4.18 – 100 kW_{el}: first law efficiency.

In Figure 4.17 one can observe that there is a certain balance among the electrical efficiencies of the different configurations, thus confirming the prediction made in Section 2.4.2, i.e. that ICE and GT solutions would present comparable efficiencies. Obviously this is valid neglecting GT DIR REG that almost reaches 30%, i.e. the value achieved by the natural gas plant (indeed, there is practically no thermodynamic reason why this should not happen).

ICE GAS efficiency is about 24%: this value could be predictable, as it is essentially the result of the product of electrical efficiency in case of natural gas feeding (30%) and gasifier cold gas efficiency (80%), since auxiliaries needs are limited. GT GAS REG almost reaches the same result, but only in the pressurised configuration. The ambient pressure one, in fact, is heavily penalised by power consumption of the syngas compressor, that passes from about 3 kW_{el} to about 28 kW_{el}, due to the larger mass flow rate to be supplied compared to the natural gas feeding: this nullifies the benefits related to the higher power output of the expander, which increases gross power output from 106 kW_{el} to 124 kW_{el}. In case of pressurised gasifier, instead, no fuel compressor is required anymore and consumption due to the air compressor required to feed the gasifier is lower (even if it is still considerable, 13 kW_{el}). Moreover, it is recalled that pressurised conditions make the gasification process more efficient (in this case working pressure is 6.5 bar; for higher scale it reaches 20 bar). This is due to two different contributions. The first one is obviously the pressure itself (cold gas efficiency is an increasing function of this parameter), whereas the second one is related to the fact that air must be compressed: since compression is in general adiabatic, air temperature increases with the pressure ratio and this results in higher performance, same as in all combustion processes. Figures 4.19 and 4.20 graphically show the effects of these two thermodynamic parameters on gasifier cold gas efficiency. Cold gas efficiency of an ambient pressure gasifier as a function of air temperature is shown in the former, in order to investigate the pure effect of feeding this quantity, whereas in the latter the pressure effect is studied in two cases: in the first one it is investigated neglecting temperature, i.e. supposing to have a pressurised air source at ambient temperature, while in the second one a real configuration of pressurised gasifier fed by air compressed, and thus heated, by a compressor is being considered (the result is a sort of composition of the two previous curves). In these analyses, design data are obviously

those adopted up to now (even if biomass drying is not performed: however, this would simply shift the curves upwards of about 2%, as shown in Figure 3.11). As one can see, air temperature increase is more effective than pressure one in raising cold gas efficiency.

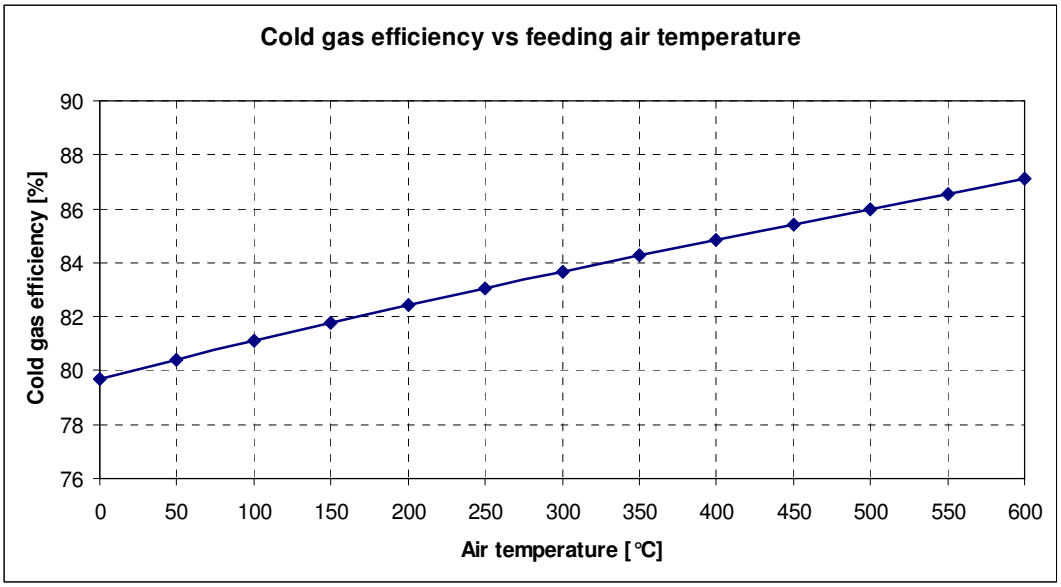

Figure 4.19 – Cold gas efficiency as a function of air temperature.

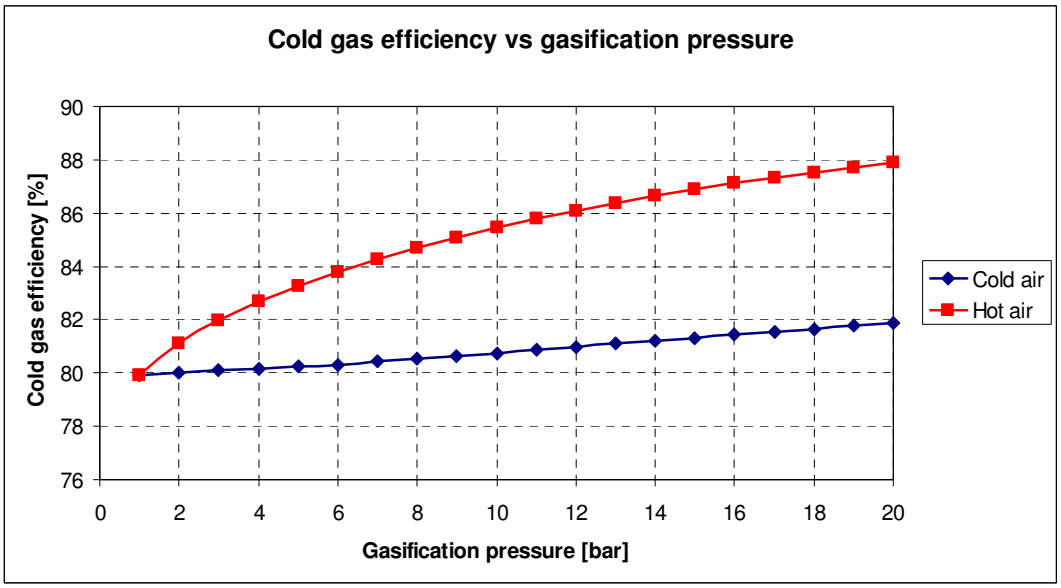

Figure 4.20 – Cold gas efficiency as a function of gasification pressure.

Returning to Figure 4.17, GT EXT CER also presents an analogous electrical efficiency, as the reduction due to the externally fired configuration is balanced by the lack of the losses related to the gasification process. On the contrary, GT EXT MET is heavily penalised by the low allowable maximum temperature, which determines a difference of about 8% compared with the previous case. As predictable, the ORC solution shows a lower efficiency than that of the other solutions (apart from GT EXT MET): 20% is exceeded only in the pure electric configuration, but at the cost of neglecting thermal heat recovery, with unacceptable consequences (at least in general) on the first law efficiency. Finally, GT HYB performance is comparable to the aforementioned ones: as predicted, the afterburning involves a η_{el} decrease compared to the natural gas case.
Concerning first law efficiency (Figure 4.18), again gasification solutions are burdened by the losses related to syngas sensible heat, which is only partially recovered. This determines a decrease of about 12 ÷ 15% compared to the methane feeding case, whereas this does not happen in the other four GT solutions keeping 75 ÷ 80%, since a stronger heat recovery is achieved against lower electrical efficiencies. The most interesting performance is however the ORC one (obviously in CHP configuration), where η_I exceeds 90%: in case of high heat demand, this solution could be suitably adopted. However, for the purposes of this work, due to its poor electric performance, it is not considered a proper choice. On the contrary, the most interesting solutions are: ICE GAS, GT GAS REG PRES, GT EXT CER and GT HYB.

4.3.2 1 MW_{el} size

Twelve solutions have been considered for 1 MW_{el} size: the three GT simple cycle solutions (GAS AMB, GAS PRES and DIR) and the combined GT GAS ORC are now added to the eight ones previously analysed.
Differently from the previous case, however, a preliminary analysis must now be carried out in order to cream off the possible versions of the GT GAS ORC solution. In fact there would be twelve theoretical configurations, then reduced to eight considering that STIG cycle is not suitable for such an application. These eight solutions are given by the combination of simple or regenerative cycle, pressurised or ambient pressure gasifier and CHP or electric ORC configuration. The objective of this phase is to

understand which cycle type (simple or regenerative) is more suitable for this application, in order to consider hereinafter only the four versions associated to it. It is important to note that in the simple cycle case the high-temperature ORC configuration (300/250°C) has been chosen, as flue gases are discharged by the turbine at about 530°C, while in the regenerative case gases are cooled in the recuperator and their exit temperature is about 315°C, which suggests the adoption of the low-temperature option (270/150°C). Results are listed in Table 4.6 and shown in Figures 4.21 and 4.22.

Cycle	Pressure	CHP/EL	Solution	η_{el} [%]	η_{I} [%]
SIM	AMB	CHP	SIM AMB CHP	19.14	68.32
		EL	SIM AMB EL	20.33	47.93
	PRES	CHP	SIM PRES CHP	22.75	72.14
		EL	SIM PRES EL	23.95	51.65
REG	AMB	CHP	REG AMB CHP	24.47	64.45
		EL	REG AMB EL	25.65	46.93
	PRES	CHP	REG PRES CHP	28.30	68.12
		EL	REG PRES EL	29.49	50.57

Table 4.6 – 1 MW_{el}: electrical and first law efficiencies of GT GAS ORC versions.

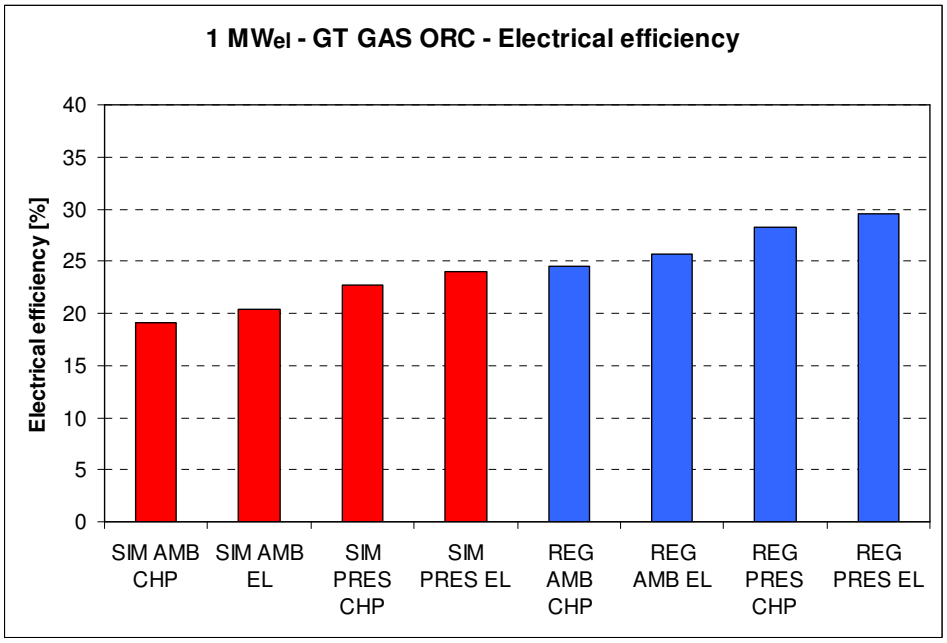

Figure 4.21 – 1 MW_{el}: electrical efficiency of GT GAS ORC versions.

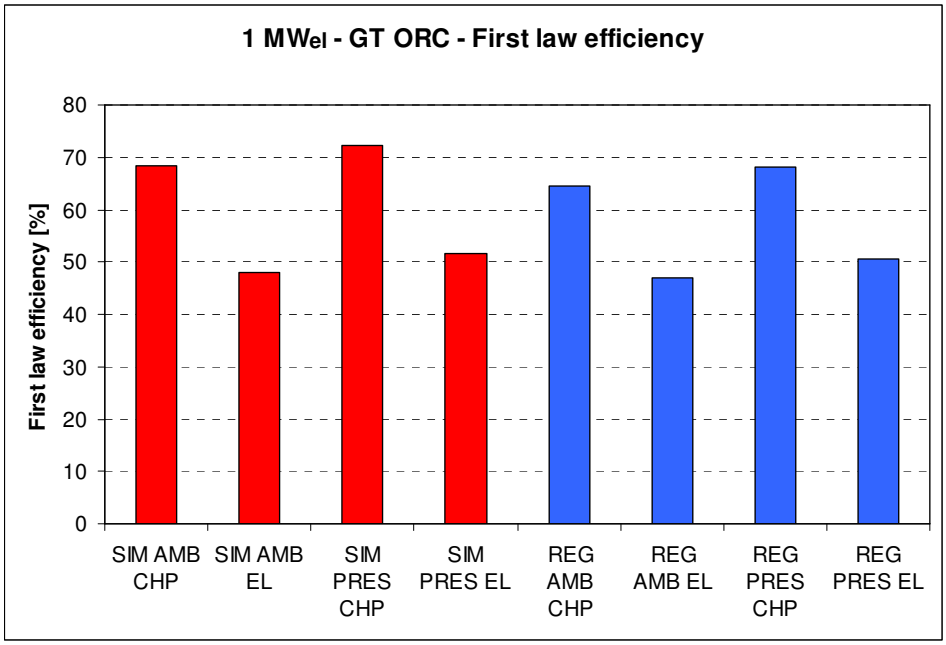

Figure 4.22 – 1 MW_{el}: first law efficiency of GT GAS ORC versions.

First of all, it must be specified that heat recovery is being effected exploiting the residual heat contained in the flue gases exiting the gas/oil heat exchanger also in case of pure electric production. Thus first law efficiency is not equal to electrical one neither in these cases. In general one can observe that pressurised solutions are more efficient than ambient pressure ones and that CHP configurations lead to slightly lower electrical efficiencies but much higher first law efficiencies than electric ones. Apart from this, Figure 4.21, shows that the regenerative cycle provides much better electric performance: a difference of 5 ÷ 6% with the corresponding simple cycle solutions has been found for all of the configurations. This means that the higher performance reached by the ORC in the latter case (due to the hotter thermal oil source) is not sufficient to compensate the regeneration effect in the gas turbine. Obviously an optimisation of the thermodynamic parameters could be performed, but it can be hypothesised that results would not change in qualitative terms, and however referring uniquely to the two described ORC configurations is considered more suitable. In conclusion, the regenerative cycle is preferable compared to the simple one (first law efficiencies are slightly lower, but obviously this can be neglected) and thus its four configurations will be considered hereinafter (naturally for the 5 MW_{el} case, too).

After this preliminary analysis, overall results for the 1 MW_{el} scale are listed in Table 4.7 and shown in Figures 4.23 and 4.24.

Group	Colour	Solution	η_{el} [%]	η_{I} [%]
1	Green	ICE GAS	31.73	69.99
2	Red	GT GAS SIM AMB	13.42	68.08
		GT GAS REG AMB	21.27	65.47
		GT GAS SIM PRES	17.07	71.96
		GT GAS REG PRES	25.15	69.25
3	Gold	GT EXT CER	24.97	79.58
		GT EXT MET	19.17	78.49
4	Light brown	GT DIR SIM	21.84	83.31
		GT DIR REG	31.68	79.85
5	Blue	ORC	17.16 (CHP) 21.00 (EL)	91.04(CHP) 21.00 (EL)
6	Purple	GT GAS ORC	24.47 (AMB CHP) 25.65 (AMB EL) 28.30 (PRES CHP) 29.49 (PRES EL)	64.45 (AMB CHP) 46.93 (AMB EL) 68.12 (PRES CHP) 50.57 (PRES EL)
7	Orange	GT HYB	26.06	79.95

Table 4.7 – 1 MW_{el}: electrical and first law efficiencies.

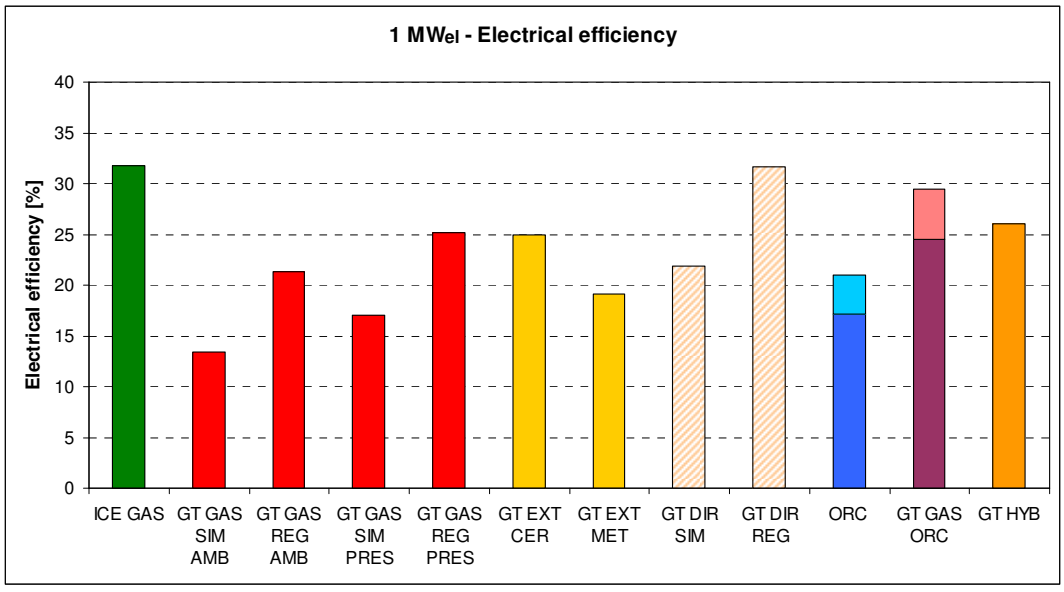

Figure 4.23 – 1 MW_{el}: electrical efficiency.

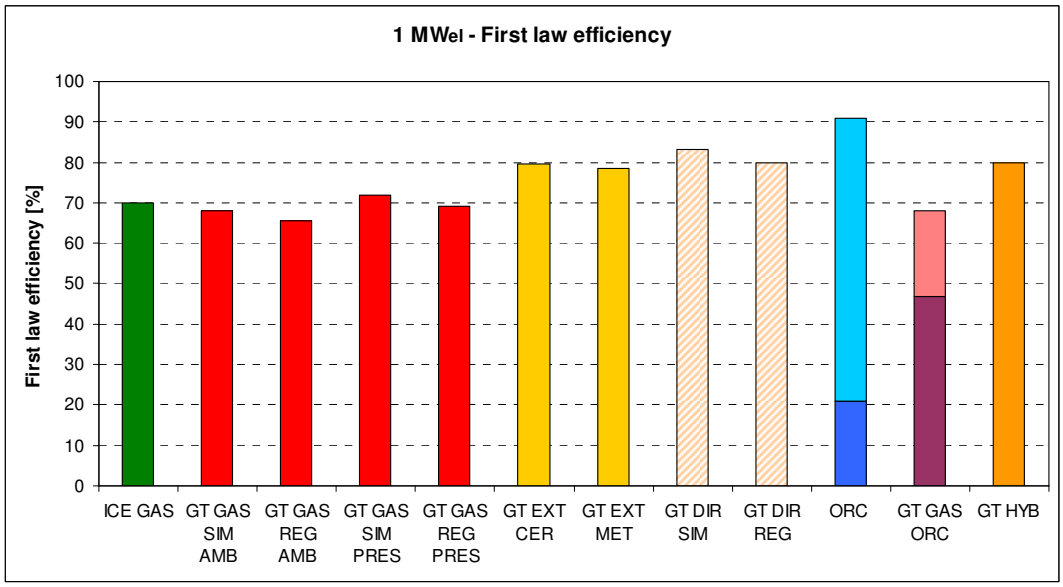

Figure 4.24 – 1 MW_{el}: first law efficiency.

Differently from the 100 kW_{el} case, where a substantial balance has been found, as far as electrical performance is concerned, the ICE GAS solution is much more efficient than plants with gas turbine, again confirming the hypotheses made in Section 2.4.2, where it was supposed that higher efficiency of a methane-fuelled internal combustion engine would be reflected on biomass-fed plants, too. As for 100 kW_{el}, the result (about 32%) is given by the product of the machine base efficiency (40%) and the gasifier cold gas efficiency (80%). In absolute terms, there is an increase of about 7% with respect to the previous case. Only GT DIR REG has an efficiency comparable to the engine, as it practically reports the performance of the natural gas regenerative turbine, but the particularity of this solution has already been discussed. On the other hand, GT DIR SIM itself, despite the direct feeding advantage, suffers the poor performance of the simple cycle gas turbine, so that electrical efficiency is low. For the same reason, among GT GAS solutions, simple-cycle ones have low efficiencies, while a good result is reached (about 25%, analogous to the previous size) only with a regenerative cycle, and in particular, with a pressurised gasifier (GT GAS REG PRES). A similar efficiency is achieved by GT EXT CER, while the configuration with a metallic heat exchanger is always penalised by low maximum temperatures (however, its performance in both pressure configurations is better than the GT GAS SIM one). As regards ORC, since efficiencies are equal to those presented for 100 kW_{el}, almost the same evaluation

proposed there is valid, although now the distance between its efficiencies and those reached by the best solutions is becoming greater. On the other hand, it is interesting to analyse the result of the combined solution, i.e. GT GAS ORC: as easily understandable, its performance is better with respect to the other GT solutions (in the pressurised pure electric case it almost reaches 30%), nevertheless ICE GAS has still a 2% higher electrical efficiency. Finally, same as in the previous case, the hybrid solution places itself at a level comparable to GT GAS REG PRES and GT EXT CER.
On the other hand, the analysis of first law efficiencies does not provide any particular indications: for plants with a gasifier this parameter is about 65 ÷ 70%, for the other solutions with a gas turbine it is about 80%, while naturally ORC (CHP) is still the best solution with its 90%: values are roughly analogous to the previous case. Concluding, what has been said above regarding ORC is valid also for GT GAS ORC too, namely that the pure electric production involves a heavy reduction of first law efficiency (- 17 ÷ 18%), allowing to get improvements of just 1% in electrical terms: therefore also in this case the cogenerative configuration (in particular coupled with a pressurised gasifier, where efficiencies are 4% higher than the ambient pressure ones) is generally preferable.
In conclusion, the most interesting solutions are analogous to those listed regarding the 100 kW_{el} case, with the addition of GT GAS ORC.

4.3.3 5 MW_{el} size

All of the sixteen solutions listed in Table 4.4 have been analysed for the last scale: apart from the twelve configurations studied regarding the 1 MW_{el} scale, STIG cycle plants for GT solutions and the combined ICE GAS ORC have been considered. As mentioned before, concerning the GT GAS ORC solution, only the regenerative cycle has been taken into account. Results are listed in Table 4.8 and shown in Figures 4.25 and 4.26, reported on the following pages. Focussing on electrical efficiencies, results are qualitatively analogous to those regarding the 1 MW_{el} scale. ICE GAS benefits from the engine's very high electrical efficiency and is well ahead of gas turbine solutions (as usual, except for those with direct solid biomass feeding): 37% against about 30% in the best cases.

Group	Colour	Solution	η_{el} [%]	η_{I} [%]
1	Green	ICE GAS	36.82	70.28
2	Red	GT GAS SIM AMB	17.95	68.72
		GT GAS REG AMB	24.87	67.82
		GT GAS VAP AMB	24.07	47.41
		GT GAS SIM PRES	22.37	73.86
		GT GAS REG PRES	29.60	72.59
		GT GAS VAP PRES	29.43	52.42
3	Gold	GT EXT CER	25.96	81.60
		GT EXT MET	15.21	79.78
4	Light brown	GT DIR SIM	26.75	83.89
		GT DIR REG	36.05	82.51
		GT DIR VAP	35.41	58.39
5	Blue	ORC	17.16 (CHP) 21.00 (EL)	91.04(CHP) 21.00 (EL)
6	Purple	ICE GAS ORC	39.22 (CHP) 39.85 (EL)	73.41 (CHP) 61.98 (EL)
		GT GAS ORC	28.62 (AMB CHP) 29.93 (AMB EL) 33.31 (PRES CHP) 34.63 (PRES EL)	67.88 (AMB CHP) 47.32 (AMB EL) 72.54 (PRES CHP) 51.82 (PRES EL)
7	Orange	GT HYB	31.62	82.85

Table 4.8 – 5 MW_{el}: electrical and first law efficiencies.

STIG cycle versions almost equalise regenerative cycle ones among plants with gas turbine in all of the three cases in which they are adopted (GAS AMB, GAS PRES and DIR). On the contrary, differently from the previous cases, GT EXT CER has a lower efficiency than the regenerative-pressurised GT GAS: this is due to the limitations imposed on the maximum working temperature at the heat exchanger (see Section 4.2.3). The same considerations proposed for the previous size are valid for GT EXT MET and ORC. Concerning the combined solutions, those with a gas turbine are again slightly less performing than ICE GAS, while ICE GAS ORC obviously reaches the highest efficiency, since the ORC contribution is added to the 37% achieved by ICE GAS. Indeed, the increase consists in just 2 ÷ 3%, as the non enormous thermal energy contained in the engine flue gases limits power production by ORC. However almost 40% is reached: an excellent result, comparable to that of large scale BIGCCs.

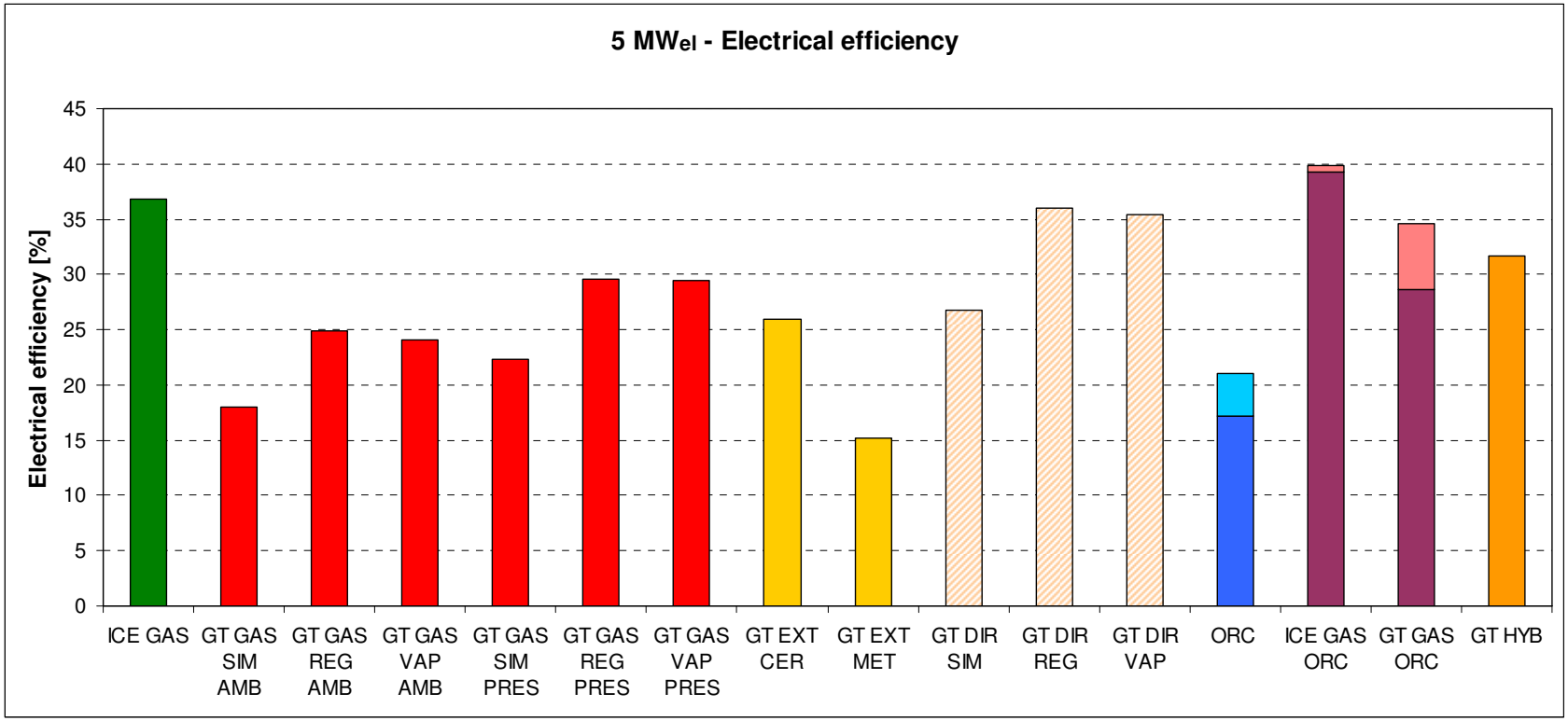

Figure 4.25 – 5 MW_{el}: electrical efficiency.

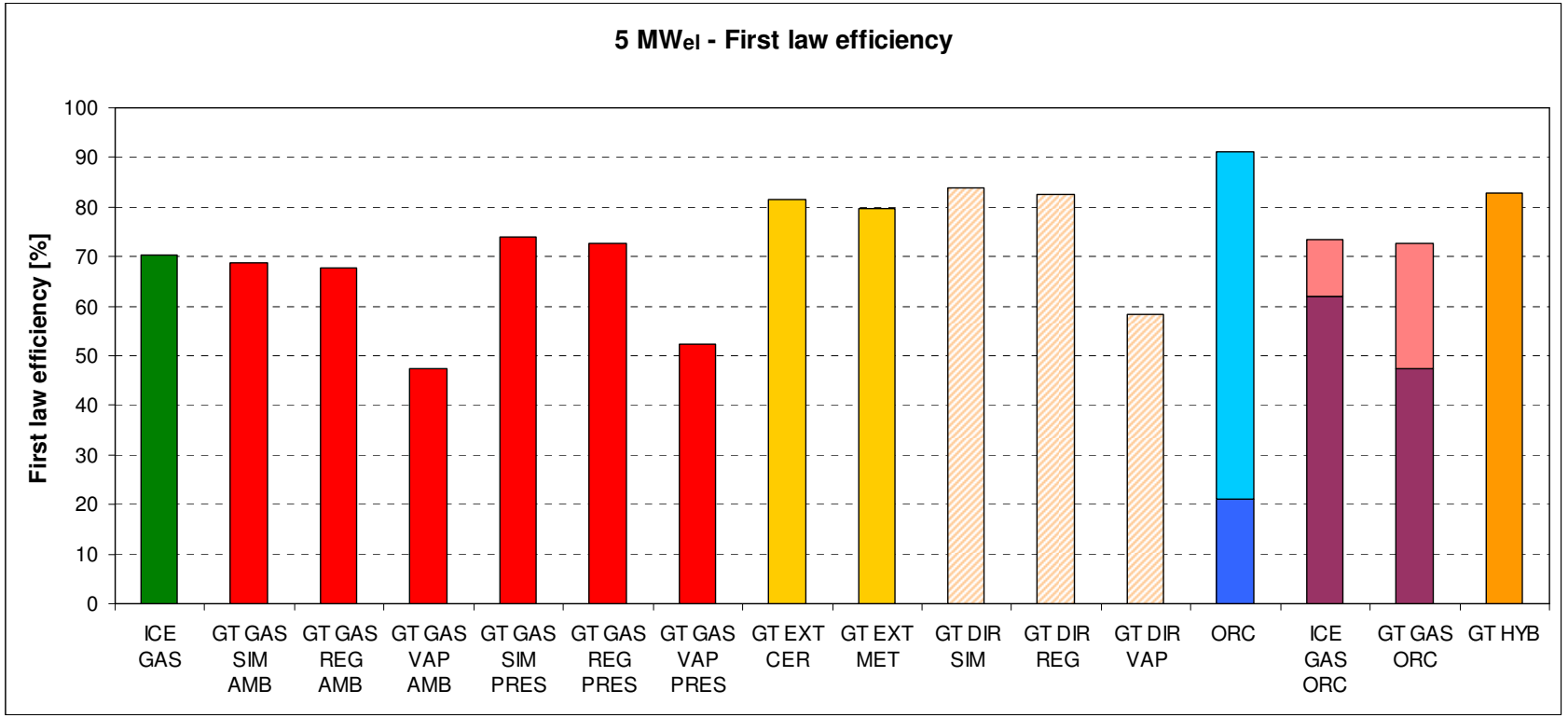

Figure 4.26 – 5 MW_{el}: first law efficiency.

Finally GT HYB as usual settles on the levels of GT GAS REG PRES, i.e. about 30%.
On the other hand, observations made in the previous sections can be proposed again for first law efficiencies, too. Here it is sufficient to note the poor performance of STIG solutions, where heat is absorbed to produce injection steam increasing electrical efficiency, but determining a strong reduction in the process heat yield.
In conclusion, the most interesting solutions are those previously mentioned, in addition, of course, to ICE GAS ORC.

4.4 Improved gasification solutions

As described in the previous chapter and shown in the plant schemes proposed in the previous pages, the gasification facility provides the recovery of syngas sensible heat by means of an air stream, that is then used to dry biomass. If very wet fuel is used, the thermal content of this air stream is mainly absorbed for this purpose and can then not be used for other applications, but if biomass moisture is low (like in the examined case, where it is recalled that wood pellets with 8.7% moisture are used), air exiting the biomass dryer still has an interesting temperature (about 200°C with the adopted design data) and therefore it can be exploited for other thermal purposes. Firstly it can be used to feed the gasifier: in Section 4.3.1 the advantages related to this operation have already been discussed. Moreover, it can be verified that air mass flow rate required for gasification is always lower than the available one, thus the surplus can be used to produce additional process heat[3].
A further optimisation could be represented by high-temperature syngas cleaning: as discussed in Chapter 1, this technology presents a lot of problems and cannot be applied

[3] To explain this point it is sufficient to perform a little analysis regarding the order of magnitude of the problem. As said, cooling air mass flow is calculated so that, given its inlet temperature equal to the ambient one and the requirements for the syngas that has to be cooled from 500°C to 60 ÷ 100°C, syngas/air heat exchanger has an effectiveness of 90%. Calculation leads to an air mass flow rate that is about double the syngas one. Moreover, syngas mass flow rate actually derives by one third from solid biomass and by two thirds from gasification air (see Figure 3.6): therefore, roughly, available hot air is normally about three times higher than required by the gasifier.

at the moment, but it is interesting to analyse the effects of feeding the power plants with syngas at 500°C (the gasifier exit temperature) without the necessity of cooling it (in this case, biomass drying is effected adopting ICE or GT exhaust gases).

Summarising, three versions of the gasification device have been analysed (for brevity reasons, the corresponding plant schemes are not graphically shown: indeed, all the configurations are very simple to figure):

1. use of the hot air exiting the dryer to feed the gasifier (pre-heat);
2. thermal heat recovery of the residual air mass flow rate in addition to the previous operation (pre-heat + heat recovery);
3. high-temperature syngas cleaning and plant feeding (hot feeding).

The analysis has been conducted on three plant samples: ambient pressure gasifier coupled with an internal combustion engine (ICE GAS) and ambient pressure or pressurised gasifier coupled with a gas turbine, signally the regenerative one, as it has proved to be the most performing one (GT GAS REG AMB and GT GAS REG PRES). Obviously results can then be transferred to the other solutions adopting this type of devices (i.e. simple and STIG cycle GT GAS and the combined plants ICE/GT GAS ORC). The reference size is 100 kW_{el}: also in this case results are qualitatively valid for the other scales too. Results, always expressed in terms of electrical and first law efficiencies, are then listed in Table 4.9 and shown in Figures 4.27 and 4.28. The base case version is obviously referred to the configuration described in Section 4.3.1.

Solution	Version	η_{el} [%]	η_{I} [%]
ICE GAS	Base case	23.78	73.42
	Pre-heat	24.45	75.45
	Pre-heat + heat recovery	24.45	78.65
	Hot feeding	28.35	81.46
GT GAS REG AMB	Base case	19.07	63.92
	Pre-heat	19.84	65.68
	Pre-heat + heat recovery	19.68	68.95
	Hot feeding	16.62	66.54
GT GAS REG PRES	Base case	22.15	66.68
	Pre-heat	22.17	68.39
	Pre-heat + heat recovery	22.07	71.05
	Hot feeding	25.08	72.32

Table 4.9 – Improved gasification solutions: electrical and first law efficiencies.

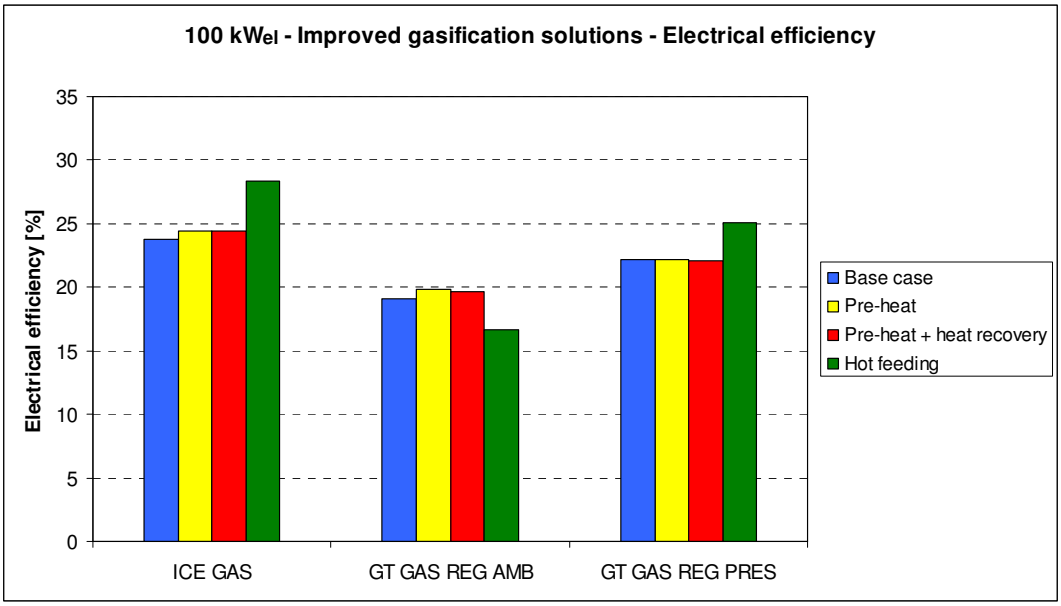

Figure 4.27 – Improved gasification solutions: electrical efficiency.

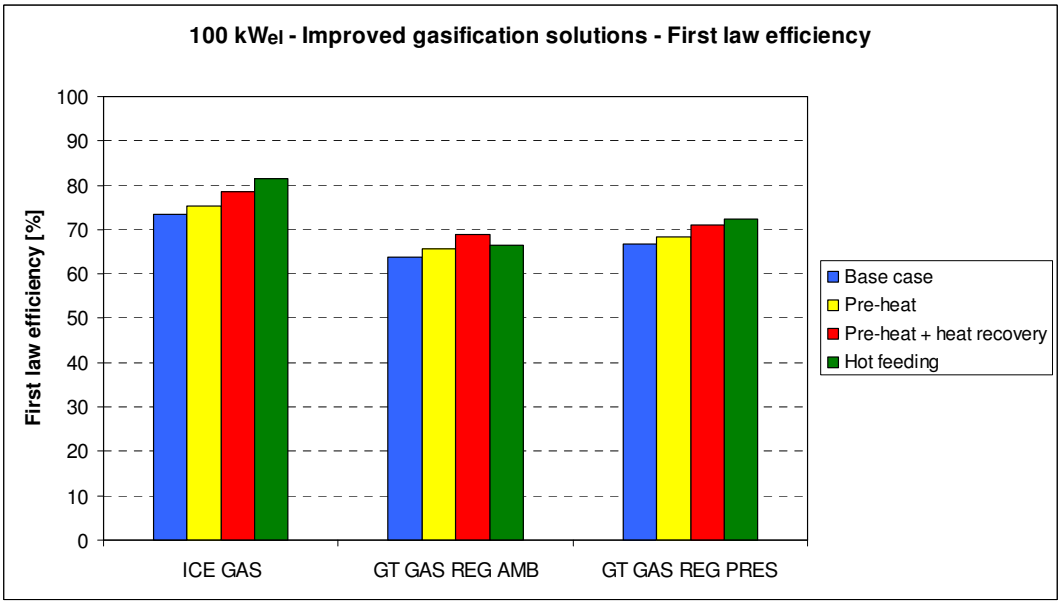

Figure 4.28 – Improved gasification solutions: first law efficiency.

Air pre-heating is undoubtedly advantageous for internal combustion engines and gas turbines with ambient pressure gasifier, since, power and useful heat being equal, higher cold gas efficiency determines a lower fuel power input, that implies an increase of about 1% in the electrical efficiency and 2% in the first law one. In case of pressurised gasifier, instead, the matter is a little different: pre-heating air, in fact, does not yield appreciable variations in the electrical efficiency. This is due to the fact that gasification air has to be compressed and thus, after exiting the dryer, the share of mass flow rate to be injected in the gasifier is sent to a compressor. Nevertheless this compression starts from high temperature (about 200°C) and therefore compression work is higher than in case of compression from ambient air. Hence the benefits related to the enhance of combustion air temperature are balanced by the higher power consumption of the compressor itself[4]. On the other hand, an increase of about 2% in first law efficiency is registered as in the previous two cases, because cold gas efficiency is higher all the same (obviously higher compressor consumption has no effect in this sense) and thus fuel power input decreases (while process heat remains almost equal).

If the residual air mass flow rate is then used for further heat recovery, thermal efficiency raises and first law one does the same (the increase is averagely 3%), electrical efficiency being constant in first analysis. Actually this is not completely true, because the head losses related to the recovery heat exchanger cause a little decrease in the power output. Indeed, this little loss has been found only in the gas turbine solutions, as for internal combustion engines exhaust gas losses have been put equal to zero for computational reasons (however the concept does not change).

Finally, in case of hypothetical fuelling with hot syngas, a considerable increase in electrical efficiency could be expected, since, power output being roughly constant, the introduction of syngas sensible heat in the combustion chamber lowers the fuel power demand and thus its required inlet mass flow rate. Actually this is what happens with ICE GAS and GT GAS PRES, where an increase of about 3 ÷ 4% is registered, nevertheless for gas turbine coupled with an ambient pressure gasifier not only this increase does not occur, but there is also a 3% reduction. The reason still lies in the high

[4] Theoretically the whole air mass flow rate could be compressed starting from ambient temperature before entering the air/syngas heat exchanger, but one could verify that this solution is worse than the previous one (two thirds of the mass flow rate would be compressed in vain).

temperature at the compressor inlet, that is 500°C: this value makes compression work raise dramatically so that power absorbed by the compressor is about half of the total gas turbine output, thus completely nullifying the benefits of high temperature injection in the combustion chamber[5]. In all of the three cases, thermal power output decreases, as syngas thermal heat recovery is no more effected and, additionally, hot gases are used to dry biomass, but thermal efficiency remains almost constant, always thanks to the fact that also fuel power input decreases. Therefore first law efficiency varies according to the electrical one, raising in case of ICE GAS and GT GAS PRES and diminishing in case of GT GAS PRES AMB.

Concluding, neglecting the last particular case of fuelling plants with hot syngas, it has been demonstrated how an optimised gasifier configuration, consisting in recovery of sensible heat from syngas aiming at feeding the gasifier with hot air and performing additional heat recovery (apart the already considered biomass drying), generally leads to higher electrical and first law efficiencies. Therefore this scheme will be taken as reference hereinafter.

4.5 Conclusions

The performance analysis described in this chapter has shown that, from a thermodynamic point of view, the most interesting solutions for the exploitation of biomass for power production are:

- internal combustion engine coupled with a gasifier (ICE GAS);
- regenerative-cycle gas turbine coupled with a pressurised gasifier (GT GAS REG PRES);
- externally fired gas turbine with a ceramic heat exchanger (GT EXT CER);
- internal combustion engine coupled with a gasifier and bottoming ORC (ICE GAS ORC);

[5] In this sense it must be also specified that the compressor exit temperature would be up to 1000°C, which would make this solution technically unfeasible as a matter of fact, apart from its thermodynamic disadvantage.

- regenerative-cycle gas turbine coupled with a pressurised gasifier and bottoming ORC (hereinafter the acronym GT GAS ORC will refer implicitly to this pattern);
- hybrid gas turbine fed by solid biomass and natural gas (GT HYB).

These solutions will be considered in the next chapter for the economic analysis. Table 4.10 summarises their electrical and first law efficiencies for the three scales. Concerning GT EXT CER and GT HYB, values are those presented in the previous sections, while for all the other solutions, all based on biomass gasification, the improved configuration described above has been considered, therefore results are a little better than those indicated before[6]. The reason why the table reports efficiencies for both cogenerative and electric configurations for ICE GAS ORC and GT GAS ORC will be explained in the next chapter.

Solution	**100 kW_{el}**		**1 MW_{el}**		**5 MW_{el}**	
	η_{el} [%]	**η_{I} [%]**	**η_{el} [%]**	**η_{I} [%]**	**η_{el} [%]**	**η_{I} [%]**
ICE GAS	24.45	78.65	32.65	75.22	37.88	75.39
GT GAS REG PRES	22.07	71.05	25.09	73.23	29.55	76.21
GT EXT CER	22.61	77.52	24.97	79.58	25.96	81.60
ICE GAS ORC	-	-	-	-	40.03 (CHP) 40.89 (EL)	79.33 (CHP) 67.43 (EL)
GT GAS ORC	-	-	28.17 (CHP) 29.37 (EL)	71.61 (CHP) 54.84 (EL)	33.18 (CHP) 34.50 (EL)	75.71 (CHP) 55.80 (EL)
GT HYB	23.62	73.68	26.06	79.95	31.62	82.85

Table 4.10 – Thermodynamic analysis: best solutions and their electrical and first law efficiencies.

[6] It is clear, however, that this little improvement does not distort the sense of the comparison among the various solutions performed in the previous sections.

Chapter 5
Economic analysis

5.1 Introduction

The previous chapter has been dedicated to the definition of the most interesting solutions from a thermodynamic point of view regarding biomass exploitation for power generation. Nevertheless it is well known that, beyond its technical performance, no engineering project can be considered desirable, if it is not accompanied by a solid financial sustainability. In this regard, the present chapter aims at identifying the best configuration in economic terms for each one of the three considered sizes among the plant solutions chosen in the previous analysis. In particular the investigation is performed referring to the Italian context (regarding legislation, costs, etc.).

The chapter is divided into three parts: the first one deals with the working hypotheses on which the analysis is based, in the second one results are shown and discussed and finally a sensitivity analysis is effected varying some significant parameters. The identified plant solutions will then be considered for the final assessment concerning the effects of biomass moisture on thermodynamic and economic performance, which will be described in Chapter 6.

In the previous chapter, focus has been brought to electrical and first law efficiencies, while the actual power output of the various plants has been neglected: this because the latter depends on the specific plant model taken as reference, while efficiencies can be considered representative of the whole plant typology performance, which is the interest of this work. In this chapter the same logics have been followed: only efficiencies have been taken into account (apart from one specific case), while net electric power output has been fixed precisely equal to 100 kW_{el}, 1 MW_{el} or 5 MW_{el}. Thus the obtained results prescind from the actual power output of the single plant and can therefore be directly compared with the different plant configurations.

5.2 Working hypotheses

5.2.1 Investment costs

Accurate estimates concerning investment costs of the analysed plants are very difficult to be performed, essentially because small-scale biomass power generation is a young field: first of all not all the considered solutions are present on the market, but a proper evaluation is not easy concerning plants that instead are commercially available too, since their market cannot be considered consolidated yet. Therefore data available in the literature are often conflicting. Many sources have been consulted to define the investment costs of the analysed plants, including real commercial offers: some of them are cited gradually during the discussion or at the end of the section. Adopted values for the three scales are listed in Table 5.1: they are expressed in €/kW_{el}. Concerning the power plants, reference values are those listed in Chapter 2.

Solution	**100 kW_{el}**	**1 MW_{el}**	**5 MW_{el}**
ICE GAS	4500	2700	2000
GT GAS REG PRES	5540	3340	2440
GT EXT CER	4000	3000	2000
ICE GAS ORC	-	-	2130
GT GAS ORC	-	3650	2690
GT HYB	2500	2000	1500

Table 5.1 – Specific investment costs (€/kW_{el}).

For internal combustion engines coupled with a gasifier (ICE GAS), reported costs are given adding the engine and the gasification system ones. These values respectively have been fixed as follows: 1200 €/kW_{el} and 3300 €/kW_{el} for the 100 kW_{el} scale, 900 €/kW_{el} and 1800 €/kW_{el} at 1 MW_{el} and finally 700 €/kW_{el} and 1300 €/kW_{el} at 5 MW_{el}.

Concerning regenerative gas turbines coupled with pressurised gasifiers (GT GAS REG PRES), it is recalled that small-size types of the latter devices are not available on the market, therefore their costs have to be estimated. In the present work, it has been

hypothesised to increase costs of above reported ambient pressure gasifiers by 30%. Resulting values are thus: 4290 €/kW_{el} at 100 kW_{el}, 2340 €/kW_{el} at 1 MW_{el} and 1690 €/kW_{el} at 5 MW_{el}. These costs are then added to the gas turbines ones, that are respectively 1250 €/kW_{el}, 1000 €/kW_{el} and 750 €/kW_{el}, giving the final values reported in the table.

In externally fired gas turbines with a ceramic/high temperature heat exchanger (GT EXT CER) the turbine and the heat exchanger itself represent the two main cost factors. Concerning the former one, the values reported few lines above have been naturally used. Regarding the latter one, the evaluation has been based on several references. In [3.5] a cost of 750 €/m^2 is proposed (obviously referring to the exchanger surface). Indeed, this value is referred to a maximum allowable temperature of 1000°C, which, in the present work, has been found on the two smallest sizes (see Section 4.2.3). On the contrary, 1100°C are reached at the 5 MW_{el} scale: however the referred value has been considered valid as well. On the other hand, in [2.14] costs of high temperature heat exchangers are estimated to be three fold the conventional ones (e.g. 304L). For the latter, two relations may be adopted, both expressed in €/m^2 (A is the exchanger area, in m^2):

- $475 \cdot A^{0.9}$ [5.1]
- $10{,}000 + 300 \cdot A^{0.95}$ [5.2]

Indeed, the second relation would be expressed in British pounds per area unit, but, considering the exchange rate, it can be suitably hypothesised to use it in terms of €/m^2. However it is easy to verify that the two formulas provide analogous results, apart from the initial gap.

From an operating point of view, firstly the heat exchanger surface was obtained[1], then the overall cost of the device was calculated by means of the three above mentioned relations and afterwards the results were converted in €/kW_{el}, being finally averaged. Reference value was then chosen rounding the latter number. Results for the three scales are listed in Table 5.2.

[1] Thermoflex™ provides this result in terms of UA, i.e. the product of overall heat transfer coefficient and the actual surface. Obviously A is easily obtained dividing that product by U, for which a value of 38 W/(m^2·K) has been used [3.5].

		Unit	100 kW_{el}	1 MW_{el}	5 MW_{el}
Heat exchanger area		m^2	173.4	1359	3547
Heat exchanger cost	[3.5]	k€	130	1019	2660
	3 × [5.1]		148	941	2232
	3 × [5.2]		151	883	2151
Heat exchanger specific cost (to power output)	[3.5]	€/kW_{el}	1300	1019	532
	3 × [5.1]		1480	941	446
	3 × [5.2]		1510	883	430
Average specific cost		€/kW_{el}	1430	948	470
Chosen specific cost		€/kW_{el}	1500	1000	500

Table 5.2 – Cost of ceramic/high temperature heat exchangers.

Apart from the gas turbine and the heat exchanger, all the other devices (such as, combustor, high temperature filters, etc) should then be additionally considered: in this work these contributions have been quantified as 50% of the sum of the two previous cost items: final results are therefore those reported in Table 5.1.

Investment costs of the combined solutions of an internal combustion engine or a gas turbine coupled with a gasifier and bottoming ORC (ICE GAS ORC and GT GAS ORC) are naturally given by the sum of the already mentioned ICE GAS or GT GAS REG PRES costs and the one of the ORC unit. Differently from what has been done up to now, in this case the evaluation must take into account the actual power output of the plants, since the additional power produced by the ORC varies according to the thermal power contained in the hot exhaust gases feeding the thermodynamic cycle and can obviously not be catalogued in advance as 100 kW_{el}, 1 MW_{el} or 5 MW_{el}. In particular, actual ORC power values are listed below. Two values are provided for each solution, concerning respectively the CHP and the electric case.

- ICE GAS ORC: 259 ÷ 351 kW_{el}
- GT GAS REG PRES (1 MW_{el}): 142 ÷ 192 kW_{el}
- GT GAS REG PRES (5 MW_{el}): 587 ÷ 794 kW_{el}

According to [5.3] and [5.4], the following installation costs regarding the ORC unit and the thermal oil circuit can be adopted for these sizes:

- ICE GAS ORC: 2300 €/kW_{el}

- GT GAS REG PRES (1 MW_{el}): 2500 €/kW_{el}
- GT GAS REG PRES (5 MW_{el}): 2000 €/kW_{el}

However it is important to note that these values are referred to the power output of the mere ORC unit, therefore they must be converted into the corresponding values referred to the whole plant power output by means of a weighted average. Power output of the topping power plants must then be considered:

- ICE GAS ORC: 1175 kW_{el}
- GT GAS REG PRES (1 MW_{el}): 5100 kW_{el}
- GT GAS REG PRES (5 MW_{el}): 5020 kW_{el}

The share of ORC generated power with respect to the overall output, always depending on the CHP or electric configuration, is then:

- ICE GAS ORC: 5 ÷ 6%
- GT GAS REG PRES (1 MW_{el}): 11 ÷ 14%
- GT GAS REG PRES (5 MW_{el}): 11 ÷ 14%

Therefore, for simplicity reasons considering an average value for the last parameter, the incidence of the ORC unit on the installation cost of the whole plant is about:

- ICE GAS ORC: 130 €/kW_{el}
- GT GAS REG PRES (1 MW_{el}): 310 €/kW_{el}
- GT GAS REG PRES (5 MW_{el}): 250 €/kW_{el}

As mentioned before, these values must finally be added to the topping plants costs (2000 €/kW_{el} for ICE GAS ORC, 3340 €/kW_{el} and 2440 €/kW_{el} for GT GAS REG PRES respectively at 1 MW_{el} and 5 MW_{el}), thus giving the costs reported in Table 5.1.

Concluding, in [4.4] a cost of about 2100 €/kW_{el} is proposed for the hybrid biomass/natural gas solution (GT HYB) at the 100 kW_{el} scale. In the present work a slightly more conservative value has been chosen instead, i.e. 2500 €/kW_{el}, as shown in the table. This value is equal to two times the mere gas turbine cost: an analogous rule has then been adopted for the two larger scales (from 1000 €/kW_{el} to 2000 €/kW_{el} for 1 MW_{el}, from 750 €/kW_{el} to 1500 €/kW_{el} for 5 MW_{el}). An evaluation of the single components costs could show that this assumption is correct.

Finally, given the specific costs reported above, it is sufficient to multiply them by 100, 1000 or 5000 to calculate the overall investment costs: results (in k€) are shown in Table 5.3 [TF] [1.8] [1.25] [2.2].

Solution	100 kW_{el}	1 MW_{el}	5 MW_{el}
ICE GAS	450	2700	10,000
GT GAS REG PRES	554	3340	12,200
GT EXT CER	400	3000	10,000
ICE GAS ORC	-	-	10,650
GT GAS ORC	-	3650	13,450
GT HYB	250	2000	7500

Table 5.3 – Overall investment costs (k€).

5.2.2 Electric energy sale price

Italian legislation provides considerable economic incentives to support power generation from renewable energies [5.5]. The whole regulation is quite complex, however for the purposes of this work it is sufficient to specify that, in general, there are two possible options: the so called Tariffa Omnicomprensiva (TO, i.e. all-inclusive tariff) and Green Certificates (GC), both lasting 15 years. The first one is applied to plants having a power output lower than 1 MW_{el} (0.2 MW_{el} for wind turbines) and provides an overall payment for the generated electricity equal to 28 c€/kWh_{el} as regards biomass. GCs are instead available for plants of any size and provide a contribution which is added to the normal electricity sale price. This contribution is given by a fixed base value multiplied by a factor varying according to the different renewable sources. The base value is equal to the difference between the constant value of 18 c€/kWh_{el} and the annual average electric energy sale price: 8 c€/kWh_{el} for the latter parameter and thus 10 c€/kWh_{el} for the green certificates have been chosen in this work. Indeed, for plants having a size lower than 1 MW_{el} a minimum electricity sale price is granted. Its calculation mechanism is not explained here, however its value is averagely 9 ÷ 10 c€/kWh_{el} at 100 kW_{el} and about 8 c€/kWh_{el} at 1 MW_{el} (thus there is a potential advantage only as regards the former scale). The aforementioned multiplicative factor for biomass depends on the biomass supply chain length: it is equal to 1.8 in case of short chain, while it is 1.3 with a long chain. Concerning this point, it is important to note that the legislative decree, which should properly define the concept of short and long chain, is still pending (ref. November 2009) and in the meantime the

1.3 factor should be used in any case. However in the present work both of the two possible scenarios have been considered, assuming that the decree will be enacted in the near future. Basing on those factors, the green certificates are equal, respectively, to 18 c€/kWh$_{el}$ and 13 c€/kWh$_{el}$ and the overall income is thus 26 c€/kWh$_{el}$ and 21 c€/kWh$_{el}$ (or 27 ÷ 28 c€/kWh$_{el}$ and 22 ÷ 23 c€/kWh$_{el}$ for 100 kW$_{el}$). One can see that the TO (whose value is independent from any considerations regarding the chain length) is more convenient than GCs on the scales of interest, therefore it has been used for 100 kW$_{el}$ and 1 MW$_{el}$. Obviously GCs have instead been adopted for 5 MW$_{el}$.
It is important to note that what described up to now is strictly valid for biomass fed plants only: on the contrary, in the hybrid solution, electric energy is sold at a price depending on the power share generated from biomass or from natural gas. Thus in the first case it will be paid according to the aforementioned incentives, while in the second case the base tariff of 8 c€/kWh$_{el}$ will be applied: the final sale price will then be given by a weighted average of the two contributions.
Concluding, one can see how high incentives really are and that it is therefore necessary to stress power generation if plants are fed with renewable energy sources.

5.2.3 Other hypotheses

- Thermal energy sale price has been fixed to 5 c€/kWh$_{th}$, which would correspond to burning natural gas having a cost of 40 c€/Sm^3 in a boiler with 85% thermal efficiency[2]; the same methane cost is applied when it is used for fuelling the hybrid solution;
- biomass cost is equal to 60 €/t for the raw material[3] (including costs of ash disposal) and to 15 €/t for its transport: in all 75 €/t;

[2] Such a methane cost is applicable in the industrial sector, while in the civil one values of 60 ÷ 70 c€/Sm^3, corresponding to 7 ÷ 9 c€/kWh$_{th}$, are usually found. However it is important to note that a possible civil application would normally imply the construction of a district heating net, which would have a considerable cost. The use of 5 c€/kWh$_{th}$ as sale price also in this case is meant to roughly take into account such a fact.

[3] It must is recalled that the considered biomass (wood having a moisture content of 8.7%) is valuable and the cost is fixed accordingly.

- yearly working period is 7000 h (i.e. 80% availability);
- the duration of the investment is fixed to 10 years: as mentioned before, economic incentives should last 15 years but considering a 7000 h/y working period, the overall life would be 70,000 h, that is essentially a limit value for the considered plants (indeed, for many of them reliability data are not even available); obviously revamping interventions may be effected to extend useful life in order to cover the whole incentive period in case;
- three scenarios have been taken into account for the thermal energy sale period, already starting from the base analysis:
  - 0 h: no heat sale
  - 2500 h: heat sale during the cold season (for heating purposes)
  - 7000 h: heat sale all over the year (industrial applications)
- it is hypothesised to take out a loan which covers 50% of the investment; loan repayment time is 8 years, while the interest rate is equal to 6%;
- maintenance bears on the investment costs at a rate of 3% for plants with internal combustion engines and 2% for plants with gas turbines, with a 2% increase every year in both of the cases;
- insurance and other charges are meant to be 1% of the investment costs;
- one equivalent operator for 100 kW_{el} and 1 MW_{el} devices and two operators for the 5 MW_{el} ones are meant to be required for plant running: the unit salary is 30,000 €, distributed on 13 months;
- the amortization period is equal to the investment one, i.e. 10 years;
- the discount rate is 6%;
- Italian legislation provides two taxes: IRES (Imposta sul Reddito delle Società, i.e. tax on the corporate income), equal to 27.5% of the earnings, and IRAP (Imposta Regionale sulle Attività Produttive, i.e. regional tax on productive activities), equal to 3.9% of the amount given by the sum of EBIT (Earning Before Interests and Takes) and job costs.

Once fixed the yearly working hours and grouped the power outputs to 100 kW_{el}, 1 MW_{el} and 5 MW_{el}, annual generated electricity in the three cases is then equal to 700 MWh_{el}, 7000 MWh_{el} or 35000 MWh_{el}. Biomass consumption is then calculated starting from the electrical efficiency of each plant, known wood lower heating value.

Thermal production instead depends on the thermal efficiency (given by the difference of first law and electrical efficiencies) and varies accordingly in the different cases.

5.3 Results

Results of the investment analysis are presented in terms of PayBack Time (PBT), Net Present Value (NPV), evaluated on 10 years, and Internal Rate of Return (IRR) of the investments, the first two ones being analysed more in depth. As in the previous chapter, they will be shown both in numerical terms and in graphic form.

5.3.1 100 kW_{el} size

Results of the analysis are listed in Table 5.4 and shown in Figures 5.1 ÷ 5.3.

Solution	PBT [years]	NPV [k€]	IRR [%]
No heat sale			
ICE GAS	5.43	174	19.27
GT GAS REG PRES	8.30	81	11.22
GT EXT CER	4.32	225	24.71
GT HYB	-	- 426	-
Heat sale: 2500 h			
ICE GAS	3.72	314	28.89
GT GAS REG PRES	5.35	221	19.60
GT EXT CER	2.99	378	36.13
GT HYB	-	- 227	-
Heat sale: 7000 h			
ICE GAS	2.40	566	45.16
GT GAS REG PRES	3.23	473	33.45
GT EXT CER	1.93	654	55.70
GT HYB	5.83	86	17.82

Table 5.4 – 100 kW_{el}: economic results.

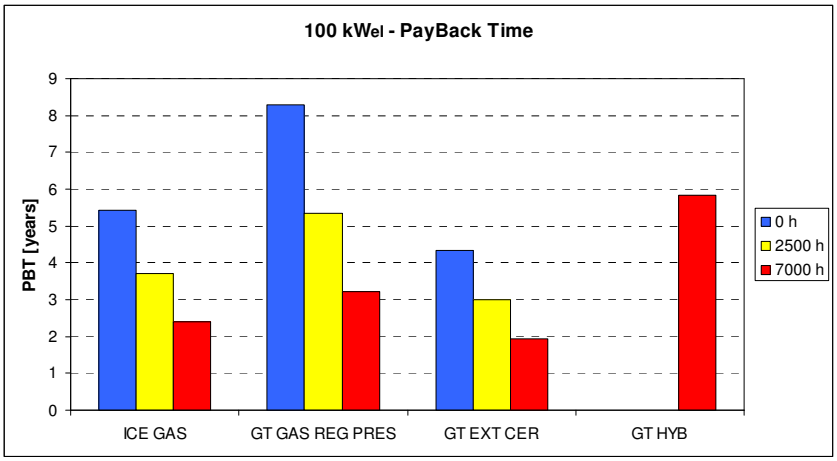

Figure 5.1 – 100 kW_{el}: PayBack Time.

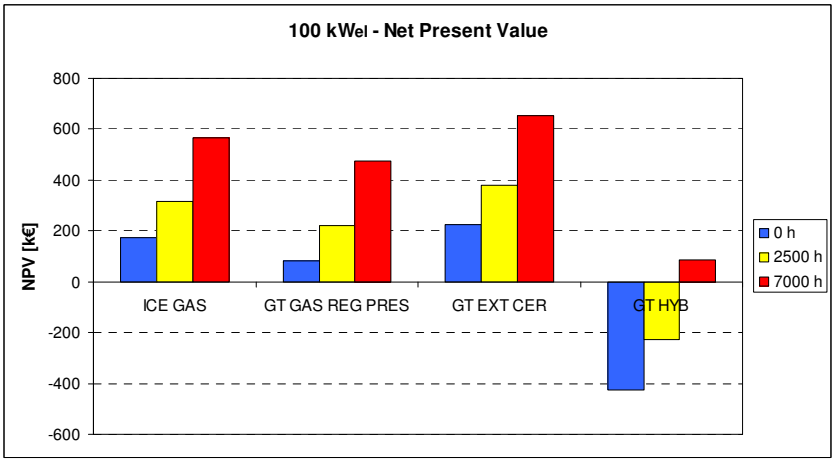

Figure 5.2 – 100 kW_{el}: Net Present Value.

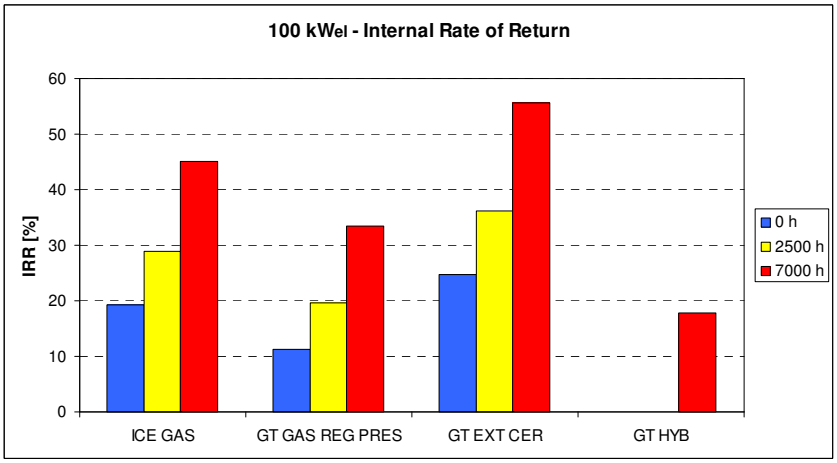

Figure 5.3 – 100 kW_{el}: Internal Rate of Return.

Observing Figure 5.1, one can immediately see that PBTs are in general attractive, despite high specific investment costs: all analysed solutions provide positive results, except for the hybrid configuration if heat sale is not performed all over the year. Besides the incidence of heat sale is clear: passing from 0 h to 7000 h sale, PayBack Times roughly halve, although incomes from heat sale are much lower, in absolute terms, than those from electricity: for instance, GT EXT CER is characterised by 196 k€ earnings from electric energy (same as all the other biomass solutions, obviously) and about 30 k€ and 85 k€ from heat in case of 2500 h or 7000 h sale respectively. Actually, also looking at Net Present Values (Figure 5.2), one can roughly say that, at least for pure biomass solutions, electricity sale allows to get the break-even point and to slightly overcome it, while heat sale provides the added value. Heat sale is even more significant for the hybrid solution. In fact, as mentioned before, this plant only partially enjoys the incentives related to renewable energies (in this configuration the overall fuel power derives from biomass at a rate of 39% and from natural gas at a rate of 61%), therefore the mere electricity sale (which now yields only 111 k€) is not sufficient to cover the investment costs and it is instead necessary to sell thermal energy to reach the break even point. However, it is important to note that the relevance of heat sale is naturally inherent in this power size: as shown in Section 4.3.1, in fact, 100 kW_{el} solutions are roughly characterised by 20 ÷ 25% electrical efficiency and averagely about 70% first law efficiency. This implies that thermal efficiency is about 45 ÷ 50%, i.e. heat production is more than twice the electricity one, and it is thus easy to understand that its recovery and sale can be decisive.

However, the best solution seems to be GT EXT CER from all points of view (PBT, NPV and IRR) and in all heat sale configurations: its electrical efficiency is lower than the ICE GAS one, but it has lower investment costs and a higher first law efficiency (due to the fact that it is not affected by the gasification losses), thus higher income from heat sale. On the other hand, GT GAS REG PRES is inevitably penalised by the installation costs (essentially the pressurised gasifier). Finally, as mentioned before, GT HYB, which could be desirable thanks to its plant simplicity, would be justified only in case of continuous thermal recovery and sale and, moreover, its performance would be quite poor compared to the other solutions also as regards this size. Besides, in case of no heat sale, its NPV is even lower than the investment cost: not only the plant does not

yield sufficient earnings to reach the break-even point, but yearly losses are also higher than incomes, so that cash flows are negative. Indeed, it is important to remember that the major interest of this work is mainly power generation, thus the most important case is given by no sale: nevertheless it is obvious that considerations concerning thermal power recovery are important as well.

5.3.2 1 MW_{el} size

Results of the analysis at 1 MW_{el} are listed in Table 5.5 and shown in Figures 5.4 ÷ 5.6.

Solution	PBT [years]	NPV [k€]	IRR [%]
No heat sale			
ICE GAS	1.62	5432	66.23
GT GAS REG PRES	2.28	4482	47.47
GT EXT CER	1.97	4776	54.50
GT GAS ORC	2.43	4534	44.65
GT HYB	3.14	1776	34.45
Heat sale: 2500 h			
ICE GAS	1.44	6255	74.63
GT GAS REG PRES	1.87	5693	57.63
GT EXT CER	1.60	6156	67.26
GT GAS ORC	2.08	5478	51.95
GT HYB	2.03	3081	53.05
Heat sale: 7000 h			
ICE GAS	1.19	7736	89.67
GT GAS REG PRES	1.42	7872	75.66
GT EXT CER	1.18	8640	89.99
GT GAS ORC	1.66	7177	64.89
GT HYB	1.25	5430	85.48

Table 5.5 – 1 MW_{el}: economic results.

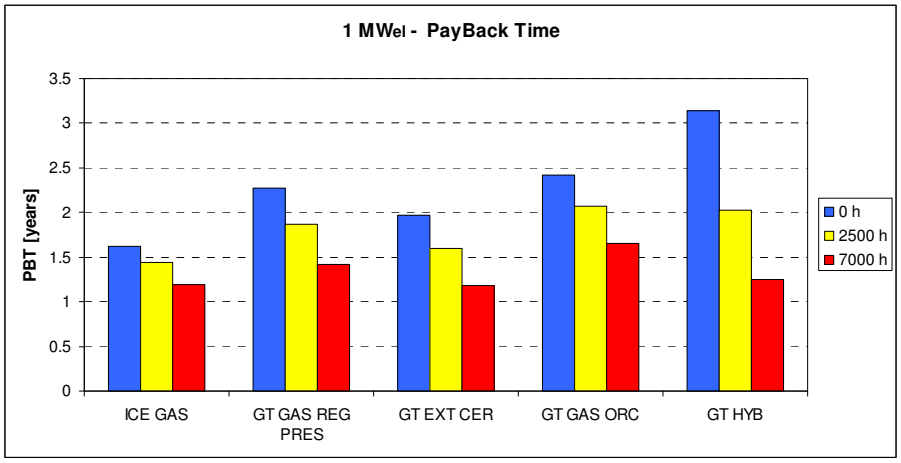

Figure 5.4 – 1 MW_{el}: PayBack Time.

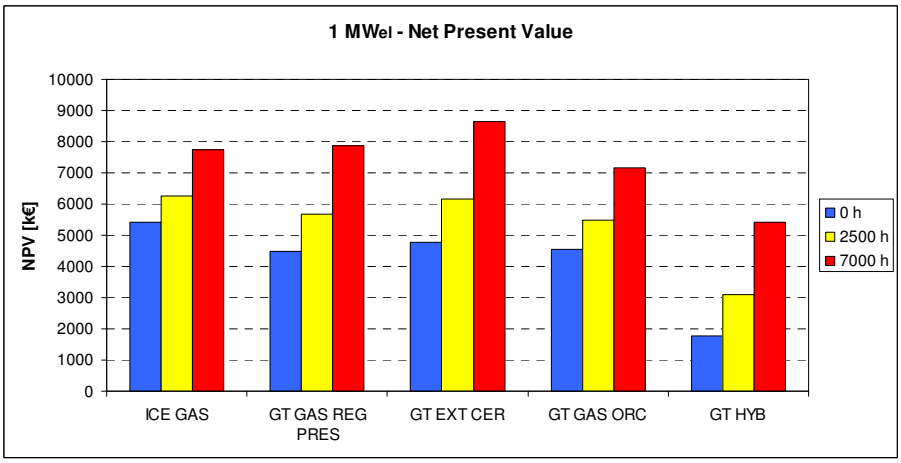

Figure 5.5 – 1 MW_{el}: Net Present Value.

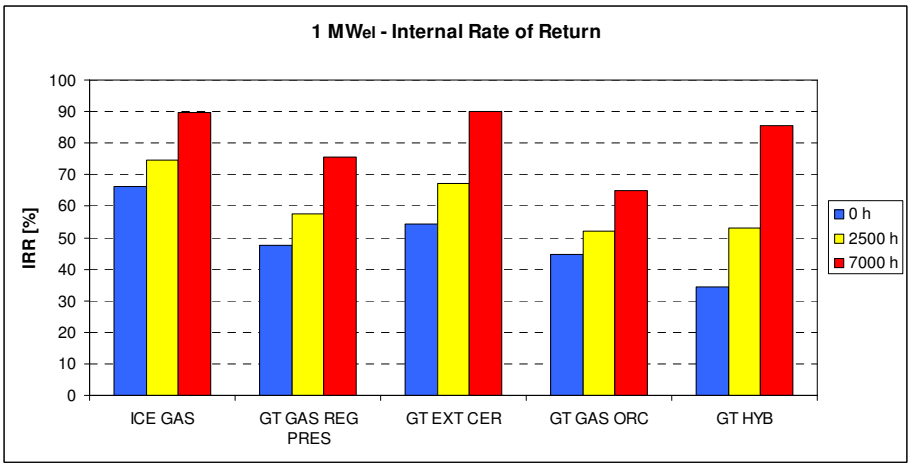

Figure 5.6 – 1 MW_{el}: Internal Rate of Return.

Figure 5.4 shows that PayBack Times are much lower now, thanks to reduced installation costs: as regards the best solutions this value is equal to 1 ÷ 1.5 years. GT HYB presents very good performance now: PBT is short enough also in case of no heat sale. Similarly to the previous case, this is essentially due to the plant configuration. As mentioned in Chapter 4, in fact, temperature of flue gas exiting the biomass combustor is 800°C regarding all of the three sizes and, given the recuperator features, this implies that air temperature entering the natural gas combustor is about 740 ÷ 750°C. Natural gas consumption is then "proportional" to the turbine inlet temperature[4]: at 100 kW_{el} this is equal to 950°C, which leads to the mentioned share of 40/60% between biomass and methane fuel power input. On the other hand, the 1 MW_{el} reference turbine is characterised by a TIT of 899°C: this involves a natural gas lower consumption required to obtain that value (temperature raise is in fact lower), which leads to an inverted share of fuel power input: about 63% biomass and 37% natural gas. Then a larger use of the renewable energy source results in higher incomes related to electric energy sale and thus to a better economic performance of the plant.

Besides, one can see that the gap existing between solutions in the three heat sale scenarios is lower than in the previous case. The reason lies in what has been discussed above: first law efficiencies are now roughly similar to the 100 kW_{el} case, but electrical ones are about five percentage points higher. This implies that thermal production is proportionally less significant and thus its incidence in the three scenarios is lower. Naturally GT HYB represents a particular case again: the concept is generally valid terms, but due to the hybrid nature of the plant, heat sale incidence is still more considerable than in the other biomass-fed solutions (although it is less dramatic than in the 100 kW_{el} case).

Observing PBTs, the most performing solution is ICE GAS, even if there is a very small difference compared with the other solutions. Indeed, GT EXT CER achieves the same performance in case of 7000 h heat sale: this is always due to higher thermal efficiencies, related to the absence of gasification losses. This point becomes even clearer concerning Net Present Values: at 0 h and 2500 h ICE GAS has the best performance, but it is overcome by GT EXT CER at 7000 h. GT HYB itself has a PBT

[4] Obviously it also depends on other parameters, like pressure ratio, turbine polytropic efficiency, etc.

that almost equals the previous two ones at 7000 h, thanks to what has been discussed before, but obviously NPV is much lower. However, it has already been mentioned that the most important scenario is 0 h sale, therefore the latter results are less important. Besides, as in the pervious case, GT GAS REG PRES proves to be less interesting than the best plants (even if it slightly overcomes ICE GAS in terms of Net Present Value in the 7000 h heat sale case, due to a better thermal efficiency). Moreover, the addition of the ORC unit (GT GAS ORC) does not yield any particular results: economic performance is essentially comparable to the base case (although being somewhat worse). Concerning the latter solution, it is important to point out that, in case of heat recovery and sale, the CHP configuration has been obviously considered, otherwise the electric one is used, in order to achieve a better performance (without any extraordinary results, though).

Finally, ICE GAS can be considered the best solution at 1 MW_{el} scale, even because GT EXT CER is based on a regenerative gas turbine, which is actually not consolidated on these scales. Differently from the 100 kW_{el}, GT HYB can represent an interesting solution, especially if heat is being sold for a long period of time during the year.

5.3.2.1 Note

In this sub-section, some considerations concerning the PayBack Times values obtained in this analysis are being proposed (they would be valid for the 5 MW_{el} case too). The purpose is to show how results (1 ÷ 1.5 years), which could seem too optimistic at first sight, are actually coherent.

First of all a comparison with photovoltaic (PV) technology has been made, carrying out some approximate estimates. In the last years, PV panels installation costs remarkably decreased, reaching about 4000 €/kW_p in case of large plants, like those being taken into account [5.6]. Nevertheless it is well known that peak kilowatt (kW_p) refers to ideal conditions in which solar radiation is equal to 1 kW_{rad}/m^2, which obviously does not occur all over the year (at certain latitudes never at all), therefore it cannot be considered a real measure of the actual plant capacity. The verifiable average solar radiation at the Italian latitudes is about 160 W_{rad}/m^2 (central Italy) [5.7], i.e. about one sixth of the peak value. As a consequence, real average capacity of solar panels is

one sixth of that declared in peak-kilowatt terms and thus real installation costs are about six times higher than indicated above, i.e. 24,000 €/kW_{el}, whereas biomass plants are costing about 3000 €/kW_{el}, which is one eighth of the previous value. Instead, concerning the incomes related to electricity sale, considerable incentives are granted to PV, too: they depend on many variables, but for the purposes of this work 40 c€/kWh_{el} can be used. This value is obviously the net gain, as there is no fuel cost. On the other hand, as shown, a 28 c€/kWh_{el} all-inclusive tariff is applied to biomass power generation at this scale. However, in this case fuel cost has to be taken into account: with the given hypotheses, it is about 5 ÷ 6 c€/kWh_{el}, consequently net gain is about 22 ÷ 23 c€/kWh_{el}, i.e. about one half compared to photovoltaic plants (potential heat sale is being neglected for simplicity reasons). Based on these data, the following calculation can quickly be made: if investment costs in case of biomass fuelling are one eighth and net gain on electric energy sale is one half of PV panels, it is reasonable to conclude that the expected PayBack Times will be in roughly one fourth. It is easy to verify that PV plants with installation cost and electricity payment like those mentioned above will have a PBT of about 8 years [5.8]: the expected biomass plants value will accordingly be 2 years, that is essentially the result of the analysis. Of course, this is just an approximate evaluation, but it permits to understand that the results shown are reasonable. Table 5.6 summarises the described concept.

	Photovoltaic	**Biomass**	**Ratio**
Investment cost [€/kW_{el}[	24,000	3000	8x
Electricity sale earning [c€/kWh_{el}]	40	23 (28 - 5)	2x
PayBack Time [years]	8	**2**	4x

Table 5.6 – Comparison between photovoltaic and biomass PBT.

For completeness reasons, it is important to note that there is another aspect contributing to lower PayBack Times, obviously being relevant for all of the three considered sizes: it is loan raising. In fact, it is well known that the amount of money obtained from the funding agency represents a reduction of the disbursement actually to be made by the investor. Clearly the sum has then to be refunded together with the related interests, engraving on the cash flows, but the break-even point will be reached

in a shorter time. Figure 5.7, for instance, graphically shows the concept taking ICE GAS configuration as reference: in particular, the progressive Net Present Values over the years for three loan conditions (100% and 50% of the whole investment and no loan) are being presented.

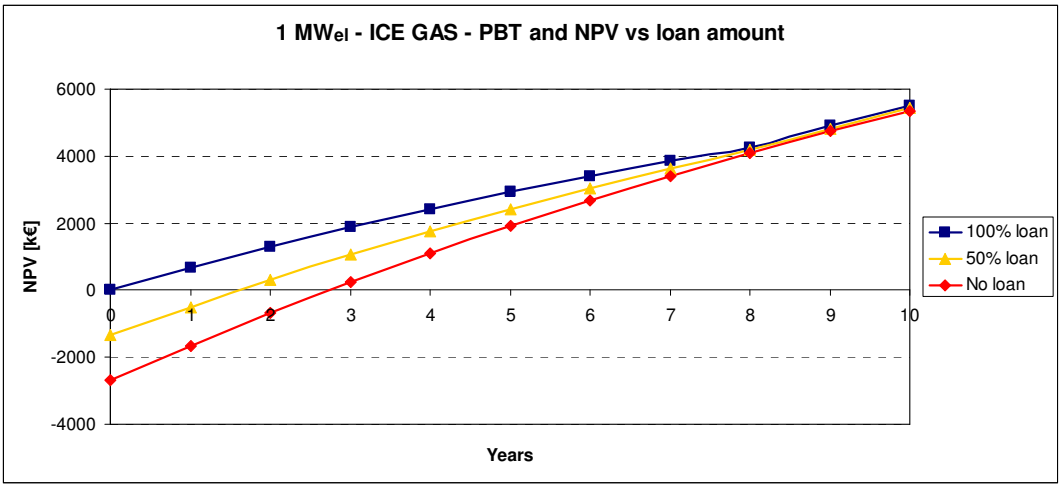

Figure 5.7 – Loan effect on Net Present Value and PayBack Time.

As specified in Section 5.2.3, in the present work a loan raise covering 50% of installation costs has been hypothesised: in the examined case, this leads to a PBT of about 1.5 years (given by the point in which the curve reaches zero). Without raising a loan, the real initial disbursement would be twofold: the absence of interests would lead to higher cash flows, so that the related NPV curve would gradually approach and finally reach the 50% one, but PBT would be considerably higher (in particular 2.75 years). On the other hand, raising a 100% loan, PayBack Time would not even be defined, since progressive Net Present Value would always be positive: actually there would not be any initial disbursement. Naturally in this case interests would be very high and final NPV again would result to be roughly equal to the other two cases (the actual value then depends on the choice of the various economic parameters).

In case of real investments, loans are always raised and thus the hypothesis made in this work can be considered correct: it is not a contrivance to keep PayBack Times low. On the other hand, the actual amount obviously varies from case to case and the effect on PBT changes accordingly.

5.3.3 5 MW_{el} size

Results of the 5 MW_{el} analysis are listed in Table 5.7 and shown in Figures 5.8 ÷ 5.10. As mentioned above, incentives for power generation are now different compared to the two previous cases, as GCs substitute TO. GCs values vary as a function of chain length, thus every solution is analysed two times, i.e. considering long chain (GC multiplicative factor K = 1.3) and short chain (K = 1.8): the brighter portions at the top of the histograms in the figures show the gap between the two configurations.

Solution	PBT [years]		NPV [k€]		IRR [%]	
	K = 1.3	K = 1.8	K = 1.3	K = 1.8	K = 1.3	K = 1.8
No heat sale						
ICE GAS	1.65	1.19	19,786	28,622	65.31	89.59
GT GAS REG PRES	2.29	1.60	16,246	25,082	47.19	67.37
GT EXT CER	1.88	1.31	16,888	25,723	57.20	81.57
ICE GAS ORC	1.70	1.24	20,303	29,139	63.24	86.05
GT GAS ORC	2.45	1.72	16,506	25,342	44.23	62.62
GT HYB	-	-	- 4,121	- 24	-	5.88
Heat sale: 2500 h						
ICE GAS	1.45	1.08	22,911	31,746	73.93	98.13
GT GAS REG PRES	1.84	1.36	21,229	30,065	58.63	78.61
GT EXT CER	1.41	1.06	23,651	32,487	75.88	100.06
ICE GAS ORC	1.51	1.13	23,348	32,184	71.13	93.87
GT GAS ORC	2.05	1.52	20,434	29,270	52.46	70.69
GT HYB	6.90	3.81	1854	5,089	14.67	28.24
Heat sale: 7000 h						
ICE GAS	1.19	0.93	28,535	37,371	89.35	113.48
GT GAS REG PRES	1.36	1.08	30,198	39,034	78.91	98.72
GT EXT CER	0.97	0.79	35,825	44,661	109.17	133.24
ICE GAS ORC	1.25	0.98	28,829	37,664	85.26	107.92
GT GAS ORC	1.60	1.26	27,504	36,340	67.07	85.12
GT HYB	2.11	1.70	11,057	14,292	51.20	63.22

Table 5.7 – 5 MW_{el}: economic results.

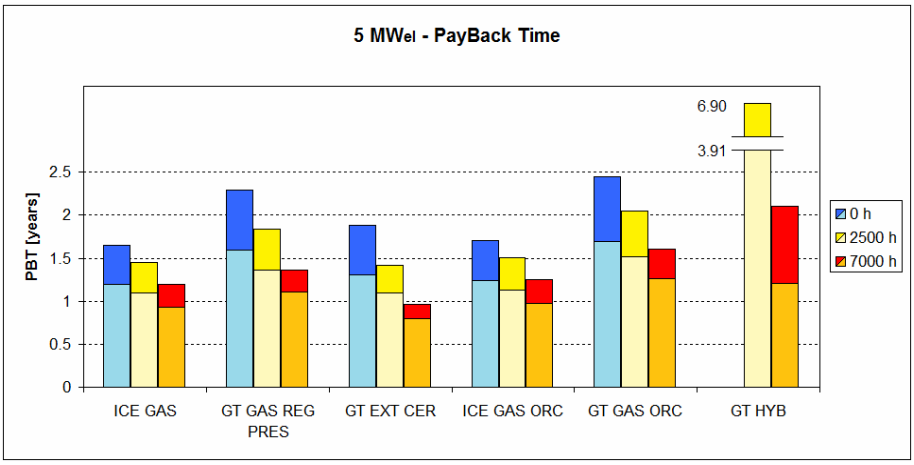

Figure 5.8 – 5 MW_{el}: PayBack Time.

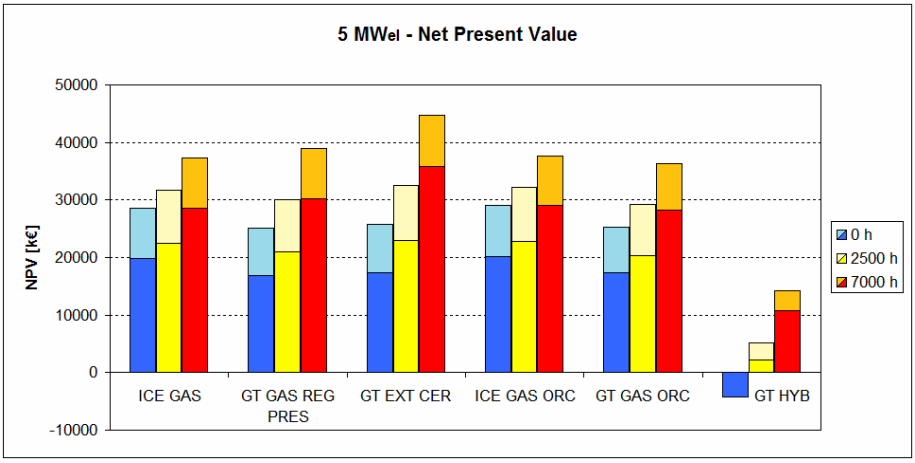

Figure 5.9 – 5 MW_{el}: Net Present Value.

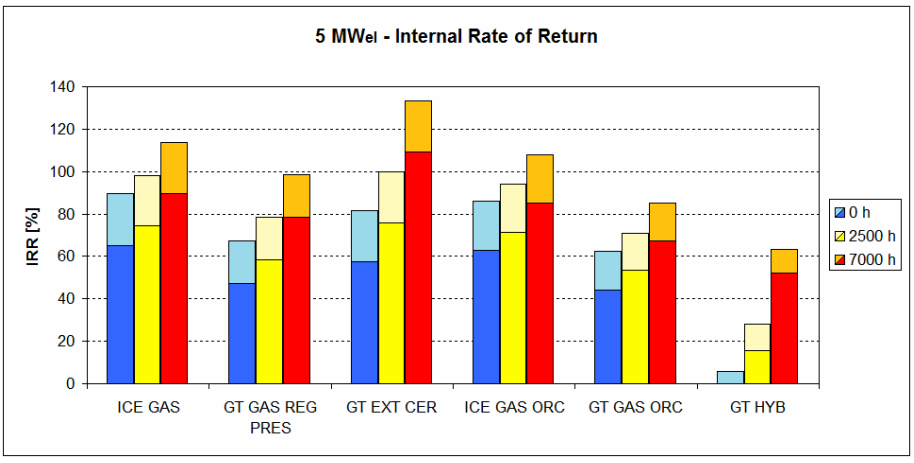

Figure 5.10 – 5 MW_{el}: Internal Rate of Return.

Analysing the proposed figures, one can immediately appreciate the chain length effect on the final results: passing from a long to a short chain, results do not change as order of magnitude, but obviously the positive effect of the associated higher incentives is shown in decreasing PBTs and increasing NPVs and IRRs (the opposite effects justify the inverted colours in the graphs).

However, generally results are not much different from those obtained in the 1 MW_{el} case, especially concerning PayBack Times, which are still 1 ÷ 1.5 years. This is essentially due to the fact that the higher electrical efficiencies achieved on this scale (30 ÷ 40% against 25 ÷ 30%) are balanced by lower economic incentives associated to green certificates. ICE GAS and GT EXT CER, again, prove to be the best solutions, according to all three economic items (PBT, NPV and IRR): similarly to the previous case, the former is preferable if only electricity is sold, while the latter becomes slightly more convenient in the two scenarios related to thermal energy sale. Economic performance of the combined solution ICE GAS ORC is very similar to the base case, i.e. ICE GAS: this means that the addition of the ORC does not lead to appreciable economical advantages, as the ORC installation cost balances the additional power output. As in the previous case, GT GAS REG PRES and the related combined solution GT GAS ORC instead denote somewhat less interesting results (again, apart from the former NPV at 7000 h). Finally, the hybrid configuration suggests considerations that are half way between those proposed for the previous scales. First of all, it is important to note that turbine inlet temperature of the reference gas turbine at 5 MW_{el} is 1093°C, i.e. a high value, that leads to a high share of natural gas power input compared to the biomass one: 63% against 37%, similarly to the 100 kW_{el} case. As discussed above, this implies low economic incentives for electric energy sale (as it mainly derives from a fossil fuel) and a consequent high incidence of heat sale, which is clearly appearing in the figures (if heat is not recovered, break-even point is not reached). Moreover, also the chain length condition, with consequently a different amount of green certificates, is proportionally more important. On the other hand, investment costs are lower than in the 100 kW_{el} case, therefore the plant rapidly moves towards desirable PBTs in case of conspicuous heat sale, although Net Present Values are limited again.

5.3.4 Conclusions

The analysis has shown that the most interesting solutions for biomass power generation from an economic point of view are GT EXT CER at 100 kW_{el} and ICE GAS at 1 MW_{el}. At 5 MW_{el} the two configurations provide similar results, even if the latter is the most performing one in case of no heat sale and thus should be preferred according to the logics of this work. Obviously, whatever stated is true from a mere numerical point of view: the actual choice of the plant configuration will then be based on various specific constraints varying from case to case.

Results are extremely attractive as regards 1 MW_{el} and 5 MW_{el}, and they are absolutely good also at 100 kW_{el}, especially if thermal energy recovery and sale is provided. The hybrid solution is interesting thanks to its low installation cost and plant simplicity, but generally only if heat is sold all over the year. Besides, the importance of the biomass or natural gas power input share regarding the economic performance has been demonstrated.

Concerning this point, a more-in-depth analysis can finally be carried out. First of all, Figure 5.11 shows the electric energy sale price progress as a function of fuel input share, from 8 c€/kWh_{el} in case of pure methane fuelling to 28, 26 or 21 c€/kWh_{el} in case of biomass use only (depending on whether all-inclusive tariff or green certificates are applied).

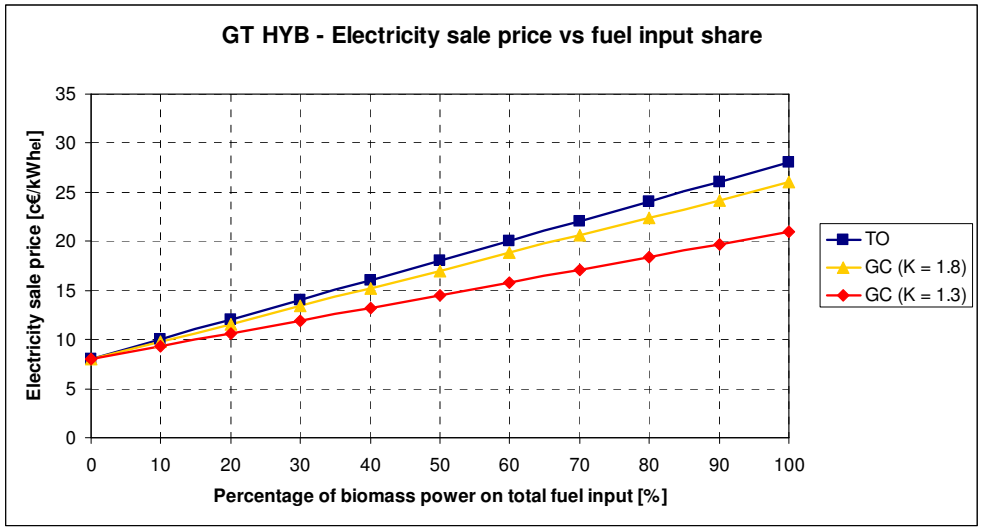

Figure 5.11 – Electric energy sale price as a function of fuel input share.

Figure 5.12, instead, shows the behaviour of PayBack Times as a function of the same parameter in the intermediate 2500 h heat sale scenario for all the considered scales.

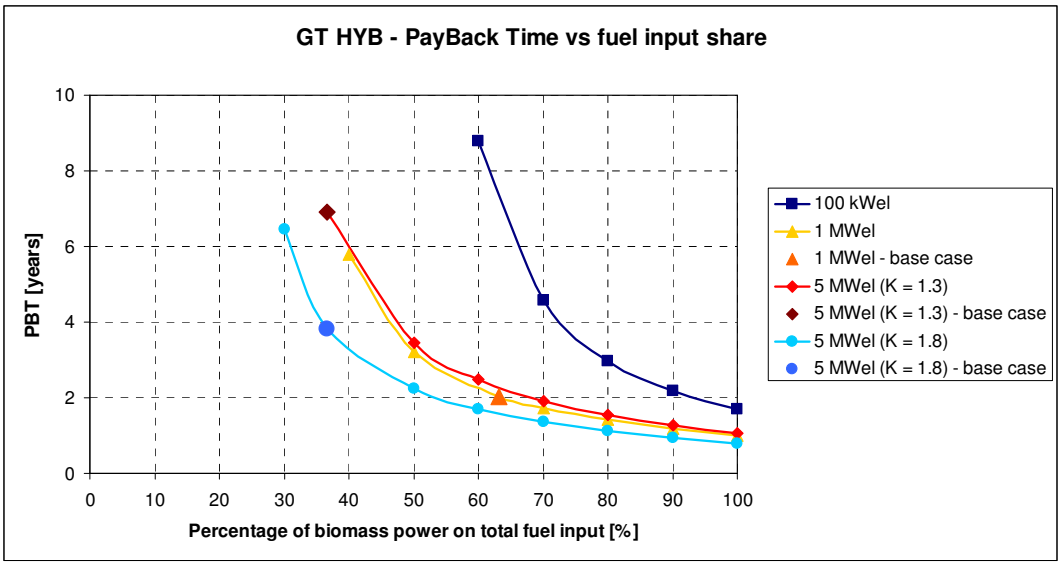

Figure 5.12 – GT HYB: PBT as a function of fuel input share.

As predictable, the 100 kW_{el} curve is the highest one, being penalised by higher specific investment costs and thus providing higher PayBack Times. On the contrary, 1 MW_{el} and long chain-5 MW_{el} give intermediate results. Curves are almost identical, as the former higher incentives balance the latter higher efficiencies, while short chain-5 MW_{el} provides the best performance. Generally one can conclude that natural gas share should not exceed 30% of fuel power input at 100 kW_{el} and 50% at the other scales, since otherwise PBTs grow dramatically. In particular in all cases PBTs are not even defined for low biomass use, the curve growing towards infinity: this is due to the mentioned fact that, with low economic incentives, not only earnings are not sufficient to reach the break-even point, but cash flows are actually negative. The operating points of the base case at 1 MW_{el} and 5 MW_{el} are additionally indicated in the figure: obviously this has not been done as regards 100 kW_{el}, since the base case at this scale does not yield an economic return. 1 MW_{el} case provides very good results thanks to the high share of biomass consumption. As mentioned, this analysis is conducted referring to 2500 h heat sale: it is quite easy to figure that results in the other two cases (0 h or 7000 h) would be shifted numerically but would be absolutely similar in qualitative terms.

5.4 Sensitivity analysis

The last part of the chapter is dedicated to an assessment of the effects on plant economic performance deriving from the variation of some parameters. In particular three quantities have been focused:

- biomass cost (raw material only), ranging between 20 ÷ 100 €/t (base case: 60 €/t);
- thermal energy sale price, ranging between 3 ÷ 7 c€/kWh$_{th}$, which corresponds to about 25 ÷ 60 c€/Sm^3 as cost of natural gas burnt in a 85% efficiency boiler (base case: 5 c€/kWh$_{th}$);
- again, yearly heat sale hours, equal to 0 h, 2500 h or 7000 h (base case: 2500 h – despite in this work, as already remembered, 0 h scenario would be more considerable, 2500 h has been taken as reference since it provides intermediate results).

For brevity reasons, only GT EXT CER at 100 kW$_{el}$ results of the analysis are presented (they are being expressed in terms of PBT). However the proposed considerations may be qualitatively transferred to the other cases and economic indicators, too. Results are shown in Figures 5.13 ÷ 5.15: in each of them, two of the three aforementioned parameters vary in the corresponding range, while the third is fixed to its base value.

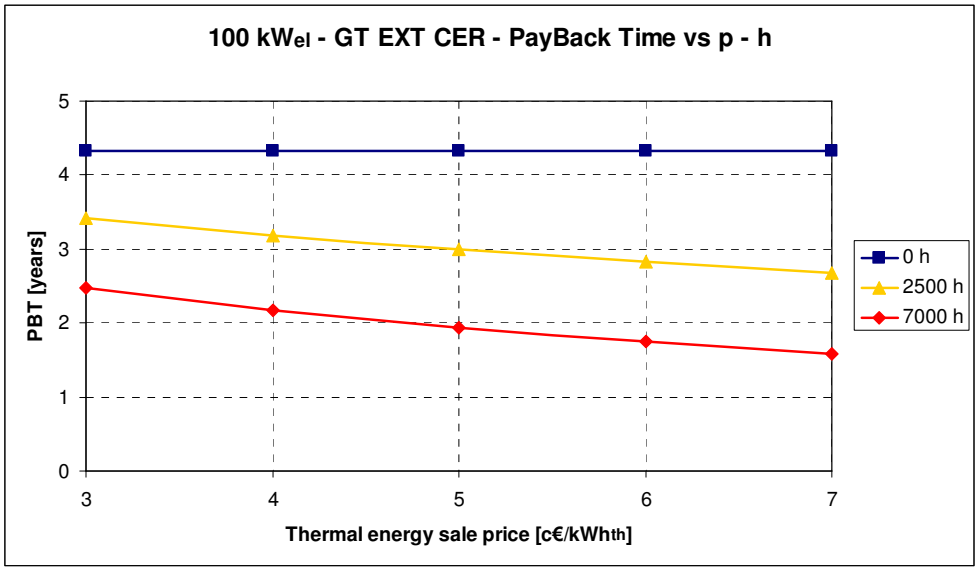

Figure 5.13 – PBT as a function of thermal energy sale price (p) and hours (h).

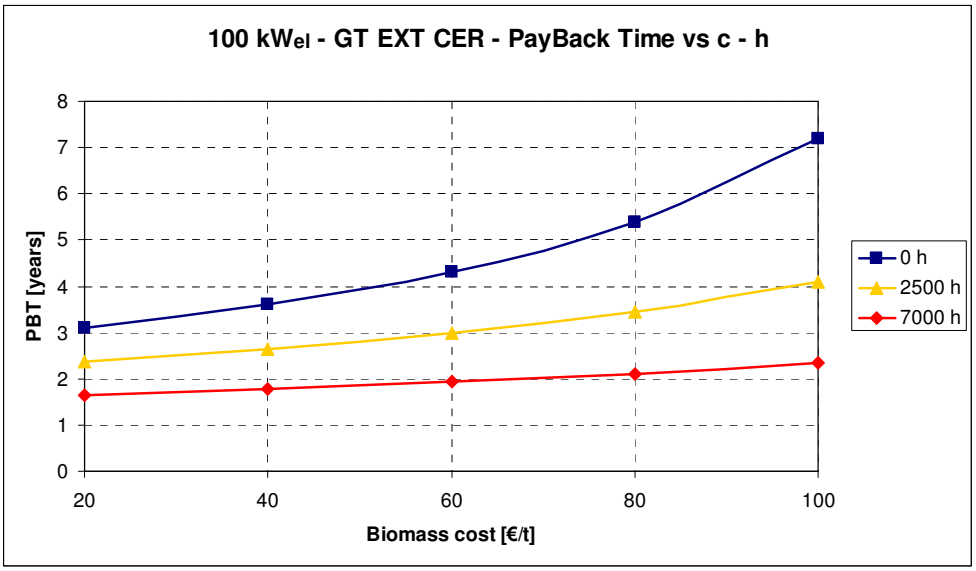

Figure 5.14 – PBT as a function of biomass cost (c) and thermal energy sale hours (h).

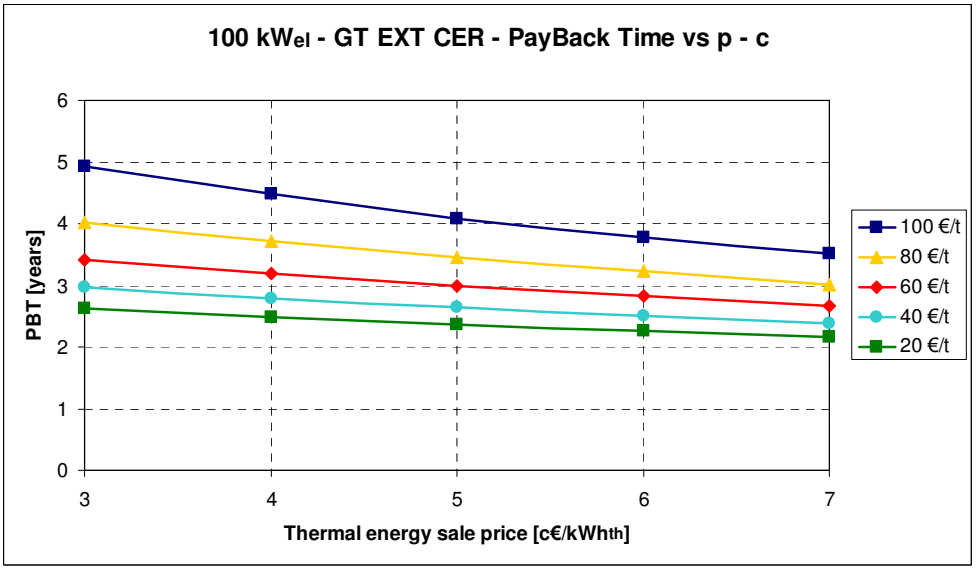

Figure 5.15 – PBT as a function of thermal energy sale price (p) and biomass cost (c).

Figure 5.13 shows the effects of increasing the thermal energy sale price at the three sale hours scenarios (with biomass cost fixed at 60 €/t): it is quite expectable to observe that PBTs decrease with increasing sale price, except for the 0 h scenario, for which this parameter is obviously irrelevant. However, the incidence is not enormous in absolute terms, the considered range being quite narrow (indeed, more external values would have been unreasonably high or low in terms of corresponding methane cost). On the other hand it is more interesting to note that the heat sale effect is not linear: the 2500 h curve is about half way between the 0 h and 7000 h ones (actually even closer to the latter than to the former), although it represents just about one third of the whole year period.

This becomes even more clear in Figure 5.14, where the thermal energy sale price is fixed at 5 c€/kWh$_{th}$, while biomass cost varies. The range of interest in this case is larger (biomass cost is influenced by several factors and can substantially vary from case to case), allowing a wider curve progress analysis. Apart from the obvious PBT increase with increasing biomass cost and diminishing heat sale hours, one can observe that the 2500 h curve is closer to the 7000 h one than to the 0 h one. Besides, the effect of increasing biomass cost is different in the three cases: it is very high without heat sale, while it gradually diminishes with increasing heat sale hours, until it becomes almost negligible in case thermal energy is being sold all over the year. The reason naturally lies in the heat sale itself: if it is performed, it allows to keep down PayBack Times.

Finally, Figure 5.15 shows how PBT varies according to thermal energy sale price and biomass cost, considering a 2500 h heat sale scenario. In the previous lines it has been stated that such a heat sale period is sufficient to limit the variation effects of the other economic parameters: this figure confirms this assumption, since all curves are very close to each other.

In conclusion, this sensitivity analysis has reasserted the relevance of heat sale as regards small-scale biomass power plant economy, showing in particular that selling thermal energy even for a not exceptionally high number of year hours (such as 2500 h) allows to limit the biomass cost raise effects. Consequences of varying thermal energy sale price are limited too, but this is also due to the fact that such values are quite standardised and may not be varied in a very wide range.

On the other hand, it is important to note that investment cost and electricity sale price (with the corresponding incentives) still remain the most important two factors for the economic analysis. Concerning this point, it is recalled that the hybrid solution, despite lower investment costs, normally requires heat to be sold all over the year, precisely because lower incentives are being granted: generally a 2500 h period is not sufficient, as it could be in case of plants fuelled with biomass only.

Chapter 6
Sensitivity analysis: moisture effects

6.1 Introduction

The analyses described in Chapters 4 and 5 have shown that externally fired gas turbines with a high temperature heat exchanger (GT EXT CER) and internal combustion engines coupled with a gasifier (ICE GAS) are the most performing biomass exploitation solutions for power generation. Having reached this conclusion represents the achievement of this thesis main objective.

A complementary sensitivity analysis is finally proposed in this chapter: in particular, the aim is to study the thermodynamic and economic effects of varying the biomass type used for plant feeding. Indeed, in Chapter 1 (see Table 1.3) it has already been shown that different wood types generally have very similar characteristics concerning their composition on dry basis (and thus their lower heating value, for instance), therefore in first analysis the only relevant point regarding different wood types is moisture. Its effects on plant performance and the usefulness of biomass drying are here investigated. The chapter is divided into two parts: firstly a preliminary analysis is proposed, where effects of gradual biomass drying with flue gases are studied from a pure thermodynamic point of view, in order to show the benefits of such an operation; secondly a more complete thermodynamic and economic study is being carried out considering three scenarios: drying with hot flue gases, no drying and natural drying.

GT EXT CER at 100 kW_{el} and ICE GAS at 1 MW_{el} have been adopted as reference plants, first of all because they have proved to be the best solutions in the previous analyses and secondly because they represent the two main ways to exploit biomass, i.e. by direct combustion of solid fuel in the former case and by conversion in syngas in the latter case.

Wood pellets have been used as fuel in all simulations, same as in the previous chapters. The actual reference composition is the one related to dry basis, which is shown in

Table 6.1[1] (LHV is equal to 18,567 kJ/kg), then moisture is varied in the different cases taken into account. Obviously, using just one single wood type allows to completely put aside any consideration concerning the actual wood composition.

FC	VM	Ash	C	H	O	N	S	Cl
17.96	81.49	0.55	50.16	6.02	43.16	0.09	0.01	0.01

Table 6.1 – Proximate and ultimate analysis of wood pellets (% w/w, db) [TF].

6.2 Preliminary analysis

As mentioned in the introduction, here it is briefly investigated how biomass drying affects thermodynamic performance, in order to demonstrate that it is a suitable operation from a technical point of view. A 20% moisture level[2] has been chosen for this analysis: the reason lies in the limits imposed to this parameter by downdraft gasifiers. This limit would not be applied to direct combustion, and therefore to GT EXT CER, but for consistency reasons it has been fixed all the same also in this case (as a matter of fact, a higher moisture level would not change the qualitative concept). Simulations have been carried out considering a progressive drying from 0% (no drying) to 100% (complete drying)[3]. Results are provided both in numerical form (reporting only the two edge values) and graphically: not only efficiencies but also powers are now being considered for completeness reasons. Plant schemes are naturally those shown in Chapter 4 (Figures 4.1 and 4.8), apart from the gasifier configuration of course (the optimised one is still being used).

6.2.1 100 kW_{el} size: GT EXT CER

Results of the simulations are reported in Table 6.2 and in Figures 6.1 and 6.2.

[1] Naturally these data could easily be derived from Table 3.1 eliminating the moisture contribution.

[2] Moisture is always meant to be calculated in weight terms and on wet basis.

[3] Indeed, normally a complete drying is not achieved, but this "ideal" case has been studied all the same.

Drying		%	0	100	Δ 0-100 (abs)	Δ 0-100 (rel,%)
Powers	P_{el}	kW	88.3	87.5	- 0.8	- 1.0
	Q_{th}		230.9	206.5	- 24.4	- 10.6
	P_{ch}		408.8	381.8	- 27.0	- 6.6
Efficiencies	η_{el}	%	21.60	22.91	+ 1.31	+ 6.1
	η_{th}		56.49	54.08	- 2.41	- 4.3
	η_{I}		78.09	76.99	- 1.10	- 1.4

Table 6.2 – GT EXT CER (100 kW_{el}): powers and efficiencies as a function of biomass drying.

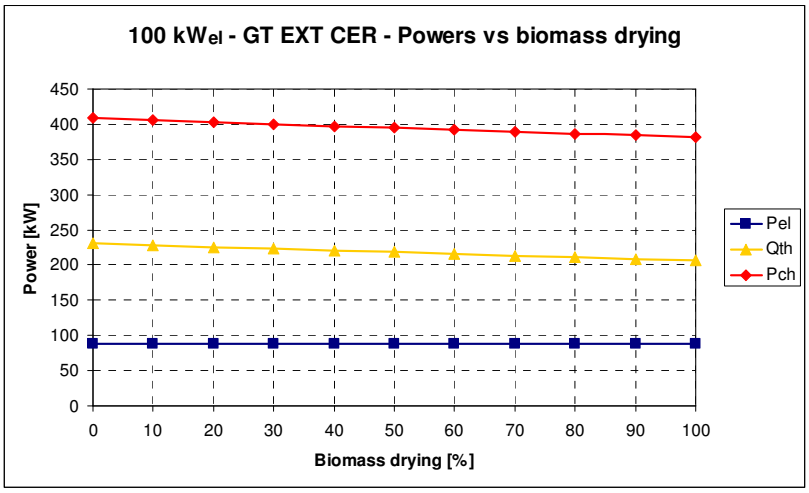

Figure 6.1 – GT EXT CER (100 kW_{el}): powers as a function of biomass drying.

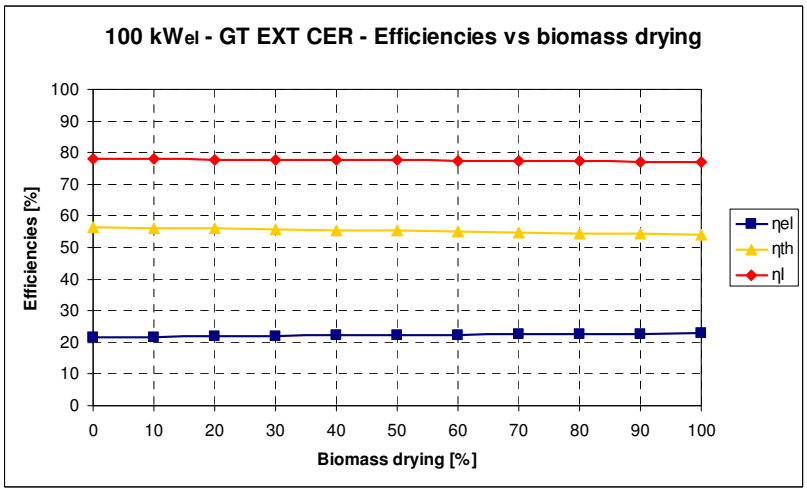

Figure 6.2 – GT EXT CER (100 kW_{el}): efficiencies as a function of biomass drying.

Focusing on Figure 6.1, electric power output remains practically unchanged: indeed, there is no reason why it should change, as all thermodynamic parameters (pressure ratio, combustor outlet temperature, etc.) are not influenced by biomass drying[4]. Actually a little reduction due to the dryer power consumption (related to the moisture evacuator), that is proportional to the removed moisture quantity, is being verified all the same. On the other hand, thermal power output considerably decreases with increasing drying, because more and more power contained in flues gases is required by the drying process itself and is thus no more available for the thermal user. Finally, chemical fuel power input to be fed into the cycle is constant, since thermodynamic cycle parameters are unvaried; nevertheless if wet biomass is supplied to the combustor additional chemical power is required to allow moisture vaporisation into the combustor itself. Therefore it is easy to understand why overall fuel power input decreases with increasing drying.

Efficiencies progress is a natural consequence of the aforementioned power behaviour (Figure 6.2). Electric power being constant and chemical one decreasing, electrical efficiency is an increasing function of biomass drying: more than one percentage point (6% in relative terms) is gained performing a complete drying. On the other hand, as thermal power decreases more than the fuel one, thermal efficiency (η_{th}) diminishes too: about two percentage points are lost (4% in relative terms). Therefore first law efficiency decreases by one point. However, as mentioned more than once, this work is mainly focusing on electric power maximisation, hence biomass drying should be considered as an advantageous operation. Indeed, this is true in general terms too, in fact it is not necessary to perform an exergy analysis to understand that the 1%-increase in electrical efficiency is much more significant than the 2%-decrease in the thermal one, considering that process heat is available at very low temperature (about 70°C), corresponding consequently to very low exergy.

6.2.2 1 MW_{el} size: ICE GAS

Results of the simulations are reported in Table 6.3 and in Figures 6.3 and 6.4.

[4] Indeed flue gas mass flow rate slightly changes if moisture is being removed or not, but the effects of this variation are negligible.

Drying		%	0	100	Δ 0-100 (abs)	Δ 0-100 (rel,%)
Powers	P_{el}	kW	942.8	949.6	+ 6.8	+ 0.7
	Q_{th}		1299.4	1205.6	- 93.8	- 7.2
	P_{ch}		3048.0	2885.9	- 162.1	- 5.3
Efficiencies	η_{el}	%	30.93	32.90	+ 1.97	+ 6.4
	η_{th}		42.64	41.78	- 0.86	- 2.0
	η_{l}		73.57	74.68	+ 1.11	+ 1.5

Table 6.3 – ICE GAS (1 MW_{el}): powers and efficiencies as a function of biomass drying.

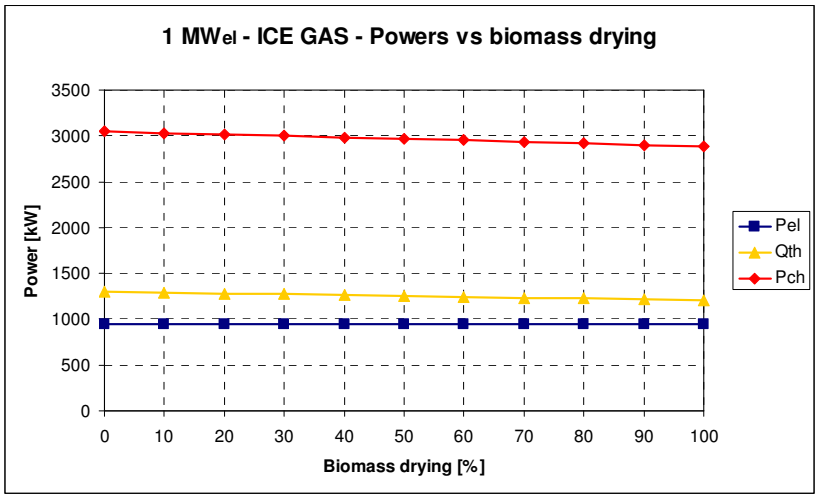

Figure 6.3 – ICE GAS (1 MW_{el}): powers as a function of biomass drying.

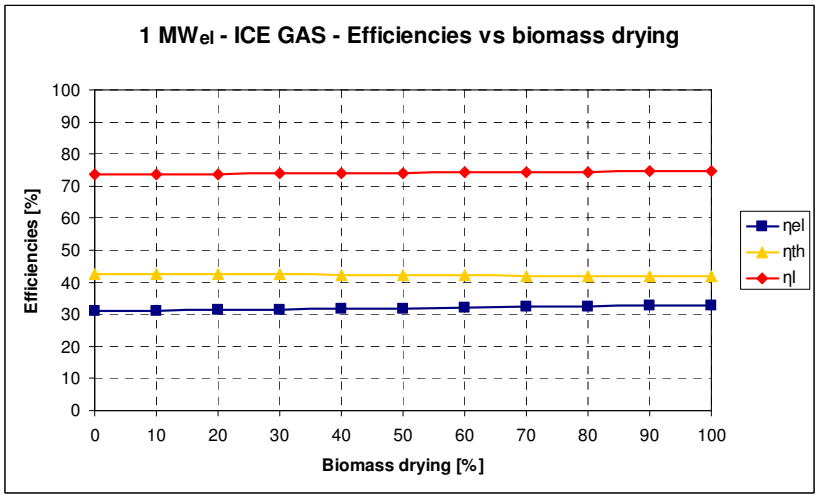

Figure 6.4 – ICE GAS (1 MW_{el}): efficiencies as a function of biomass drying.

One can observe that plant response to progressive biomass drying is similar to the previous case, even if some important differences can be found.

Electric power output is roughly constant (engine operation is not influenced by moisture), but in this case a little increase instead of a decrease is being verified (Figure 6.3). In fact dryer power consumption raises with biomass drying, like in GT EXT CER, but on the other hand gasifier and cleaning section consumptions diminish, as they are proportional to the fuel mass flow rate, which decreases as well both concerning solid fuel input and syngas output. In fact providing an additional power input is still required if wet biomass is charged into the gasifier, whereas overall required fuel mass flow rate diminishes if dried biomass is being used. Moreover cold gas efficiency increases and this leads to a lower syngas mass flow rate characterised by a much higher LHV (fuel power input in the engine has to be constant). Consequently chemical fuel power input decreases with increasing drying, exactly as in the previous case. A progress similar to the GT EXT CER at 100 kW_{el} has been found concerning thermal power too, as it is gradually used to perform drying. Moreover one can note that both chemical and thermal power diminutions are roughly of the same order of magnitude compared to the previous case in relative terms, even if the latter is now less relevant, essentially due to the lower heat supply temperature.

Regarding efficiencies (Figure 6.4), the electrical one obviously raises (about two percentage points in absolute terms, i.e. six points in relative ones), since electric power output increases and chemical power input decreases. Thermal efficiency instead decreases, although less than in the previous case: about 1% in absolute terms and 2% in relative ones. As a consequence of higher electrical efficiency increase and lower thermal efficiency decrease, differently from the previous case, first law efficiency now raises: therefore there is no doubt concerning the convenience of biomass drying.

6.2.3 Conclusions

This brief analysis has shown that progressive biomass drying involves considerable advantages from a thermodynamic point of view, both as regards GT EXT CER and ICE GAS. In both cases electrical efficiency increases, while thermal one decreases. The actual progress leads to a first law efficiency decrease in the former case and to an

increase in the latter. An exergy analysis could however show that the operation would be advantageous in the first case too, like it is undoubtedly in the second one[5]. This explains why biomass drying has always been performed in the thermodynamic analysis described in Chapter 4 [6.1] [6.2] [6.3].

6.3 Complete analysis

Once proven the thermodynamic convenience of gradual artificial biomass drying, a more-in-depth analysis is finally proposed, still adopting GT EXT CER at 100 kW_{el} and ICE GAS at 1 MW_{el}. The purpose of this section is to compare the performance of three scenarios starting from different moisture contents. The scenarios are the following:

- full drying using hot flue gases, analogously to the previous section;
- no drying;
- natural drying (seasoning), which allows to lower moisture content down to 20%, as discussed in Chapter 1.

In this analysis a wider moisture level range is being considered: in particular the maximum content is fixed to 60%, which is the highest practical value for biomass combustion. The natural drying scenario is therefore applied exclusively in the moisture range 20 ÷ 60% and is equal to no drying at 20%.

It is important to note, however, that all of the three cases can completely be taken into consideration as regards GT EXT CER, while the no drying scenario can only partially be applied to ICE GAS. As mentioned, in fact, at the gasifier input biomass moisture must be lower than 20% (by chance exactly the value reached by natural drying), therefore, in case of higher initial level, biomass must be dried (artificially or naturally) at least down to this value. Thus no drying is not a possible option beyond that value. On the other hand, it is suitable if the initial moisture content is already lower than 20%.

Reference plants are those so far adopted, obviously eliminating the dryer in case of no drying and substituting it with a sort of free-dryer which simulates seasoning in case of

[5] Then it is clear that the energy demand of the specific process fed by the plant could lead to different evaluations.

natural drying. Nevertheless gas drying has required a little plant variation. It could be shown, in fact, that thermal power absorbed by air stream from hot syngas is just sufficient to dry biomass having a maximum moisture content of about 30%, therefore it has been hypothesised to perform biomass drying using hot flue gas exiting the engine[6]. Gas exiting the dryer is then naturally used to produce further process heat; on the other hand, air stream heated up by hot syngas is still being used partly to feed the gasifier and partly to supply additional process heat.
In this case the assessment is effected not only from a thermodynamic, but also from an economic point of view, in order to investigate the overall suitability of the different options.

6.3.1 Thermodynamic analysis

As in the previous analysis, results are provided both in numerical and in graphic form. Nevertheless now all numeric results are shown, as in many cases the behaviour of the various parameters is not linear. Absolute and relative variations between the edge values are also provided. It is expectable that hot gas drying will provide results similar to those proposed in the previous case, even if conditions are not exactly the same and thus some differences may be found. Finally it is easy to predict that at 0% moisture content no drying and gas drying cases will provide the same result (except for one particular case), since under those conditions, there is no difference between the two scenarios.

6.3.1.1 100 kW_{el} size: GT EXT CER

Results are summarised in Table 6.4 and shown in Figures 6.5 ÷ 6.10.

[6] As specified in Charter 3, hot flue gas temperature is 515°C. This could lead to potential pyrolysis phenomena in the wood, but for simplicity this issue has been neglected.

Full hot gas drying						
Moisture [%]	**P_{el} [kW]**	**Q [kW]**	**P_{ch} [kW]**	**η_{el} [%]**	**η_{th} [%]**	**η_{I} [%]**
0	88.5	218.7	394.7	22.42	55.41	77.83
8.7	88.1	214.0	389.7	22.61	54.91	77.52
20	87.5	206.5	381.8	22.91	54.08	76.99
30	86.7	197.7	372.5	23.28	53.07	76.35
40	85.7	186.0	360.2	23.80	51.64	75.44
50	84.3	169.7	342.9	24.60	49.49	74.09
60	82.3	145.2	316.9	25.96	45.80	71.76
Δ 0-60 (abs)	- 6.2	- 73.5	- 77.8	+ 3.54	- 9.61	- 6.07
Δ 0-60 (rel,%)	- 7.0	- 33.6	- 19.7	+ 15.8	- 17.3	- 7.8
No drying						
Moisture [%]	**P_{el} [kW]**	**Q [kW]**	**P_{ch} [kW]**	**η_{el} [%]**	**η_{th} [%]**	**η_{I} [%]**
0	92.7	221.3	401.9	23.05	55.07	78.12
8.7	92.6	226.4	407.7	22.72	55.53	78.25
20	92.6	235.1	417.7	22.17	56.28	78.45
30	92.6	246.6	430.8	21.48	57.23	78.71
40	92.5	263.8	450.6	20.53	58.54	79.07
50	92.4	293.2	484.4	19.08	60.53	79.61
60	92.2	355.3	555.4	16.60	63.96	80.56
Δ 0-60 (abs)	- 0.5	+ 134.0	+ 153.5	- 6.45	+ 8.89	+ 2.44
Δ 0-60 (rel,%)	- 0.5	+ 60.6	+ 38.2	- 28.0	+ 16.1	+ 3.1
Natural drying (down to 20%)						
Moisture [%]	**P_{el} [kW]**	**Q [kW]**	**P_{ch} [kW]**	**η_{el} [%]**	**η_{th} [%]**	**η_{I} [%]**
20	92.6	235.1	417.7	22.17	56.28	78.45
30	92.6	235.3	407.7	22.71	57.70	80.41
40	92.6	235.3	394.2	23.49	59.67	83.16
50	92.6	235.3	375.7	24.65	62.61	87.26
60	92.6	235.3	350.2	26.45	67.19	93.64
Δ 20-60 (abs)	0.0	+ 0.2	- 67.5	+ 4.28	+ 10.91	+ 15.19
Δ 20-60 (rel,%)	0.0	+ 0.1	- 16.2	+ 19.3	+ 19.4	+ 19.4

Table 6.4 – GT EXT CER (100 kW_{el}): powers and efficiencies in the three drying scenarios.

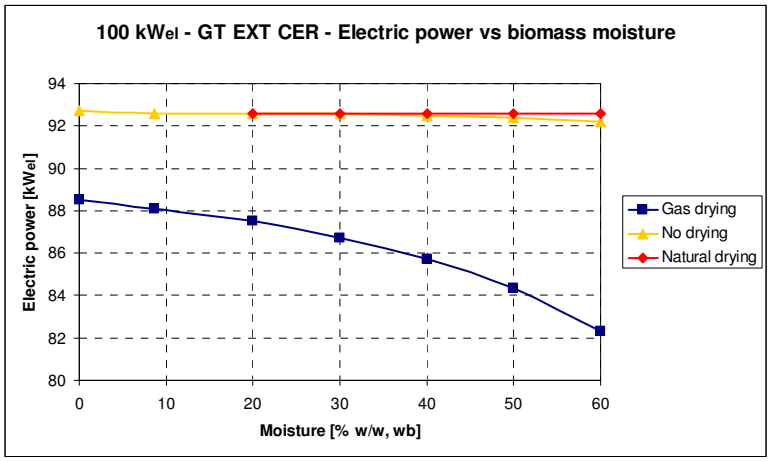

Figure 6.5 – GT EXT CER (100 kW_{el}): electric power in the three drying scenarios.

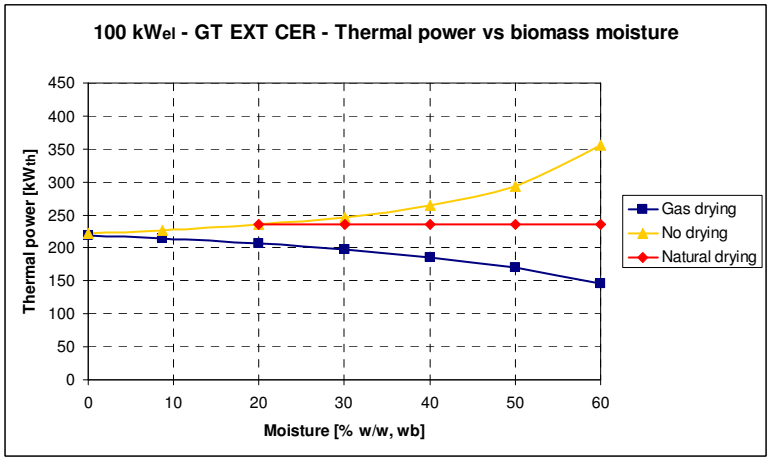

Figure 6.6 – GT EXT CER (100 kW_{el}): thermal power in the three drying scenarios.

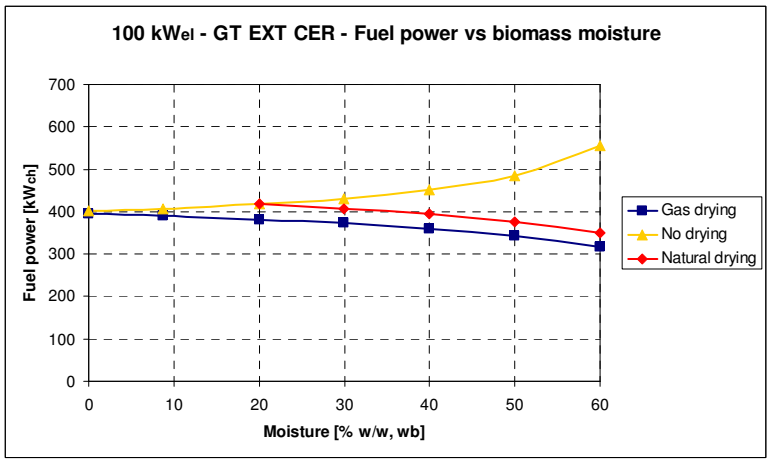

Figure 6.7 – GT EXT CER (100 kW_{el}): fuel power in the three drying scenarios.

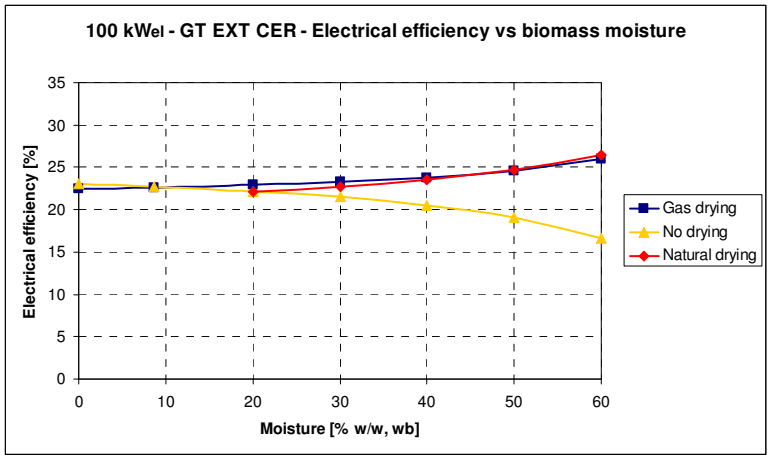

Figure 6.8 - GT EXT CER (100 kW_{el}): electrical efficiency in the three drying scenarios.

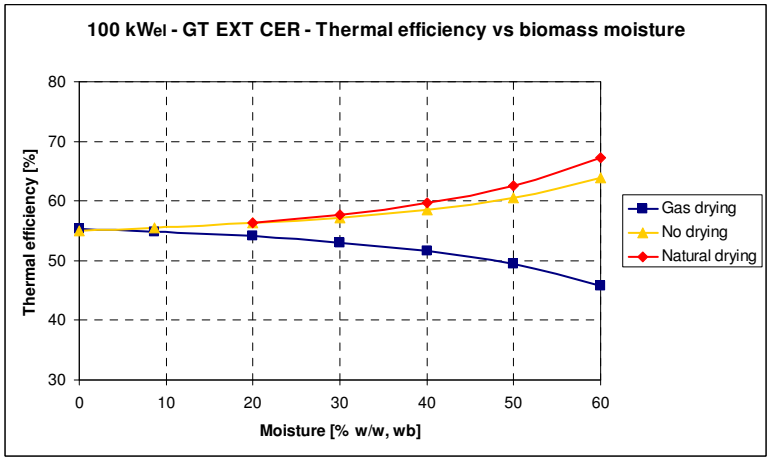

Figure 6.9 - GT EXT CER (100 kW_{el}): thermal efficiency in the three drying scenarios.

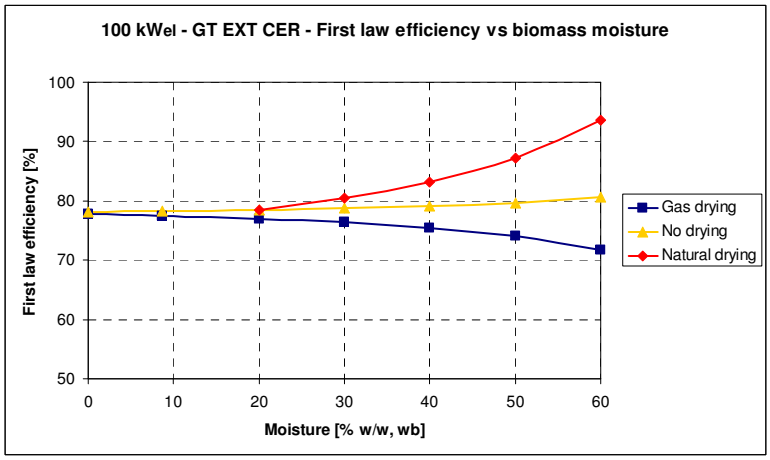

Figure 6.10 - GT EXT CER (100 kW_{el}): first law efficiency in the three drying scenarios.

Electric power (Figure 6.5) is similar in all scenarios. In case of no or natural drying, this quantity is practically constant, as cycle parameters are not varied. The same should be valid also for hot gas drying, but a reduction can be observed again, still due to the increasing moisture evacuator power consumption. This decrease is considerable (about 7% in relative terms), as a consequence of the high maximum moisture content. As mentioned, the 0% moisture result should be equal to no drying, since drying is actually not performed: however the presence of the dryer determines head losses, hence a lower useful pressure ratio in the turbine and a lower power output.

Neglecting thermal power for the time being and focusing on the chemical fuel one (Figure 6.7), one can see that it increases considerably in case of no drying, otherwise it decreases. As discussed before, the reason lies in the moisture latent heat: if drying is not being carried out, the vaporisation takes place in the combustor and thus an additional wood mass flow is required to fuel the process (a 38% relative increase in chemical power is registered). Nevertheless, considering gas drying, the situation is slightly different from the previous analysis. In fact a gradual drying starting from a certain moisture content was performed in that case, and thus water was always partly injected in the combustor with its latent heat (apart from the case of complete drying, obviously), which immediately justified the necessity of supplying an additional fuel power. Instead now biomass drying starts from different moisture levels, but drying is always supposed to be complete, therefore moisture never enters the combustor: wood fed into the combustor is always completely dry and thus the same mass flow rate of dry fuel is required, i.e. the chemical power input in the combustor is constant in all cases. If then a certain amount of moisture is contained in the starting wood, overall mass flow rate is accordingly higher. Nevertheless, the chemical power contained in that overall wet wood mass flow rate is lower than the one contained in the same quantity of dry wood, still due to the moisture latent heat[7]: this difference obviously raises with increasing moisture, finally explaining the required chemical power reduction (numerically the relative reduction is about 20%). In case of natural drying the concept is similar: a simple shift can be noted in the figure, due to the fact that drying is performed down to 20% and not to 0%.

[7] For instance, 1 kg of dry wood has a higher LHV than 1.1 kg of wet wood with 0.1 kg of moisture, since the latent heat of the latter is to be accounted.

Concerning thermal power (Figure 6.6), one can observe a considerable increase with moisture if drying is not performed (+60%). The reason lies in what has just been described: an increasing wood mass flow rate is required with increasing moisture and this makes a higher gas mass flow rate available for the thermal process. On the other hand, wet biomass removes more and more heat from the hot stream with increasing moisture in case of gas drying, and thus the useful thermal power output decreases in this scenario (by about one third). Finally thermal power remains unvaried in case of natural drying. In all cases, in fact, wood enters the combustor with a moisture content of 20% and thus operating conditions do not vary: thermal power available for the process is always the same.

Efficiencies behaviour is a consequence of power results. Concerning electrical efficiencies (Figure 6.8), natural and artificial drying cases lead to an increase (+3.5/4% absolute, +16/19% relative, respectively), since electric power remains unvaried (or very slightly decreases), while fuel power decreases considerably. Moreover, absolute results are analogous. On the other hand, it diminishes (-6% and -28%) if drying is not realised, because, electric power being constant, the chemical one increases.

The progress of thermal efficiencies (Figure 6.9) is in general less easy to predict. Both thermal and chemical powers increase in case of no drying: numerically the former contribution is proportionally more effective and thus thermal efficiency raises (+9% absolute, +16% relative). In case of artificial drying, instead, both of the two considered power decrease: again, the thermal diminution is more effective, hence thermal efficiency decreases (-10% and -17%). Finally, natural drying leads to a thermal efficiency increase (+11% absolute, +19% relative), due to the constancy of thermal power and the diminution of the chemical one.

First law efficiency can finally be evaluated starting from the two previous parameters (Figure 6.10). The electrical efficiency increase is roughly equal to the thermal efficiency decrease in case of no drying, therefore first law efficiency is about constant. On the contrary, a considerable increase is registered in case of natural drying (+15% in absolute terms, +19% in relative ones), due to the fact that both electrical and thermal efficiencies raise with moisture. Finally gas drying denotes analogous results to the previous analysis: thermal efficiency diminution is higher than electrical increase, and thus first law efficiency diminishes (-6% and -8%).

In conclusion, from a thermodynamic point of view, one can say that natural drying (if possible, clearly) is undoubtedly a suitable option, as it determines both electric and thermal performance increase with increasing moisture. As regards artificial drying, electrical and thermal efficiencies behave oppositely but, again, the 3.5% electric increase must be considered more significant, in exergy terms, than the 10% thermal power loss. Finally, no drying allows to achieve very high thermal production with increasing moisture, but electrical efficiency is heavily penalised.

6.3.1.2 1 MW_{el} size: ICE GAS

Results are summarised in Table 6.5 and shown in Figures 6.11 ÷ 6.16.

Full hot gas drying						
Moisture [%]	**P_{el} [kW]**	**Q [kW]**	**P_{ch} [kW]**	**η_{el} [%]**	**η_{th} [%]**	**η_{I} [%]**
0	960.5	1262.8	2944.8	32.62	42.88	75.50
8.7	958.5	1229.9	2906.9	32.97	42.31	75.28
20	953.8	1178.3	2852.0	33.44	41.32	74.76
30	949.4	1115.4	2781.5	34.13	40.10	74.23
40	938.8	1023.5	2683.2	34.99	38.14	73.13
50	929.5	899.9	2535.7	36.40	35.49	71.89
60	913.9	687.9	2289.9	39.91	30.04	69.95
Δ 0-60 (abs)	- 46.6	- 574.9	- 654.9	+ 7.29	- 12.84	- 5.55
Δ 0-60 (rel,%)	- 4.9	- 45.5	- 22.2	+ 22.3	- 29.9	- 7.4
No drying						
Moisture [%]	**P_{el} [kW]**	**Q [kW]**	**P_{ch} [kW]**	**η_{el} [%]**	**η_{th} [%]**	**η_{I} [%]**
0	964.1	1278.9	2966.0	32.51	43.11	75.62
8.7	959.2	1292.8	3003.0	31.94	43.04	74.98
20	950.2	1315.5	3072.0	30.93	42.83	73.76
Δ 0-20 (abs)	- 13.9	+ 36.6	+ 106.0	- 1.58	- 0.28	- 1.86
Δ 0-20 (rel,%)	- 1.4	+ 2.9	+ 3.6	- 4.9	- 0.6	- 2.5
Natural drying (down to 20%)						
Moisture [%]	**P_{el} [kW]**	**Q [kW]**	**P_{ch} [kW]**	**η_{el} [%]**	**η_{th} [%]**	**η_{I} [%]**
20	950.2	1315.5	3072.0	30.93	42.83	73.76
30	950.2	1315.9	2996.2	31.71	43.92	75.63
40	950.2	1315.5	2894.6	32.83	45.44	78.27
50	950.2	1315.6	2755.1	34.49	47.75	82.24
60	950.2	1315.7	2543.0	37.36	51.74	89.10
Δ 20-60 (abs)	0.0	+ 0.2	- 529.0	+ 6.43	+ 8.91	+ 15.34
Δ 20-60 (rel,%)	0.0	0.0	- 17.2	+ 20.8	+ 20.8	+ 20.8

Table 6.5 – ICE GAS (1 MW_{el}): powers and efficiencies in the three drying scenarios.

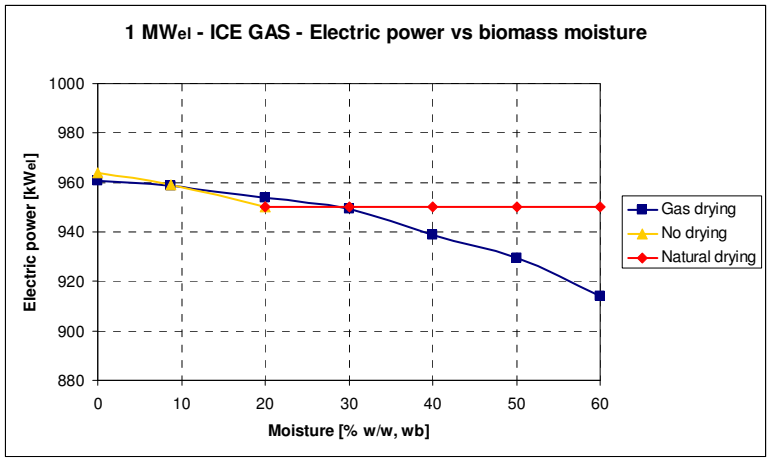

Figure 6.11 – ICE GAS (1 MW_{el}): electric power in the three drying scenarios.

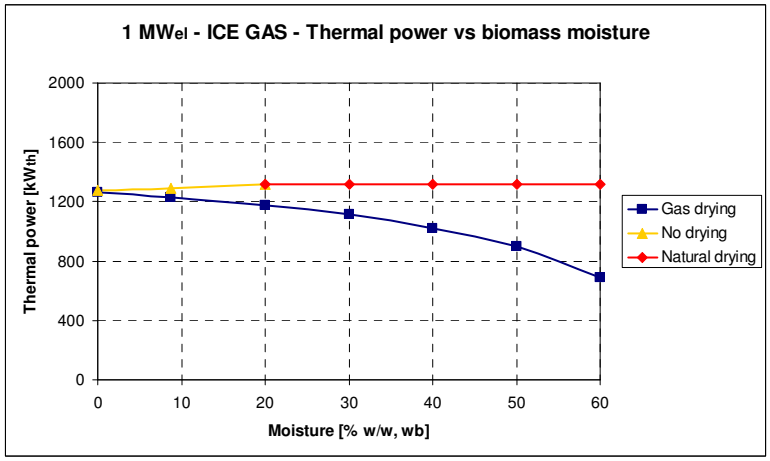

Figure 6.12 – ICE GAS (1 MW_{el}): thermal power in the three drying scenarios.

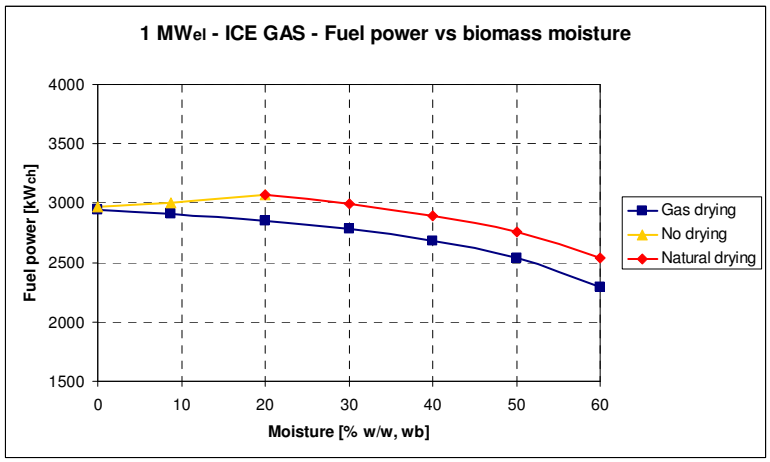

Figure 6.13 – ICE GAS (1 MW_{el}): fuel power in the three drying scenarios.

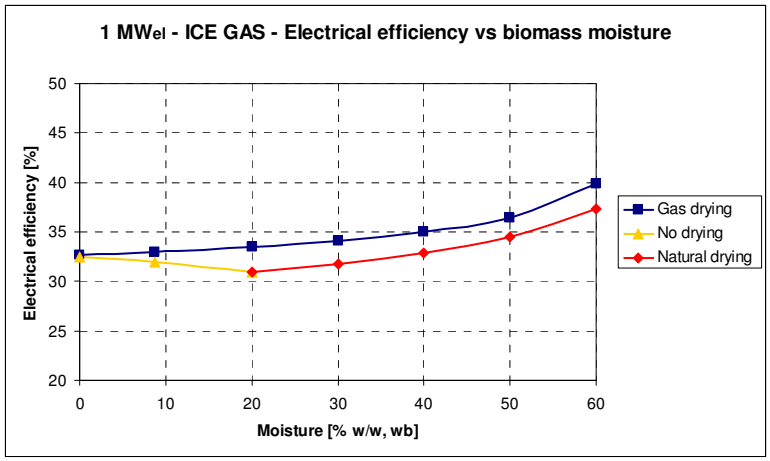

Figure 6.14 – ICE GAS (1 MW_{el}): electrical efficiency in the three drying scenarios.

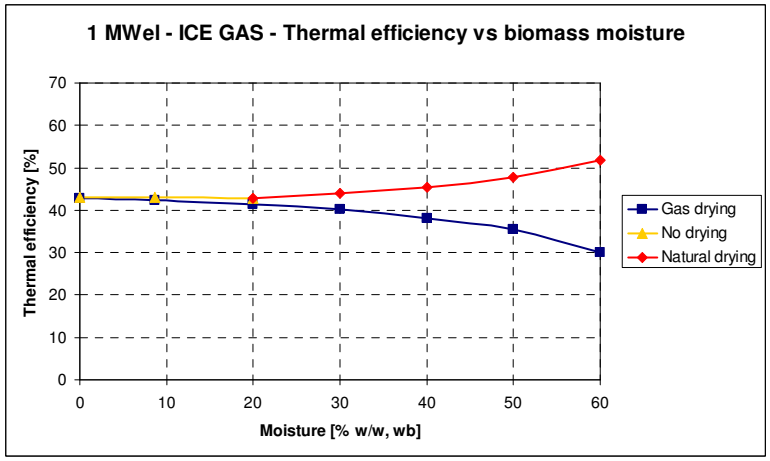

Figure 6.15 – ICE GAS (1 MW_{el}): thermal efficiency in the three drying scenarios.

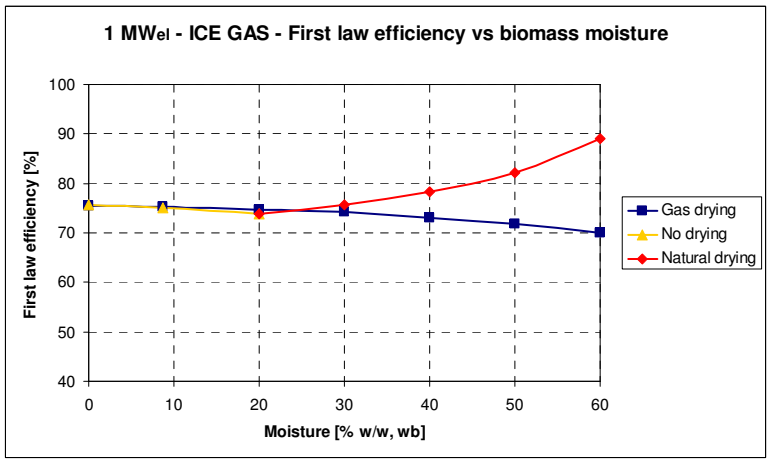

Figure 6.16 – ICE GAS (1 MW_{el}): first law efficiency in the three drying scenarios.

All the main previously proposed remarks are in general valid here too, therefore the discussion will be shorter. As mentioned before, the no drying case is being taken into consideration only up to 20%, because this is the maximum allowable wood moisture content for downdraft gasifiers.

In case of artificial drying, electric power (Figure 6.11) decreases with increasing moisture (-5%), due to the gradually increasing moisture evacuator power consumption. Differently from the scenario considered in the preliminary analysis, in fact, in this case there is no effect related to gasifier and syngas cleaning auxiliaries consumption, since biomass is now completely dried from any initial moisture content, and thus the mass flow rate treated by the gasifier (solid fuel) and by the cleaning section (syngas) is always the same. If drying is performed the natural way, the electric power output does not change, as the cycle is not influenced by the different moisture input. A little diminution (just over 1%) is found only in case of no drying, because wood and syngas mass flow rates slightly increase with moisture, and so do the auxiliaries consumptions.

The progress of thermal power (Figure 6.12) is well known, at least as regards gas and natural drying: in the former case, thermal power available for the process decreases with increasing moisture due to the increasing power demand for drying (it almost halves); in the latter case useful heat output does not change. An increase with increasing moisture is instead found regarding no drying (+3%): as already discussed, syngas mass flow rate grows and so does recoverable sensible heat.

The behaviour of chemical powers (Figure 6.13) is practically identical to the GT EXT CER case (Figure 6.7): moisture latent heat makes fuel power grow if drying is not carried out (+4%), otherwise a decrease is found (-22% as regards gas drying and -17% in case of natural drying).

Electrical efficiencies (Figure 6.14) behave as in the GT EXT CER case as well, diminishing in case of no drying (-1.5% absolute and -5% relative) and increasing in the other two cases: +7% absolute and +22% relative with artificial drying, +6.5% absolute and +22% relative with natural drying. Differently from GT EXT CER, however, the gas drying curve is slightly higher than the natural drying one.

Thermal efficiencies (Figure 6.15) denote a strong decrease as regards gas drying (-13% absolute, -30% relative), a considerable increase regarding natural drying (+9% and + 21%) and a certain constancy in case of no drying, again same as in the previous case.

Finally, first law efficiencies (Figure 6.16) grow in case of natural drying and decrease in the artificial one, roughly in equal measure as in the previous case both in absolute and relative terms. No drying, instead, denotes a little variation as regards GT EXT CER (compared to the corresponding moisture range, obviously), being characterised by a slight decrease in place of the substantial constancy previously found (-2% absolute and -2.5% relative), essentially due to higher electrical penalisation.
In conclusion, the same remarks presented in the previous case can be proposed here as well: biomass drying, both artificial or natural, determines a plant performance improvement, while the use of wet biomass involves a thermodynamic penalisation.
On the other hand, it is now necessary to verify that biomass drying is advantageous also from an economic point of view.

6.3.2 Economic analysis

The economic analysis described in this section has been performed basing on the same hypotheses discussed in Chapter 5 (including the 2500 h heat sale period), except for two important parameters: biomass cost (still referring to raw material) and specific investment costs.
Concerning the former, it is recalled that a cost of 60 €/t was assumed for the analysis. Nevertheless this value is valid for the reference moisture content, that is 8.7% (corresponding to a LHV equal to 16,784 kJ/kg). If then the latter varies, the biomass lower heating value, and thus its energy content, will vary accordingly too: in particular, increasing the former, it will decreases. Therefore it is not possible to adopt the same cost for all the considered moisture contents: for simplicity reasons, in this work it has been assumed to fix a direct proportionality between biomass cost and its lower heating value, starting from the aforementioned base values (Table 6.6 and Figure 6.17).
Plant specific investment costs have been listed in Table 5.1. In particular, they are equal to 4000 €/kW_{el} for GT EXT CER and 2700 €/kW_{el} for ICE GAS. Those values include the dryer cost, as this device has been considered in all base configurations. On the other hand, in this analysis there are two scenarios (no drying and natural drying) where the dryer is not present, therefore its cost must be subtracted from the aforementioned values to obtain the investment costs in these two cases. In particular

300 €/kW_{el} have been chosen for GT EXT CER and 200 €/kW_{el} for ICE GAS: the corresponding overall investment costs are therefore 3700 €/kW_{el} and 2500 €/kW_{el}, as summarised in Table 6.7.

Moisture [%]	LHV [kJ/kg]	Cost [€/t]
0	18,567	66.4
8.7	16,784	60.0
20	14,364	51.3
30	12,264	43.8
40	10,164	36.3
50	8,061	28.8
60	5,961	21.3

Table 6.6 – Biomass lower heating value and cost as a function of moisture content.

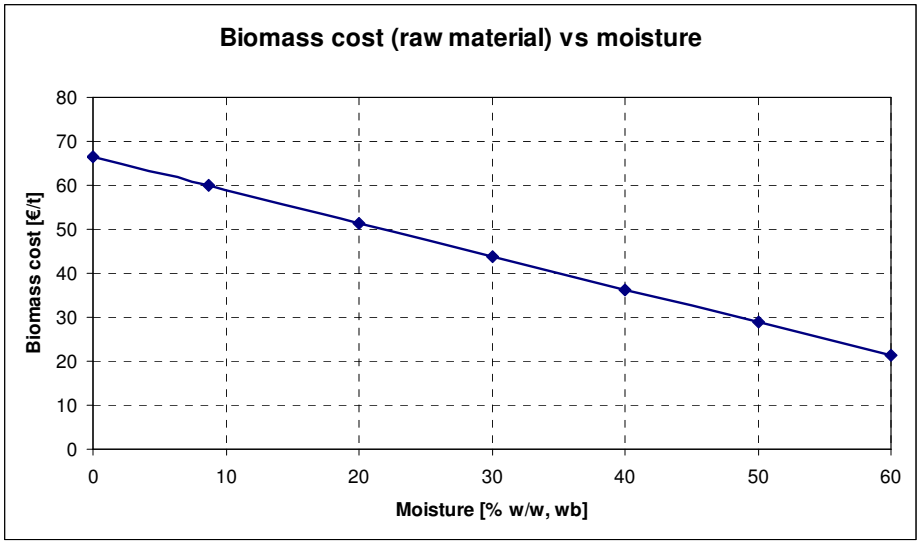

Figure 6.17 – Biomass cost as a function of moisture content.

Solution	Gas drying	*Dryer cost*	No drying and natural drying
GT EXT CER	4000	*300*	3700
ICE GAS	2700	*200*	2500

Table 6.7 – Plant specific investment costs (€/kW_{el}) in the three drying scenarios.

6.3.2.1 Results and discussion

Results of the economic analysis are provided in one single section, as they are very similar in the two cases. In particular, PayBack Times and Net Present Values have been calculated, while Internal Rates of Return have been neglected. Results are listed in Table 6.8 and 6.9 and shown in Figures 6.18 ÷ 6.19 (PBT) and 6.20 ÷ 6.21 (NPV).

100 kW_{el} – GT EXT CER						
Moisture [%]	**PBT [years]**			**NPV [k€]**		
	Gas drying	**No drying**	**Natural drying**	**Gas drying**	**No drying**	**Natural drying**
0	2.96	2.64	-	384	412	-
8.7	2.99	2.67	-	378	407	-
20	3.05	2.71	2.71	369	399	399
30	3.12	2.77	2.73	358	387	395
40	3.22	2.87	2.76	343	370	390
50	3.37	3.05	2.79	322	341	383
60	3.64	3.44	2.86	289	285	371
Δ 0-60 (abs)	+ 0.68	+ 0.8	+ 0.15	- 95	- 127	- 28
Δ 0-60 (rel,%)	+ 23.0	+ 30.3	+ 5.5	- 24.7	- 30.8	- 7.0

Table 6.8 – GT EXT CER (100 kW_{el}): economic results in the three drying scenarios.

1 MW_{el} – ICE GAS						
Moisture [%]	**PBT [years]**			**NPV [k€]**		
	Gas drying	**No drying**	**Natural drying**	**Gas drying**	**No drying**	**Natural drying**
0	1.43	1.30	-	6293	6485	-
8.7	1.44	1.31	-	6259	6434	-
20	1.45	1.32	1.32	6197	6339	6339
30	1.46	-	1.33	6128	-	6314
40	1.48	-	1.34	6026	-	6281
50	1.51	-	1.35	5890	-	6233
60	1.56	-	1.36	5707	-	6164
Δ 0-60 (abs)	+ 0.13	+ 0.02	+ 0.04	- 586	- 146	- 175
Δ 0-60 (rel,%)	+ 9.1	+ 1.5	+ 3.0	- 9.3	- 2.3	- 2.8

Table 6.9 – ICE GAS (1 MW_{el}): economic results in the three drying scenarios.

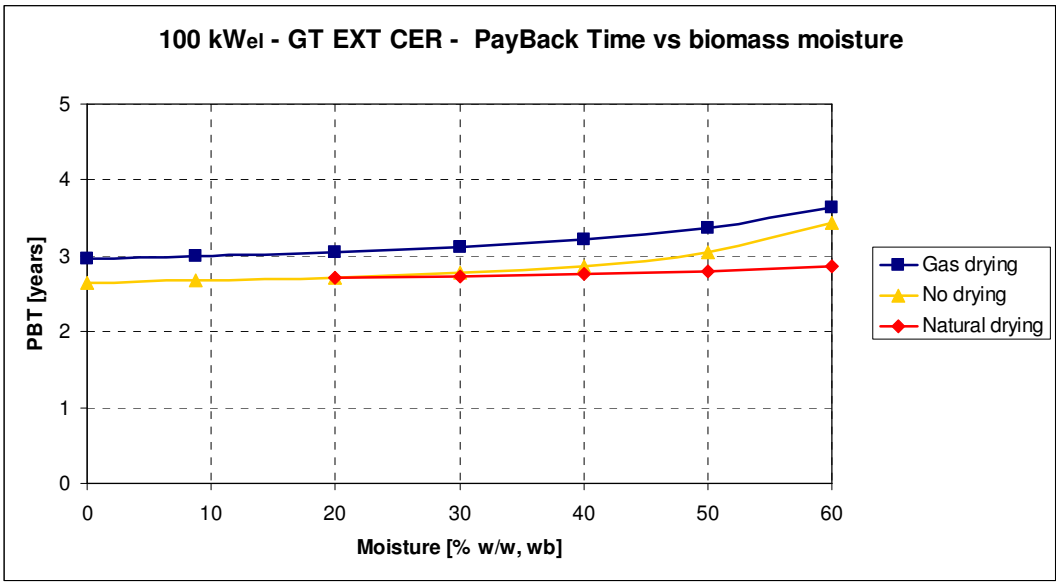

Figure 6.18 - GT EXT CER (100 kW_{el}): PayBack Time in the three drying scenarios.

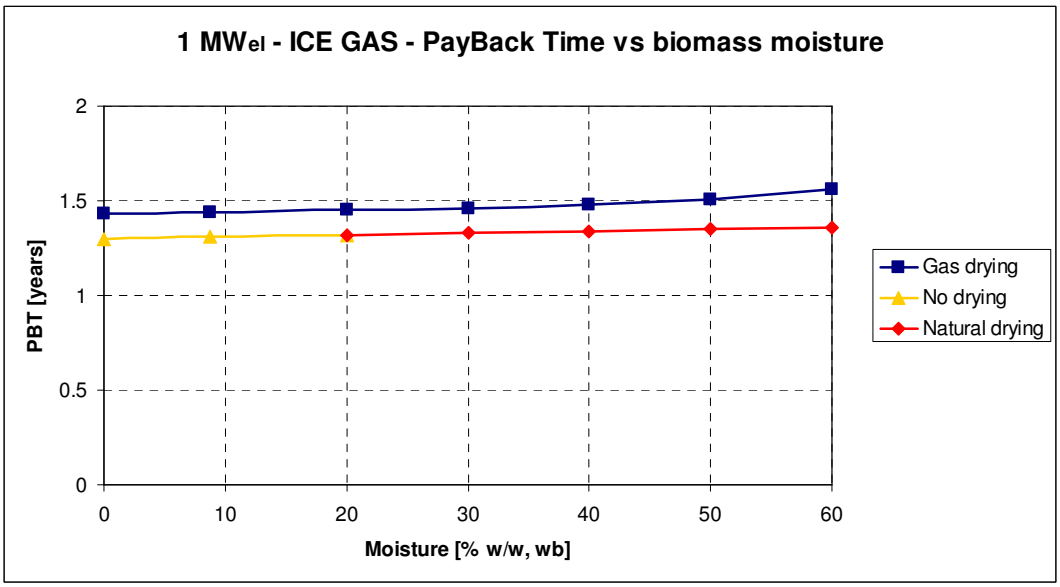

Figure 6.19 – ICE GAS (1 MW_{el}): PayBack Time in the three drying scenarios.

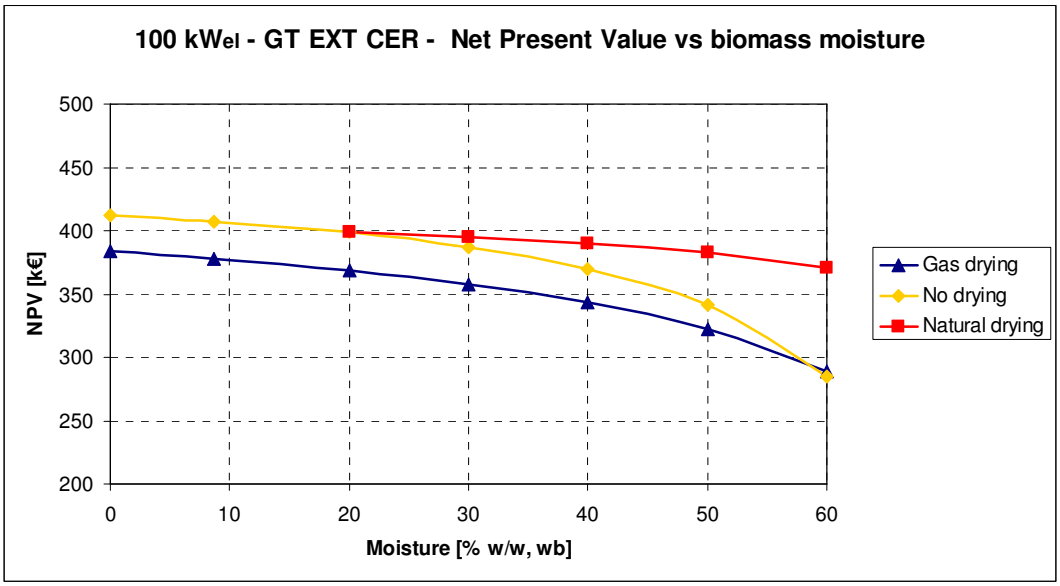

Figure 6.20 - GT EXT CER (100 kW_{el}): Net Present Value in the three drying scenarios.

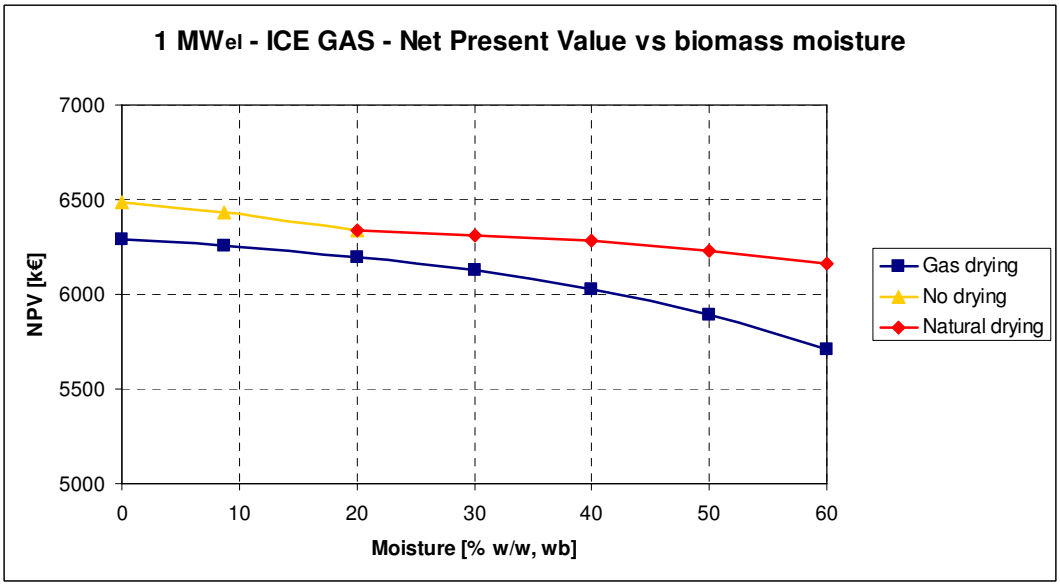

Figure 6.21 – ICE GAS (1 MW_{el}): Net Present Value in the three drying scenarios.

Firstly one can note that PayBack Times slightly increase and Net Present Values slightly decrease with increasing moisture in both cases and in all scenarios: the main reason lies in biomass transport costs. As mentioned in Chapter 5, in fact, a cost of 15 €/t is fixed to quantify this item, independently from the biomass energy content. Therefore if moisture increases, a higher biomass quantity is required, and thus costs grow proportionally. On the other hand, costs of raw material do not change considerably, as the higher required biomass quantity is roughly balanced by lower specific costs. Actually, as inferable from the previous discussions, a little increase is found in the no drying case, and an analogous decrease in the other two cases, but they are small variations.

However, the most important and immediate observation regards gas drying performance: it is the worst solution from an economic point of view, despite its good technical results which have been previously discussed; PayBack Time curve is shifted upwards compared to the other two solutions, while the Net Present Value one is accordingly shifted downwards both for GT EXT CER and ICE GAS. The reason lies in the dryer cost, which heavily penalises this solution. Therefore the best option is to directly feed biomass in the combustor or in the gasifier when the initial moisture content is already lower than 20%; natural drying, if possible, is instead preferable when the moisture content is higher than 20%. If the latter solution were not applicable, gas drying would be mandatory in case of ICE GAS, due to the moisture limits which have already been discussed; on the contrary, solid biomass combustion, which occurs in GT EXT CER, allows the use of wet biomass and thus no drying is possible: results show that thermodynamic disadvantages of such an option are more than balanced by the economic benefits related to the non-installation of the dryer.

Finally, it is clear that these are general conclusions: a lot of other issues should then be considered from a practical point of view, for instance the corrosion problems related to the use of wet biomass which could affect the heat exchanger in externally fired gas turbines [6.1] [6.2].

Conclusions and future work

The aim of this thesis was to provide a full overview on small-scale wood fired power generation technologies, in order to identify the most performing solutions from a thermodynamic and an economic point of view.

Results of the performance simulations show that the most efficient configurations are the following:

- internal combustion engine coupled with a gasifier;
- regenerative gas turbine coupled with a pressurised gasifier;
- externally fired gas turbine with a ceramic/high temperature heat exchanger;
- bottoming organic Rankine cycle coupled with the former two listed solutions.

Achievable electrical efficiencies are about 25% at 100 kW_{el}, 30% at 1 MW_{el} and 35 ÷ 40% at 5 MW_{el}.

Feeding gas turbines directly with solid biomass would provide excellent performance, but this is normally considered an unfeasible option. On the other hand, a hybrid gas turbine solution fed with natural gas and solid biomass has been studied, providing good efficiencies, although it is only partially renewable.

A more-in-depth analysis has additionally shown that a proper heat recovery from the syngas cooling process in gasification devices results in a considerable efficiency increase, both in electrical and thermal terms.

The most efficient solutions, together with the hybrid gas turbine, have been subject to an economic analysis. This study has shown that the externally fired gas turbine with a high temperature heat exchanger is the most convenient solution at 100 kW_{el}, while an internal combustion engine coupled with a gasifier is preferable at 1 MW_{el}. At 5 MW_{el} these two solutions provide similar results: the former is more performing if heat can be sold for a long period during the year, otherwise the latter is more suitable. If power generation is being focused, then an internal combustion engine coupled with a gasifier should be preferred.

Thanks to considerable incentives provided by the Italian legislation, economic performance is very attractive: PayBack Times of the cited best solutions are about $2 \div 4$ years at 100 kW_{el} and just $1 \div 1.5$ years at the two larger scales, the actual value depending on the period of the year when recovery heat can be sold. Concerning this point, thermal energy recovery and sale is not generally mandatory like in natural gas plants, but its positive effects are clear.

The hybrid gas turbine proves to be an interesting option too, thanks to low investment cost, if generated heat is sold all over the year and/or the natural gas power input share is small.

A sensitivity analysis has also shown that the variation of some economic parameters (heat sale price, biomass cost, etc.) has a limited effect on the overall performance, especially if heat is sold for an appreciable number of hours during the year.

Finally, biomass drying has positive effects on thermodynamic performance, but carrying out such an operation with hot flue gases is unprofitable because of the dryer cost: if the plants allows to burn wet biomass and natural drying is not possible (which otherwise is always convenient), it is better to perform no fuel drying.

Basing on this work, a very wide range of activities can be planned. First of all a broad plant model library has been created in Thermoflex™: these models could be used for deeper performance simulations, as in this work the reliability of this software has been proven also for such plant typologies. On the other hand, the identified most performing solutions can be developed with specific numeric, modelling or experimental tools: for instance, gasification and syngas cleaning processes or high temperature/ceramic heat exchanger operation may be focussed. Moreover, combined plants with an internal combustion engine or a gas turbine coupled with bottoming ORC have proven to deserve attention: these solutions are penalised by high investment costs, but are thermodynamically very performing, especially the former one. For instance, one research activity could be the coupling of topping and bottoming plants.

References

Special reference

[TF] Thermoflex™ library data

1. Biomass and technologies for its exploitation

[1.1] IAC (InterAcademy Council), Lighting the way: toward a sustainable energy future, Amsterdam, The Netherlands, 2007

[1.2] IEA (International Energy Agency), World Energy Outlook, Paris, France, 2008

[1.3] IEA (International Energy Agency), Key World Energy Statistics, Paris, France, 2009

[1.4] F. Reale, Soluzioni innovative per impianti basati sulla micro-turbina a gas: analisi energetica e ambientale, Tesi di dottorato, Università degli Studi di Napoli "Federico II", 2007

[1.5] IPCC (Intergovernmental Panel on Climate Change), Fourth Assessment Report (AR4), Geneva, Switzerland, 2007

[1.6] UN (United Nations), Kyoto Protocol to the United Nations Framework Convention on Climate Change (UNFCCC), Kyoto, Japan, 1997

[1.7] Commission of the European Communities, Proposal for a directive of the European Parliament and of the Council on the promotion of the use of energy from renewable sources, Brussels, Belgium, January 2008, approved in December 2008

[1.8] D. Cocco, C. Palomba, P. Puddu, Tecnologie delle energie rinnovabili, Servizi Grafici Editoriali, Padova, 2008

[1.9] Commission of the European Communities, Biomass action plan, Brussels, Belgium, 2005

[1.10] EurObserv'ER, Solid biomass barometer, Paris, France, 2006

[1.11] Italian Government, Position paper – Energy: issues and challenges for Europe and for Italy, Roma, 2007

[1.12] ITABIA (Italian Biomass Association), I traguardi della bioenergia in Italia – Elementi chiave per gli obiettivi al 2020: rapporto 2008, Roma, 2009

[1.13] ENEA (Ente per le Nuove tecnologie, l'Energia e l'Ambiente), Rapporto energia e ambiente 2006, Roma, 2007

[1.14] ENEA (Ente per le Nuove tecnologie, l'Energia e l'Ambiente), Rapporto sul recupero energetico da rifiuti urbani in Italia, 2^ edizione, Roma, 2009

[1.15] Ambiente Italia, Italia: uno scenario low carbon 2020, Milano, 2009

[1.16] F. Fantozzi, P. Bartocci, C. Buratti, Agroforestry biomass availability assessment in Umbria region, preliminary results, Proceedings of the 16th European Biomass Conference and Exhibition, Valencia, Spain, 2-6 June 2008

[1.17] L. Zullo, G. Fiorese, M. Gatto, G. Guariso, S. Consonni, Stima della disponibilità di biomassa e alternative di utilizzo energetico: un'applicazione alla provincia di Piacenza, Atti del XV congresso della Società Italiana di Ecologia, Torino, 12-14 settembre 2005

[1.18] R. Infascelli, S. Faugno, S. Pindozzi, L. Boccia, Disponibilità di biomasse agro-forestali e residui di potature in Campania, Atti del IX Convegno Nazionale dell'Associazione Italiana di Ingegneria Agraria, Ischia Porto (NA), 12-16 settembre 2009

[1.19] GSE (Gestore dei Servizi Energetici, former Gestore dei Servizi Elettrici), Statistiche sulle fonti rinnovabili in Italia – Anno 2008, Roma, 2009

[1.20] TERNA (Rete Elettrica Nazionale), Dati statistici sull'energia elettrica in Italia, Roma, 2009

[1.21] Governo Italiano, Libro bianco per la valorizzazione energetica delle fonti rinnovabili, Roma, 1999

[1.22] F. Lucia, Potenzialità dei biocombustibili solidi nelle province italiane: metodologia e stima, Tesi di laurea, Università degli Studi di Napoli "Federico II", 2004

[1.23] TERNA (Rete Elettrica Nazionale), Previsioni della domanda elettrica in Italia e del fabbisogno di potenza necessario – Anni 2009-2019, Roma, 2009

[1.24] ISES (International Solar Energy Society) ITALIA, Biomasse per l'energia: guida per progettisti, impiantisti e utilizzatori, Roma, 2004

[1.25] A. Bartolazzi, Le energie rinnovabili, Hoepli editore, Milano, 2006

[1.26] ITABIA (Italian Biomass Association), Le biomasse per l'energia e l'ambiente: rapporto 2003, Roma, 2005

[1.27] R. Moro, P. Pinamonti, M. Reini, ORC technology for waste-wood to energy conversion in the furniture manufacturing industry, Thermal Science, Vol. 12, N. 4, pp. 61-73, October 2008

[1.28] S. Gaur, T. B. Reed, Thermal data for natural and synthetic fuels, Marcel Dekker, New York, NY, USA, 1998

[1.29] P. Lacquaniti, Analisi e valutazione delle tecnologie energetiche nell'ambito della pianificazione energetico-ambientale della regione Lombardia. Il caso studio "Kyoto Enti Locali", Tesi di laurea, Università degli Studi di Milano-Bicocca, 2008

[1.30] S. van Loo, J. Koppejan, The handbook of biomass combustion and co-firing, Earthscan, London, United Kingdom, 2008

[1.31] L. Damiani, La gassificazione delle biomasse: analisi delle prestazioni con l'utilizzo di modelli di simulazione, Tesi di dottorato, Università degli Studi di Genova, 2009

[1.32] M. Balat, Gasification of biomass to produce gaseous products, Energy Sources, Part A: Recovery, Utilization and Environmental Effects, Vol. 31, N. 6, pp. 516-526, January 2009

[1.33] EUBIA (European Biomass Industry Association), Gasification, www.eubia.org

[1.34] M. Baratieri, P. Baggio, B. Bosio, M. Grigiante, G. A. Longo, The use of biomass syngas in IC engines and CCGT plants: a comparative analysis, Applied Thermal Engineering, Vol. 29, N. 16, pp. 3309-3318, November 2009

[1.35] H. Spliethoff, Status of biomass gasification for power production, IFRF (International Flame Research Foundation) Combustion Journal, N. 200109, November 2001

[1.36] P. Hasler, T. Nussbaumer, Gas cleaning for IC engine applications from fixed bed biomass gasification, Biomass and Bioenergy, Vol. 16, N. 6, pp. 385-395, June 1999

[1.37] CTI (Comitato Termotecnico Italiano), Materiale del corso di formazione: Produzione di energia attraverso processi di gassificazione di biomasse solide (Ciclo di corsi: Produzione di energia da biomasse con particolare riferimento alle potenze inferiori ai 1000 kW), Milano, 5 ottobre 2009

2. Small-scale power plants

[2.1] M. A. Paisley, M. J. Welch, Biomass gasification combined cycle opportunities using the future energy Silvagas® gasifier coupled to Alstom's industrial gas turbines, GT2003-38294, Proceedings of the ASME Turbo Expo, Atlanta, GA, USA, 16-19 June 2003

[2.2] E. Macchi, S. Campanari, P. Silva, La microcogenerazione a gas naturale, Polipress, Milano, 2006

[2.3] Deutz Power Systems, TCG 2016 K engine technical data, www.deutz.com

[2.4] Encyclopaedia Britannica, Internal-combustion engine, www.britannica.com

[2.5] Garrett, Turbo Systems Tech Center, www.turbobygarrett.com

[2.6] A. Perdichizzi, Prestazioni di impianti di cogenerazione per applicazioni industriali, Atti del convegno: La sicurezza nell'uso del gas ed ottimizzazioni energetiche, Bergamo, 20-21 settembre 1996

[2.7] General Electric Aircraft Engines, LM2500, www.geae.com

[2.8] G. Lozza, Turbine a gas e cicli combinati, Progetto Leonardo, Società editrice Esculapio, Bologna, 2006

[2.9] C. Rodgers, Microturbine cycle options, 2001-GT-0552, Proceedings of the ASME Turbo Expo, New Orleans, LA, USA, 4-7 June 2001

[2.10] Capstone Turbine Corporation, C30, www.capstoneturbine.com

[2.11] T. Matsunuma, H. Yoshida, N. Iki, T. Ebara, S. Sodeoka, T. Inoue, M. Suzuki, Micro gas turbine with ceramic nozzle and rotor, GT2005-68711, Proceedings of the ASME Turbo Expo, Reno-Tahoe, NV, USA, 6-9 June 2005

[2.12] F. Vanini, Impianto di micro turbina a gas alimentato a biomassa, Tesi di laurea, Università degli Studi di Firenze, 2004

[2.13] J. E. D. Gauthier, Analysis of indirectly fired gas turbine power systems, GT2007-27226, Proceedings of the ASME Turbo Expo, Montreal, Canada, 14-17 May 2007

[2.14] M. Kautz, U. Hansen, The externally fired gas turbine (EFGT-Cycle) and simulation of the key components, Proceedings of the 3rd European Congress on the Economics and Management of Energy in Industry, Estoril-Lisbon, Portugal, 6-9 April 2004

[2.15] S. B. Ferreira, P. Pilidis, M. A. R. Nascimento, A comparison of different gas turbine concepts using biomass fuel, 2001-GT-0559, Proceedings of the ASME Turbo Expo, New Orleans, LA, USA, 4-7 June 2001

[2.16] A. Traverso, L. Magistri, R. Scarpellini, A. Massardo, Demonstration plant and expected performance of an externally fired micro gas turbine for distributed power generation, GT2003-38268, Proceedings of the ASME Turbo Expo, Atlanta, GA, USA, 16-19 June 2003

[2.17] Turboden, Products, www.turboden.eu

[2.18] I. Obernberger, P. Thonhofer, E. Reisenhofer, Description and evaluation of the new 1,000 kW_{el} Organic Rankine Cycle process integrated in the biomass CHP plant in Lienz, Austria, Euroheat & Power, Vol. 10, N.1, pp. 18-25, January 2002

[2.19] G. Bonetti, Simulazione di un gruppo a vapore a fluido organico (ORC) cogenerativo, Tesi di laurea, Università degli Studi di Trieste, 2004

[2.20] S. Quoilin, Experimental study and modeling of a low temperature Rankine cycle for small scale cogeneration, Degree Thesis, University of Liège, 2007

[2.21] A. Duvia, M. Gaia, Cogenerazione a biomassa mediante turbogeneratori ORC Turboden: tecnologia, efficienza, esperienze pratiche ed economia, Atti del convegno: Energia prodotta dagli scarti del legno – opportunità di cogenerazione nel distretto del mobile, Pordenone, 11 novembre 2004

[2.22] A. Germek, Dimensionamento di impianti di cogenerazione asserviti ad una minirete di teleriscaldamento, Tesi di laurea, Università degli Studi di Bergamo, 2008

[2.23] U.S. Department of Energy, Energy Efficiency & Renewable Energy, Fuel Cells, www.eere.energy.gov

3. Working hypotheses and preliminary analysis

[3.1] Thermoflow, www.thermoflow.com

[3.2] Savona Combustion Laboratory, Dipartimento di Macchine, Sistemi Energetici e Trasporti (DIMSET/SCL), University of Genoa, proxy.sv.inge.unige.it/SCL/

[3.3] R. Karamarkovic, V. Karamarkovic, Energy and exergy analysis of biomass gasification at different temperatures, Energy, Vol. 35, N. 2, pp. 537-549, February 2010 (available online in November 2009)

[3.4] Caema, Gassificatori a biomassa, www.caemaenergia.com

[3.5] D. Cocco, P. Deiana, G. Cau, Ottimizzazione di uno scambiatore di calore ad alta temperatura per impianti EFGT alimentati con biomasse, Atti del 58° Congresso ATI (Associazione Termotecnica Italiana), Padova, 8-12 Settembre 2003

[3.6] J. Jayasuriya, A. Manrique, R. Fakhrai, J. Fredriksson, T. Fransson, Gasified biomass fuelled gas turbine: combustion stability and selective catalytic oxidation of fuel-bound nitrogen, GT2006-90988, Proceedings of the ASME Turbo Expo, Barcelona, Spain, 8-11 May 2006

[3.7] E. O. Oluyede, J. N. Phillips, Fundamental impact of firing syngas in gas turbines, GT2007-27385, Proceedings of the ASME Turbo Expo, Montreal, Canada, 14-17 May 2007

[3.8] P. Ouimette, P. Seers, Numerical comparison of premixed laminar flame velocity of methane and wood syngas, Fuel, Vol. 88, N. 3, pp. 528-533, March 2009

[3.9] A. L. Boehman, O. Le Corre, Combustion of syngas in internal combustion engines, Combustion Science and Technology, Vol. 180, N. 6, pp. 1193-1206, June 2008

[3.10] G. Fiorenza, La gassificazione della biomassa: stato dell'arte ed esempi pratici di piccola e media taglia, Presentazione al convegno: Valorizzazione energetica della biomassa legnosa e del biogas, Fiera Klimaenergy, Bolzano, 25 settembre 2009

[3.11] Cummins, Generator sets, www.cumminspower.com

[3.12] H. E. Stassen, H. Knoef, Theoretical and practical aspects on the use of LCV-gas from biomass gasifiers in internal combustion engines, Proceedings of the international conference: Gasification and pyrolysis of biomass – State of the art and future prospects, edited by M. Kaltschmitt and A.V. Bridgwater, CPL Press, Newbury, United Kingdom, pp. 269–281, 1997

[3.13] Deutz Power Systems, TBG 620 K engine technical data, www.deutz.com

[3.14] Turbec, T100 technical information, www.turbec.com

[3.15] G. Lagerström, M. Xie, High performance & cost effective recuperator for micro-gas turbine, GT-2002-30402, Proceedings of the ASME Turbo Expo, Amsterdam, The Netherlands, 3-6 June 2002

[3.16] T. C. Hung, Waste heat recovery of organic Rankine cycle using dry fluids, Energy Conversion and Management, Vol. 42, N. 5, pp. 539-553, March 2001

4. Thermodynamic analysis

[4.1] J. Kaikko, J. L. H. Backman, L. Koskelainen, J. Larjola, Optimum operation of externally-fired microturbine in combined heat and power generation, GT2007-28264, Proceedings of the ASME Turbo Expo, Montreal, Canada, 14-17 May 2007

[4.2] J. Kaikko, L. Koskelainen, J. L. H. Backman, J. Larjola, Optimal design of a heat exchanger for an externally-fired microturbine in combined heat and power generation, GT2008-51244, Proceedings of the ASME Turbo Expo, Berlin, Germany, 9-13 June 2008

[4.3] M. Pelzmann, H. Haselbacher, Combustion chamber for a directly wood particle fired gas turbine, GT-2002-30076, Proceedings of the ASME Turbo Expo, Amsterdam, The Netherlands, 3-6 June 2002

[4.4] D. Chiaramonti, G. Riccio, F. Martelli, Preliminary design and economic analysis of a biomass fed micro-gas turbine plant for decentralised energy generation in Tuscany, GT2004-53546, Proceedings of the ASME Turbo Expo, Vienna, Austria, 14-17 June 2004

[4.5] L. Y. Bronicki, D. N. Schochet, Bottoming organic cycle for gas turbines, GT2005-68121, Proceedings of the ASME Turbo Expo, Reno-Tahoe, NV, USA, 6-9 June 2005

[4.6] I. Vaja, A. Gambarotta, Internal combustion engine (ICE) bottoming with organic Rankine cycles (ORC), Energy, Vol. 35, N. 2, pp. 1084-1093, February 2010 (available online in July 2009)

5. Economic analysis

[5.1] G. Franchini, G. Nurzia, Heat exchangers design in a single stage LiBr-water absorption machine: thermodynamic and economic optimisation, Proceedings of the Conference: Heat Transfer in Components and Systems for Sustainable Energy Technologies, Chambéry, France, 18-20 April 2007

[5.2] I. C. Kemp, Pinch analysis and process integration, Butterworth-Heinemann, Elsevier, Oxford, United Kingdom, 2007

[5.3] I. Peretti, Application of ORC units in sawmills: technical-economic considerations, Proceeding of the wood energy information day, Killadeas, United Kingdom, 19 November 2008

[5.4] A. Duvia, A. Guercio, C. Rossi di Schio, Technical and economic aspects of biomass fuelled CHP plants based on ORC turbogenerators feeding existing district heating networks, Proceedings of the 17th European Biomass Conference and Exhibition, Hamburg, Germany, 29 June - 03 July 2009

[5.5] GSE (Gestore dei Servizi Energetici, former Gestore dei Servizi Elettrici), Support for renewable energy sources, www.gse.it

[5.6] A. Lorenzoni, Speciale fotovoltaico: costi e prospettive della tecnologia, Il giornale dell'ingegnere, Vol. 58, N. 16, 1 ottobre 2009

[5.7] ENEA (Ente per le Nuove tecnologie, l'Energia e l'Ambiente), Atlante italiano della radiazione solare, Calcoli, www.solaritaly.enea.it

[5.8] GSE (Gestore dei Servizi Energetici, former Gestore dei Servizi Elettrici), Guida al conto energia, Roma, 2009

6. Sensitivity analysis: moisture effects

[6.1] B. Elmegaard, B. Qvale, G. Carapelli, P. de Faveri Tron, Open-cycle indirectly fired gas turbine for wet biomass fuel, Proceedings of the conference: Efficiency, Costs, Optimization, Simulation and Environmental Impact of Energy Systems (ECOS), Istanbul, Turkey, 4-6 July 2001

[6.2] B. Elmegaard, B. Qvale, Analysis of indirectly fired gas turbine for wet biomass fuels based on commercial micro gas turbine data, GT-2002-30016, Proceedings of the ASME Turbo Expo, Amsterdam, The Netherlands, 3-6 June 2002

[6.3] M. Bolhàr-Nordenkampf, H. Hofbauer, Biomass gasification combined cycle thermodynamic optimisation using integrated drying, GT2004-53269, Proceedings of the ASME Turbo Expo, Vienna, Austria, 14-17 June 2004